ENTROPY-BASED INFERENCE AND CALIBRATION METHODS FOR CIVIL ENGINEERING SYSTEM MODELS UNDER UNCERTAINTY

Thesis submitted in accordance with the requirements of the University of Liverpool for the degree of Doctor in Philosophy

by

Abdullah YASSIN-KASSAB

January 1998

ABSTRACT

Jaynes' maximum entropy formalism, based on Shannon's informational measure of uncertainty, is used in this thesis to infer solutions to two different civil engineering system models under uncertainty; those being water distribution networks and structural trusses. In this regard, the following problems, formalised as questions, are investigated.

1. By appreciating the applicability of the entropy of network flows as a surrogate measure of reliability in water distribution networks, how can maximum entropy flows be calculated in a looped network when only the external inflows and outflows and the direction of pipe flows are available, without requiring mathematical programming techniques or iterative processes, so that they can be incorporated in one of the linearized least-cost optimum design methods without inducing any extra complexity into the formulation?
2. How can various types of information which might be available in real water distribution networks be used to infer most-likely pipe flows and their corresponding pipe characteristics in a looped network, thus opening up the possibility of calibrating computer models of existing water networks without requiring a physical measurement of the network pipe flows which might be expensive and time consuming?
3. Is it possible to extend the entropy-based method of designing reliable water networks to structural trusses bearing in mind the striking similarities between the two systems?

In an attempt to answer the above questions, the following aspects of the present research are established.

1. Visualising network pipe flows as path flows supplying demand nodes from the network sources, and appreciating that the demand of any node served by more than one path from any source should be distributed equally amongst all

the paths supplying that node from that source, the maximum entropy flows in a looped network are such that the ratio of the probabilities of path flows from each pair of sources to a demand node reachable from the corresponding pair of sources is the same for every demand node supplied by this pair of sources in the network. Accordingly, a very simple algorithm for calculating maximum entropy flows in general looped networks is developed. Its simplicity and efficiency is noted. An algorithm using a path-based entropy function, capable of calculating directly the maximum entropy value of network flows, is derived.

2. A compound entropy formula representing pipe characteristics and pipe flows in water distribution networks is derived. A calibration model is then developed by maximizing the compound network entropy formula subject to available information such as external flows for multiple load cases, pipe diameters and lengths, nodal pressure heads and nodal equilibrium equations along with conservation laws of energy for all load cases considered around network loops. It is shown that the calibration method is very accurate for networks designed to carry maximum entropy flows and less accurate for other conventionally designed networks.

3. An attempt is made to design reliable structural trusses to carry maximum entropy bar axial forces calculated by visualising bar axial forces as force flows. This attempt shows that flow entropy concept seems to have little significance in respect of structural reliability. However, unsuspected difficulties regarding extending the scalar methodologies developed in water distribution networks to the vectorial domain of structural trusses are highlighted. Also, the difference between reliability concepts in the two systems is observed.

ACKNOWLEDGEMENT

I would like to thank my supervisor, Professor Andrew B. Templeman for his invaluable guidance, support, encouragement and enormous amount of discussion time which I have received during the course of this research.

Also, my sincere thanks go to all members of my family and to my lovely wife for their endless encouragement and patience during the period of my absence.

I would also like to thank the University of Tishreen and the ministry of Higher Education in Syria for the financial support which I have been given all the way through.

Finally, I would like to thank all my friends and colleagues here in Liverpool for their help and kind friendship which I have enjoyed during the happy and difficult times.

Abdullah YASSIN-KASSAB

To my wife Rabia and our families.

TABLE OF CONTENTS

CHAPTER 1

INTRODUCTION **1**

1.1 INTRODUCTION 1

1.2 MOTIVATIONS AND OBJECTIVES OF THE PRESENT RESEARCH 2

1.3 LAYOUT OF THESIS 4

CHAPTER 2

THE MAXIMUM ENTROPY FORMALISM AND ITS APPLICATIONS IN WATER DISTRIBUTION NETWORKS **6**

2.1 INTRODUCTION 6

2.2 SHANNON'S INFORMATIONAL ENTROPY 7

2.2.1ENTROPY OF FINITE PROBABILITY SCHEMES 8

2.2.2 PROPERTIES OF SHANNON'S ENTROPY 10

2.2.2.1 THE UNIQUENESS THEOREM 11

2.3 THE MAXIMUM ENTROPY FORMALISM 12

2.3.1 INTERPRETATIONS BEHIND THE MAXIMUM ENTROPY FORMALISM 15

2.4 THE CONTINUOUS CASE OF THE MAXIMUM ENTROPY FORMALISM 15

2.5 APPLICATIONS OF THE MAXIMUM ENTROPY FORMALISM IN CIVIL ENGINEERING 16

2.6 ENTROPY APPLICATIONS IN WATER DISTRIBUTION NETWORKS 19

2.6.1 OPTIMUM DESIGN OF WATER DISTRIBUTION NETWORKS 20

2.6.1.1 CONSTITUTIVE EQUATIONS 20

2.6.1.1.1 HEAD LOSS EQUATIONS 20

2.6.1.1.2 CONTINUITY EQUATIONS 21

2.6.1.1.3 ENERGY CONSERVATION EQUATIONS 21

2.6.1.1.3.1 LOOP EQUATIONS 21

2.6.1.1.3.2 PATH EQUATIONS 22

2.6.1.2 WATER NETWORK FLOW ANALYSIS 22
2.6.1.2.1 HARDY-CROSS METHOD 22
2.6.1.3 WATER NETWORK LEAST COST DESIGN FORMULATION 24
2.6.1.3.1 COST OBJECTIVE FUNCTION 24
2.6.1.3.2 PRACTICAL CONSTRAINTS 24
2.6.2 MAXIMUM ENTROPY FLOWS IN WATER DISTRIBUTION NETWORKS 27
2.6.2.1 FLOW ENTROPY FUNCTIONS OF AWUMAH, GOULTER AND BHATT 28
2.6.2.2 FLOW ENTROPY FUNCTIONS OF TANYIMBOH AND TEMPLEMAN 32
2.6.2.3 CALCULATING MAXIMUM ENTROPY FLOWS IN NETWORKS 38
2.6.2.4 PATH-BASED ALGORITHM FOR CALCULATING MAXIMUM ENTROPY FLOWS IN SINGLE-SOURCE NETWORKS 41
2.6.3 ENTROPY AND RELIABILITY IN WATER NETWORKS 43
2.6.3.1 SOME DEFINITIONS AND MEASURES OF RELIABILITY 44
2.6.3.2 CORRELATION BETWEEN ENTROPY AND RELIABILITY 47
2.6.3.3 ENTROPY-BASED OPTIMUM DESIGN OF RELIABLE WATER NETWORKS 49

CHAPTER 3
MATHEMATICAL SIMILARITIES IN THE SYSTEM MODELS OF ENGINEERING NETWORKS 55
3.1 INTRODUCTION 55
3.2 OPTIMUM DESIGN OF STRUCTURAL TRUSSES 57
3.2.1 CONSTITUTIVE EQUATIONS 57
3.2.1.1 BAR FORCE EQUILIBRIUM EQUATIONS 57
3.2.1.2 COMPATIBILITY EQUATIONS 58
3.2.1.3 CHARACTERISTIC FORCE-STRAIN RELATIONSHIP EQUATIONS ..58
3.2.2 METHODS OF ANALYSIS 58
3.2.2.1 FLEXIBILITY METHOD 59
3.2.2.2 STIFFNESS METHOD 60

3.2.3 DISCRETE OPTIMUM DESIGN FORMULATION 61
3.2.3.1 WEIGHT OBJECTIVE FUNCTION 62
3.2.3.2 OTHER CONSTRAINTS 62
3.2.4 SOLUTION METHODS 64
3.2.4.1 SEGMENTAL OPTIMUM DESIGN METHOD 65
3.3 STRUCTURAL RELIABILITY 68
3.3.1 PROBABILISTIC RELIABILITY ANALYSIS 69
3.3.1.1 THE FUNDAMENTAL CASE 69
3.3.1.2 APPROXIMATE STRUCTURAL RELIABILITY METHODS 71
3.3.1.3 RELIABILITY ANALYSIS OF STRUCTURAL SYSTEMS 75
3.3.2 PROBABILITY-BASED DESIGN 80
3.3.3 DAMAGE TOLERANT DESIGN 83
3.4 SIMILARITIES IN THE ENGINEERING NETWORK SYSTEM MODELS 86
3.4.1 ANALYSIS PROBLEM 88
3.4.1.1 CONSTITUTIVE EQUATIONS 88
3.4.1.2 ANALYSIS PROBLEM FORMULATION AND SOLUTION METHODS 89
3.4.2 OPTIMUM DESIGN PROBLEM 92
3.4.3 RELIABILITY PROBLEM 94

CHAPTER 4

CALCULATING MAXIMUM ENTROPY FLOWS IN MULTI-SOURCE, MULTI-DEMAND GENERAL NETWORKS 104
4.1 INTRODUCTION 104
4.2 MULTI-PATH FLOWS AND THEIR EQUILIBRIUM EQUATIONS FOR MULTI-SOURCE NETWORK 105
4.3 PATH FLOW PROBABILITIES AND PATH ENTROPY FUNCTION OF WATER NETWORKS 108
4.4 ALFA METHOD 111
4.5 PATH-BASED ALGORITHMS FOR CALCULATING MAXIMUM ENTROPY FLOWS IN GENERAL WATER NETWORKS 116
4.6 SUMMARY AND CONCLUSION 126

CHAPTER 5

NUMERICAL APPLICATIONS OF THE ALFA METHOD ALGORITHMS 131

5.1 INTRODUCTION 131

5.2 EXAMPLE 1 132

5.3 EXAMPLE 2 137

5.4 EXAMPLE 3 139

5.5 COMMENTS ON THE SUPER-SOURCE APPROACH 142

5.6 SUMMARY AND CONCLUSION 144

CHAPTER 6

CALIBRATION METHOD FOR GENERAL WATER DISTRIBUTION NETWORKS 152

6.1 INTRODUCTION 152

6.2 PIPE FLOW PROBLEM 154

6.2.1 ENTROPY OF NETWORK FLOWS 155

6.2.2 MAXIMUM ENTROPY FLOWS 157

6.3 PIPE CHARACTERISTIC PROBLEM 158

6.3.1 ENTROPY OF NETWORK PIPE CHARACTERISTICS 158

6.3.2 MAXIMUM ENTROPY PIPE CHARACTERISTICS 159

6.4 COMPOUND PROBLEM 160

6.4.1 COMPOUND NETWORK ENTROPY 162

6.4.2 MAXIMUM ENTROPY FLOWS AND CORRESPONDING MAXIMUM ENTROPY PIPE CHARACTERISTICS 163

6.4.3 MULTIPLE-LOAD CASE 166

6.5 SUMMARY 168

CHAPTER 7

NUMERICAL APPLICATIONS OF THE WATER DISTRIBUTION NETWORK CALIBRATION METHOD 170

7.1 INTRODUCTION 170

7.2 EXAMPLE 1 171

7.2.1 DISCUSSION 173
7.3 EXAMPLE 2 175
7.3.1 ORIGINAL LOAD CASE 1 177
7.3.2 MULTIPLE LOAD CASE WITH UNCHANGED PIPE FLOW DIRECTIONS 179
7.3.2.1 MULTIPLE LOAD CASE (1+2) 179
7.3.2.2 MULTIPLE LOAD CASE (1+2+3) 181
7.3.3 MULTIPLE LOAD CASE WITH CHANGING PIPE FLOW DIRECTIONS 183
7.3.3.1 MULTIPLE LOAD CASE (1+4) 183
7.3.3.2 MULTIPLE LOAD CASE (1+4+5) 185
7.3.4 DISCUSSION 187
7.3.4.1 ORIGINAL LOAD CASE 1 187
7.3.4.2 MULTIPLE LOAD CASE WITH UNCHANGED PIPE FLOW DIRECTIONS 189
7.3.4.3 MULTIPLE LOAD CASE WITH CHANGING PIPE FLOW DIRECTIONS 190
7.4 SUMMARY AND CONCLUSION 193

CHAPTER 8

ENTROPY-BASED STRUCTURAL APPLICATIONS 200
8.1 INTRODUCTION 200
8.2 STRUCTURAL FORCE FLOW DIAGRAM 201
8.2.1 VERTICAL COMPONENT OF FORCE FLOW DIAGRAM 203
8.2.2 HORIZONTAL COMPONENT OF FORCE FLOW DIAGRAM 203
8.3 MAXIMUM ENTROPY BAR AXIAL FORCES 204
8.4 MAXIMUM ENTROPY OPTIMUM STRUCTURAL DESIGN 206
8.5 CONVENTIONAL OPTIMUM STRUCTURAL DESIGN 211
8.6 MAXIMUM ENTROPY DESIGN AND CONVENTIONAL DESIGN RELIABILITY COMPARISON 212
8.7 DISCUSSION 216
8.8 SUMMARY AND CONCLUSION 223

CHAPTER 9

SUMMARY, CONCLUSIONS AND RECOMMENDATIONS FOR FUTURE WORK 231

9.1 INTRODUCTION 231

9.2 SUMMARY OF THE PRESENT WORK AND ITS MAIN CONCLUSIONS 234

9.3 RECOMMENDATIONS FOR FUTURE WORK 241

REFERENCES 245

APPENDIX A

WALTERS' APPROACH FOR CALCULATING MAXIMUM ENTROPY FLOWS IN GENERAL WATER SUPPLY NETWORKS 261

APPENDIX B

THE ALFA METHOD COMPUTER PROGRAMME 271

APPENDIX C

SOME OF THE ALFA METHOD COMPUTER PROGRAMME APPLICATIONS OF CHAPTER 5 278

APPENDIX D

THE CAMONET COMPUTER PROGRAMME 290

APPENDIX E

SOME OF THE CAMONET COMPUTER PROGRAMME APPLICATIONS OF CHAPTER 7 301

APPENDIX F

SOME OF THE EZLP COMPUTER PROGRAMME APPLICATIONS OF CHAPTER 8 322

APPENDIX G

THE TRUSS2D COMPUTER PROGRAMME 330

FIGURE CAPTIONS

CHAPTER 2

Figure 2.1 Water supply network 52

Figure 2.2 Single-source network 53

Figure 2.3 Equal path flows from the source to each demand node 53

Figure 2.4 Maximum entropy flows for the network of Figure 2.2 found by superposing the path flows of Figure 2.3 54

Figure 2.5 Number of paths to each node for the network of Figure 2.2 54

CHAPTER 3

Figure 3.1 Typical structural truss 97

Figure 3.2 Truss with redundant bars replaced by external applied loads 97

Figure 3.3 Conventional and segmental axial force bars 98

Figure 3.4 The fundamental case 98

Figure 3.5 Single distribution of strength R for a given load L 99

Figure 3.6 Different distributions of strength R for positive and negative load 99

Figure 3.7 Concept of residual strength 100

Figure 3.8 Concept of factor of safety 100

Figure 3.9 Reliability index for two variables 101

Figure 3.10 Weakest link model 102

Figure 3.11 Fail safe model 102

Figure 3.12 Typical water supply network 103

CHAPTER 4

Figure 4.1 Two-source network 128

Figure 4.2 Equal path flows from each source to each reachable demand node 128

Figure 4.3 Maximum entropy flows for the network of Figure 4.1 obtained by maximizing the nodal entropy function of the network 129

Figure 4.4 Maximum entropy flows for a three-source network obtained by maximizing the nodal entropy function of the network 129
Figure 4.5 Maximum entropy flows for the two-source network of Figure 4.1 130

CHAPTER 5

Figure 5.1 Maximum entropy flows for the network of Example 1 146
Figure 5.2 Maximum entropy flows for the network of Example 2 147
Figure 5.3 Maximum entropy flows for the network ofExample 3 148
Figure 5.4 The reversed network of the two-source network of Example 1 with a new global node numbering scheme 149
Figure 5.5 Maximum entropy flows for a two-source network adapted from Tanyimboh and Templeman (1993b) 150
Figure 5.6 Maximum entropy flows for the two-source network of Figure 5.5 having the flow direction in link 1-2 reversed 151

CHAPTER 7

Figure 7.1 The one-source network of Example 1 adapted from Tanyimboh and Templeman (1993c) 196
Figure 7.2 The one-source network of the original load case of Example 1 197
Figure 7.3 Two load cases of Example 2 with unchanged pipe flow directions comparing with the original load case of Figure 7.2 198
Figure 7.4 Two load cases of Example 2 with changing flow direction in some pipes comparing with the original load case of Figure 7.2 199

CHAPTER 8

Figure 8.1 A sample indeterminate structural truss 226
Figure 8.2 The truss of Figure 8.1 with the two redundant bars replaced by their bar axial forces 226

Figure 8.3 The vertical component of force flow diagram of the truss of Figure 8.1 227
Figure 8.4 The horizontal component of force flow diagram of the truss of Figure 8.1 227
Figure 8.5 Precompressing of bars 1-4 and 2-3 in the maximum entropy design of the truss of Figure 8.1 228
Figure 8.6 The maximum entropy design of the truss of Figure 8.1 under precompressing applied loads 228
Figure 8.7 Removing of bar 1-3 case which has to be added to the maximum entropy design results to give case 1 of damage tolerance analysis 229
Figure 8.8 Increasing the load at joint 5 case which has to be added to the maximum entropy design results to give case 4 of resilience analysis 229
Figure 8.9 Case 1 of damage tolerance analysis for the conventional design with bar 1-3 being removed 230
Figure 8.10 Case 4 of resilience analysis for the conventional design with the external load at joint 5 being increased 230

TABLE CAPTIONS

CHAPTER 4

Table 4.1 The maximum entropy path flows and their probabilities for the two-source network of Figure 4.1 with S^*=2.3885315 112

Table 4.2 The maximum entropy path flows and their probabilities for the three-source network of Figure 4.4 with S^*=2.594634 113

CHAPTER 5

Table 5.1 The path flow probabilities and the corresponding path flows for the two-source network of Figure 5.1 calculated by the alfa method with S^p=3.748957 134

Table 5.2 The path flow probabilities and the corresponding path flows for the three-source network of Figure 5.2 calculated by the alfa method with S^p=3.028466 138

Table 5.3 The path flow probabilities and the corresponding path flows for the three-source network of Figure 5.3 calculated by the alfa method with S^p=2.923974 141

CHAPTER 7

Table 7.1 Pipe data for the one-source network of Figure 7.1 and pipe diameters designed by Tanyimboh and Templeman (1993c) to carry maximum nodal entropy pipe flows with S_f= 1.915 172

Table 7.2 Maximum entropy pipe flows and corresponding maximum entropy pipe characteristics and their probabilities along with pipe head losses for the network of Example 1 obtained by the CAMONET computer programme for four different runs ...173

Table 7.3 Pipe data for the network of Figure 7.2 and pipe flows and head losses calculated by the Hardy-Cross method 175

Table 7.4 Actual pipe flows and corresponding pipe head losses calculated by the Hardy-Cross method for load cases 2, 3, 4 and 5 shown in Figures 7.3 and 7.4 176

Table 7.5 Maximum entropy pipe flows for load case 1 of Example 2, obtained by the CAMONET computer programme for seven different runs 177

Table 7.6 Maximum entropy pipe characteristics for load case 1 of Example 2, obtained by the CAMONET computer programme for seven different runs 178

Table 7.7 Maximum entropy pipe head losses for load case 1 of Example 2, obtained by the CAMONET computer programme for seven different runs 178

Table 7.8 Maximum entropy pipe flows for multiple load case (1+2) of Example 2, obtained by the CAMONET computer programme for run 179

Table 7.9 Maximum entropy pipe characteristics for multiple load case (1+2) of Example 2, obtained by the CAMONET computer programme for runs 8-12 180

Table 7.10 Maximum entropy pipe head losses for multiple load case (1+2) of Example 2, obtained by the CAMONET computer programme for runs 8-12 180

Table 7.11 Maximum entropy pipe flows for multiple load case (1+2+3) of Example 2, obtained by the CAMONET computer programme for runs 13-17 181

Table 7.12 Maximum entropy pipe characteristics for multiple load case (1+2+3) of Example 2, obtained by the CAMONET computer programme for runs 13-17 182

Table 7.13 Maximum entropy pipe head losses for multiple load case (1+2+3) of Example 2, obtained by the CAMONET computer programme for runs 13-17 182

Table 7.14 Maximum entropy pipe flows for multiple load case (1+4) of Example 2, obtained by the CAMONET computer programme for runs 18-22 183
Table 7.15 Maximum entropy pipe characteristics for multiple load case (1+4) of Example 2, obtained by the CAMONET computer programme for runs 18-22 184
Table 7.16 Maximum entropy pipe head losses for multiple load case (1+4) of Example 2, obtained by the CAMONET computer programme for runs 18-22 184
Table 7.17 Maximum entropy pipe flows for multiple load case (1+4+5) of Example 2, obtained by the CAMONET computer programme for runs 23-27 185
Table 7.18 Maximum entropy pipe characteristics for multiple load case (1+4+5) of Example 2, obtained by the CAMONET computer programme for runs 23-27 186
Table 7.19 Maximum entropy pipe head losses for multiple load case (1+4+5) of Example 2, obtained by the CAMONET computer programme for runs 23-27 186
Table 7.20 Deviations of pipe characteristic results from the actual values for the network of Example 2 along with the sums of the square errors for runs 4-27 192

CHAPTER 8

Table 8.1 Bar axial forces of the truss of Figure 8.1, calculated by bar force equilibrium equations in terms of redundant axial bar forces Fax_{14} and Fax_{23} 202
Table 8.2 Maximum entropy bar axial forces of the truss of Figure 8.1, calculated by solving the vertical component of force flow diagram (Figure 8.3) using the alfa method programme 205
Table 8.3 Input data of Problem 5 for maximum entropy optimum design of the truss of Figure 8.1 207

Table 8.4 Maximum entropy optimum design of the truss of Figure 8.1, obtained by solving Problem 5 using the EZLP linear programming algorithm 208

Table 8.5 Initial bar axial forces and joint deflection components for the maximum entropy discrete optimum design of the truss of Figure 8.1, calculated by the TRUSS2D programme 208

Table 8.6 Maximum entropy bar axial forces in the truss of Figure 8.1, generated by adding the extra bar axial forces induced by precompressing of bars 1-4 and 2-3 by forces 32.200 and 26.914 KN respectively to the initial bar axial forces induced by the external applied loads 210

Table 8.7 Final joint deflection components in the maximum entropy design of the truss of Figure 8.1, generated by adding the extra joint deflection components caused by precompressing of bars 1-4 and 2-3 to the initial deflection components caused by the external applied loads 210

Table 8.8 Last iteration results of the conventional discrete optimum design of the truss of Figure 8.1, obtained by five iterations of analysis, optimization and rounding up process of the segmental optimum structural design method using TRUSS2D and EZLP computer programmes 212

Table 8.9 Bar axial force results of damage tolerance analysis for the maximum entropy design of the truss of Figure 8.1 213

Table 8.10 Joint deflection component results of damage tolerance analysis for the maximum entropy design of the truss of Figure 8.1.....214

Table 8.11 Bar axial force results of resilience analysis for the maximum entropy design of the truss of Figure 8.1 214

Table 8.12 Joint deflection component results of resilience analysis for the maximum entropy design of the truss of Figure 8.1 214

Table 8.13 Bar axial force results of damage tolerance analysis for the conventional design of the truss of Figure 8.1 215

Table 8.14 Joint deflection component results of damage tolerance analysis for the conventional design of the truss of Figure 8.1 215
Table 8.15 Bar axial force results of resilience analysis for the conventional design of the truss of Figure 8.1 216
Table 8.16 Joint deflection component results of resilience analysis for the conventional design of the truss of Figure 8.1 216
Table 8.17 Maximum entropy design and conventional design results for the truss of Figure 8.1 with some statistical comparison 217
Table 8.18 Reliability analysis for the maximum entropy design of the truss of Figure 8.1 221
Table 8.19 Reliability analysis for the conventional design of the truss of Figure 8.1 221

NOTATION

*	superscript denoting the optimum value of a variable.
-	superscript of a random variable to indicate its mean value.
+ve	positive value.
-ve	negative value.
$\in$	belong to.
Σ	sum.
∞	infinity.
$\int$	integral.
$\prod$	product.
$\forall$	for all.
$\sqcap$	intersection.
$\sqcup$	union.
$\sqsubset$	subset.
α	dimensionless conversion factor for units.
α_i	alfa value corresponding to source node i in a network.
α_{ij}	characteristic value of pipe ij in a network.
β	safety index.
β_{ij}	safety index of component ij.
γ	constant cost coefficient for pipes in a network.
$[\delta]$	column vector of nodal displacement components in a truss.
δ_{jh}	horizontal component of the nodal displacement of node j in a truss.
δ_{jv}	vertical component of the nodal displacement of node j in a truss.
Δ_i	discrepancy between actual and estimated characteristic value of pipe in a network.
Δ_{ij}	deformation of bar ij in a truss.
Δq_l	equal change in the flows in loop l in a network.
η_b	axial force in bar b of the determinate sub-truss caused by the external applied loads only.
Θ_{ij}	the angle that bar ij makes with the horizontal in a truss.

μ	Lagrange multiplier.
ξ_{br}	axial force in bar b of the determinate sub-truss due to unit load applied at the nodes at the ends of redundant bar r.
ρ_{ij}	material density of bar ij in a truss.
σ_{com}	maximum permissible compressive stress in a truss.
σ_{ij}	axial stress in bar ij in a truss.
$\sigma_{L,ij}$	standard deviation of the external load applied to bar ij in a truss.
σ_{n-1}	sample standard deviation.
$\sigma_{R,ij}$	standard deviation of the resistive strength of bar ij in a truss.
σ_{ten}	maximum permissible tensile stress in a truss.
$\sigma(x)$	standard deviation of a random variable x.
ϕ	cumulative normal distribution function.
a_{jn}	effective number of independent paths to node n through link jn in a network.
A_D	set of commercially available discrete bar sizes of a truss.
A_{ij}	cross-sectional area of bar ij in a truss.
A_{min}	smallest bar size allowed in a truss.
cos	cosine of an angle.
C	total cost of pipes in a network.
C_{ij}	Hazen-Williams coefficient of pipe ij in a network.
CAMONET	calibration model for water networks.
d_k	number of paths in which link k is a member in a network.
D_D	set of commercially available discrete pipe diameters for a network.
D_{ij}	diameter of pipe ij in a network.
D_{max}	maximum pipe diameter allowed in a network.
D_{min}	minimum pipe diameter allowed in a network.
e_1	exponent of the diameter in the cost function for pipes in a network.
E_{ij}	elastic modulus of bar ij in a truss.
f(x)	probability density function.
F(x)	cumulative probability distribution function.
$F_s(q_s^{ind})$	network entropy function defined in terms of the independent flows.

$F_{s,r}(q_{s,r}^{ind})$	network entropy function defined in terms of the independent flows for load case r.
Fax_{ij}	axial force in bar ij in a truss.
$Fax_{ij,k}$	virtual axial force in bar ij associated with virtual unit force at joint k in a truss.
[Fex]	column vector of nodal externally applied force components in a truss.
Fex_{jh}	horizontal component of the external load applied at node j in a truss.
Fex_{jv}	vertical component of the external load applied at node j in a truss.
Fn( )	function defined in terms of items indicated in the parentheses.
$<Fn_j>$	expected value of the jth expectation constraint.
FM_i	ith failure mode.
g(X)	performance state function.
h_{ij}	head loss in pipe ij in a network.
h_p	head loss along path p in a network.
$h_{p,r}$	head loss along path p for load case r in a network.
$H_{max,n}$	maximum desirable head at node n in a network.
$H_{min,n}$	minimum desirable head at node n in a network.
H_n	total head at node n in a network.
H_s	total head at source node s in a network.
I_D	set of all demand nodes in a network.
$I_{D,i}$	set of all demand nodes reachable from source node i in a network.
I_S	set of all source nodes in a network.
$I_{S,j}$	set of all source nodes supplying node j in a network.
IJ	set of all the links in a network; set of all the bars in a truss.
IJ_l	set of all the links in loop l in a network.
$IJ_{l,r}$	set of all the links in loop l for load case r in a network.
IJ_p	set of all the links in path p in a network.
$IJ_{p,r}$	set of all the links in path p for load case r in a network.
k_i	main curvature of the limit state surface at the most probable failure point.

K	arbitrary positive constant.
[K]	stiffness matrix.
Kg	kilogram.
KN	kilonewton.
l_{bd}	length of segment d in bar b in a truss.
ln	the natural logarithmic function.
log	the logarithmic function to the base 10.
ltr	litre.
L	external load applied to a structural component.
Le_{ij}	length of link ij in a network; length of bar ij in a truss.
m	metre.
mm	millimetre.
M	number of finite schemes.
(n)	superscript denoting iteration number.
nl_{jn}	number of links in all the paths supplying node n using link jn in a network.
npt_{jn}	number of paths to node n using link jn in a network.
N	number of outcomes or events.
NB	number of bars in a truss.
ND_n	set of all the nodes or links immediately downstream of node n in a network.
NDB	number of commercially available discrete bars in the set A_D for a truss.
NDL_n	set of all the nodes or links immediately downstream of node n, which belong to a loop containing node n in a network.
NEC	number of expectation constraints.
NK	number of joints whose displacements are to be restricted in a truss.
NLC	number of load cases in a network.
NLK	number of links in a network.
NLP	number of loops in a network.
NM	number of members in a system.
NN	number of nodes in a network or a truss.

NP	number of paths having known head losses in a network.
NP_r	number of paths having known head losses in for load case r in a network.
NP_{ij}	number of paths from source node i to demand node j in a network.
NR	number of redundant bars in a truss.
NS	number of sources in a network.
NU_n	set of all the nodes or links immediately upstream of node n in a network.
o_i	ith outcome or event.
O_i	ith finite scheme.
p_{0n}	fraction of total inflow of source node n provided by its external inflow in a network.
$p_{\alpha,ij}$	probability that link ij has pipe characteristic value of α_{ij} in a network.
p_f	probability of failure.
$p_{f,ij}$	probability of failure of component ij.
p_f(system)	probability of system failure.
p_i	probability of ith outcome or event.
p_{ij}	probability of the outcome or event identified by ij.
p_{n0}	fraction of total inflow of demand node n satisfying its demand in a network.
$p_{p,ij}$	probability that path flow $q_{p,ij}$ supplied by source i reaches demand node j in a network.
p_s	probability of survival.
$p_{s,ij}$	probability of survival of component ij.
p_s(system)	probability of system survival.
p( )	probability of the outcome or event indicated in the parentheses.
P_{0n}	fraction of the total supply provided by source node n in a network.
P_n	total probability of flow arriving at node n by all possible paths in a network.
P_{n0}	fraction of the total supply consumed at demand node n in a network.

q_{0n}	external inflow at node n in a network.
q_{ij}	flow in pipe ij from node i to node j in a network.
$q_{ij,n}$	flow in pipe ij associated with sub-network n.
q_n	external inflow or outflow at node n.
q_{n0}	external outflow at node n in a network.
$q_{p,ij}$	path flow from source node i to demand node j in a network.
q_s	vector representing the flows in a network.
q_s^{ind}	vector representing the independent flows in a network.
$q_{s,r}^{ind}$	vector representing the independent flows for load case r in a network.
Q_0	sum of the link flows of a network.
Q_n	sum of link inflows at node n in a network.
$Q_n^{\sim}$	sum of the link inflows and outflows at node n in a network.
R	resistive strength of a structural component.
R_n	negative resistive strength of a structural component.
R_p	positive resistive strength of a structural component.
RS	residual strength.
sec	second.
sin	sine of an angle.
S	entropy of a probabilistic system; compound network entropy.
S^i	network entropy based on inflows at all nodes.
S^o	network entropy based on outflows at all nodes.
S^p	network entropy based on path flows.
S_0	entropy of the distribution of supplies or demands in a network.
S_0^d	entropy of the distribution of the demands in a network.
S_0^s	entropy of the distribution of the source supplies in a network.
S_α	network pipe characteristic entropy.
S_f	network flow entropy.
S_i^p	entropy of path flows supplied by source node i in a network.
S_n	entropy of node n in a network.
S_n^i	entropy of inflows at node n in a network.
S_n^o	entropy of outflows at node n in a network.

S_n'	modified entropy of node n in a network.
$S_n\tilde{}$	entropy of node n based on both nodal inflows and outflows in a network.
SF	factor of safety.
SNK_n	sub-network n.
t_{nj}	transmissivity from node j to node n in a network.
T_0	total supply or demand in a network.
$T_{i,n}$	total outflows at node i associated with sub-network n.
T_n	total flow reaching or leaving node n in a network.
v_{ij}	flow velocity in pipe ij in a network.
v_{max}	maximum flow velocity in a network.
v_{min}	minimum flow velocity in a network.
W	total weight of truss bars.
Z^+	the set of positive integers.

CHAPTER 1

INTRODUCTION

1.1 INTRODUCTION

In civil engineering projects, it is very common for engineers to deal with situations where some of the data needed in the analysis and design procedure is unavailable or uncertain. Load and strength data in structural reliability analysis, for example, have to be fitted by some available analytical probability distributions which are needed for estimating failure probability from their respective overlapping tail regions. Also, there is uncertainty associated with future orders in every productive industry such as the ready-mixed concrete industry, where prior probabilities for such orders need to be estimated for each mix. For such cases and many more, involving data uncertainty, an engineering judgement or a so-called "educated guess" is usually used to estimate the missing information so that progress on the analysis or design procedure can be made. However, such judgement or guess may sometimes introduce significant errors into subsequent calculations. For example, choosing different probability distributions to represent load and strength data in structural reliability analysis produces errors in reliability estimates measured in orders of magnitude (Basu and Templeman, 1985). Also, the evaluation of prior probabilities for future orders in the ready-mixed concrete industry, for example, should be done objectively, not arbitrarily, and should not be affected by any personal bias. Consequently, a rigorous inference method for estimating most-likely, or least-biased, performance estimates from partial information has to be adopted for such cases of uncertainty so that no arbitrary guesses have to be made to fill in the missing information if sensible data estimates are to be sought.

Recently, Jaynes' maximum entropy formalism (Jaynes, 1957) based on Shannon's informational entropy measure of uncertainty (Shannon, 1948) has been used in such cases as those outlined above to infer most-likely values for unknown probabilities

subject to available and incomplete information. The applicability of the maximum entropy formalism, however, has not been limited only to the obvious cases of inferring least-biased probability values. It has been used to generate solutions to a wide range of civil engineering problems where the available information is incomplete or uncertain, provided that the sought missing information can be somehow cast in a probabilistic fashion as required by Shannon's informational entropy. The present research is concerned with developing methods of logical inference based on the maximum entropy formalism for two different civil engineering system models under uncertainty; those being water supply networks and structural trusses.

1.2 MOTIVATIONS AND OBJECTIVES OF THE PRESENT RESEARCH

In recent years, water supply networks have been the subject of much research concerning least-cost optimum design and reliability. Entropy-based applications in water supply networks have also been studied. Tanyimboh and Templeman (1993a) used the maximum entropy formalism to calculate most-likely flows in water distribution networks for which only supply and demand flows and the topology of the networks, along with pipe flow directions, are assumed be available. Other data such as lengths, diameters and roughness coefficients of the network pipes which may have been lost or may have changed over time as in the case of old water distribution networks are assumed not be available. In this case, the available information is insufficient to uniquely determine the flows in the network pipes. Physical measurements of pipe flows for such networks may be expensive and time consuming. By modelling network pipe flows probabilistically using the relative frequency interpretation of probability, Tanyimboh and Templeman (1993a) were able to develop a nodal flow entropy function of network pipes, and by maximizing it subject to equilibrium equations only they obtained a nonlinear programming model for calculating most-likely flows in water distribution networks with incomplete information. In another paper, Tanyimboh and Templeman (1993c) showed that entropy of pipe flows in water distribution networks can be used as a surrogate measure of reliability. By adding an entropy constraint to the least-cost optimum design formulation of water networks, they obtained a good compromise between cost

and reliability which is desirable in urban water distribution networks. However, the least-cost optimum design formulation for water supply networks is one of non-linear programming, and adding an entropy constraint, which is also non-linear, to the formulation makes the problem more difficult to solve and computer time consuming. Many attempts have been made in the literature to linearize the least-cost design formulation of water supply networks. The method of Alperovits and Shamir (1977) is one of them. Therefore, simplifying the problem of calculating maximum entropy flows in water networks so that it can be incorporated into such a linearized least-cost design method without inducing any extra complexity would be most beneficial. Part of the present research aims to develop a path-based method capable of estimating most-likely flows in multi-source, multi-demand general networks without requiring any mathematical programming techniques or iterative processes.

The entropy-based methods of calculating maximum entropy flows in water distribution networks mentioned so far have assumed that only supply and demand flows and the topology of the networks, along with pipe flow directions, are assumed to be available. In practical situations, however, other data such as pipe lengths and pipe diameters may also be available. Also, pressure heads at some network nodes can be measured quite cheaply and easily. Additionally, the estimated pipe flows must satisfy the conservation laws of energy around the network loops. All the above information may be available in old and inaccessible water supply networks in which only pipe characteristics and hence pipe flows are not known. The main objective of the present research is to show how such normally available information can be incorporated into one single model capable of estimating most-likely pipe flows and corresponding pipe characteristics in old water distribution networks, and to demonstrate that such a model can be used as a calibration method for calculating pipe flows and pipe characteristics for inaccessible water networks which are as close as possible to the actual values.

The second area covered in the present research is the optimum design of indeterminate structural trusses. It is well appreciated that structural trusses and water supply networks share similar characteristics in terms of pictorial representations.

Templeman (1992b) showed that such aspects of similarity can be extended almost fully to include terms such as physical quantities, constitutive equations, methods of analysis and design and even some reliability approaches. He concluded that such very close similarity between the two systems enables methods of analysis and design of structural trusses to be used in water supply networks and vice versa. An attempt is made in this thesis to design a reliable structural truss to carry maximum entropy bar axial forces calculated in a similar way to that of calculating maximum entropy flows in water networks. The resulting truss design is tested against reliability and damage tolerance approaches.

To sum up, the objectives of the research presented in this thesis are:

1. To develop a simple quick method of calculating maximum entropy flows in multi-source, multi-demand general networks without requiring mathematical programming techniques or iterative processes.
2. To produce an entropy-based inference model capable of calibrating inaccessible water supply networks in which only pipe characteristics, and hence pipe flows, are not available.
3. To apply the concept of network pipe flow entropy to structural trusses by calculating maximum entropy axial forces in truss bars, and then to obtain reliable structural trusses by designing them to carry those calculated maximum entropy bar axial forces.

1.3 LAYOUT OF THESIS

Including this introductory chapter, the thesis is divided into nine chapters. The background materials needed to understand the contents of this thesis are given in Chapters 2 and 3. In Chapter 2, Shannon's informational entropy and the maximum entropy formalism are introduced along with a review of water distribution networks concerning analysis, optimum design and reliability approaches. Applications of the maximum entropy formalism in civil engineering in general and in water distribution networks in particular are also reviewed in that chapter. In Chapter 3, analysis,

optimum design and reliability methods for structural trusses are reviewed. Also, Chapter 3 examines aspects of similarity between structural trusses and water distribution networks.

The new material presented in this thesis is distributed throughout Chapters 4 to 8. Chapter 4 introduces a path-based method of calculating maximum entropy flows in water distribution networks with incomplete information. Neither mathematical programming techniques nor iterative processes are required in the method which is illustrated in Chapter 5 by means of three sample network examples exhibiting different aspects which might be encountered in real water distribution networks. Chapters 6 and 7 are devoted to the mathematical model of calibrating inaccessible water distribution networks for which only pipe characteristics and corresponding pipe flows are not available. The theory behind the development of the calibration model is presented in Chapter 6, while applications of the model on two network examples are left to Chapter 7. Moving away from water distribution networks, Chapter 8 is an attempt to obtain a reliable structural truss by designing it to carry maximum entropy bar axial forces calculated in a similar way to that of calculating maximum entropy flows in water distribution networks. The resulting design is compared with a conventional design of the same truss by testing both designs against reliability and damage tolerance approaches.

Finally, the main conclusions of Chapters 4 to 8 and some recommendations for future work are summarized and discussed in Chapter 9. All computer programmes written to solve the new methods developed in the present research along with some sample input and output files of some illustrative examples solved by those programmes are given in the end of this thesis as appendices.

CHAPTER 2

THE MAXIMUM ENTROPY FORMALISM AND ITS APPLICATIONS IN WATER DISTRIBUTION NETWORKS

2.1 INTRODUCTION

Entropy is a known concept for scientists in the context of *classical thermodynamics* in which the entropy concept was first originated and defined as a function of some macroscopic properties which are experimentally observable such as temperature, pressure and volume. This entropy is non-probabilistic in nature and known as *classical entropy.*

In *statistical mechanics* which is concerned with the microscopic states of matter, entropy evolved further and was used in a probabilistic sense to measure the uncertainty associated with a particular micro-state. This entropy has no explicit reference to information and is known as *statistical entropy.*

It was Shannon (1948) who first used entropy in new contexts which are unrelated to thermodynamics. He related entropy to information by introducing entropy as a measure of the amount of information or uncertainty about the possible outcomes of a probabilistic experiment, enabling the information content of different probability distributions to be compared quantitatively. This kind of entropy is referred to as *informational entropy* and is described in detail shortly due to its direct relevance to the present research.

Shannon's measure of uncertainty was the inspiration which led Jaynes (1957) to his revolutionary formalism in the history of science. Before Jaynes' (1957) astonishing

paper, Shannon's entropy was merely a measure of uncertainty in a probability distribution, provided that all probabilities are known. In the case of unknown prior probabilities which in practice is often the case, Jaynes (1957) suggested using the Shannon's entropy measure in a reverse sense to infer a probability distribution which would have the maximum entropy, that is a distribution which would have the maximum information available without introducing any unconscious arbitrary assumptions about choosing some probability distribution which appears to fit the available data. This criterion is known as *the maximum entropy formalism* which is the core of the present work and is described fully in this chapter.

The maximum entropy formalism of Jaynes has opened up a wide range of applications for the Shannon entropy in all areas of civil engineering. Special attention will be given in this chapter to water distribution network applications which have recently attracted attention in tackling the difficulties associated with including reliability in water distribution designs.

In this chapter, Shannon's informational entropy is first presented along with some of its important properties. Then, the maximum entropy formalism is introduced, with a survey of its applications in civil engineering. Finally, literature on water distribution network analysis and design is reviewed, and the water distribution network entropy major applications are described.

2.2 SHANNON'S INFORMATIONAL ENTROPY

Shannon (1948) was interested in *information theory* and in particular in the ways in which information can be conveyed via a message. In his work, he needed to develop a way of measuring the levels of information or uncertainty in different probability distributions. For example, consider the probabilistic experiment of tossing a coin. If the coin is perfectly fair, the probability of obtaining a head (H) is obviously equal to the probability of obtaining a tail (T) and is equal to 0.5. Suppose now the coin is loaded such that the probability of tossing a head is 0.95, and the probability of tossing a tail is 0.05. Clearly, the first probability distribution represents more

uncertainty than the second distribution in which the result of the experiment is almost surely the head. In the first case, any prediction is very uncertain.

Furthermore, imagine a fair three-faced coin. For such a coin, it is clear that the probability of obtaining any face of its three faces in the next toss is 1/3. Comparing this experiment with that of the fair two-faced coin, the amount of uncertainty associated with the former experiment is greater than that associated with the latter one, since the chance of having the right prediction of the next toss is one-in-two for the fair two-faced coin, while the chance is one-in-three for the fair three-faced coin.

Analysing such types of experiments, Shannon (1948) raised the following question; how can the degree of uncertainty in any finite probability scheme be measured quantitatively? In this section, Shannon's entropy measure of uncertainty is presented. Some of its properties along with the well-established *Uniqueness Theorem* of the measure are given.

2.2.1 ENTROPY OF FINITE PROBABILITY SCHEMES

Before Shannon's entropy measure of uncertainty is presented, a finite probability scheme has to be defined first.

In *probability theory*, a set of events or outcomes is said to b*e mutually exclusiv*e if one, and only one, of them can occur at each trial. Also, if it happens that one of these events must occur at each trial, then the set is *exhaustive* and it represents a *complete system*. The events of such a complete system together with their corresponding probabilities form a *finite scheme*. Let us denote the events or outcomes of a finite scheme by o_i, and the corresponding probabilities by p_i, i=1,...,N, where N is the number of events or outcomes. Thus the finite scheme O is given by:

$$O = (o_i, p_i) \quad i=1,...,N \tag{2.1}$$

The probabilities of such a scheme are non-negative and satisfy the normality condition since they form a complete system. That means:

$$p_i \geq 0 \quad \forall i \tag{2.2}$$

and,

$$\sum_{i=1}^{N} p_i = 1 \tag{2.3}$$

Every probabilistic scheme has some degree of uncertainty associated with it. A scheme with probabilities (0.5, 0.5), for example, has more uncertainty than a scheme with probabilities (0.95, 0.05). Moreover, there is more uncertainty about a scheme with probabilities (1/3, 1/3, 1/3) than a scheme with probabilities (0.5, 0.5) although both of them are uniform distributions. From these types of examples Shannon (1948) extrapolated a set of desiderata which a sought measure of uncertainty must satisfy. He found that the only form which would satisfy his desiderata and therefore can be used as a general measure of uncertainty is the following function represented by a finite probability scheme:

$$S = -K \sum_{i=1}^{N} p_i \log p_i \tag{2.4}$$

where S is the entropy or amount of uncertainty; K is an arbitrary positive constant which depends on a suitable choice for the units of measure; and the logarithms can take any arbitrary but fixed base. However, natural logarithms are used throughout this thesis. Also, it is defined that 0 log 0 = 0. See Jones (1979) and Khinchin (1953) for example. Finally, the probabilities p_i which represent a finite scheme are non-negative, exhaustive, mutually exclusive and satisfy the normality condition of Eq. (2.3).

Shannon's measure of uncertainty, Eq. (2.4) , can also be regarded as a measure of information depending on the measurement being taken before or after the experiment. When an experiment is performed, the actual outcomes are known and the uncertainty concerning the results of the experiment is removed. Therefore, the information gained by the experiment is equal to the amount of uncertainty removed by performing it. Consequently, Shannon's entropy is rigorously considered as a measure of uncertainty or amount of information. See Guiasu (1977) and Kapur (1989).

2.2.2 PROPERTIES OF SHANNON'S ENTROPY

Next are presented the properties of Shannon's entropy, some of which are simply expected of a reasonable measure of uncertainty. For more details and other properties, Khinchin (1953), Guiasu (1977), Kapur and Kesavan (1987) and Kapur (1989) are the recommended references that the interested reader may consult.

1. Shannon's function $S_N(p_1,...,p_N)$ is a continuous and symmetric function provided that 0 ln 0 is always replaced by 0. Thus S is invariant when the outcomes are rearranged among themselves.
2. $S_N(p_1,...,p_N) \geq 0$

   The function takes its minimum value (0) only if one of the properties is unity and the rest of them are zero. Such a scheme obviously contains no uncertainty.
3. $S_N(p_1,...,p_N) = S_{N+1}(p_1,...,p_N,0)$

   This is expected as an impossible outcome does not affect the amount of uncertainty about any scheme.
4. $S_N(p_1,...,p_N) \leq S_N(1/N,...,1/N)$

   The function takes its maximum value when all the events are equally likely, i.e. in a scheme with uniform distribution, which agrees with one's expectation.
5. S is a monotonically increasing function of the number of outcomes N, since its maximum value is: $S_N(1/N,...,1/N) = K \ln N$.
6. The entropy function S is a concave function. Since x ln x is a well-known convex function, $\sum p_i \ln p_i$ is a convex function and $S=-\sum p_i \ln p_i$ is a concave one. Therefore, its local maximum value of K ln N is a global maximum.
7. The joint entropy of two mutually dependent schemes is the entropy of one scheme plus the conditional entropy of the other. i.e.

$$S(O_1O_2) = S(O_1) + S(O_2 \backslash O_1) = S(O_2) + S(O_1 \backslash O_2) \tag{2.5}$$

where $S(O_1O_2)$ is the joint entropy of two mutually dependent schemes O_1 and O_2 whose entropies are $S(O_1)$ and $S(O_2)$ respectively; $S(O_2\backslash O_1)$ is the conditional entropy of scheme O_2 provided that O_1 first occurs, and $S(O_1\backslash O_2)$ is the conditional entropy of O_1 given that O_2 has occurred. Defining the two finite schemes O_1 and O_2 as: $O_1 = (o_i, p_i)\ \forall i$, and $O_2 = (o_j, p_j)\ \forall j$, the conditional

entropy $S(O_2\backslash O_1)$ is given by:

$$S(O_2\backslash O_1) = -K \sum_i p(o_i) \sum_j p(o_j\backslash o_i) \ln p(o_j\backslash o_i) \qquad (2.6)$$

in which $p(o_i)$ is the probability of event o_i in the scheme O_1 and $p(o_j\backslash o_i)$ is the conditional probability of event o_j in the scheme O_2 given that event o_i in the scheme O_1 has occurred.

Eq. (2.5) shows that the interchange of the positions of two schemes has no effect on the joint entropy of these two schemes. In the case of two mutually independent schemes, it is obvious that:

$$S(O_2\backslash O_1) = S(O_2) \qquad (2.7a)$$

and,

$$S(O_1\backslash O_2) = S(O_1) \qquad (2.7b)$$

since each scheme has no effect on the occurrence of the other. Therefore:

$$S(O_1O_2) = S(O_1) + S(O_2) \qquad (2.8)$$

This means that the joint entropy of two mutually independent schemes is the sum of their separate entropies.

The above properties of Shannon's entropy are actually the requirements which any reasonable measure of uncertainty has to satisfy. They stem from the actual meaning of the concept of uncertainty. However, Shannon's entropy is the only possible function to satisfy these properties. (See Khinchin (1953) for example). Its uniqueness is stated next as a theorem.

2.2.2.1 THE UNIQUENESS THEOREM

Let $S_N(p_1,...,p_N)$ be a function defined for any integer N and all values of p_i , i=1,...,N, are non-negative and satisfy the normality condition of Eq. (2.3). Suppose this function has the following properties:

1. $S_N(p_1,...,p_N)$, $\forall N$, is a continuous function with respect to all its arguments.
2. For a given N and for $\Sigma\ p_i = 1$, i=1,...,N, S_N takes its largest value for $p_i=1/N$, i=1,...,N.
3. $S(O_1O_2) = S(O_1) + S(O_2\backslash O_1)$.
4. $S_N(p_1,...,p_N) = S_{N+1}(p_1,...,p_N,0)$.

The only possible function to satisfy the above requirements is the entropy function of Shannon which has the form:

$$S = -K \sum_{i=1}^{N} p_i \ln p_i \qquad (2.4)$$

where K is an arbitrary positive constant.

The proof of the above theorem is in no way necessary for the present research. However, details can be found elsewhere. See Khinchin (1953) for example.

2.3 THE MAXIMUM ENTROPY FORMALISM

Consider a random variable x which may take several discrete values x_i, i=1,...,N, in a random process. Suppose the probability that x has the value x_i, i=1,...,N, i.e. $p_i=p(x=x_i)$ cannot be determined by the available information about the process under examination. What is the best estimate of such probabilities and how can they be found?

An early attempt to solve this problem was Laplace's Principle of *insufficient reason* in which two events are to be considered equally likely if there is no reason to think otherwise. Therefore, the uniform probability distribution should be adopted if there is no other distribution which can be justified.

Unfortunately, Laplace's Principle does not help a situation in which there are reasons for thinking otherwise, i.e. in a situation where the uniform distribution does not fit because of the presence of some information which might be available about the process being considered. Such information may be things like the mean and standard

deviation of the x_i, $\forall i$, and may take the form:

$$\sum_{i=1}^{N} p_i \, Fn_{ji}(x) = \langle Fn_j \rangle \quad j=1,...,NEC \tag{2.9}$$

where $\langle Fn_j \rangle$, $\forall j$, is the expected value of the function $Fn_{ji}(x)$, $\forall i$, and NEC is the number of the expectation constraint functions. These NEC constraints together with the axiomatic normality condition constraint of Eq. (2.3) are assumed to be less than the number of p_i, i=1,...,N, i.e. NEC+1<N so that there are many distributions which will fit the available information (Eqs. (2.3) and (2.9)). Which of these distributions should be selected and why?

Jaynes (1957) recognized that every probability distribution which fits the available information has a different value of Shannon's entropy. Since entropy is a measure of uncertainty, a distribution which has the maximum value of entropy within the limitation of the available information must have maximum uncertainty, must be maximally noncommittal to missing information and must contain minimum bias. Jaynes stated:

> "In making inference on the basis of partial information we must use that probability distribution which has maximum entropy subject to whatever is known. This is the only unbiased assignment we can make; to use any other would amount to arbitrary assumption of information which by hypothesis we do not have."

Mathematically, the above selection criterion, which is known as the maximum entropy formalism, is equivalent to maximizing Shannon's entropy function of Eq. (2.4) subject to the given information of Eqs. (2.3) and (2.9). i.e.

Problem 1

$$\textit{Maximize} \quad S/K = -\sum_{i=1}^{N} p_i \ln p_i \quad \forall p_i \tag{2.4}$$

Subject to:

$$\sum_{i=1}^{N} p_i = 1 \tag{2.3}$$

$$\sum_{i=1}^{N} p_i \, Fn_{ji}(x) = \langle Fn_j \rangle \quad j=1,...,NEC \tag{2.9}$$

$$p_i \geq 0 \quad i=-1,...N \tag{2.2}$$

Problem 1 is the classical maximum entropy problem. Its analytical solution can be found by examining the stationarity of its Lagrangean and is:

$$p_i = \frac{\exp\left[\sum_{j=1}^{NEC} \mu_j \, Fn_{ji}\right]}{\sum_{i=1}^{N} \exp\left[\sum_{j=1}^{NEC} \mu_j \, Fn_{ji}\right]} \quad i=1,...,N \tag{2.10}$$

in which μ_j, j=1,...NEC, are the Lagrange multipliers associated with the expectation constraints, Eq. (2.9) in Problem 1. However, the Lagrange multipliers μ_j, j=1,..., NEC, in Eq. (2.10) are unknown and have to be calculated first if the maximum entropy probabilities of Eq. (2.10) are to be determined. This can be done by substituting Eqs. (2.10) back into the expectation constraints of Eqs. (2.9) in Problem 1, and solving the NEC non-linear equations for the NEC Lagrange multipliers. Then, the maximum entropy probabilities of Eqs. (2.10) can be calculated. This is rather awkward and tedious. However, Templeman and Li (1985) showed how the Lagrange multipliers in Eqs. (2.10) may be determined more easily by realizing that Problem 1 is a *convex programming problem* and it should have a dual form of an unconstrained minimization problem which may be easier to solve directly than Problem 1. Consequently, they were able to calculate the Lagrange multipliers by solving the dual unconstrained minimization problem very easily using a standard library subroutine for unconstrained nonlinear programming. It should be noted that the resulting maximum entropy distribution of Eq. (2.10) is a unique global maximum point for Problem 1 due to the convexity of the problem.

2.3.1 INTERPRETATIONS BEHIND THE MAXIMUM ENTROPY FORMALISM

The maximum entropy formalism may be regarded as an extension of Laplace's principle of insufficient reason in which there is no information given about a probability scheme except that all the probabilities sum to unity. In such a case, maximizing the entropy subject to the normality condition only results in a uniform probability distribution which concurs with the principle of insufficient reason. However, the maximum entropy distribution is uniquely determined by virtue of the positive reason of being maximally noncommittal to missing information, instead of the negative one that there was no reason to think otherwise.

Moreover, any gain in information leads to an extra constraint in the maximum entropy formalism and consequently reduces the entropy value of the system. Conversely, any gain in entropy means loss of information.

Finally, the maximum entropy formalism has the potential power of discovering some physical laws that are yet undiscovered. Jaynes (1979) argued that if the actual probability distribution of a probabilistic experiment departs from the maximum entropy prediction, then there must exist another new constraint beyond that used in the calculation. Thus the maximum entropy formalism brings out the physics by showing that some constraints have been ignored, and if such constraints are unknown the maximum entropy formalism has the property of discovering them.

2.4 THE CONTINUOUS CASE OF THE MAXIMUM ENTROPY FORMALISM

In a situation of a continuous random process, the maximum entropy formalism is still applicable. However, an integral over the continuous domain should replace the summations and probability density functions must be used instead of the discrete probabilities. Therefore, the continuous case of the maximum entropy formalism has the following form:

$$\textit{Maximize} \quad S/K = -\int_a^b f(x) \ln (f(x))\, dx \quad \forall f(x) \tag{2.11}$$

Subject to:

$$\int_a^b f(x)\, dx = 1 \tag{2.12}$$

$$\int_a^b Fn_j(x)\, f(x)\, dx = \langle Fn_j \rangle \quad j=1,...,NEC \tag{2.13}$$

in which x is a continuous random variable; $\langle Fn_j \rangle$, $\forall j$, is the expected value of the function $Fn_j(x)$; and f(x) is a probability density function.

The continuous entropy formula of Eq. (2.11) is defined in terms of a probability density function, so it may not be invariant under variable transformation. Moreover, the continuous entropy, when $N \rightarrow \infty$, is strictly not the limit of the discrete entropy whose properties therefore can not be extended to the continuous case. However, the solution of the continuous maximum entropy formalism can be obtained following the same process as for the discrete case, but this is not considered here since this research is concerned with discrete probabilities only.

2.5 APPLICATIONS OF THE MAXIMUM ENTROPY FORMALISM IN CIVIL ENGINEERING

The maximum entropy formalism has been used in applications of many areas of science and engineering due to its simplicity and efficiency of generating solutions to a wide range of problems where the available information is not complete. Only applications in civil engineering areas, some of which were surveyed by Templeman (1992a, 1993), are presented here, while other applications from widely different fields can be found in a reference such as Levine and Tribus (1979) for example. However, the use of entropy in optimization processes is mentioned here due to its general significance, while water supply network applications are left to the next section because of their close relevance to the present research.

Li (1987) and Templeman and Li (1987, 1989) have used the maximum entropy formalism in optimization processes in an attempt to develop a radically different method of solving constrained nonlinear programming problems in order to match the sophistication of nonlinear engineering design applications. They looked at the problem in a probabilistic context and incorporated the principle of the maximum entropy into the process to improve convergence towards the optimum solution. Such an entropy-based approach was used by Li and Templeman (1988) in optimum truss sizing problems and was found to be very effective and encouraging to use in more difficult structural optimization problems.

In a more obvious application of the maximum entropy formalism, Basu (1981) and Basu and Templeman (1984, 1985) used the formalism to fit available probabilistic data. They argued that fitting different probability distributions to probabilistic data in most engineering problems is based on an *ad hoc* selection criteria which introduce bias into the calculations. In the 1984 paper, they showed that over a wide range of different distributions the maximum entropy distribution was the nearest to the actual distribution being examined. In the second paper, they estimated the failure probability of a structure by using the maximum entropy probability distribution to represent random loads and strengths in structural reliability analysis. They demonstrated that such an entropy-based approach produced a more logical and rigorous method to generate accurate failure probabilities, casting doubt upon the conventional treatment of structural reliability.

In another application, decision-making analysis is the key process in any productive industry regarding the uncertainty associated with future orders. Thus, the evaluation of prior probabilities for such orders should be made objectively and should not be affected by any personal bias. Munro and Jowitt (1978) realized this fact and used therefore the maximum entropy formalism in the ready-mixed concrete industry to estimate the least biased probability distribution associated with the orders for each mix. They showed the ability of the entropy-based method to reproduce the common sense decisions associated with simple examples and continue to make consistent judgements when common sense decision-making becomes more difficult.

Traffic engineering has attracted many entropy-based applications concerning the estimation of the origin-destination matrix or the so-called trip matrix from limited data. A typical transportation problem is to minimize the total travelling cost between origins and destinations subject to available information about the total flows leaving and entering each origin and destination respectively. Erlander (1977) added an entropy constraint to the problem in order to preserve a desired level of accessibility between all origins and destinations. He stated that a network with a low value of entropy has a low level of accessibility, and vice versa. Also, Van Zuylen and Willumsen (1980) and Bell (1983) used entropy to estimate the most probable set of origin-destination movements that are consistent with available information. Van Zuylen and Willumsen (1980), however, developed two models, the first of which was to realize the trip matrix in the most number of ways by maximizing the entropy of the trip movements, and the second was to minimize the information content of a limited number of observations on the road network. A similar approach has been used to estimate turning flows at road junctions. Mountain et al. (1983a, 1983b, 1986a, 1986b) showed that the entropy-based approach leads directly to the *gravity model* which is well known in roundabout turning flow problems.

Finally, entropy applications have reached open channel flow studies. In a sequence of papers, Chiu (1987, 1988, 1989, 1991) has used the maximum entropy formalism in modelling the distributions of the velocity, shear stress and suspended sediment concentration in open channel flows. He argued that the uncertainties surrounding these distributions which are due to the inherent randomness and man's ignorance can be overcome by maximizing their individual probability density function entropies subject to some conservation laws and others which govern fluid motion in open channels.

Clearly, the above applications and others show that the maximum entropy formalism can be used to generate solutions to wide problems where the available information is not complete and is not directly concerned with probability distributions either.

2.6 ENTROPY APPLICATIONS IN WATER DISTRIBUTION NETWORKS

In recent years the role of entropy in the analysis and design of water distribution networks has been the subject of much research. Its participation may be classified into two main areas, first as a method of estimating the most likely pipe flow rates in looped water networks, where the available data is insufficient to uniquely determine the pipe flows, and second as a surrogate measure of reliability.

The problem of not having enough information to determine the unique pipe flow rates may occur in buried old networks where much of the information may be lost or may have changed over time. Also, a physical measurement of the pipe flow rates of such networks may be expensive and time consuming. Therefore, the behaviour of the system in buried networks contains uncertainty which is not in the physical system itself but in the inability of the engineer to determine uniquely that behaviour due to the lack of some needed information. The presence of such uncertainty makes a possible role for the maximum entropy formalism to play. This role is described fully in this section due to its relevance to the present work.

The second area, the issue of reliability, is very important in urban water distribution networks. However, there is no comprehensive definition of this reliability in the literature because of its complexity and because of some uncertainty surrounding it. This uncertainty comes from the fact that reliability in water distribution networks is connected with issues naturally centring around uncertainty. Such issues are component failures, durations of their repairs or replacements, sufficiency of pressure, variations in demands and supplies, etc. Again, this uncertainty invokes an opportunity for entropy to play a part in the reliability of water networks. In this section, a review of entropy applicability as a surrogate measure of reliability in water networks is presented, and how such a measure could be incorporated in the optimum design of water networks is described. Before that, are briefly reviewed, some conventional methods of analysis and design of optimum water distribution networks along with the constitutive equations which govern the motion of water in networks.

2.6.1 OPTIMUM DESIGN OF WATER DISTRIBUTION NETWORKS

The optimum design of water networks presented here is for general networks in which the layout and external flows, including the direction of flow in each link, are specified and the length and the roughness coefficient of each pipe are known. The objective function of the problem is the least capital cost of a pipe network, and the constraints are the constitutive equations and some other constraints arising from practical considerations. Before the least capital cost design problem is stated, the constitutive equations are presented and the most common method of analysis is described.

2.6.1.1 CONSTITUTIVE EQUATIONS

These include the head loss equations for each pipe, the flow equilibrium equations at each node and the loop and path equations for the conservation of energy. However, the effects of pumps and valves on those equations are not considered here.

2.6.1.1.1 HEAD LOSS EQUATIONS

The head loss in pipes is defined as the energy loss per unit weight. This is caused by frictional resistance of pipe walls to the fluid motion and due to the viscosity of the fluid. It also occurs due to bending or changing of the cross-section of the pipes. Only frictional head losses are considered here. The most practical approximation of friction head loss is the Hazen-Williams equation which is used throughout this thesis and is given by:

$$h_{ij} = \frac{\alpha \; Le_{ij} \left(\frac{q_{ij}}{C_{ij}}\right)^{1.852}}{D_{ij}^{4.87}} \quad \forall ij \in IJ \tag{2.14}$$

in which h_{ij} and q_{ij} are, respectively, the head loss and the flow rate in pipe ij which both are positive in the direction of flow; α is a dimensionless conversion factor for units (α=10.67 in S.I. units); Le_{ij}, D_{ij} and C_{ij} are the length, the internal diameter and the Hazen-Williams coefficient of pipe ij respectively; and IJ is the the set of all the

links in the network.

Other equations may be used for head losses such as the Darcy-Weisbach equation which needs some iterative scheme in its calculations. See Jeppson (1976) for more details.

2.6.1.1.2 CONTINUITY EQUATIONS

All the inflows and outflows at each node must be in an equilibrium state. i.e.

$$\sum_{j \in NU_n} q_{jn} - \sum_{k \in ND_n} q_{nk} = q_n \quad n=1,...,NN \tag{2.15}$$

where NN is the total number of nodes, NU_n is the set of the upstream nodes of all internal inflows at node n, and ND_n is the set of the downstream nodes of all internal outflows at node n. In the above equations, q_n is the external flow at node n, $\forall n$, which is a supply for a positive value and a demand for a negative value.

It should be noted that only the first (NN-1) continuity equations of Eqs. (2.15) are required for analysis since the continuity at the last node will automatically be satisfied if all external inflows and outflows are known and are in balance.

2.6.1.1.3 ENERGY CONSERVATION EQUATIONS

2.6.1.1.3.1 LOOP EQUATIONS

The net head loss around each loop in a pipe network should be equal to zero. Therefore:

$$\sum_{ij \in IJ_l} h_{ij} = 0 \quad l=1,...,NLP \tag{2.16}$$

in which IJ_l is the set of all links in loop l and NLP is the number of loops which must satisfy the following equation:

$$NLK = NN + NLP - 1 \tag{2.17}$$

where NLK is the number of links in the network.

2.6.1.1.3.2 PATH EQUATIONS

If the heads at any two nodes in a network are known, then the total head loss along any path between these two nodes must equal the difference between their heads, which is usually known as path head loss. Thus:

$$\sum_{ij \in IJ_p} h_{ij} = h_p \quad p=1,...,NP \tag{2.18}$$

in which IJ_p is the set of all links in path p, $\forall p$; h_p is the known path head loss; and NP is the number of paths whose head losses are known and must satisfy the following equation:

$$NP \leq NN - 1 \tag{2.19}$$

It must be noted that a path may contain one link only. Also, the NP paths must be chosen so that equations (2.18) are linearly independent, i.e. each path must have some information which is not already contained in any other path.

2.6.1.2 WATER NETWORK FLOW ANALYSIS

The analysis problem is to estimate the pipe flow rates in a network whose pipe lengths, diameters and roughness characteristics are known and the external flows are specified. However, there are many methods to solve this problem, and the most commonly-used one is the Hardy-Cross method which is described next.

2.6.1.2.1 HARDY-CROSS METHOD

In this method initial flow rates must be chosen first for all the pipes in the network and they must satisfy the continuity equations (2.15). Then the current flow rates are

corrected in each loop sequentially so that:

$$q_{ij}^{(n)} = q_{ij}^{(n-1)} + \Delta q_l^{(n)} \quad \forall l, \forall ij \in IJ_l \tag{2.20}$$

in which $q_{ij}^{(n-1)}$ is an estimated flow rate; $\Delta q_l^{(n)}$ is a correction to be applied to all link flows in loop l; $q_{ij}^{(n)}$ is the corrected flow rate; and n is an iteration number.

To calculate $\Delta q_l^{(n)}$ which is needed for corrections, the head loss equations (2.14) are reconstructed as:

$$h_{ij}^{(n)} = \frac{\alpha \, Le_{ij} \, [q_{ij}^{(n-1)} + \Delta q_l^{(n)}]^{1.852}}{C_{ij}^{1.852} \, D_{ij}^{4.87}} \quad \forall l, \forall ij \in IJ_l \tag{2.21}$$

and the loop equations (2.16) as:

$$\sum_{ij \in IJ_l} h_{ij}^{(n)} = 0 \quad \forall l \tag{2.22}$$

which can be reconstructed as:

$$\Delta q_l^{(n)} = \frac{-\sum_{ij \in IJ_l} h_{ij}^{(n-1)}}{1.852 \sum_{ij \in IJ_l} \frac{h_{ij}^{(n-1)}}{q_{ij}^{(n-1)}}} \quad \forall l \tag{2.23}$$

in which:

$$h_{ij}^{(n-1)} = \frac{\alpha \, Le_{ij} \, (q_{ij}^{(n-1)})^{1.852}}{C_{ij}^{1.852} \, D_{ij}^{4.87}} \tag{2.24}$$

The resulting value of $\Delta q_l^{(n)}$ of Eq. (2.23) can then be used in Eq. (2.20) to estimate new flow rates. Correcting all flow rates in all loops completes one iterative cycle. The above process is repeated again by correcting each loop in turn until the magnitudes of all loop corrections become very small.

Although the method is very time consuming especially for a network with many loops since it corrects the flow rates in the loops sequentially rather than simultaneously, it is very simple and is used in this thesis. Other methods exist but are not presented here, such as the Linear Theory method which was developed by Wood

and Charles (1972) and the Newton-Raphson method (Martin and Peters, 1963). See Shamir and Howard (1968) for examples.

2.6.1.3 WATER NETWORK LEAST COST DESIGN FORMULATION

The least capital cost design of a pipe network described here is for general networks having the layout and external flows including flow directions in the links prespecified and the lengths and roughness coefficients of the pipes known. The formulation consists of minimizing the capital cost of the pipes subject to the constitutive equations presented earlier and to other practical constraints which are presented later. The variables in this formulation are the diameters of the pipes, the flow rates and hence the corresponding head losses in the links.

2.6.1.3.1 COST OBJECTIVE FUNCTION

The objective function considered here is the capital cost of the pipes only and may be expressed in several forms including:

$$C = \gamma \sum_{ij \in IJ} Le_{ij} D_{ij}^{e_1} \qquad (2.25)$$

in which C is the total cost of pipes; γ is a coefficient which depends on the units of D_{ij}; and e_1 is an empirical coefficient.

2.6.1.3.2 PRACTICAL CONSTRAINTS

These include flow velocity constraints, nodal pressure constraints, pipe diameter constraints and non-negativity of flow constraints.

1. Flow velocity constraints:

$$v_{min} \le v_{ij} = \frac{4q_{ij}}{\pi D_{ij}^2} \le v_{max} \quad \forall ij \in IJ \qquad (2.26)$$

where v_{ij} is the flow velocity in pipe ij; and v_{max} and v_{min} are respectively the

maximum and minimum velocities allowed in the links.

2. Nodal pressure constraints:

$$H_{\min,n} \leq H_n = H_s - \sum_{ij \in IJ_n} h_{ij} \leq H_{\max,n} \quad \forall n \tag{2.27}$$

in which H_s is the head pressure at source s; IJ_n is the set of all links along a selected path from source s to node n; and $H_{max,n}$ and $H_{min,n}$ are respectively the maximum and minimum heads allowed at node n.

3. Pipe diameter constraints:

$$D_{\min} \leq D_{ij} \in D_D \leq D_{\max} \quad \forall ij \in IJ \tag{2.28}$$

in which D_D is the set of commercially available discrete pipe diameters; and D_{max} and D_{min} are respectively the maximum and minimum diameters allowed in the network.

4. Non-negativity of flows:

$$q_{ij} \geq 0 \quad \forall ij \in IJ \tag{2.29}$$

Having defined the objective function and the constraints which are to be satisfied in the design, the following formulation of the least capital cost of a pipe network can now be constructed as Problem 2 with some of the constraints rearranged.

Problem 2

$$\textit{Minimize} \quad C = \gamma \sum_{ij \in IJ} Le_{ij} D_{ij}^{e_1} \quad \forall D_{ij} \tag{2.25}$$

Subject to:

$$h_{ij} = \frac{\alpha \; Le_{ij} \left(\frac{q_{ij}}{C_{ij}}\right)^{1.852}}{D_{ij}^{4.87}} \quad \forall ij \in IJ \tag{2.14}$$

$$\sum_{j \in NU_n} q_{jn} - \sum_{k \in ND_n} q_{nk} = q_n \quad n=1,...NN-1 \tag{2.15}$$

$$\sum_{ij \in IJ_l} h_{ij} = 0 \quad l=1,...,NLP \tag{2.16}$$

$$\sum_{ij \in IJ_p} h_{ij} = h_p \quad p=1,...,NP \tag{2.18}$$

$$\frac{\pi \; v_{\min}}{4} \leq \frac{q_{ij}}{D_{ij}^2} \leq \frac{\pi \; v_{\max}}{4} \quad \forall ij \in IJ \tag{2.30}$$

$$H_s - H_{\max,n} \leq \sum_{ij \in IJ_n} h_{ij} \leq H_s - H_{\min,n} \quad \forall n \tag{2.31}$$

$$D_{\min} \leq D_{ij} \in D_D \leq D_{\max} \quad \forall ij \in IJ \tag{2.28}$$

$$q_{ij} \geq 0 \quad \forall ij \in IJ \tag{2.29}$$

Problem 2 is formulated as one of non-linear constrained optimization and can be solved by any standard constrained non-linear programming algorithm assuming that the pipe diameters are continuous-valued, i.e. relaxing the discreteness constraint of Eq. (2.28). However, from a practical point of view, the diameter variables should be obtained as discrete values and must be chosen from a set of discrete sizes representing commercially available pipes. Yates, Templeman and Boffey (1984) showed that this requirement makes Problem 2 extremely difficult to solve.

Consequently, they suggested that good approximate solution methods should be sought rather than attempting to solve Problem 2 directly. Many attempts have been made to simplify Problem 2, and the Linear Programming Gradient method (Alperovits and Shamir, 1977) and the method of Quindry, Brill and Liebman (1981) are considered the main two approaches used in the literature for solving Problem 2. However, these methods and others have no relevance to the present work, and therefore they are not described here. The interested reader may consult the two papers mentioned above for details.

Finally, it should be noted that Problem 2 is formulated for one demand pattern. However, it can be easily formulated for multiple demand patterns by including a set of constraints for each demand pattern in turn. Obviously, the multiplicity of demand patterns makes Problem 2 more difficult to solve.

Having presented some methods of analysis and design of optimum water distribution networks, the maximum entropy flows in water networks are described next, followed by reviewing entropy as a surrogate measure of reliability.

2.6.2 MAXIMUM ENTROPY FLOWS IN WATER DISTRIBUTION NETWORKS

Consider the case of a buried water network in which much of the information needed to uniquely determine the pipe flow rates is missing. Such information are lengths, diameters of pipes and roughness properties which are assumed not to be available. However, source flow rates, demand flow rates and the topology of the network with arc flow directions are assumed to be known. Under these circumstances, how can the most likely pipe flow rates in the network be estimated?

Suppose this network has NLK links connecting NN nodes. Therefore, there are NLK unknowns, those being the flow rates in all NLK links. Also, it can be recalled from the previous subsection that there are NN-1 independent continuity equations which relate those NLK unknowns together. If the network has no loops, i.e. is a branched

network, then Eq. (2.17) shows that the number of unknowns equals NN-1 with NLP, the number of loops, equal to zero. Therefore, in such a case, the available NN-1 continuity equations are sufficient to determine uniquely the NN-1 pipe flow rates in the system. In general, water distribution networks are looped, in which case there are NN-1 equations with NN+NLP-1 unknowns [Eq. (2.17)], i.e. there are more unknowns than continuity equations available and, consequently, there are many possible flow rate distributions which satisfy those available equations. The maximum entropy formalism of Jaynes (1957), described earlier in this chapter, suggests choosing the distribution which has the maximum entropy value and satisfies the available information. The hurdle arising here is how pipe flow rates in a network can be expressed in a probabilistic way as required by Shannon's entropy and hence by the maximum entropy formalism. In this subsection, entropy functions for a flow network suggested by Awumah et al. (1990, 1991) are presented first, followed by those developed by Tanyimboh and Templeman (1993a) which are found to be rigorous and therefore are chosen to be the basis from which the entropy formulations of a network developed in this thesis are derived. Then, the maximum entropy flows in a network calculated by Tanyimboh and Templeman (1993a) are described and their relevance to the present work is highlighted. Finally, a path-based approach for calculating maximum entropy flows in single-source networks is presented.

2.6.2.1 FLOW ENTROPY FUNCTIONS OF AWUMAH, GOULTER AND BHATT

In an attempt to cast pipe flow rates in a water distribution network in a probabilistic form as required by Shannon's entropy, Awumah, Goulter and Bhatt (1990, 1991) started investigating the flows in links incident on a node n. They argued that the probability quantities in Shannon's entropy function of Eq. (2.4) may be regarded as the fractions of total flows into node n carried by each link incident on that node. Therefore, the following function could be used as an entropy measure of node n in a network after setting K in Eq. (2.4) to unity:

$$S_n = -\sum_{j \in NU_n} \frac{q_{jn}}{Q_n} \ln \frac{q_{jn}}{Q_n} \quad \forall n \tag{2.32}$$

in which S_n is the entropy of node n,$\forall$n; NU_n, $\forall$n, represents the upstream nodes of link inflows at node n; q_{jn} is the flow in link jn, $\forall j \in NU_n$; and Q_n is the sum of the link flows entering node n and is given by:

$$Q_n = \sum_{j \in NU_n} q_{jn} \quad \forall n \tag{2.33}$$

Awumah et al. (1990, 1991) then expanded Eq. (2.32) to the whole network. They argued that, in order to derive an entropy function for the whole network, it is important, regarding the overall network performance, to replace Q_n by Q_0, which is the sum of the flows in all the links in the network, before summing up the entropies of all the nodes in the network together. Therefore, the entropy of the network may be given by the following formula:

$$S = \sum_{n=1}^{NN} \left(\sum_{j \in NU_n} \frac{q_{jn}}{Q_0} \ln \frac{q_{jn}}{Q_0} \right) \quad \forall n \tag{2.34}$$

in which S is the entropy of the network; NN is the number of nodes in the network; and Q_0 is given by:

$$Q_0 = \sum_{ij \in IJ} q_{ij} \tag{2.35}$$

in which IJ is the set of all the links in the network.

Eq. (2.34) is the basic entropy formula from which all the modified entropy functions used by Awumah et al. (1990, 1991, 1992) have been derived.

It should be noted that the probability-like quantities, (q_{jn}/Q_0), $\forall j \in NU_n, \forall n$, used in Eq. (2.34) are not mutually exclusive as the flow in a link exiting node n is dependent on the flow in a link incident on that node. This violates the basic requirement of Shannon's entropy and, therefore, Eq. (2.34) is not rigorously formulated.

However, Awumah et al. (1990, 1991) transformed Eq. (2.34) into another function by substituting (q_{jn}/Q_0) by $(q_{jn}Q_n)/(Q_nQ_0)$ without changing it. The transformed equation is therefore (see Awumah et. al (1990) for the derivation):

$$S = \sum_{n=1}^{NN} \frac{Q_n}{Q_0} S_n - \sum_{n=1}^{NN} \frac{Q_n}{Q_0} \ln \frac{Q_n}{Q_0} \tag{2.36}$$

in which S_n is the entropy of node n and is given by Eq. (2.32).

Some attempts have been made by Awumah et al. (1990, 1991) to modify Eq. (2.32). In the first paper, Awumah et al. (1990) realized that the entropy of a node n given by Eq. (2.32) treats the node n in isolation without considering the connectivity of that node to the rest of the network. They argued that the number of alternate paths from a source to a demand node passing through each link incident on that demand node should be accounted for. Therefore, they introduced the following function:

$$S_n = -\sum_{j \in NU_n} \frac{q_{jn}}{Q_n} \ln \frac{q_{jn}}{a_{jn} Q_n} \quad \forall n \tag{2.37}$$

in which $a_{jn}, \forall j \in NU_n, \forall n$, is the effective number of independent paths to node n through link jn, and is given by:

$$a_{jn} = npt_{jn} \left[1 - \frac{\sum_{k=1}^{nl_{jn}} (d_k - 1)}{\sum_{k=1}^{nl_{jn}} d_k}\right] \quad \forall n, \forall j \in NU_n \tag{2.38}$$

in which $npt_{jn}, \forall n, \forall j \in NU_n$, is the number of dependent or independent paths to node n through the link jn; nl_{jn}, $\forall n$, $\forall j \in NU_n$, is the number of links in the npt_{jn} paths; d_k is the number of paths in which link k is a member.

In the second paper, Awumah et al. (1991) presented another approach to modify Eq. (2.32) by considering the transmissivity of entropy from one node to another which is immediately downstream to it. They approximated this transmissivity by the ratio of the flow entering the downstream node from its immediate upstream node to the total flow entering that upstream node. i.e.

$$t_{nj} = \frac{q_{jn}}{Q_j} \quad \forall n, \forall j \in NU_n \tag{2.39}$$

in which t_{nj}, $\forall n$, $\forall j \in NU_n$, is the transmissivity from node j to node n. Therefore, Eq. (2.32) can be extended to include this transmissivity parameter as follows:

$$S_n' = S_n + \sum_{j \in NU_n} t_{nj} S_j' \quad \forall n \tag{2.40}$$

in which S_n' is the modified entropy of node n; S_j' is the modified entropy of node j, $\forall j \in NU_n$. Therefore, to calculate the modified entropy of any node, the modified entropy of its all upstream nodes must be calculated first.

Finally, it may be noted that all nodal entropy functions presented so far have been defined in terms of link inflows only. No consideration was given to the outflow links which may become inflow links to the node being considered in the event of a link failure. Obviously, this may only happen to outflow links which are part of a loop since flow reversal cannot occur in a link which does not belong to a loop. To allow for such a situation, Awumah et al. (1990) expanded Eq. (2.37) to the following equation:

$$S_n^{\sim} = -\sum_{j \in NU_n} \frac{q_{jn}}{Q_n^{\sim}} \ln \frac{q_{jn}}{a_{jn} Q_n^{\sim}} - \sum_{k \in NDL_n} \frac{q_{nk}}{Q_n^{\sim}} \ln \frac{q_{nk}}{a_{nk} Q_n^{\sim}} \quad \forall n \tag{2.41}$$

in which $S_n^{\sim}$ is the new entropy of node n, $\forall n$; NDL_n is the set of all nodes immediately downstream of the node n,$\forall n$, which belong to a loop containing node n; $Q_n^{\sim}$ is the total of all flow leaving and entering node n from the set of nodes NU_n and to the set of nodes NDL_n respectively. i.e.

$$Q_n^{\sim} = \sum_{j \in NU_n} q_{jn} + \sum_{k \in NDL_n} q_{nk} \quad \forall n \tag{2.42}$$

The above Eqs. (2.37), (2.40) and (2.41) can then be substituted for S_n in the basic function of Eq. (2.36) to obtain the entropy of the network. It will be recalled here that Eq. (2.34) is questionable as it is based on probability-like quantities which are not mutually exclusive. Since Eq. (2.36) is equivalent to Eq. (2.34), therefore, all the

entropy functions presented earlier are not rigorously founded. Also, the quantities (Q_n/Q_0) used in Eq. (2.36) are not probabilities as there is double counting in Q_0. This makes Eq. (2.36) incorrect theoretically from an entropy viewpoint. Moreover, the entropy functions of Awumah, Goulter and Bhatt do not directly account for the external inflows and outflows in the network. Although the external inflows and outflows may be known, they have to be considered in entropy functions because of the uncertainty surrounding the contributions of the source supply at each node to the total flow reaching that node, and also surrounding the contributions of the total inflow to satisfy abstraction at a demand node. Tanyimboh and Templeman (1993a) realized the above weaknesses and proposed alternate and more rigorous flow entropy functions which are presented next.

2.6.2.2 FLOW ENTROPY FUNCTIONS OF TANYIMBOH AND TEMPLEMAN

In general looped water networks, the flow entering or leaving node n, $\forall n$, by link jn, $\forall j \in NU_n$ or link nk, $\forall k \in ND_n$, respectively, depends on whether or not flow has reached the node n. In other words, the probability of the flow entering node n, $\forall n$, by link jn, $\forall j \in NU_n$, and the probability of the flow leaving node n, $\forall n$,by link nk, $\forall k \in ND_n$, are both conditional upon the probability that flow has reached that node n. Therefore, the conditional entropy formula of Khinchin (1953), which was presented earlier in this chapter as Eq. (2.6), has to be used if the entropy of node n in a network is to be defined. Tanyimboh (1993) and Tanyimboh and Templeman (1993a) realized the above fact and used a multiple probability space to formulate a rigorous entropy function for general water distribution networks in which each node must have either an external inflow or outflow. They introduced two conditional finite probability schemes for each node representing respectively the flow entering and leaving node n, $\forall n$, as follows:

$$p_{jn} = \frac{q_{jn}}{T_n} \quad \forall n,\ \forall j \in NU_n \tag{2.43}$$

$$p_{nk} = \frac{q_{nk}}{T_n} \quad \forall n,\ \forall k \in ND_n \tag{2.44}$$

where p_{jn} is the conditional probability that flow, which is destined to reach node n, $\forall n$, uses link jn, $\forall j \in NU_n$; p_{nk} is the conditional probability that flow, which is destined to pass through node n, $\forall n$, is included in q_{nk}, $\forall k \in ND_n$; T_n represents the total flow reaching or leaving node n, $\forall n$, i.e.

$$T_n = \sum_{j \in NU_n} q_{jn} = \sum_{k \in ND_n} q_{nk} \quad n=1,...,NN \tag{2.45}$$

It should be noted that NU_n and ND_n used in Eqs. (2.43), (2.44) and (2.45) include respectively any external inflow and outflow. Defining q_{0n} and q_{n0} being respectively the external inflow and outflow at node n, $\forall n$, then Eqs. (2.43) and (2.44) respectively include the following probabilities:

$$p_{0n} = \frac{q_{0n}}{T_n} \quad \forall n \in I_s \tag{2.46}$$

$$p_{n0} = \frac{q_{n0}}{T_n} \quad \forall n \in I_D \tag{2.47}$$

in which I_s and I_D respectively are the sets of source nodes and demand nodes in the network; p_{0n}, $\forall n \in I_s$, is the probability that a source node receives its total inflow T_n from its external inflow q_{0n}; p_{n0}, $\forall n \in I_D$, is the probability that a demand node uses its total inflow T_n to satisfy its demand q_{n0}.

Tanyimboh (1993) and Tanyimboh and Templeman (1993a) stated that the two finite probability schemes represented by Eqs. (2.43) and (2.44) are conditional upon the probability that flow reaches node n, $\forall n$, by all possible paths. Considering the conditional probability scheme of Eq. (2.44) which is associated with flow splitting processes, and applying the conditional entropy function of Eq. (2.6), Tanyimboh and Templeman (1993a) were able to define the entropy of a node n in a general network as follows:

$$S_n^o = -P_n \sum_{k \epsilon ND_n} p_{nk} \ln p_{nk} \quad n=1,...,NN \tag{2.48}$$

in which S_n^o is the entropy of node n associated with the outflows from that node n, $\forall n$; ND_n is the set of all downstream nodes of link outflows from node n, $\forall n$, including any demand; P_n is the total probability of flow arriving at node n, $\forall n$, by all possible paths. Tanyimboh and Templeman (1993a) showed how P_n, $\forall n$, can be calculated in a rather laborious way. However, algebraic manipulation of P_n, $\forall n$, gives the following convenient equation (see Tanyimboh and Templeman, 1993b, for its proof):

$$P_n = \frac{T_n}{T_0} \quad \forall n \tag{2.49}$$

in which T_0 is the total supply or demand, i.e.

$$T_0 = \sum_{n \epsilon I_s} q_{0n} = \sum_{n \epsilon I_D} q_{n0} \tag{2.50}$$

Having defined the conditional entropy of node n, $\forall n$, the conditional entropy of the entire network can then be defined using the general form of Eq. (2.5), which has the form:

$$S(O_1O_2...O_M) = S(O_1) + S(O_2 \backslash O_1) + ... + S(O_m \backslash O_1O_2...O_{m-1}) + ...$$

$$+ S(O_M \backslash O_1O_2...O_{M-1}) \quad M=2,3,... \; ; 2<m \epsilon Z^+<M \tag{2.51}$$

in which $S(O_1O_2...O_{M-1})$ is the joint entropy of M number of schemes; Z^+represents the set [0,1,2,3,...].

The first term of Eq. (2.51) represents the entropy of an absolute rather than a conditional finite scheme. Such an absolute scheme in a water network is a scheme representing the fraction of the total supply provided by source node n, $\forall n \in I_s$. i.e.

$$P_{0n} = \frac{q_{0n}}{T_0} \quad \forall n \in I_s \tag{2.52}$$

Therefore, in accordance with Eq. (2.51), Tanyimboh and Templeman (1993b, 1993c) introduced the following function which defines the entropy of a general water network as follows:

$$S^o = S_0^s + \sum_{n=1}^{NN} S_n^o \tag{2.53}$$

in which S^o is the network entropy based on the outflows; S_n^o is the conditional entropy of outflows, including any demand, at node n, $\forall n$, as given by Eq. (2.48); S_0^s is the entropy of the distribution of T_0 amongst the sources and is given by:

$$S_0^s = -\sum_{n \in I_s} P_{0n} \ln P_{0n} \tag{2.54}$$

where P_{0n} is given by Eq. (2.52).

The sample water supply network used by Tanyimboh and Templeman (1993a) and shown here as Figure 2.1 is used next to demonstrate the above equations.

If the supply, demand and link flows are specified in Figure 2.1a, and the associated probabilities are shown in Figure 2.1b, then the following equations can be obtained:

$T_0 = q_{01} + q_{02}$ [Eq. (2.50)]

$T_1 = q_{13} + q_{14} = q_{01}$

$T_2 = q_{23} + q_{24} = q_{02}$

$T_3 = q_{34} + q_{35} + q_{30}$

$T_4 = q_{46} + q_{40}$

$T_5 = q_{56} + q_{50}$

$T_6 = q_{60}$ [Eq. (2.45)]

$P_{01} = q_{01} / T_0$; $P_{02} = q_{02} / T_0$ [Eq. (2.52)]

$p_{13} = q_{13} / T_1$; $p_{14} = q_{14} / T_1$

$p_{23} = q_{23} / T_2$; $p_{24} = q_{23} / T_2$

$p_{34} = q_{34} / T_3$; $p_{35} = q_{35} / T_3$; $p_{30} = q_{30} / T_3$

$p_{46} = q_{46} / T_4$; $p_{40} = q_{40} / T_4$

$p_{56} = q_{56} / T_5$; $p_{50} = q_{50} / T_5$

$p_{60} = q_{60} / T_6 = 1$ [Eq. (2.44)]

Also, P_n, $\forall n$, can be calculated as the probability of flow arriving at node n, $\forall n$, by all possible paths. P_3, for example, can be calculated as follows. Flow can arrive at node 3 by two routes; those being 1-3 and 2-3. The probability of flow arriving at node 3 by route 1-3 is $P_{01}p_{13}$, and by route 2-3 is $P_{02}p_{23}$. Thus, P_3 is the sum of those two probabilities, i.e. $P_{01}p_{13} + P_{02}p_{23}$. Using the above approach, P_n, $\forall n$, are:

$P_1 = P_{01}$

$P_2 = P_{02}$

$P_3 = p_{13}P_1 + p_{23}P_2$

$P_4 = p_{14}P_1 + p_{24}P_2 + p_{34}P_3$

$P_5 = p_{35}P_3$

$P_6 = p_{46}P_4 + p_{56}P_5$

It should be noted that the above probabilities may be obtained by applying Eq. (2.49) which is very easy to use. At this stage, Eqs. (2.54) and (2.48) can be used to produce the following entropy functions:

$S_0^s = - P_1 \ln P_1 - P_2 \ln P_2$

$S_1^o = - P_1 [p_{13} \ln p_{13} + p_{14} \ln p_{14}]$

$S_2^o = - P_2 [p_{23} \ln p_{23} + p_{24} \ln p_{24}]$

$S_3^o = - P_3 [p_{34} \ln p_{34} + p_{35} \ln p_{35} + p_{30} \ln p_{30}]$

$S_4^o = - P_4 [p_{46} \ln p_{46} + p_{40} \ln p_{40}]$

$S_5^o = - P_5 [p_{56} \ln p_{56} + p_{50} \ln p_{50}]$

$S_6^o = - P_6 [p_{60} \ln p_{60}] = 0$

S_6^o being zero can be justified by the fact that there is no uncertainty about splitting the flow leaving node 6 as there is only one outflow at node 6, this being q_{60}. Finally,

the total outflow entropy of the network can be calculated using Eq. (2.53):

$$S^o = S_0^s + S_1^o + S_2^o + S_3^o + S_4^o + S_5^o + S_6^o.$$

It should be noted that the network entropy given by Eq. (2.53) is based on the conditional finite probability scheme of Eq. (2.44) which represents the outflows from node n, $\forall$n. Tanyimboh (1993) produced a similar network entropy function based on the inflows at node n, $\forall$n, which are represented by Eq. (2.43) as follows:

$$S^i = S_0^d + \sum_{n=1}^{NN} S_n^i \qquad (2.55)$$

in which S^i is the network entropy based on the inflows; S_n^i is the conditional entropy of inflows, including any source supply, at node n, $\forall$n, and is given by:

$$S_n^i = - P_n \sum_{j \in NU_n} p_{jn} \ln p_{jn} \quad n=1,...,NN \qquad (2.56)$$

where P_n is given by Eq. (2.49) and p_{jn} is given by Eq. (2.43). Also, in Eq. (2.55), S_0^d is the entropy of the distribution of T_0 amongst the demand nodes, i.e.

$$S_0^d = -\sum_{n \in I_D} P_{n0} \ln P_{n0} \qquad (2.57)$$

where P_{n0} is the fraction of the total demand consumed at node n, $\forall n \in I_D$, and is given by:

$$P_{n0} = \frac{q_{n0}}{T_0} \quad \forall n \in I_D \qquad (2.58)$$

It should be noted that the entropy of the outflows, S^o, which is given by Eq. (2.53) must equal the entropy of the inflows, S^i, which is given by Eq. (2.55). This can be seen by contemplating Eq. (2.5). However, the network entropy of the outflows, S^o, is used in this thesis, and the superscript o is therefore dropped hereafter.

2.6.2.3 CALCULATING MAXIMUM ENTROPY FLOWS IN NETWORKS

Returning to the problem of determining the most likely flows in a buried network in which only the supplies and demands, and the flow directions in the links are assumed to be available, it has been suggested, according to Jaynes' maximum entropy formalism, that the flow distribution which has the maximum entropy and satisfies the available information must be used. Having defined the appropriate entropy function for network flows, Tanyimboh and Templeman (1993a) calculated the maximum entropy flows in a looped network by maximizing the network entropy of Eq. (2.53) subject to the nodal flow equilibrium equations, Eqs. (2.15). However, the network entropy of Eq. (2.53) is defined in terms of probabilities, while the variables in the nodal equilibrium equations are the link flows. To simplify the optimization process, Tanyimboh and Templeman (1993a) reformulated the network entropy in terms of flows. This can easily be done by substituting Eqs. (2.44), (2.45), (2.47), (2.49) and (2.50) in Eq. (2.48), and substituting Eqs. (2.50) and (2.52) in Eq. (2.54), then Eqs. (2.48) and (2.54) can be substituted in Eq. (2.53) to obtain the new network entropy in terms of link flows, which may have the form:

$$S = F_s (q_s) \tag{2.59}$$

in which $F_s(q_s)$ is the network entropy defined in terms of all link flows.

Maximizing the network entropy of Eq. (2.59), therefore, subject to the nodal equilibrium equations, Eqs. (2.15), contains NLK variables, this number being the number of links in the network. However, if the first (NN-1) independent equilibrium equations, Eqs. (2.15), are substituted in the network entropy of Eq. (2.59), the size of the optimization process can be reduced from NLK number of variables to NLK-(NN-1) variables, those being the independent flows whose number is NLP, the number of loops, as shown in Eq. (2.17). Under these transformations, the nodal equilibrium equations are no longer needed in the optimization process as they are satisfied implicitly in the network entropy which may now have the form:

$$S = F_s (q_s^{ind}) \tag{2.60}$$

in which q_s^{ind} is the vector of all independent flows in the network; $F_s(q_s^{ind})$ is the network entropy defined in terms of q_i^{ind}, i=1,...,NLP.

Tanyimboh and Templeman (1993a) exploited the above simplifications to calculate the maximum entropy flows in a general looped network. They maximized Eq. (2.60) subject to non-negativity of all link flows to enforce the flow directions specified in the links. The optimization problem which they proposed is presented next as Problem 3.

Problem 3

$$\textit{Maximize} \quad S = F_s (q_s^{ind}) \tag{2.60}$$

subject to:

$$q_i = Fn_i (q_s^{ind}) \geq 0 \quad i=1,...,NLK \tag{2.61}$$

in which q_i is the flow in link i, i=1,...,NLK, derived from the equilibrium equations, Eqs. (2.15), and defined in terms of the independent flows (q_s^{ind}).

Problem 3 is a convex programming problem because the objective function of Eq. (2.60) is concave as it is the sum of a set of concave functions of the form $-\sum p_i \ln p_i$, and also the constraints in Problem 3, which are linear, represent a convex set. Therefore, Problem 3 has a unique global maximum point which can be obtained using any standard constrained non-linear programming algorithm. However, Tanyimboh and Templeman (1993a) solved Problem 3 as an unconstrained optimization problem after eliminating the non-negativity constraints of Eq. (2.61) by arguing that the maximum entropy solution will be expected to have flows which are as uniform as possible without any being equal to zero. Moreover, the network entropy of Eq. (2.60) will be undefined in the infeasible region, thus satisfying the non-negativity constraints implicitly in the objective function.

It should be noted that the multiple probability space models produced by Tanyimboh and Templeman (1993a) for general networks are capable of solving parallel networks. A water network is said to be parallel if it has no links connected in series, i.e. each link in a parallel network operates independently of the rest. This implies that each link connects a source node to a demand node. Tanyimboh and Templeman (1993a) applied the multiple probability space model to a parallel network and maximized the network entropy function of Eq. (2.53) subject to its nodal equilibrium equations. The resulting maximum entropy flows were shown to be as follows:

$$q_{nk}^{*} = \frac{q_{0n}\, q_{n0}}{T_0} \quad \forall nk \in IJ \tag{2.62}$$

in which q_{nk}^{*} is the maximum entropy flow in link nk, $\forall nk \in IJ$; the * is used herein to denote the optimal value. The result of Eq. (2.62) corresponds to the well-known gravity model of transportation engineering, see Erlander (1977) for example. This may give further emphasis on the general correctness of the approach.

Finally, it may be noted that the above approach of determining the least biased flows proposed by Tanyimboh and Templeman (1993a) is for general water networks in which only the supply and demand, and the flow directions in the links are assumed to be available. However, other information may be available such as lengths and diameters of the pipes and the pressure head of any node in the network. Also, the conservation of energy around each loop must be satisfied. Unfortunately, the maximum entropy flows problem proposed by Tanyimboh and Templeman (1993a) and presented here as Problem 3 is not able to cover the new information which may be available in general networks. The above issues are investigated in Chapter 6, and a new optimization problem is proposed to incorporate the new available information in one general model.

2.6.2.4 PATH-BASED ALGORITHM FOR CALCULATING MAXIMUM ENTROPY FLOWS IN SINGLE-SOURCE NETWORKS

The problem of calculating maximum entropy flows in networks proposed by Tanyimboh and Templeman (1993a) and presented earlier as Problem 3 involves non-linear programming. A different and simpler path-based approach was described by Tanyimboh and Templeman (1993b) to calculate maximum entropy flows in single-source networks.

Considering any demand node served by more than one path from the source, Tanyimboh and Templeman (1993b) argued that, according to the maximum entropy formalism, the demand of that node should be divided equally amongst all paths supplying it if there is no further information about those paths. Therefore, each demand node should be treated in turn, and the final maximum entropy flow in each link is then obtained by summing the flows in all paths passing that link. To demonstrate the above approach, the single-source network example used by Tanyimboh and Templeman (1993b) is considered here and is shown as Figure 2.2. The equal path flows from the source to each demand node are shown in Figure 2.3. For example, node 5 is served by three paths 1-2-5, 1-2-3-5 and 1-3-5, each of which must carry 8 units of flows; that is one-third of the demand of node 5. Finally, for each link, the flow for all paths through that link are summed to obtain the maximum entropy flow for that link. The resulting maximum entropy link flows are shown in Figure 2.4. They are identical to those obtained by solving Problem 3 computationally for the network of Figure 2.2. Tanyimboh and Templeman (1993b) presented algorithms for the proposed method. They are a node numbering algorithm, a node weighting algorithm and a flow distribution algorithm.

The same single-source network of Figure 2.2, which is shown now in Figure 2.5, is used next to demonstrate the above algorithms. First, all nodes in the network are numbered according to the node numbering algorithm. The source node is given the number 1, then the rest of the nodes are numbered in an ascending sequence starting with any node for which all upstream nodes have already been numbered. The

numbering of nodes 4 and 5 is arbitrary and may be interchanged.

The next step is to calculate the number of paths from the source to each node using the node weighting algorithm, and then to enclose that number, as a weight of the node, in a box next to it. This can be done by assigning a weight of 1 to the source node, then, in ascending node numbering sequence, the weight of each node is equal to the sum of the weights assigned to all nodes immediately upstream of it. Consequently, the weight of node 2 is equal to the weight of node 1, and the weight of node 3 is the sum of the weights of nodes 1 and 2, that is 1+1=2. Similarly, the weight of node 4 equals the weight of node 1 plus the weight of node 3, and the weight of node 5 is the sum of the weights of nodes 2 and 3, which, in both cases, equals 3. It may be noted that the node numbering algorithm ensures that all nodes immediately upstream of the node being considered have been weighted.

Finally, the flow distribution algorithm is used to determine maximum entropy link flows. The total outflow at a node is shared among the inflowing links at that node in proportion to the upstream nodal weights. The flow distribution algorithm operates in descending node number order. Therefore, starting with node 5, the flow in link 2-5 is obtained by multiplying 24, this being the total outflow at node 5, by the ratio 1/3 which is the ratio between the weights of nodes 2 and 5. The flow in link 3-5 equals 24 multiplied this time by the ratio 2/3, this being the ratio between the weights of nodes 3 and 5. Similarly, considering node 4, the flow in links 1-4 and 3-4 can be obtained by multiplying 15 by the ratios 1/3 and 2/3 respectively. At this stage, the flow in the links ending at node 3 can be calculated. The total outflows at that node equal its demand plus the flows in links 3-4 and 3-5, resulting in 36 units. Consequently, the flow in links 1-3 and 2-3 will share the total outflows at node 3 equally due to the equality of the weights of the immediate upstream nodes of these two links. The only link left is link 1-2 whose flow is equal to 36, this being the total outflows at node 2, multiplied by the ratio 1/1.

The above algorithms are rigorous for single-source networks. They produce identical results to those given by solving Problem 3 in a much simpler and quicker method as

it is not iterative and does not involve linear or non-linear programming. Unfortunately, the above simple method is not capable of handling general multi-source networks. Walters (1995) has pointed out that the attempt of Tanyimboh and Templeman (1993b) to extend the simple single-source algorithm to multiple sources by means of a super-source concept is actually incorrect. He showed how it should correctly be used in a rather unwieldy method. In Chapter 4, a relatively simple algorithm based on the path concept is proposed for calculating maximum entropy flows for general multi-source networks without involving linear or non-linear programming.

Having reviewed the use of entropy in estimating the most likely flows in water networks, the second application of entropy in water distribution networks as a surrogate measure of reliability is presented next.

2.6.3 ENTROPY AND RELIABILITY IN WATER NETWORKS

The efficiency of the design of water distribution networks in urban areas depends on both the cost optimization and reliability of the system. The cost aspects of water supply systems have been discussed earlier in this chapter and incorporated in the least-cost optimum design of water distribution networks which is presented herein as Problem 2. Templeman (1982) argued that if this cost optimization design problem is formulated for a network with a prespecified looped layout it leads inevitably towards an implicit tree-type branched network where a few minimum diameter loop-completing pipes, whose existence is ensured by the minimum diameter constraints, do not provide spare capacities which are not immediately required by the design demand pattern. In contrast, the basic requirement of reliability in water supply networks is to provide alternate flow paths to each demand node by means of loops in order to prevent or at least reduce the possibility of isolating some demand points from the rest of the network in the event of random components failures. These alternate paths must have adequate capacities to be usable under various adverse conditions for which the network was not specifically designed. Therefore, it is essential to incorporate some measures of reliability in the optimum design problem

of water supply networks.

However, there is no comprehensive definition of the reliability of water distribution networks in the literature. Although some reliability definitions have been established, their practical applications for general networks are extremely complicated (see Valliant, 1979 and Provan and Ball, 1983). Consequently, including such complex reliability analysis in the optimum design problem, which is itself very difficult to solve (Yates, Templeman and Boffey, 1984), makes it even worse. It can then be concluded that a surrogate and simple measure of reliability has to be sought and included in the optimum design of water networks in such a way that optimizing this surrogate measure optimizes to some acceptable extent the overall reliability of the network. Awumah et al. (1990, 1991, 1992) and Tanyimboh and Templeman (1993c) used entropy as a surrogate measure of reliability in water distribution networks. Before reviewing entropy as a surrogate measure of reliability, some definitions and measures of actual reliability in water supply networks are presented next.

2.6.3.1 SOME DEFINITIONS AND MEASURES OF RELIABILITY

Two types of reliability may be recognized within a water distribution network. These are mechanical reliability and hydraulic reliability. Mechanical reliability reflects the need for any component in the network to be operational at any time, and it is affected by the layout of all components and their individual mechanical reliability. On the other hand, hydraulic reliability is concerned with the ability of the system to satisfy all required nodal demands under severe conditions, and it depends on mechanical reliability and the hydraulic performance of the network.

Tung (1985) defined the mechanical reliability of a network as the probability that all demand nodes are reachable from a source. Therefore, the unreliability can be identified as the probability that at least one demand node is isolated. Also, Wagner, Shamir and Marks (1988a) used two definitions for mechanical reliability, first as the probability that a given demand node in a system is reachable from at least one source, and second as the probability that all demand nodes in a system are connected

to a source.

The problem of testing the reachability and connectivity in water supply networks has been found to be extremely difficult to solve (Provan and Ball, 1983). However, some methods for solving this problem exist. Tung (1985) showed that the *minimum cut set* approach is the most efficient method for calculating the mechanical reliability of water networks. A minimum cut set is a minimum set of system components whose simultaneous failure will cause the failure of the system. The complement of the sum of failure probabilities of all minimum cut sets will give a lower bound for system reliability.

Wagner, Shamir and Marks (1988a) showed that reachability and connectivity measures can be used to identify unreliability in a system due to lack of network interconnections or unreliable components. Connection to a source, however, is only a necessary but not a sufficient condition to insure that a given node is functional. A sufficient supply for a reachable and fully connected node may not be satisfied at adequate pressure. Therefore, measures of hydraulic reliability should be defined and calculated to estimate the overall reliability of a network. Wagner, Shamir and Marks (1988a) defined the hydraulic reliability of a water network as the probability that a system can meet a specified level of flow at each demand node. They showed that calculating this measure should be made for a simplified representation of the network in question. In another paper, Wagner, Shamir and Marks (1988b) showed that simulation-based analysis of water networks under random component failures enables other reliability measures to be identified such as the duration of the longest period of failure at any node, the duration of the longest period of reduced service at any node and the failure event in which the greatest total shortfall occurred.

Also, Bao and Mays (1990) defined the hydraulic reliability of a system as the probability that the system can provide the demanded flow rates at the required pressure head. Based on this definition, they introduced nodal reliability as the probability that the actual pressure head at a given demand node is greater than or equal to the required minimum pressure head at that node. They concluded that overall

system reliability can be identified as one of the following three measures, first as the minimum nodal reliability in the system, that is the reliability of the most unreliable node, second as the mean of all nodal reliabilities, and third as the weighted average of the nodal reliabilities, that is the weighted mean of all nodal reliabilities weighted by the corresponding nodal demands.

Finally, Fujiwara and De Silva (1990) defined reliability in terms of the expected minimum flow delivered as the complement of the ratio of the expected minimum total shortfall in flow to the total demand. For calculating the expected minimum total shortfall, they calculated the minimum shortfall for each state of the network which has only one failed link. The expected minimum total shortfall can then be calculated as the sum of the minimum shortfall for each state weighted by the corresponding state probability.

The problem of calculating hydraulic reliability defined in terms of the probability of sufficient supply is extremely difficult to solve (Valliant, 1979). Its exact calculation requires the analysis of all reduced network configurations due to random component failures, which is time consuming. Many approximations, therefore, have been made in this regard. The interested reader may consult the papers from which the above measures of reliability were taken.

It can therefore be concluded that concatenating the optimum design problem of water networks with reliability is extremely complicated. Su, Mays, Duan and Lansey (1987), Fujiwara and De Silva (1990) and Cullinane, Lansey and Mays (1992) are some of many models in the literature which optimize network reliability explicitly within the framework of the optimum design problem of water distribution networks. The details of those models have no relevance to the present work and are left to the interested reader who may consult the papers from which those models were taken.

However, reliability can implicitly be optimized within the framework of the least cost optimum design of water networks which is formulated earlier in this chapter as Problem 2. This can be done by considering multiple demand patterns in the problem

including very adverse cases. In this case, a set of constraints for each demand pattern has to be added to the problem. It has been seen that Problem 2 is extremely difficult to solve. Thus this difficulty will increase with each additional load case.

Armed with the above arguments, the need for simple and easy-to-calculate surrogate measures of reliability is vital. It has been discussed earlier in this section that the uncertainty surrounding reliability invokes an opportunity for entropy to play a role in the issue of reliability in water distribution networks. In the following subsections, the correlation between entropy and reliability is discussed, followed by some models incorporating entropy as a surrogate measure of reliability in the optimum design problem of water supply networks.

2.6.3.2 CORRELATION BETWEEN ENTROPY AND RELIABILITY

Apart from uncertainty which correlates entropy to reliability of water distribution networks as discussed earlier in this section, other factors which strengthen this correlation are presented next.

It has been shown earlier in this chapter that the maximum entropy formalism selects the most uniform distribution among all the probability distributions which satisfy the available information. It is therefore logical to predict that applying the maximum entropy formalism in water distribution networks results in flows and diameters of all links to be as uniform as possible. Much research has demonstrated that uniformity in pipe diameters and flows increases the reliability of the network. Rowell and Barnes (1982) argued that a pipe with an extremely high hydraulic gradient is dissipating energy at an excessive rate and should be replaced by a larger, more efficient pipe, while a pipe with an extremely low hydraulic gradient should be replaced by a smaller pipe. This is consistent with the common design restriction on flow velocity within the network pipes, which forces large pipes with small flows to be replaced by smaller pipes, and small pipes with large flows to be replaced by larger pipes. The above rearrangement of pipe diameters suggested by Rowell and Barnes (1982) leads to a network in which all pipes are fairly similar in diameter. Also, Goulter and Coals

(1986) recommended minimizing the differences in the reliabilities of all pipes connected to each node in order to improve network reliability. Tanyimboh and Templeman (1993c) showed how such a recommendation leads inevitably to uniformity of all diameters in the network.

Turning to flow uniformity, Walters (1988) showed that splitting the flow equally between the pipes converging at each node could improve the reliability of the network. Also, Awumah, Goulter and Bhatt (1991) demonstrated that maximizing the level of uniformity in capacities of the links incident upon the demand nodes tends to improve network reliability.

The above arguments show that the desirability of uniformity for pipe diameters and flows in water supply networks puts entropy and reliability on the same track. Awumah, Goulter and Bhatt (1990) used the entropy-based function of Eq. (2.41) as a measure of redundancy at node n, $\forall n$, in water supply networks. As shown earlier in this chapter, this measure of redundancy has accounted for redundancy being transmitted from upstream, and allowed for flow reversal in case of pipe failures. The overall redundancy of the network can then be calculated using Eq. (2.36). Awumah et al. (1990) assessed the above entropy-based redundancy measure by comparing it to two well-known parameters; the Nodal Pair Reliability parameter and Percentage of Demand Supplied at Adequate Pressure parameter. The first parameter measures the probability that a pair of nodes are successfully connected, and the second parameter assesses the hydraulic performance of the network under failure of a link in the network. The above comparison showed that the entropy measure of Eq. (2.36) is very sensitive to changes in the network reliability as measured by the above two comparative parameters.

Another entropy-based measure presented earlier in this section as Eq. (2.40) has been used by Awumah et al. (1991) as a measure of global redundancy at node n,$\forall n$, in a water network. They demonstrated that the above measure reflects the network performance indicated by the percentage of flow supplied under a range of link failures, and can be used to produce reliable designs without the need for large

numbers of load patterns or intensive iterative approaches which are normally required.

Also, Tanyimboh and Templeman (1993a) calculated the maximum entropy flows, presented earlier as Problem 3, for the network shown in Figure 2.1. They observed that the link flows in the lower half of the network are the same for any combination of source flows at nodes 1 and 2 totalling the same amount of units. From a reliability viewpoint, this would result in a considerable degree of invulnerability to possible variations in the source flows.

Finally, the above relationship between entropy and reliability has been demonstrated graphically by Awumah and Goulter (1992) who obtained two trade off curves for different designs based on a range of layouts. The first trade off curve is cost vs entropy which is defined by Eqs. (2.36) and (2.37). The second trade off curve is cost vs reliability which is defined by the average node pair reliability of the network. Awumah and Goulter (1992) showed that the above two trade off curves are very similar. They concluded that this similarity makes entropy a good surrogate measure for network reliability.

Having established the strong relationship between entropy and reliability in water distribution networks, some models for incorporating entropy into the optimum design of water supply networks are presented next.

2.6.3.3 ENTROPY-BASED OPTIMUM DESIGN OF RELIABLE WATER NETWORKS

Two approaches have been used in the literature to incorporate entropy as a measure of reliability in the optimum design of water distribution networks. The first approach is to maximize the network entropy subject, in addition to the usual hydraulic constraints, to a constraint on the total capital cost of the network. The second approach is to minimize the total cost of the network subject, in addition to the necessary hydraulic constraints, to an entropy constraint which either restricts the

minimum permissible level of entropy of the network as a whole, or at each node individually.

Awumah and Goulter (1992) used the first approach to produce a non-linear cost-constrained entropy maximizing model which was able to design both the layout and pipe diameters for a network. The objective function was the overall entropy function of Eq. (2.36) using the nodal entropy function of Eq. (2.41). The model was first run without the budget constraint on a sample looped network to determine the maximum entropic reliability of the network with maximum network cost. The model was then rerun for successively lower cost limits until no further cost reductions were possible, in which case the network has collapsed into a branched tree network without loops. In each run, the reliability of each resulting network has been calculated using the well-known Nodal Pair Reliability parameter. It has been shown that the model produced, at each lower budget limit, a network with a lower overall network entropic redundancy which reflected the changes in the nodal pair reliability of the network.

Turning to the second approach of incorporating entropy in the optimum design of water networks, Awumah, Goulter and Bhatt (1991) used this approach in their design model by imposing minimum permissible levels of value of the entropy function of Eq. (2.40) at each demand node in the cost-optimization formulation. They showed that imposing such constraints together with simultaneous inclusion of only five load cases produced solutions for a particular problem that were very close to those obtained by a well accepted design approach which used an intensive iterative approach involving 37 different load patterns.

Also, instead of restricting entropy at each demand node, Tanyimboh and Templeman (1993c) proposed a model in which the network entropy of Eq. (2.53) has been restricted for the network as a whole in the least cost optimum design problem presented earlier in this chapter as Problem 2. The model was run on a sample single-source network for five different levels of entropy. Under two kinds of emergency which were single link failures and fire fighting loads, the flexibility of the resulting five designs has been tested using two indices. The first index was the notional head

required at the source to satisfy all demands. This can be determined by finding the maximum value of the head loss in any path from the source to any terminal node added to the minimum desirable head at that node. The second index was the total amount of energy that the network dissipates per unit time. This can be calculated by summing the products of all flows and head losses in the links, multiplied by the density of water and acceleration due to gravity. Tanyimboh and Templeman (1993c) showed that the model was able to produce a design which can cope with eventualities for which the network was not specifically designed. They added that such resilient designs can be obtained without a substantial increase in cost.

To end this chapter, it may be concluded that entropy has a very important role to play in water distribution networks. However, other kinds of network exist such as structural trusses which are mathematically similar to water supply networks in terms of model formulations and methods of analysis and design. This similarity invokes entropy to play a part in the optimum design of structural trusses. In the next chapter, literature on analysis and design methods for structural trusses along with structural reliability and damage tolerance approaches is reviewed, followed by a full description of the mathematical similarities in engineering network models. The use of entropy in the optimum design of structural trusses is investigated in Chapter 8.

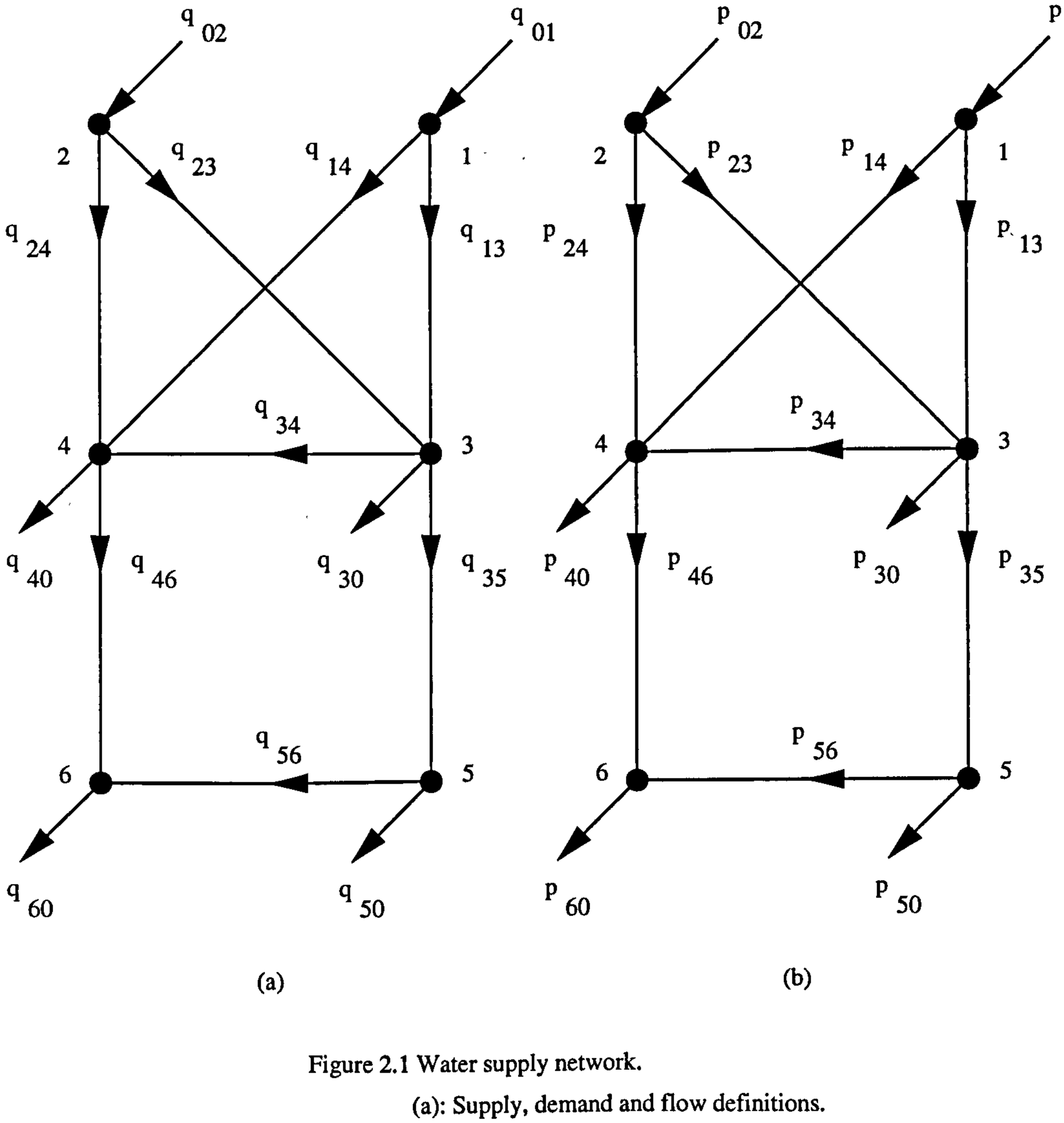

Figure 2.1 Water supply network.

(a): Supply, demand and flow definitions.

(b): Probability definitions.

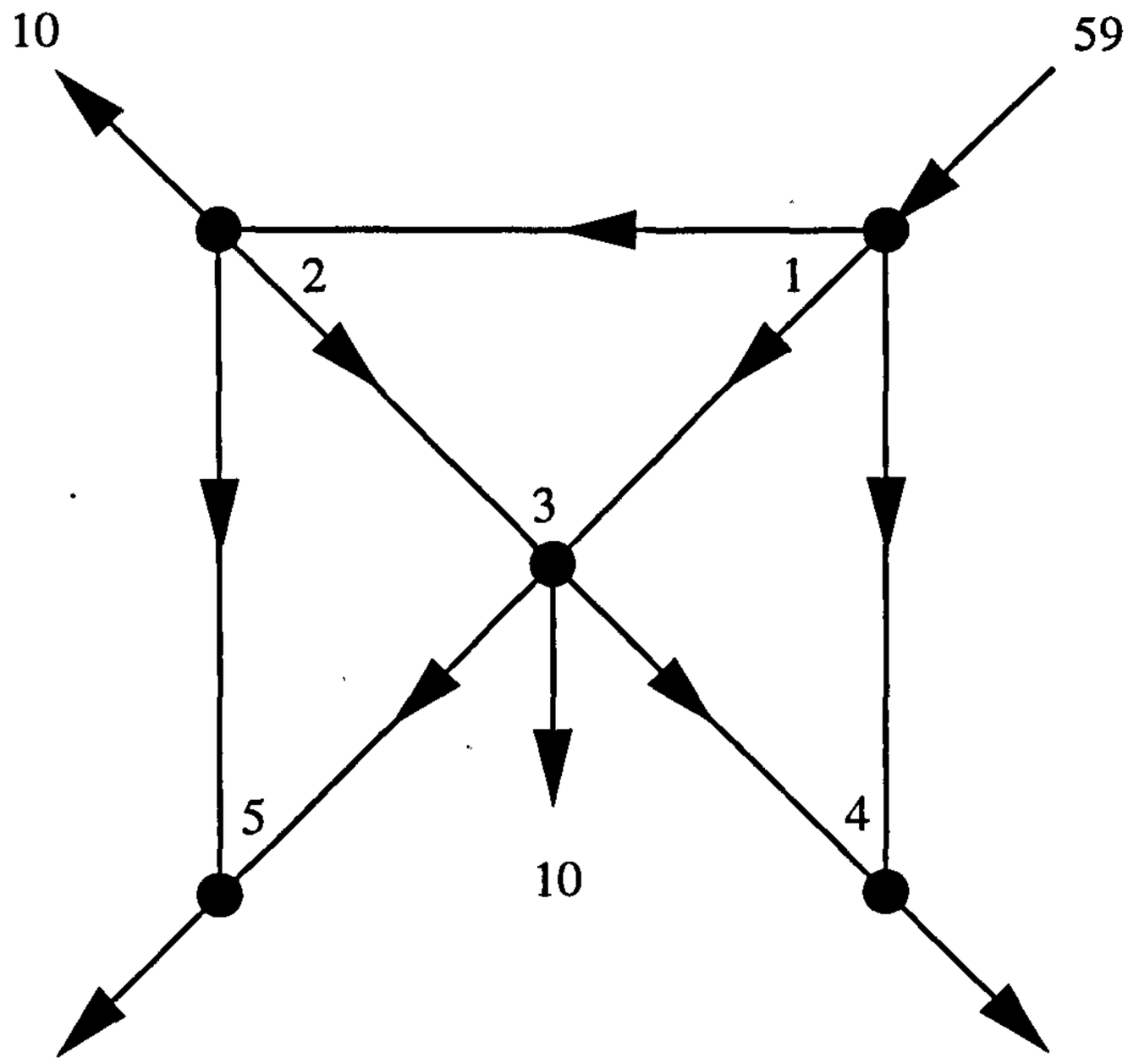

Figure 2.2 Single-source network

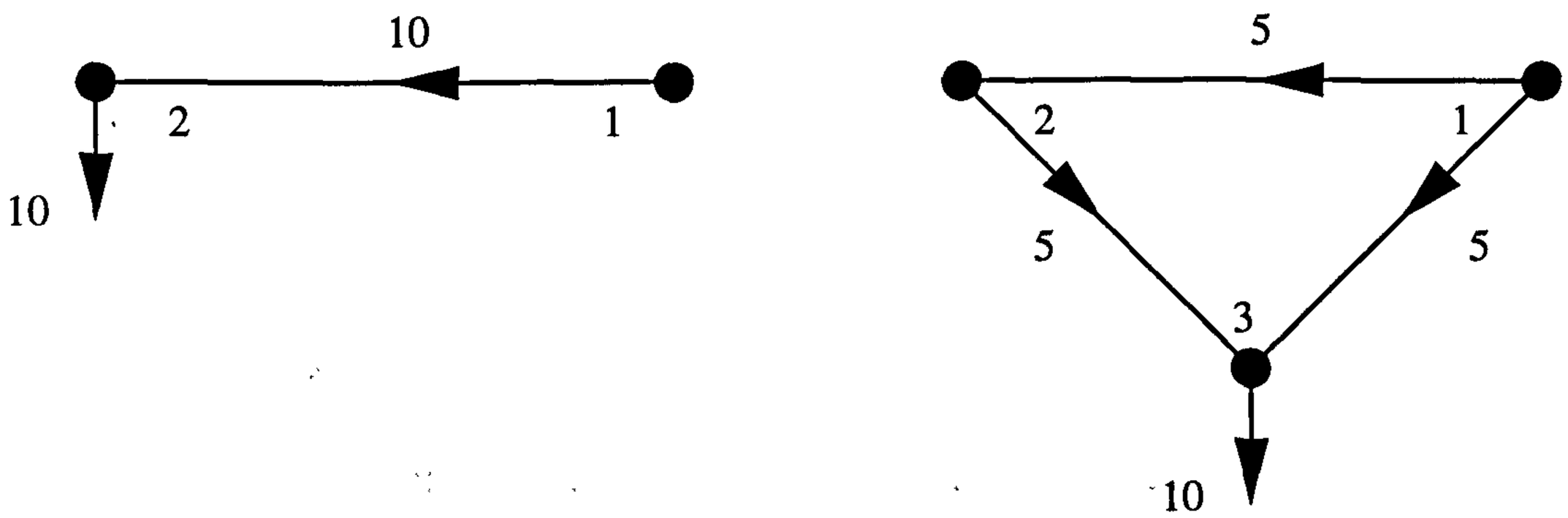

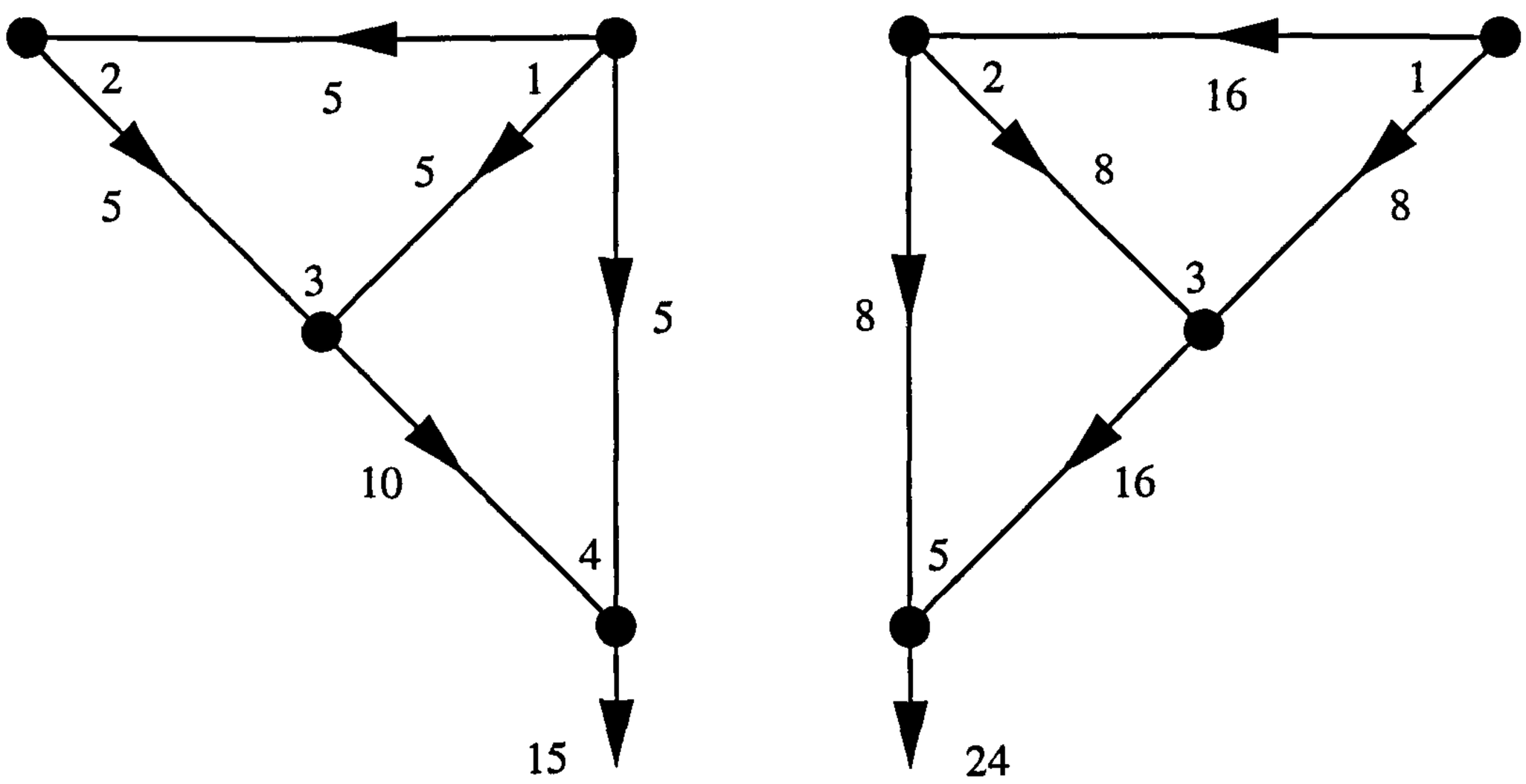

Figure 2.3 Equal path flows from the source to each demand node

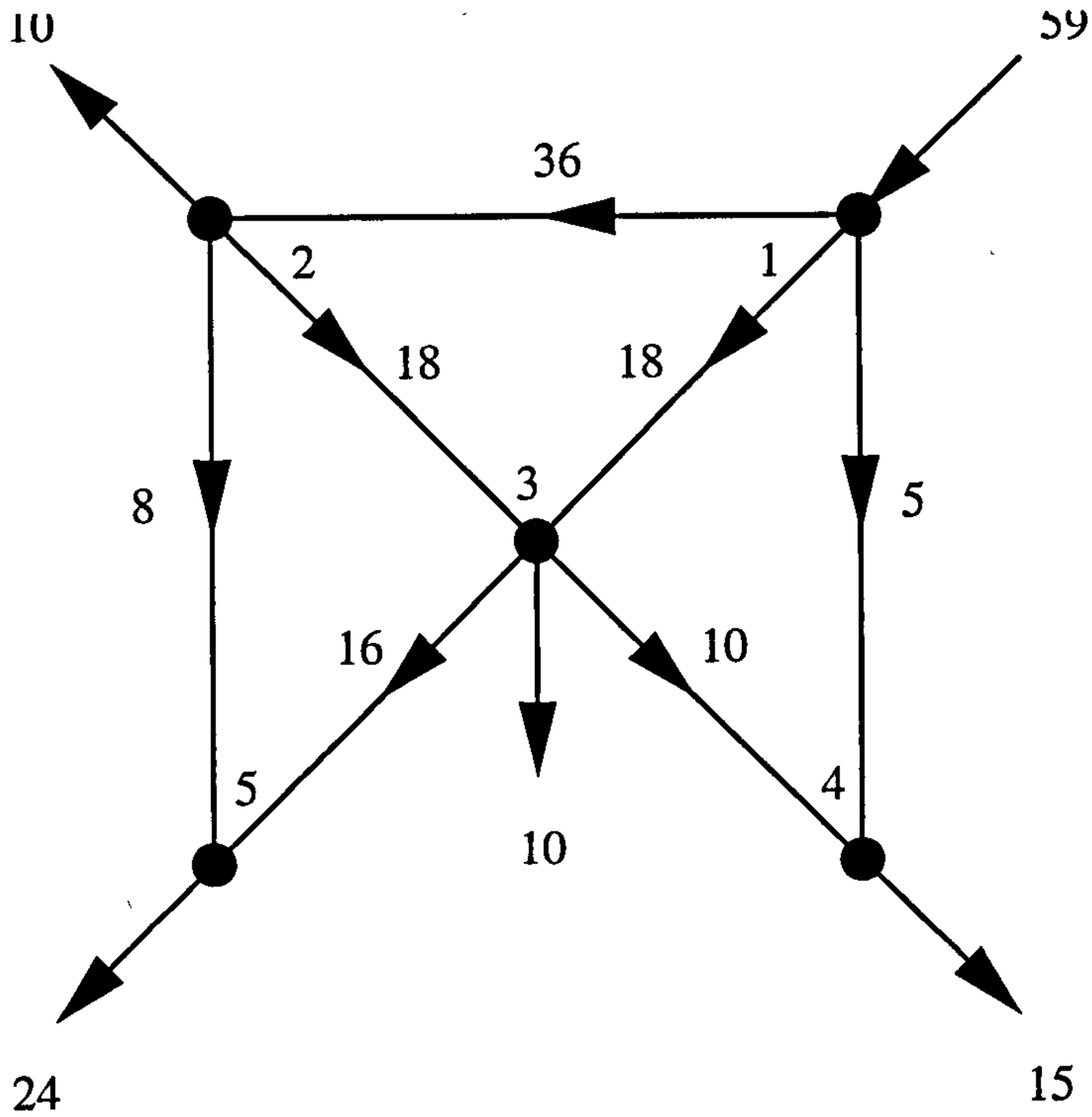

Figure 2.4 Maximum entropy flows for the network of Figure 2.2 found by superposing the path flows of Figure 2.3

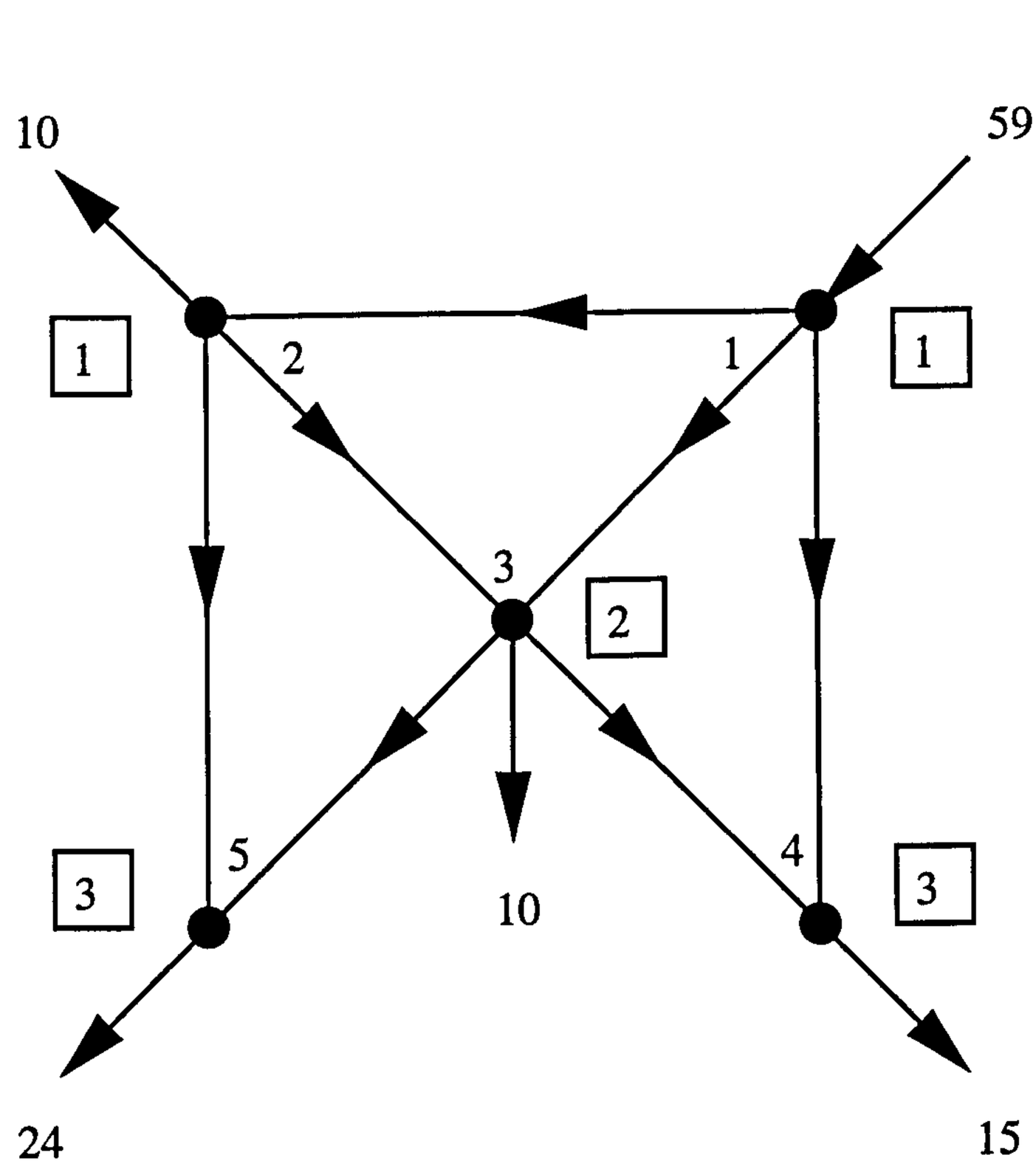

Figure 2.5 Number of paths to each node for the network of Figure 2.2

CHAPTER 3

MATHEMATICAL SIMILARITIES IN THE SYSTEM MODELS OF ENGINEERING NETWORKS

3.1 INTRODUCTION

This chapter explores in detail aspects of similarity between structural trusses and water supply networks. A review of both systems is needed to illustrate these similarities comprehensively. In the previous chapter, water supply networks were fully reviewed in terms of analysis, optimum design and reliability approaches. A similar study for structural truss models is therefore presented in this chapter before their similarities to water supply networks are investigated. These similarities enable both structural trusses and water supply networks to be included in the same general class of potentiated networks.

In graph and network theory, a graph is defined as a set of nodes connected together by a set of arcs, and a network is a graph whose arcs carry directed or undirected flows. A potentiated network is defined as a network whose nodes have some potentials which functionally depend upon the arc flows of the network. Whether this functional dependence of nodal potentials upon the arc flows is linear or nonlinear, the corresponding networks are respectively classified as linear or nonlinear potentiated networks which both together form a small sub-set of general graphs and networks.

Many engineering networks such as water supply networks, gas transmission networks and electrical power distribution networks belong to the same general class of nonlinear potentiated networks. It is well appreciated that they all share similar characteristics in terms of network representation, physical quantities, constitutive

equations and methods of analysis and design.

Structural trusses are an important class of engineering structures with their familiar pictorial representation of node-arc graphs. Engineers can easily recognize the similarity between structural trusses and the other engineering networks, such as water supply systems, in terms of pictorial representations. Spillers (1972) showed that this kind of similarity between structural trusses and water supply networks, which share in the commonality with other potentiated networks, can be extended to the sets of constitutive equations only. However, by a close contemplation of the system mathematical models of engineering networks, Templeman and Yates (1984) and Templeman (1992b) were able to demonstrate that this obvious network representational similarity between structural trusses and the general class of potentiated networks, of which the water supply system is an example, can be extended almost fully to include terms such as physical quantities, constitutive equations, methods of analysis and design and even reliability approaches. This is very interesting and instructive as these mathematical similarities enable structural trusses to be expressible as linear potentiated networks which form a special case of the more general class of nonlinear potentiated networks such as water supply networks. Consequently, the existing methods of analysis and optimum and even reliable design of structural trusses could be used for water supply networks and vice versa. In the present work, the concept of network entropy presented in this thesis is applied to indeterminate structural truss design methods, and the resulting designs are tested against reliability and damage tolerance approaches.

In this chapter, the constitutive equations of structural trusses along with the existing methods of analysis and optimum design are introduced, then a review of structural reliability analysis is investigated followed by the probabilistic approach to design and the concept of damage tolerant design. Finally, a full description of the mathematical similarities between structural trusses and water supply networks is presented in terms of analysis, optimum design and reliability approaches.

3.2 OPTIMUM DESIGN OF STRUCTURAL TRUSSES

The optimum design of structural trusses presented here is for general pin-jointed plane trusses in which the layout and external applied loads are prespecified and the length and the elastic modulus of the material of each bar are known. The objective function of the problem is the weight function of the truss, and the design variables are the cross-sectional areas of the truss bars. The constraints are the constitutive equations and some other constraints which limit nodal displacements, bar stresses and bar sizes. Before the optimum design problem is stated, the constitutive equations are presented and the most common methods of analysis are described.

3.2.1 CONSTITUTIVE EQUATIONS

Figure 3.1 shows a typical structural truss with its physical quantities conventionally defined. The constitutive equations include the bar force equilibrium equations at each node, the compatibility equations and the characteristic force-strain relationship equations for each bar of the truss.

3.2.1.1 BAR FORCE EQUILIBRIUM EQUATIONS

At each node, all the horizontal components of the external applied loads acting at that node and the axial forces carried by the bars connected to that same node must be in an equilibrium state. The same applies for the vertical components as the truss equilibrium is vectorial and hence there are two equilibrium equations per node, i.e.

$$\sum_{i=1}^{NN} Fax_{ij} \sin \theta_{ij} + Fex_{jv} = 0 \quad j=1,...,NN \tag{3.1a}$$

$$\sum_{i=1}^{NN} Fax_{ij} \cos \theta_{ij} + Fex_{jh} = 0 \quad j=1,...,NN \tag{3.1b}$$

where Fax_{ij} is the axial force in bar ij, $\forall$ij; θ_{ij} is the angle that bar ij makes with the horizontal; NN is the total number of nodes; Fex_{jv} and Fex_{jh} are respectively the vertical and horizontal components of the external applied loads acting at node j,

j=1,...,NN.

It should be noted that only (2NN-3) equilibrium equations of Eqs. (3.1a,b) are usable since the external load vectors must be in equilibrium and three of the equilibrium equations become linear combinations of the (2NN-3) equations mentioned above. However, the three displacement vector components available at the points of truss supports will balance out the loss of these three equilibrium equations.

3.2.1.2 COMPATIBILITY EQUATIONS

The axial deformation of each bar must be compatible with the nodal displacement components at the bar ends. i.e.

$$\cos \theta_{ij} (\delta_{jh}-\delta_{ih}) + \sin \theta_{ij} (\delta_{jv}-\delta_{iv}) = \Delta_{ij} \quad \forall ij \in IJ \tag{3.2}$$

in which δ_{jh} and δ_{jv} are respectively the horizontal and vertical nodal displacement components of node j; Δ_{ij} is the deformation of bar ij; and IJ is the set of all the bars in the truss.

3.2.1.3 CHARACTERISTIC FORCE-STRAIN RELATIONSHIP EQUATIONS

For the most usual case of a linear elastic bar material, the deformation of each bar can be written in terms of the axial bar forces as follows:

$$\Delta_{ij} = \frac{Le_{ij}\, Fax_{ij}}{A_{ij}\, E_{ij}} \quad \forall ij \in IJ \tag{3.3}$$

where Le_{ij}, A_{ij} and E_{ij} are respectively the length, the cross-sectional area and the elastic modulus of bar ij, $\forall ij$.

3.2.2 METHODS OF ANALYSIS

The analysis problem is to estimate the axial bar forces and the nodal displacement components in a truss whose bar lengths, cross-sectional areas and the elastic modulus

of bar materials are known and the external applied loads are specified. As discussed earlier, there are (2NN-3) usable equilibrium equations of Eqs. (3.1a,b) with NB axial bar forces as unknowns, where NB is the number of bars in the truss. If NB=2NN-3 there will be 2NN-3 linear equations in (2NN-3) unknown bar forces which can be determined uniquely by solving these equations by Gaussian elimination. Substituting the resulting bar forces into Eqs. (3.3) gives bar deformations which can then be used to determine uniquely the nodal displacement components directly from Eqs. (3.2).

Note that the case where NB=2NN-3 corresponds to a statically determinate truss. In the case of an indeterminate truss where NB>2NN-3, the available (2NN-3) nodal equilibrium equations will be insufficient to obtain unique values for bar forces, and thus the analysis problem becomes more complex. Many methods exist to solve this problem (see Coates, Coutie and Kong, 1994). Next are presented the main two methods used in the literature. They are the force or flexibility method and the displacement or stiffness method.

3.2.2.1 FLEXIBILITY METHOD

In this method, the redundant [NR=NB-(2NN-3)] bars, where NR is the number of redundant bars, are removed and replaced by external loads equal to the unknown axial forces in the removed bars Fax_r, r=1,...,NR, as shown in Figure 3.2. The axial bar forces can then be calculated in terms of the unknown forces in the removed bars as follows:

$$Fax_b = \eta_b + \sum_{r=1}^{NR} \xi_{br}\, Fax_{NB-NR+r} \quad b=1,...,NB-NR \tag{3.4a}$$

$$Fax_b = Fax_{NB-NR+r} \quad b=NB-NR,...,NB;\ r=1,...,NR \tag{3.4b}$$

where η_b, b=1,...,NB-NR, are bar forces in the determinate sub-truss caused by the external applied loads only; and the terms ($\Sigma\xi_{br}Fax_{NB-NR+r}$, b=1,...,NB-NR; r=1,...,NR) are the extra forces in these bars caused by the unknown forces ($Fax_{NB-NR+r}$, r=1,...,NR) in the redundant bars.

At this stage, the nodal displacement components at the end nodes of the redundant bars can be calculated for the determinate sub-truss. They must be compatible with the axial deformations in the redundant bars. Therefore, there is a compatibility requirement for each redundant bar. These can be set up directly by means of virtual work as follows:

$$\sum_{b=1}^{NB-NR} \frac{Fax_b\ \xi_{br}\ Le_b}{A_b\ E_b} + \left(\frac{Fax\ Le}{A\ E}\right)_{NB-NR+r} = 0 \quad r=1,...,NR \tag{3.5}$$

in which Fax_b is the axial force in bar b, b=1,...,NB-NR, of the determinate sub-truss as given by Eqs. (3.4a); ξ_{br} is the axial force in bar b of the determinate sub-truss due to unit load applied at the nodes at the ends of redundant bar r, r=1,...,NR; and the term $(Fax\ Le/A\ E)_{NB-NR+r}$ is the axial deformation in redundant bar r.

Eqs. (3.5) are NR equations with NR unknown axial forces of NR redundant bars existing in the truss. Solving these equations gives the redundant bar forces $Fax_{NB-NR+r}$, r=1,...,NR, which can then be substituted into Eqs. (3.4) to give the axial bar forces Fax_b, b=1,...,NB, for the whole indeterminate truss. Eqs. (3.3) and (3.2) can now be used to determine the axial bar deformations and nodal displacement components for each node in the truss.

Although the method described above is widely used in the literature, it is difficult to programme for general use. However, other methods exist such as the stiffness method for which a general-purpose program is easy to write. Its use requires no understanding of structural mechanics, and it is described next.

3.2.2.2 STIFFNESS METHOD

In this method which is also called the displacement method, bar forces Fax_{ij}, $\forall ij \in IJ$, are expressed in terms of nodal displacement components by simply substituting Eqs. (3.3) into Eqs. (3.2) and rearranging the resulting equations to yield the following equations:

$$Fax_{ij} = \frac{A_{ij}\,E_{ij}}{Le_{ij}} [\cos\theta_{ij}\,(\delta_{jh}-\delta_{ih})+\sin\theta_{ij}\,(\delta_{jv}-\delta_{iv})] \quad \forall ij \in IJ \tag{3.6}$$

which are then substituted into Eqs. (3.1) to give the following equations with the well-known matrix form:

$$[K]\,[\delta] = [Fex] \tag{3.7}$$

in which [δ] is a column vector of (2NN-3) unknown nodal displacement components; [Fex] is a column vector of (2NN-3) nodal externally applied force components; and [K] is the stiffness matrix with (2NN-3)x(2NN-2) known constants.

Eqs. (3.7) are a system of (2NN-3) linear equations in (2NN-3) unknown nodal displacement components δ_{iv} and δ_{ih}, i=1,...,NN, with three of these components already known at the points of supports. Solving these linear equations yields all the nodal displacement components which can then be substituted into Eqs. (3.6) to give the axial bar forces in the truss.

It must be noted that the above methods of truss analysis are for linear trusses. Other methods exist for general nonlinear trusses in which Eqs. (3.3) are nonlinear. This is the case of trusses with nonlinear materials or with large displacements. The minimum energy method is the most appropriate method for such structures, but it is rarely used for the usual linear structures for which the above described methods are simpler and more efficient.

3.2.3 DISCRETE OPTIMUM DESIGN FORMULATION

The minimum weight design of structural trusses described here is for general indeterminate pin-jointed plane trusses having the layout and external applied loads prespecified and the lengths and the material characteristics for the bars known. The formulation consists of minimizing the weight of the bars subject to the constitutive equations presented earlier and to other constraints which are presented later. The variables in this formulation are the cross-sectional areas of the bars, the axial bar

forces and the nodal displacement components at the joints of the truss.

3.2.3.1 WEIGHT OBJECTIVE FUNCTION

The objective function considered here is the weight of the bars of the truss and is given by:

$$W = \sum_{ij \in IJ} \rho_{ij} \, Le_{ij} \, A_{ij} \tag{3.8}$$

in which W is the total weight of bars; and ρ_{ij} is the material density of bar ij, $\forall ij \in IJ$.

3.2.3.2 OTHER CONSTRAINTS

These are the constraints which limit nodal displacements, bar stresses and bar sizes.

1. Nodal displacement constraints:

$$\sum_{ij \in IJ} \frac{Fax_{ij} \, Fax_{ij,k} \, Le_{ij}}{A_{ij} \, E_{ij}} \leq \delta_k \quad k=1,...,NK \tag{3.9}$$

in which $Fax_{ij,k}$ is the virtual force in bar ij associated with virtual unit force at joint k whose displacement must be limited to δ_k, k=1,...,NK; NK is the number of joints whose displacements are to be restricted.

2. Bar stress constraints:

$$\sigma_{ten} \leq \sigma_{ij} = \frac{Fax_{ij}}{A_{ij}} \leq \sigma_{com} \quad \forall ij \in IJ \tag{3.10}$$

where σ_{ij} is the axial stress in bar ij, $\forall ij \in IJ$, assuming positive for compression and negative for tension; σ_{ten} and σ_{com} are respectively the maximum permissible tensile and compressive stresses in the truss bars. Note that σ_{com} may be assumed lower than the absolute value of σ_{ten} to allow the buckling effects to be taken implicitly into account.

3. Bar size constraints:

$$A_{ij} \in A_D \geq A_{min} \quad \forall ij \in IJ \tag{3.11}$$

in which A_D is the set of commercially available discrete bar sizes; and A_{min} is the smallest bar size allowed in the truss.

Having defined the objective function and the constraints which are to be satisfied in the design, the following formulation of the minimum weight of a structural truss can now be constructed as Problem 4 which is formulated for one load case, but it can easily be formulated for multiple load cases by including a set of constraints for each load case in turn.

Problem 4

$$Minimize \quad W = \sum_{ij \in IJ} \rho_{ij} \, Le_{ij} \, A_{ij} \tag{3.8}$$

subject to:

$$\sum_{i=1}^{NN} Fax_{ij} \sin \theta_{ij} + Fex_{jv} = 0 \quad j=1,...,NN \tag{3.1a}$$

$$\sum_{i=1}^{NN} Fax_{ij} \cos \theta_{ij} + Fex_{jh} = 0 \quad j=1,...,NN \tag{3.1b}$$

$$\cos \theta_{ij} \, (\delta_{jh} - \delta_{ih}) + \sin \theta_{ij} \, (\delta_{jv} - \delta_{iv}) = \Delta_{ij} \quad \forall ij \in IJ \tag{3.2}$$

$$\Delta_{ij} = \frac{Le_{ij} \, Fax_{ij}}{A_{ij} \, E_{ij}} \quad \forall ij \in IJ \tag{3.3}$$

$$\sum_{ij \in IJ} \frac{Fax_{ij} \, Fax_{ij,k} \, Le_{ij}}{A_{ij} \, E_{ij}} \leq \delta_k \quad k=1,...,NK \tag{3.9}$$

$$\sigma_{ten} \leq \sigma_{ij} = \frac{Fax_{ij}}{A_{ij}} \leq \sigma_{com} \quad \forall ij \in IJ \tag{3.10}$$

$$A_{ij} \in A_D \geq A_{\min} \quad \forall ij \in IJ \tag{3.11}$$

3.2.4 SOLUTION METHODS

Although Problem 4 has been formulated for indeterminate trusses, it can also be used for determinate trusses for which Eqs. (3.2) and (3.3) may be omitted from the formulation as they are no longer necessary for calculating Fax_{ij} and $Fax_{ij,k}$. For indeterminate trusses, however, modern structural optimization practice uses iterative processes for solving Problem 4. The bar forces Fax_{ij} and $Fax_{ij,k}$ for each member of the truss are first calculated for an initial design and are held constant during the optimization which gives new bar sizes. For each iteration, the bar forces are calculated using the updated bar sizes. The process continues until a converged optimum design is reached. It is therefore assumed that numerical values for all bar forces Fax_{ij} and $Fax_{ij,k}$ will always be available when needed.

The optimization phase of Problem 4 is a nonlinear constrained optimization which can be solved by any standard constrained nonlinear programming algorithm assuming that the bar sizes are continuous-valued, i.e. relaxing the discreteness constraint of Eq. (3.11). However, from a practical point of view, the cross-sectional areas variables should be obtained as discrete values and must be chosen from a set of discrete sizes representing commercially available bars. Yates, Templeman and Boffey (1982) showed that this requirement makes Problem 4 extremely difficult to solve even for the simplest possible case of a statically determinate truss with a single displacement constraint.

Indeed, the combinatorial nature of the discrete optimum design requires enumerating designs containing all possible combinations of discrete member sizes and selecting the best combination of them. If NDB is the number of commercially available discrete bars in the set A_D from which the NB bars of the truss have to be chosen,

then there are $(NDB)^{NB}$ designs to be examined in order to a globally optimum discrete design can be guaranteed. This is enormously expensive in computer time. Although many methods have been developed to prune down the number of designs to be examined such as the Branch and Bound method (see Garfinkel and Nemhauser, 1972), the run time needed for the enumeration explodes exponentially as the number of the truss bars increases. Yates, Templeman and Boffey (1982) concluded that completely rigorous discrete optimum design methods cannot exist and research effort should be directed towards developing heuristic methods which have the goal of obtaining non-rigorous but very close discrete optimum designs. Templeman (1988a) reviewed some of those methods and discussed their practical capabilities for real structural trusses needs. Most of the methods apply some approximate rounding processes on the continuous optimum design to convert it to a discrete one. These methods are based on the idea that the continuous optimum design forms a close lower bound to the discrete optimum. This is fairly true for cases in which the discrete set of sizes to choose from is large and the sizes cover the size range fairly evenly. Practical design considerations however require a small set of discrete sizes to be used in the design for which the continuous optimum design does not form a very useful lower bound. The segmental optimum design method proposed by Templeman and Yates (1983) appreciates these practical considerations and does not use the continuous optimum design in any way. It is not enumerative and it turns out to be one of the most effective methods available for discrete optimum design. Therefore, it has been chosen to be used in this thesis, and it is described next.

3.2.4.1 SEGMENTAL OPTIMUM DESIGN METHOD

This method transforms ingeniously Problem 4 from a nonlinear programming problem to linear optimization by introducing artificial bars made up of several segments, each of known discrete size but unknown segment length, to replace the conventional bars with known lengths but unknown cross-sectional areas. This is due to the fact that the optimization phase of Problem 4 is nonlinear in respect to the cross-sectional areas of the bars but linear in terms of bar lengths. Figure 3.3 illustrates the assumed transformations for a single bar. The number of segments in

each bar should equal the number of discrete sizes in the set A_D, so all sizes are represented among the segments. Obviously, the total lengths of the segments in each bar must be equal to the known length of the conventional bar. Thus for each bar b, b=1,...,NB, in the truss, the following relationship must hold:

$$\sum_{d=1}^{NDB} l_{bd} = Le_b \quad b=1,...,NB \tag{3.12}$$

in which l_{bd} is the unknown length of segment d, d=1,...,NDB, in bar b, b=1,...,NB.

Assuming that axial bar forces in Problem 4 are available when needed, Eqs. (3.1), (3.2) and (3.3) may be omitted from the segmental optimum design formulation. Also, Eqs. (3.10) and (3.11) can be removed from the formulation provided that the set of discrete sizes A_D is chosen so that no segment will violate stress limits or minimum size limits. Therefore, the segmental optimum design can be formulated as follows:

Problem 5

$$Minimize \quad W = \sum_{b=1}^{NB} \sum_{d=1}^{NDB} \rho_b A_d l_{bd} \tag{3.13}$$

subject to:

$$\sum_{b=1}^{NB} \sum_{d=1}^{NDB} \frac{Fax_b Fax_{bk} l_{bd}}{A_d E_b} \le \delta_k \quad k=1,...,NK \tag{3.14}$$

$$\sum_{d=1}^{NDB} l_{bd} = Le_b \quad b=1,...,NB \tag{3.12}$$

$$l_{bd} \ge 0 \quad b=1,...,NB;\ d=1,...,NDB \tag{3.15}$$

Problem 5 is a linear programming problem with NBxNDB non-negative variables and NB+NK constraints. It can be solved easily by any standard linear programming algorithm to yield a segmental optimum design which has some members composed

of several segments and the rest having a single discrete segment. The sought discrete design can then be found by rounding up the multi-segment members by replacing the smaller sized segments by the same size as the largest segment. Templeman and Yates (1983) showed that the number of multi-segment members involved in the rounding is very small and equal to the number of active displacement constraints at the optimum. They concluded that the resulting rounded up segmental optimum design forms a very close upper bound to the discrete optimum design.

The above method can be used for determinate and indeterminate general structural trusses. However, the three phases of the method, i.e. the analysis, optimization and rounding process, should be made iteratively for indeterminate trusses. The only disadvantage of the method is the enormous increase of the number of variables. This is somewhat compensated by the fact that the problem is linear. However, the increased number of variables can be reduced quite effectively by grouping the members of the truss into several groups, each containing several members which are required to have the same bar size due to symmetrical needs or due to some similarities in structural purposes of the members.

Finally, it should be noted that Problem 5 is formulated for one load case. It can easily be formulated for multiple load cases by including a set of constraints for each load case in turn. Also, discrete material properties can be included in the method by assuming that the material of each bar of the truss is not known and must be selected from a set of available discrete materials, thus introducing member segments, each has a known discrete cross-sectional area and known discrete material properties but has an unknown length. This assumption, however, does not affect the nature of the method but does increase the size of the segmental linear programming problem enormously.

3.3 STRUCTURAL RELIABILITY

Optimum structural design problems, of which Problem (4 or 5) is an example, are constructed in a way that the objective functions and constraint functions are assumed to be deterministic, and the design parameters, namely the load and the strength, are considered as deterministic variables, i.e. they are assigned constant values. In reality, however, they are random variables. It is not possible for example to predict a unique value for a wave load acting on offshore platforms. Also, the strength of concrete used in structures may take several values depending on many factors which are out of the designer's control. The worst combination approach based on maximum value of load and minimum value of strength has been used in the conventional deterministic design approach to compensate for the uncertainty associated with the design parameters. Obviously, the worst combination approach becomes economically unreasonable for structures subjected to loading with a broad spectrum such as nuclear reactors, offshore platforms, etc. Also, safety factors are used in the design process to account for the randomness of the design parameters and to compensate for the designer's ignorance of the exact behaviour of the structure under loading in its lifetime and for the effect of fabrication and construction. Such safety factors are assigned deterministic values based on experience and can be found in all standard codes of practice. Again, these safety factors are random as they are related to the design random variables (Freudenthal, 1956).

It may be concluded from the above discussion that the conventional deterministic approach to design does not produce a structure with a required level of safety. To guarantee such a safety, however, a probabilistic approach incorporating the uncertainty associated with the randomness of the design parameters has to be adopted. In the next section, probabilistic analysis methods, which are known as reliability analysis methods, for a single structural component and then for the entire structure are presented, followed by the probabilistic approach to design with review of its applications over the last three decades. Then, the concept of damage tolerant design used frequently in structural design is introduced.

3.3.1 PROBABILISTIC RELIABILITY ANALYSIS

The analysis of a structure in a probabilistic sense to determine its level of safety is known as reliability analysis. The reliability of a structure may be described as the probability that the structure will survive under the expected external loads applied to it in its lifetime. This probability of survival p_s is the complement of the probability of failure p_f of the corresponding structure, i.e.

$$p_s = 1 - p_f \tag{3.16}$$

To calculate the probability of failure of a structure, the failure modes have to be selected first in order to identify the limit state function which separates the safe state from the failure state. The failure modes may be the axial mode as in the case of trusses, or axial, bending and shear modes as in the case of rigid frame structures, etc. After the failure modes have been selected, the analysis of the structure is carried out on the basis of the mean values of the load and strength in order to estimate the effect of external load on the structure. Then, the reliability analysis may take place to measure the level of safety of the structure by means of calculating the probability of its failure. Many reliability techniques to estimate the probability of structural failure exist. Some of them are discussed next over the basic problem in the field of structural reliability which is called the fundamental case.

3.3.1.1 THE FUNDAMENTAL CASE

This is the situation of a single structural component with resistive strength R carrying an external load L as shown in Figure 3.4. Both strength R and load L are assumed to have predefined statistical distribution functions, and must be presented on the same scale; they are both axial forces in the fundamental case. The failure mode of this very basic case is the axial mode. Two ranges of strength may be identified in the axial mode, the compression and the tension range which are denoted as positive and negative strength respectively. Obviously, positive strength will resist positive load and negative strength will resist negative load. The two ranges of strength may have a single or different distribution functions. Freudenthal et al. (1966) assumed a single

distribution of the strength R for a given load L. This case is illustrated in Figure 3.5. Assuming that the distributions of R and L are independent and stating that the failure occurs whenever the magnitude of load is greater than strength, Freudenthal et al. (1966) derived the following equation for calculating the probability of failure:

$$p_f = p(R<L) = \int_0^{\infty} F_R(l)\, f_L(l)\, dl \qquad (3.17)$$

or equivalently:

$$p_f = \int_0^{\infty} [1-F_L(r)]\, f_R(r)\, dr \qquad (3.18)$$

in which $f_L(l)$ and $f_R(r)$ are the probability density functions of load and strength respectively; F_R and F_L are the cumulative probability distribution functions of strength and load respectively.

Ang and Amin (1968) developed other equations for calculating p_f assuming that the strength has two different distribution functions over the two random variables R_p and R_n representing the positive and negative strength respectively. This is illustrated in Figure 3.6. They stated that the failure occurs whenever positive strength is less than positive load or negative strength is greater than negative load. p_f is expressed as:

$$p_f = p[(R_p<L,\ L>0) \bigcup (R_n>L,\ L\leq 0)]$$

$$= \int_0^{\infty} [1-F_L(r_p)]\, f_{R_p}(r_p)\, dr_p + \int_{-\infty}^{0} F_L(r_n)\, f_{R_n}(r_n)\, dr_n \qquad (3.19)$$

or equivalently:

$$p_f = \int_0^{\infty} F_{R_p}(l)\, f_L(l)\, dl + \int_{-\infty}^{0} [1-F_{R_n}(l)]\, f_L(l)\, dl \qquad (3.20)$$

in which f_{Rp} and f_{Rn} are the probability density functions of positive and negative strength respectively; F_{Rp} and F_{Rn} are the cumulative probability distribution functions of positive and negative strength respectively.

Eqs. (3.17) through (3.20) have been derived directly from the distributions of load and strength. However, other equations may be derived using the residual strength RS=R-L (see Figure 3.7) or the factor of safety SF=R/L (see Figure 3.8). The probability of failure for such models may be estimated as (see Ang and Tang, 1984):

$$p_f = p(RS=R-L<0) = \int_{-\infty}^{0} f_{RS}(rs)\, drs = F_{RS}(0) \tag{3.21}$$

for the residual strength model, and:

$$p_f = p(SF=R/L<1) = \int_{0}^{1} f_{SF}(sf)\, dsf = F_{SF}(1.0) \tag{3.22}$$

for the factor of safety model. In Eq. (3.21), RS is the random variable of residual strength; f_{RS} and F_{RS} are respectively the probability density function and the cumulative probability distribution function of residual strength. In Eq. (3.22), SF is the random variable of factor of safety SF; f_{SF} and F_{SF} are the probability density function and the cumulative probability distribution function of factor of safety respectively.

3.3.1.2 APPROXIMATE STRUCTURAL RELIABILITY METHODS

The integral equation technique just presented, Eqs. (3.17-3.22), is based on the integration of the joint probability density function of the random variables over the failure domain. This can generally be expressed as:

$$p_f = p[g(X)<0] = \int_{g(X)<0} f_X(x)\, dx \tag{3.23}$$

where $f_X(x)$ is the joint probability density function of a vector X of N random variables x_i, i=1,...,N; g(X) is the performance state function which, when equal to zero, produces a limit state function which separates the failure domain from the safe domain.

The probability of failure calculated by using numerical integration of Eq. (3.23) can alternatively be calculated by a Monte Carlo simulation technique (see Robinstein,

1981). In this technique, NT sets of sample values of x_i, i=1,...,N, are randomly generated and the performance state function $g(x_i)$ is evaluated for each set x_i. The probability of failure is then estimated as the ratio of the number of events that yield $g(x_i)<0$ to the total number of trials NT. Melchers (1987) demonstrated that the number of trials NT is required to be much larger than $1/p_f$ (for example, NT≅$100/p_f$ as suggested by Bjerager, 1990) in order to achieve a good estimate of p_f.

Both the integration technique and the Monte Carlo simulation technique require the joint probability density function $f_X(x)$ or each of the individual probability density functions of each random variable to be constructed which is practically impossible due to scarcity of statistical data. However, it is quite common to use some analytical distributions to fit the available data. It is recalled here from Chapter 2 that Basu and Templeman (1984, 1985) showed that such selection of available analytical distributions to fit the available statistical data is a source of systematic error which affects to a large extent the estimation of probability of failure. They used the maximum entropy formalism presented in Chapter 2 as Problem 1 to generate the least biased distribution functions using the first four central moments of the residual strength random variable. Then, they performed the numerical integration of Eq. (3.23) to estimate the probability of failure.

However, it is impractical to calculate p_f from Eq. (3.23) by using numerical integration or Monte Carlo simulation due to computational inefficiency. Consequently, many approximate reliability methods have been developed, and Monte Carlo solutions have been practically restricted to verify or validate these approximate methods. Most of the approximate reliability methods use only the first two moments of the statistical data, i.e. the mean value and standard deviation. Cornell (1969) produced a very simple equation to measure the reliability by means of an index called the safety index and denoted as β:

$$\beta = \frac{\bar{g}(X)}{\sigma(g)} \tag{3.24}$$

where $\bar{g}(X)$ is the mean value of g (X); and $\sigma(g)$ is the standard deviation of g(X).

Assuming the random variable g(X) is normally distributed, the first order approximation of p_f may be written as:

$$p_f = \Phi(-\beta) = 1-\Phi(\beta) \tag{3.25}$$

where $\phi(.)$ is the cumulative normal distribution function.

For the fundamental case where g(X)=R-L, Eq. (3.24) becomes:

$$\beta = \frac{\overline{R} - \overline{L}}{\sqrt{\sigma_R^2 + \sigma_L^2}} \tag{3.26}$$

in which $\overline{R}$ and $\overline{L}$ are the mean values of strength and load respectively; σ_R and σ_L are respectively the standard deviations of strength and load. If R and L are assumed to be normally distributed, then g(X) may be considered as normally distributed and hence p_f can be calculated from Eq. (3.25).

Eq. (3.24) is a very simple technique of reliability analysis. It produces an exact result for linear performance functions, e.g. Eq. (3.26) for the fundamental case. In the case of nonlinear performance functions where only two moments are available, a linearization procedure by means of the first-order expansion of the Taylor series is carried out at the mean value of g(X). The mean value first-order second-moment technique, however, leads to erroneous estimates for highly nonlinear performance functions or for large coefficients of variation. A more rigorous and accurate method but computationally more intensive has been proposed by Hasofer and Lind (1974) who recommended that the first-order linearization of the performance function be done at the most probable failure point which should lie on the failure surface and which corresponds to the maximum likelihood of failure occurrence. Assuming that the random variables are continuous, uncorrelated and normally distributed, and introducing the reduced variables as $y_i = (x_i-\overline{x}_i)/\sigma(x_i)\ \forall i$, where y_i, i=1,...,N, are the reduced variables, Hasofer and Lind (1974) defined the safety index β as the minimum distance from the origin to the failure surface in the reduced space (see Figure 3.9 for the case of two variables; load and strength). They demonstrated that, for the fundamental case, the distance from the origin to the failure boundary (R-L=0) in the

reduced space is found to be equal to β calculated by Eq. (3.26).

The Hasofer-Lind method, which is called the advanced first-order second-moment method and which is later extended by Rackwitz and Fiessler (1978) to include random variable distribution information, approximates the general hypersurface g(X) by its tangent plane at the most probable failure point. The method works well as long as the limit state surface is nearly flat in the neighbourhood of the most probable failure point. However, when the performance function is highly nonlinear and hence the limit state surface is non-flat, the limit state surface is approximated by a paraboloid or a sphere at the most probable failure point using a second-order approximation techniques. Several second-order approximations of p_f have been derived such as Tvedt's three-term formulas (Tvedt, 1983) and Breitung's asymptotic (Breitung, 1984). The simplest second-order approximation of p_f is the one derived by Breitung (1984) which is based on a paraboloid fitting and it may be written as:

$$p_f = \Phi(-\beta) \prod_{i=1}^{N-1} (1-\beta k_i)^{-1/2} \qquad (3.27)$$

in which k_i $\forall i$, denote the main curvatures of the limit state surface at the most probable failure point, taken positive for a surface curved towards the origin.

Eq. (3.27) is a simple second-order approximation of p_f and it yields good results for rather large values of β, but it is of limited use only for $\beta k_i<1$. Recently, a second-order reliability method based on new approximations has been derived by Koyluoglu and Nielsen (1994). The new approximations are more complicated than Eq. (3.27) but they give better results and can be used for all values of β and all curvatures.

Higher-order approximation methods of reliability analysis are also available, e.g. Hong and Lind (1996), Grandhi and Wang (1997), etc. However, the higher-order approaches are very complicated and computationally expensive with a large number of variables. Therefore, different approaches have been developed to improve the approximation accuracy without using second or higher-order approximations. Based on the first-order reliability methods of Hasofer and Lind (1974) and Rackwitz and

Fiessler (1978), Wang and Grandhi (1994, 1996) produced an efficient safety index calculation algorithm for structural reliability analysis. They used adaptive nonlinear approximation models of the performance function in the original space (1994) and later in the standard normal space (1996) by selecting some appropriate intervening variables. The algorithm was found to be efficient and robust for several cases involving large coefficients of variation, non-normal distribution of random variables and highly nonlinear and complex performance functions.

Finally, the hypercone method presented by Mebarki, Lorrain and Bertin (1990, 1991) is worth mentioning here. The method considered the whole geometry of the failure domain however irregular and distorted it is without applying any approximations. However, only lower and upper bounds of p_f, instead of a unique value of p_f, could be found by respectively inscribing and circumscribing the failure domain by two idealized domains constituted by a set of hypercone sections. The method showed that the values of p_f deduced from the Hasofer-Lind index and those obtained by Monte Carlo simulations are within the lower and upper bounds found by the hypercone method, while the values of p_f calculated under the assumption that the state random variable g(X) might follow a normal distribution, Eq. (3.24), were found to be slightly inaccurate.

3.3.1.3 RELIABILITY ANALYSIS OF STRUCTURAL SYSTEMS

The structural analysis methods presented in the last two sections may be applied to the fundamental case in order to estimate the probability of its failure. Any structure, however, can be idealized by a set of fundamental cases. Once the p_f's for those fundamental cases are determined, p_f of the entire structure can then be found by a suitable combination of the fundamental cases found in the structure. The weakest-link model and the fail-safe model are the two most widely-used combination models available, and they are presented next.

1. Weakest-link model:

This model is illustrated in Figure 3.10. In this model which is also called the chain-type series model, system failure occurs if any element fails. The strength of the system would therefore be equal to the strength of its weakest element. Obviously, all statically determinate structures fall into this category. Freudenthal et al. (1966) were the first to introduce this model by stating that the probability of system failure equals the probability of the occurrence of at least one member failing, that is:

$$p_f(system) = p(FM_1 \cup FM_2 \cup \ldots \cup FM_{NM}) \tag{3.28}$$

in which p_f(system) is the probability of system failure; NM is the number of members in the structure; FM_i, i=1,...,NM, denotes the event of member i failing; $p(FM_1 \cup FM_2 \cup \ldots \cup FM_{NM})$ denotes the probability of the occurrence of at least one of the events FM_i, i=1,...,NM.

2. Fail-safe model:

This model is illustrated in Figure 3.11. In this model which is also called the parallel model, system failure occurs only when several elements exceed their strength capacity. Generally, all statically indeterminate structures may be modelled as fail-safe structures. However, some structures which are often mdelled as fail-safe structures may actually follow the weakest-link model. Moses and Stevenson (1970) argued that indeterminate elastic trusses with brittle members, i.e. they carry zero load after failing, with relatively small numbers of redundant members can be analyzed by the weakest-link model. This is due to the fact that the redistribution of loads following the failure of any member will trigger the failure of other members. Also, Moses and Stevenson (1970) and Moses (1974) demonstrated that in indeterminate trusses with small strength variability compared with the variability of the applied loads, like the case of dynamic loadings, system failure will be considered when any member fails. Moses and Stevenson (1970) concluded that the reliability of most indeterminate elastic trusses can be analyzed by finding the probability that any member fails under any load condition. This rather simplifies the problem, but surely determines a

conservative estimation of p_f of the entire structure.

In general, most indeterminate structures must be modeled by the fail-safe model. In this model, the failure of several members which constitutes system failure forms a single failure mode. There are usually many failure modes in fail-safe structures. The probability of system failure is therefore equal to the probability of the occurrence of at least one failure mode being reached. This is similar to the weakest-link model. Zimmerman et al. (1993), for example, illustrated that a rigid-plastic structure can be modelled as a series system with each element of the series being a failure mechanism. Therefore, Eq. (3.28) can be applied for fail-safe structures by replacing the probability of union of all NM members failing by the probability of union of all failure modes. Consequently, failure modes and their probabilities have to be identified first before the weakest-link model can be applied. This is a complicated task especially for large structures where a large number of potential failure modes exists. In such cases, therefore, numerous alternate paths have to be generated, yielding a large number of combinations of members which produce failure.

Many methods for identifying failure modes are available. Recent methods, however, simplify the problem by searching for the most dominant and significant failure modes based on their contributions to the estimate of the system probability of failure. Zimmerman et al. (1993) and Xiao and Mahadevan (1994) introduced such methods. These methods and others are not presented here since the interest of the present study concentrates on general linear trusses which as shown earlier can be analyzed by assuming system failure occurs when any member fails. However, a comprehensive review of available failure mode identification methods can be found in the two papers mentioned above.

It should be recalled at this point that once the failure modes have been identified and their probabilities of occurrence have been calculated (Tang and Melchers, 1988), the probability of system failure can then be calculated using Eq. (3.28) with failure mode replacing member failure. Therefore, the term "failure mode" will replace the term "member failure" hereafter in this thesis even for the weakest-link model since the

failure of a member may be considered as a failure mode having one member failing.

The calculation of the probability of system failure as the union of all possible failure modes, Eq. (3.28), requires the knowledge of the degree of dependence between all failure modes. Usually, the conservative assumption of independent failure modes is used. Therefore, from basic probability considerations (see Ang and Tang, 1975, for example) Eq. (3.28) becomes:

$$p_f(system) = 1 - \prod_{i=1}^{NM} [1 - p(FM_i)] \tag{3.29}$$

in which $p(FM_i)$ is the probability of failure mode i, i=1,...,NM; where NM being the number of failure modes.

However, the events of failure modes are not independent. For series systems, for example, the same random variable of applied load appears in each component failure event. Kjerengtroen and Wirsching (1984) demonstrated that the conservative assumption of Eq. (3.29) may produce weight penalties of more than 10% for chain-like series structures. Also, failure modes identified in parallel structural systems are not independent as they share some elements and resist the same loadings (Stevenson and Moses, 1970).

However, the degree of dependence between different failure modes is not clear due to the involvement of random quantities. Therefore, system reliability analysis is simplified by the use of upper and lower bounds on the exact value of failure probability. The efficiency of the bounds is dependent on how close the bounds are to each other. Cornell (1967) produced upper and lower bounds on system probability of failure by assuming independent and perfectly correlated (i.e. maximally dependent) failure modes respectively. Assuming independent modes, Cornell's upper bound may be obtained as Eq. (3.29). While assuming failure modes are maximally dependent, Cornell's lower bound would be equal to the maximum value of all mode failure probabilities. Thus, Cornell's upper and lower bound formula has the form:

$$Max\ p(FM_i) \le p_f(system) \le 1-\prod [1-p(FM_i)] \quad i=1,...,NM \tag{3.30}$$

Cui and Blockley (1991) argued that Cornell's bounds, Eq. (3.30), seems to exclude possible values varying between minimum dependence and independence. They showed that upper and lower bounds should be evaluated by the assumption of minimum and maximum dependence models respectively, and the independence model is a special case of dependence which lies between the above extreme models. The resulting upper and lower bound formula which is known as the unknown dependence model was shown to have the form (Cui and Blockley, 1991):

$$Max\ p(FM_i) \le p_f(system) \le \sum p(FM_i) \quad i=1,...,NM \tag{3.31}$$

for values of $p(FM_i)<<1$, i=1,...,NM. It should be noted here that Cornell's upper bound in Eq. (3.30) may be approximated by the upper bound of Eq. (3.31) for very small failure probabilities as recommended by Cornell (1967).

More accurate but more complicated bounds of system probability of failure are those due to Ditlevsen (1979). Unlike Cornell's bounds, they are based on all the pairwise mode intersection failure probabilities in addition to all single mode failure probabilities. The lower bound has the form:

$$p_f(system) \ge p(FM_1) + \sum_{i=2}^{NM} \max\ [p(FM_i) - \sum_{j=1}^{i-1} p(FM_i \cap FM_j)\ ,\ 0] \tag{3.32}$$

in which $p(FM_i \cap FM_j)$ is the failure probability of the intersection of failure mode i and j, while the upper bound has the form:

$$p_f(system) \le \sum_{i=1}^{NM} p(FM_i) - \sum_{i=2}^{NM} \max_{for j<i} p(FM_i \cap FM_j) \tag{3.33}$$

It should be noted that Ditlevsen's bounds calculated by Eqs. (3.32) and (3.33) may be influenced by the ordering chosen for failure modes, and the closest bounds need not correspond to the same ordering used for the lower and upper bounds.

Finally, a completely different approach to measuring structural reliability has been proposed by Wu, Blockley and Woodman (1993a, 1993b) by means of vulnerability

analysis. A structural system was represented hierarchically in terms of clusters of structural rings which contain a sequence of members connected by a set of joints. A failure scenario which transforms each structural ring into a mechanism has been identified. Then, the effort required to transform a ring into a mechanism for each failure scenario has been calculated under the name "damage demand". The most robust ring will be the one with maximal damage demand, while the ring with minimal damage demand will be the most vulnerable one which will be used as a measure of the relative robustness of the whole structure. Such vulnerable rings will enable the identification of the most vulnerable parts of a structure so that they may be suitably protected and monitored.

Having presented the most widely used methods of structural reliability analysis, their practical applications in structural design are reviewed next.

3.3.2 PROBABILITY-BASED DESIGN

The structural reliability analysis methods presented in the previous sections have been used frequently in the literature to assess the reliability of existing structures (Trautner and Frangopol, 1990) and to examine the reliability of analysis and design methods used in different codes of practice, for example the analysis of holonomic elastoplastic trusses (Katsuki, Frangopol and Ishikawa, 1993a, 1993b), cable-stayed bridge design (Bruneau, 1992), prestressed concrete beams (Al-Harthy and Frangopol, 1994) and nonlinear analysis of reinforced concrete structures (Val, Bljuger and Yankelevsky, 1997). Although structural reliability analysis methods can be criticised at philosophical, theoretical and practical levels (Templeman, 1988b) and they lead sometimes to inaccurate results due to the approximate models and simplified analysis procedures adopted (Karamchandani, 1990), they are widely used in the practical design of offshore and nuclear structures and are approaching code of practice status for general structures.

Much research has been carried out in the last two or three decades in an attempt to formalize probability-based design methods in a code format starting from

(Cornell,1969), (Ang and Cornell, 1974), (Ravindra, Lind and Siu, 1974) and (Ellingwood and Ang, 1974) through (Ditlevsen and Madsen, 1989) and (Galambos, 1990) and finishing with (Ellingwood, 1994) and (Mrazik and Krizma, 1997). Although the final format of probability-based design has not yet been reached, the probability-based optimum structural design approach is well established and its applications are intensively published in the literature.

In the probability-based optimum approach, the weight or cost of a structure is minimized subject to constraints on the structural probability of failure. Alternatively, the probability of failure of the entire structure is minimized subject to an allowable structural weight or cost. Another approach is to minimize the total cost of the structure which includes the initial cost and cost of failure. In this approach, minimizing the cost of failure will automatically minimize the probability of failure of the entire structure, hence enhancing structural reliability. The first approach, however, is the most used approach in the literature. Hilton and Feigen (1960) used this approach to minimize the weight of a structure for a given reliability assuming that failures of individual components of the structure are statistically independent. Kalaba (1961) extended Hilton and Feigen's (1960) formulation to include the cost of materials. Also, Switsky (1964) used Hilton and Feigen's (1960) approach to conclude that in order to achieve minimum weight, member sizes have to be selected so that the probability of failure of each member is proportioned with its weight.

Unlike the above works, Moses and Kinser (1967) considered the correlation between failure mode events. They showed that significant weight savings could be obtained assuming that failure modes are dependent. Also, Moses and Stevenson (1970) used the dependence model in the collapse mechanism approach and the fail-safe criterion for optimizing a framed structure. Based on failure mode events, Takada, Kohama and Miyamura (1994) presented an efficient search technique to pursue predominant combinations of failure modes which were used in Ditlevsen's upper bound of system probability of failure. The resulting failure probability was constrained in the optimization process to minimize the weight of a space truss. Alternatively, the selected dominant failure modes have been added step by step by Murotsu, Shao and

Watanabe (1994) to the set of constraints to facilitate the optimization of redundant structures.

Kwak and Lee (1987) developed a sensitivity analysis formulation for reliability-based optimization using the advanced first-order second-moment approach of Hasofer and Lind (1973). For one-bay, two storey frame design, they used the upper bound of system failure probability of Eq. (3.31) in their formulation. Moreover, Liu and Moses (1992) presented an optimization model for truss structures with system reliability constraints. In searching for an appropriate system reliability measure, they showed that the average of upper and lower bounds of reliability corresponding to Ditlevsen's bounds of probability of failure was the most efficient measure of system reliability. They demonstrated that optimizing a truss with constraints on this average reliability measure would decrease the weight of the original truss and also would improve its reliability, while deterministic optimization would decrease the weight and the reliability simultaneously.

Chang, Ger and Cheng (1994) used two objective functions, weight and cost, to optimize steel structures subjected to seismic loadings. They showed that the optimum weight increased rapidly with the increase of coefficient of variation of the earthquake load especially at high reliability levels. They also demonstrated that the optimum weight was sensitive to the type of load distribution used. In the cost objective function approach, the cost of failure was included with the initial cost in the total cost function. The reliability of the structure increased when this total cost function was minimized as this will minimize the cost of failure and hence failure probability.

Recently, Borri and Speranzini (1997) proposed an algorithm for optimum structures with prefixed reliability requirements. They showed that the proposed algorithm can be implemented within any Finite Element code provided that this code contains an internal minimization routine. At each iteration of the objective function minimization process, structural analysis was performed to define the limit state condition and the reliability index was calculated in an internal loop by minimizing the distance between the origin of the space of the standardized independent normally distributed variables

and a point that respects the limit condition. The algorithm was applied on a three-dimensional truss structure with a large number of random variables and demonstrated that the algorithm is unaffected by problem size.

Finally, it should be noted that all the above applications are based on handling uncertainties associated with random variables, namely load and strength, which can be represented statistically by probability distributions. However, other uncertainties such as quality of construction, importance of the structure, skill of engineers, accuracy of analysis methods, etc. cannot be statistically modelled. Templeman (1987) showed how such fuzzy uncertainties can be incorporated into reliability-based optimum structural design formulation along with statistical uncertainties.

3.3.3 DAMAGE TOLERANT DESIGN

The conventional structural design methods aim to satisfy serviceability limit state requirements such as excessive deformation or crack formation, and ultimate limit state requirements such as plastic collapse or instability occurrences. The minimum strength required for the structure to fulfil these requirements is called the intact strength. For safety considerations, the concept of safety factor has been introduced into design methods to achieve a structure having strength beyond its intact strength by a margin called reserve strength which is determined by the amount of load beyond the working load the structure can carry before it collapses.

The above conventional methods, however, do not consider the behaviour of structures under some damage conditions which lie intermediate between the start of the unserviceability state and the final collapse state. Such damage conditions may play a significant role in the design methods if a structure has to be designed to sustain some damage without leading to a complete failure, as is the requirement for many structures. The damage conditions may be considered as complete damage of one member or more depending on the type of the structure and its importance. Consequently, structures must be designed to have some extra strength so a structure can exhibit damage tolerance once a member has failed. The minimum strength of the

structure among all expected damage conditions is called the residual strength.

Arora et al. (1980) defined a damage tolerant structure as a structure capable of performing its basic function even after it sustains a specified level of damage. Mistree (1983) and Shupe and Mistree(1987) suggested that a damage tolerant structure must have intact strength, reserve strength and residual strength in order to resist respectively initial failure, failure due to service loads exceeding design loads and further failure after the initial failure. Obviously, statically determinate structures cannot be designed to have residual strengths as the presence of all members is necessary for the structure not to collapse. For statically indeterminate structures, the failure of one member will not necessarily lead to complete failure. However, unless these structures have been very carefully designed and their configurations have been carefully chosen, failure of the most critical member may cause overloading for other members and possibly failure of more members leading to progressive collapse of the structure.

Designing a structure to be damage tolerant will inevitably lead to increase of its weight and hence its cost. A compromise between reserve strength, residual strength and cost, therefore, has to be adopted. Mistree (1983) presented a formulation of such a compromise criterion for damage tolerant design problems based on goal programming techniques (Ignizio, 1982). In his formulation, two types of constraints were included, system constraints and goal constraints. System constraints were defined to specify that the system capability to demand ratio for each failure mode should be greater or equal to factor of safety. Capability of a system may be defined as its strength, and the load or stress applied on the system may be considered as its demand. Two types of system constraints were included, catastrophic failure constraints, which may be due to buckling, for example, and non-catastrophic failure constraints, which may be due to tension, for example. Catastrophic failure constraints included those for the intact structure where factor of safety represents the reserve strength for a specific failure mode, and those for the damaged structure where the factor of safety for each failure mode represents the residual strength. The damaged structure was considered as the structure with one member failed. The non-catastrophic

constraints, on the other hand, were considered only for the intact structure. Bounds on the design variables and proportionality constraints to ensure that system components can be fabricated were also included in the system constraints.

The system constraints, however, will ensure the feasibility of the design but will not prevent the capability to demand ratios from being very large. The aim of the goal constraints was to prevent such large ratios and hence to produce a good feasible design. This was done by targeting the average capability to demand ratio among all failure modes to be equal to the target factor of safety for catastrophic and non-catastrophic constraints. Also, the cost of the structure should not exceed a specific cost. To achieve the above requirements as closely as possible, Mistree (1983) relaxed those requirements by introducing some deviation variables which were added to the above goals to produce goal constraints. The damage tolerant design problem became as follows. Given input data, find the design deviation variables to satisfy system and goal constraints by minimizing the set of deviation variables. Shupe and Mistree (1987) added some preference indices to the deviation variables in the objective function to be minimized. These ensure that some goal constraints are preferred to others. They applied the formulation on a thirteen-bar truss regarding the compromise between cost and reserve strength only. This application demonstrated the applicability and the accuracy of the formulation.

Frangopol et al. (1991) used optimum design formulation techniques to optimize damage tolerant structures. They minimized weight subject to constraints regarding the serviceability, ultimate load-carrying capacity and residual capacity requirements. Serviceability requirements demanded that elastic displacement at any section should not exceed an allowable value. Ultimate load-carrying capacity, on the other hand, should not be below a required capacity of the system. Finally, the minimum capacity of the damaged structure among all possible damage conditions (each member has been removed in turn) should be greater or equal to a required residual capacity of the system. The above formulation was applied to a five-bar truss for brittle and ductile materials showing that the rate of increase in reliability is much greater than the rate of increase of volume.

Finally, the concept of residual strength for damage tolerance has been used in reliability-based design methods. In their work which is presented in the previous section, Liu and Moses (1992) designed a sample truss by optimizing its weight subject to a prespecified system reliability constraint for the intact structure. The optimal design exhibited a decrease in weight and increase in reliability. However, examining this design further showed that such design was not safe during its expected damaged lifetime. Removing one of its members will decrease its reliability dramatically. Applying extra constraints regarding the residual reliability for each possible damage condition (each member has been removed in turn), Liu and Moses (1992) were able to obtain a damage tolerant structure with only a slight increase in weight.

Having presented the concept of structural damage tolerance and its applications, the review of structural truss models is now completed. It is recalled here that the aim of this chapter is to demonstrate the similarities between structural trusses and water supply networks in terms of analysis, optimum design and reliability approaches. This is described next.

3.4 SIMILARITIES IN THE ENGINEERING NETWORK SYSTEM MODELS

Figures 3.1 and 3.12 show respectively the familiar pictorial presentation of a typical structural truss and a water supply network. Both are illustrated by means of a set of IJ arcs connected by a set of NN nodes. The arcs represent bars or members for the truss and pipes or links for the water network. The nodes are truss joints or pipe junctions. For both cases, the external actions are applied at the nodes only. For the water network, these external actions are supply and demand flows q_n, which can be defined to be positive for demands and negative for supplies. On the other hand, the external actions applied on the truss are the external applied loads Fex_j including support reactions. In the truss case, each external load has a vertical and a horizontal component with positive directions chosen as shown in Figure 3.1. Each component for each external load can be considered to be equivalent to a demand flow if it is positive or a supply flow if it is negative, according to the directions defined in Figure

3.1.

Moreover, each node is associated with a nodal potential quantity which for the water network is the water pressure head H_i, and for the truss is the nodal displacement δ_i which again has two components, vertical and horizontal. Also, each arc has several quantities associated with it. For the water network, these quantities are the internal flow q_{ij} which is positive for the direction of the flow, the head loss quantity h_{ij} which is defined as the difference between pressure heads of the pipe ends and is positive for the direction of the flow, the pipe effective length Le_{ij}, the internal diameter of the pipe D_{ij} and a physical constant C_{ij} associated with pipe characteristic of roughness coefficient. On the other hand, each bar of the truss has similar quantities corresponding to those mentioned above. The axial force for each bar Fax_{ij} can be expressed as a force flow corresponding to the pipe flow q_{ij} of the water network. The axial force flow is defined to be positive for a compressive force and negative for a tensile force. However, bar forces are vectorial quantities and each has two components which can be calculated for a known layout and geometry of the truss. Also, each bar has an axial deformation quantity Δ_{ij} corresponding to the head loss h_{ij} of each pipe of the water network. This deformation is positive for compressive force and negative for tensile force. The remaining quantities associated with each bar of the truss are bar length Le_{ij}, cross-sectional area A_{ij} and the elastic modulus of the bar material E_{ij}. Those correspond respectively to the pipe length Le_{ij}, internal diameter of the pipe D_{ij} and the physical constant C_{ij} for the water network.

The above physical quantities for the truss and water network shown in Figure 3.1 and 3.12 respectively are evidently closely similar. The only difference is the vectorial nature of some of the truss quantities. Other striking similarities are discussed in the remainder of this chapter.

3.4.1 ANALYSIS PROBLEM

This includes constitutive equations, analysis problem formulation and solution methods.

3.4.1.1 CONSTITUTIVE EQUATIONS

The constitutive equations for the truss shown in Figure 3.1, namely bar force equilibrium equations, compatibility equations and characteristic force-strain relationship equations, were presented in section (3.2.1) of this chapter and for convenience are rewritten here as follows:

$$\sum_{i=1}^{NN} Fax_{ij} \sin \theta_{ij} + Fex_{jv} = 0 \quad j=1,...,NN \tag{3.1a}$$

$$\sum_{i=1}^{NN} Fax_{ij} \cos \theta_{ij} + Fex_{jh} = 0 \quad j=1,...,NN \tag{3.1b}$$

$$\cos \theta_{ij} (\delta_{jh}-\delta_{ih}) + \sin \theta_{ij} (\delta_{jv}-\delta_{iv}) = \Delta_{ij} \quad \forall ij \in IJ \tag{3.2}$$

$$\Delta_{ij} = \frac{Le_{ij}\, Fax_{ij}}{A_{ij}\, E_{ij}} \quad \forall ij \in IJ \tag{3.3}$$

For the water network problem shown in Figure 3.12, it is recalled from section (2.6.1.1) in Chapter 2 that the corresponding constitutive equations can be written as:

$$\sum_{j \in NU_n} q_{jn} - \sum_{k \in ND_n} q_{nk} = q_n \quad n=1,...,NN \tag{3.34}$$

$$H_i - H_j = h_{ij} \quad \forall ij \in IJ \tag{3.35}$$

$$h_{ij} = \frac{\alpha\, Le_{ij} \left(\frac{q_{ij}}{C_{ij}}\right)^{1.852}}{D_{ij}^{4.87}} \quad \forall ij \in IJ \tag{3.36}$$

where Eq. (3.35) is a special case of Eq. (2.18) considering paths which contain one link only.

The above two sets of constitutive equations hold a great deal of similarity. Eqs. (3.1a,b) and (3.34) are nodal flow continuity equations which connect the arc flows (force flows or water pipe flows) in a linear fashion. Also, Eqs. (3.2) and (3.35) are linear functions representing loss of nodal potentials on an arc (bar deformations or head losses). Finally, the arc flows and arc losses of nodal potentials are linked by Eqs. (3.3) and (3.36) which contain equivalent quantities. The difference between the two sets of the constitutive equations is related to these two relationship equations [Eqs. (3.3) and (3.36)]. They are linear for structural trusses, and highly nonlinear for water supply networks. However, for nonlinear trusses (nonlinear materials, large displacements, etc.) Eqs. (3.3) become nonlinear making them more closely similar to Eqs. (3.36).

3.4.1.2 ANALYSIS PROBLEM FORMULATION AND SOLUTION METHODS

Templeman and Yates (1984) described the similarities in analysis problem formulation and solution methods for trusses and water networks. For both cases, the analysis problem is to find the unknown arc flows (force flows or water pipe flows) and the unknown nodal potentials (nodal displacements or nodal pressure heads) which satisfy the set of constitutive equations [Eqs. (3.1a,b) to (3.3) or Eqs. (3.34) to (3.36)] provided that all other physical quantities are known. The only difference between the two formulations is that the problem is linear for linear trusses while it is nonlinear for water networks due to the nonlinearity of Eqs. (3.36). However, the nonlinearity of water network analysis formulation makes the problem more complicated but does not affect the similarity in concept and methods as will be seen later.

Two cases of analysis problem can be identified for each of the truss and water networks, the determinate case and the indeterminate case. In the determinate case, the number of unknown arc flows (force flows or water pipe flows) equals the number of usable continuity equations [Eqs. (3.1a,b) or Eqs. (3.34)]. It is recalled here that the

number of usable continuity equations for a structural truss is 2NN-3 (see section 3.2.2), and for a water network is NN-1 (see section 2.6.1.1.2 in Chapter 2). This corresponds to a statically determinate truss and a branched water network respectively. For this determinate case, continuity equations [Eqs. (3.1a,b) or Eqs. (3.34)] can easily be solved to give unique values for all arc flows (force flows or water pipe flows). Substituting these arc flows into arc flows-arc potential losses relationship equations [Eqs. (3.3) or Eqs. (3.36)] gives arc potential losses (bar deformations or head losses) which in turn are substituted into arc potential loss equations [Eqs. (3.2) or Eqs. (3.35)] to yield unique values for nodal potentials (nodal displacement components or nodal pressure heads) and thus the analysis problem is solved. Note that the nonlinearity of the water network analysis problem for the determinate case does not introduce any difficulties since the nonlinear equations [Eqs. (3.36)] are solved only after all water link flows have already been calculated from Eqs. (3.34).

The indeterminate case, however, is more complicated as the number of unknown arc flows (force flows or water pipe flows) is greater than the number of usable continuity equations. This corresponds to a statically indeterminate truss and a looped water network. For this indeterminate case, the continuity equations are not sufficient to determine unique values of the arc flows (force flows or water pipe flows), and a simultaneous solution of all the constitutive equations is therefore necessary to solve the problem. The presence of nonlinear Eqs. (3.36) in water network problems introduces further difficulties since these nonlinear equations are involved in the required simultaneous solution of the corresponding constitutive equations. Analytical solution methods for indeterminate water networks aim to linearize Eqs. (3.36) first and then to solve the resulting set of linear equations in ways which turn out to be similar to those used for the indeterminate truss analysis problem.

The flexibility method and the stiffness method presented earlier in this chapter are the most widely used methods for the indeterminate structural truss analysis problem. The parallel methods for the looped water network analysis problem are respectively the Newton-Raphson method of Martin and Peters (1963) and the linear theory method

of Wood and Charles (1972).

In the Newton-Raphson method, the redundant pipes (one pipe for each loop) are removed and replaced by external flows equal to the unknown internal water flows in the removed pipes. Then the internal link flows for all the pipes in the resulting branched network can be calculated in terms of the unknown redundant flows. The resulting flows are substituted into nonlinear Eqs. (3.36) which are then linearized by a Taylor series expansion to yield linear head loss equations for all pipes in terms of initial link flows for the redundant pipes and flow rate increments (see Martin and Peters, 1963). At this stage the compatibility equations, which require the sum of head losses around each loop to be zero, can be set up to yield a number of equations equal to the number of loops with the same number of unknown flow rate increments. Solving these linear equations iteratively gives the required flow rate increments necessary to correct all the pipe flow rates so that the sum of head losses around each loop is restored to zero. Hence, all pipe flows are calculated and the analysis problem is solved.

The above method is constructed in a way very similar to the flexibility method for truss analysis presented earlier in this chapter. However, the Hardy-Cross method (see section 2.6.1.2.1 in Chapter 2) which uses a one-at-a-time approach to solve the nonlinear equations of the water network analysis problem has no counterpart for truss analysis problem as this problem is linear.

In the linear theory method (Wood and Charles, 1972), the pipe flows are expressed in terms of unknown pressure heads by eliminating pipe head loss terms from Eqs. (3.35) and (3.36). The resulting nonlinear pipe flow equations are linearized by a Taylor series expansion using initial pressure head values and unknown nodal pressure head increments (see Wood and Charles, 1972). The resulting linear pipe flow equations are solved iteratively to give the required pressure head increments which then are used to give the pressure heads and hence the pipe flows. Apart from the necessary iterative procedure, the linear method is similar to the stiffness method used for truss analysis problem.

Finally, it is worth mentioning here that the energy index method of Kaya and Simon (1974) for water network analysis is closely similar to minimum energy analysis of trusses which is usually used for nonlinear cases such as trusses with nonlinear materials or with large displacements. This method was not presented when structural trusses were reviewed earlier in this chapter as the present work is concerned with linear trusses only. Therefore, the corresponding parallel method for water network (Kaya and Simon, 1974) is not presented here.

3.4.2 OPTIMUM DESIGN PROBLEM

Cheng and Ma (1989) and Templeman (1992b) pointed out the similarity between optimum design problem formulations for water networks and structural trusses. Both formulations were presented earlier as Problem 2 and Problem 4 respectively. For both problems, the arc size quantities (pipe diameters or bar cross-sectional areas), the arc flows (water pipe flows or force flows) and the nodal potentials (nodal pressure heads or nodal displacements) are the unknowns in the optimum design problem formulations. The objective function is cost which has to be minimized subject to the constitutive equations [Eqs. (3.34) to (3.36) or Eqs. (3.1a,b) to (3.3)] and to other constraints (see Problem 2 presented in Chapter 2 and Problem 4 presented earlier in this chapter). Note that the objective function used for trusses in Problem 4 is the weight function whose minimization leads directly to cost minimization. The other constraints used for optimum water network design formulation (Problem 2) are flow velocity constraints, nodal pressure constraints and pipe diameter constraints. The parallel constraints for optimum structural truss design formulation (Problem 4) are respectively bar stress constraints, nodal displacement constraints and bar size constraints.

The similarity between the two optimum design formulations is obvious. Both formulations are nonlinear programming problems having similar objective functions and parallel constraints with similar variables. Also, they both produce implicit determinate systems (branched water network or determinate truss) if one pattern of external applied actions (supplies and demands or external applied loads) are used in

the formulations. For reliability considerations, many patterns of external actions have to be used for both formulations making the problem extremely expensive in computer time. Moreover, the requirements that arc sizes (pipe diameters or bar cross-sectional areas) have to be chosen from a commercially available set of discrete sizes make both problems extremely difficult to solve (Yates, Templeman and Boffey, 1984, 1982). For these reasons and others, simplified methods have been developed to solve both problems. They turn out to be closely similar as has been demonstrated by Templeman (1992b).

The segmental truss optimum design method developed by Templeman and Yates (1983) and presented earlier in this chapter as Problem 5 is actually inspired by the optimum water network design method of Alperovits and Shamir (1977) who similarly transformed the problem, after specifying initial values for pipe flows, into a linear programming problem by replacing each pipe by several segments each of known diameter, chosen from discrete available sizes, but of unknown length. The resulting linear programming problem can then be easily solved to produce optimum design for the specified flows with few pipes having more than one segment. Quindry, Brill and Liebman (1981) showed how the initial pipe flows may be changed to further reduce the cost. The multi-segment pipes may later be rounded up in a similar way to that used for the segmental truss optimum design method.

Other methods which show some aspects of similarity can be found in the literature. The most obvious parallels may be those of Lai and Schaake (1969) and McKeown (1977) for water networks and structural trusses respectively. Both methods linearize the optimum problem by specifying a set of nodal potentials (nodal pressure heads or nodal displacements) and finding the optimum design for the specified nodal potentials. Quindry et al. (1981) and McKeown (1989) described how those nodal potentials may be changed to further reduce the cost of water networks and structural trusses respectively.

The above examples are not exclusive but surely demonstrate the similarity in the optimum design problem. Consequently, it can be concluded that structural trusses and

water supply systems are similar in many aspects. However, one aspect is still to be discussed which is reliability, and it is presented next.

3.4.3 RELIABILITY PROBLEM

It has been shown in the previous chapter and earlier in this chapter that designing optimum systems for both water supply networks and structural trusses should be based on a compromise between cost and reliability. A reliable system (water system or truss system) must meet some basic requirements under complete performance system conditions to satisfy specified applied actions (supply and demand flows or external applied loads). Also, such systems should be flexible and damage tolerant. Flexibility is defined as the ability of the system to carry applied actions other than those designed for, and damage tolerability is concerned with the behaviour of the system under some damage conditions.

The basic requirements of the reliability of water supply networks have been identified in Chapter 2 as mechanical reliability and hydraulic reliability. The mechanical reliability of a water network is defined as the probability that all demand nodes are connected and reachable from a source, while the hydraulic reliability is defined as the probability that a system can meet a specified level of flow at each demand node. Only hydraulic requirements have to be examined further for expected different supply/demand patterns (e.g. fire fighting requirements) to achieve a flexible network since the network is still undamaged and its mechanical reliability has already been tested, while both mechanical and hydraulic requirements have to be considered for each damage condition (usually each link in turn is assumed to be failed) to obtain a damage tolerant network.

On the other hand, structural reliability, as shown earlier in this chapter, is defined as the probability that load does not exceed strength. Both load and strength are treated as random variables fitted by some known probability distributions. Flexibility analysis for structural trusses is rarely done explicitly by considering different load cases since the variation of loads is accounted for by using probability distributions. However,

damage tolerant design is widely used in structures. A structure must be designed to have residual strength for some damage conditions in order to exhibit damage tolerance once any member of the structure has failed.

Comparing the reliability approaches for both water networks and structural trusses shows that basic reliability requirements for both systems are completely different. Water supply system design approaches do not use supply and demand flows and pipe carrying capacities as random variables as structural design methods do. Also, these latter methods have nothing to do with connectivity and reachability requirements considered by the former methods.

However, looking at damage tolerance approaches for both systems shows some aspects of similarity. Templeman (1992b) described some of these aspects. He argued that redundancy for both systems is necessary but not sufficient to produce reliable systems. The alternative paths (alternative supply paths or alternative load paths) provided by redundant systems (looped networks or indeterminate trusses) may be not usable in the event of some failure unless they have been designed to do so. The alternative path approach is well recognized in water network design methods and is widely used in structures in terms of damage tolerant design methods as shown earlier in this chapter.

However, designing a structure to be capable of fulfilling its full performance capacity with any one member failed is quite expensive. Therefore, a reduced performance is acceptable for a system to exhibit in its damaged state. Liu and Moses (1992) used this reduced performance approach to design a reliable and damage tolerant truss. Templeman (1992b) showed how such as approach can be applied on a simple network example.

Regarding reliability of water supply systems, it is recalled here from Chapter 2 that Tanyimboh and Templeman (1993c) used entropy as a surrogate measure of water network reliability, and by incorporating this measure into the optimum design formulation they produced a reliable, flexible and damage tolerant network. The

entropy-based method has been found to be very simple and very efficient for water supply systems. The simplicity and the efficiency of the entropy water network method and the huge similarities between water supply and truss systems demonstrated earlier in every aspect, even in some reliability approaches, suggests possible structural applications. The entropy-based method for calculating maximum entropy flows in water distribution networks presented in Chapter 4 is applied to structural truss design methods in Chapter 8 where the resulting truss designs are tested against reliability and damage tolerance approaches, and compared to conventional designs.

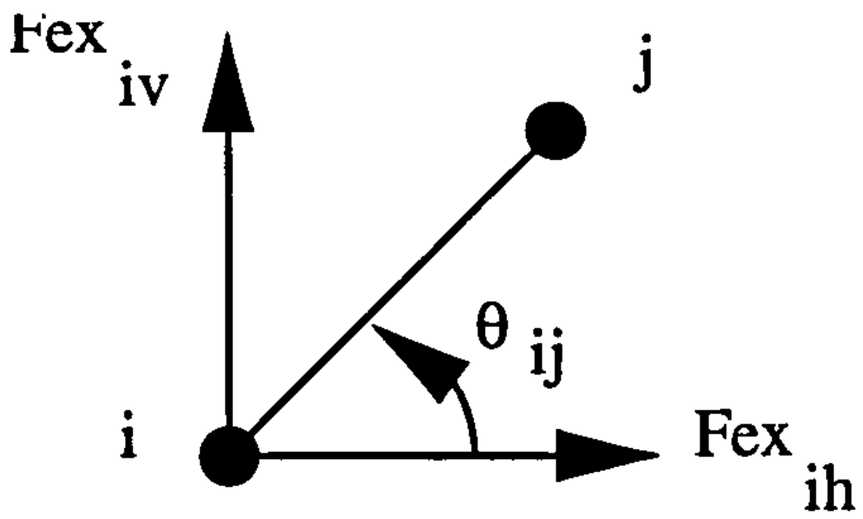

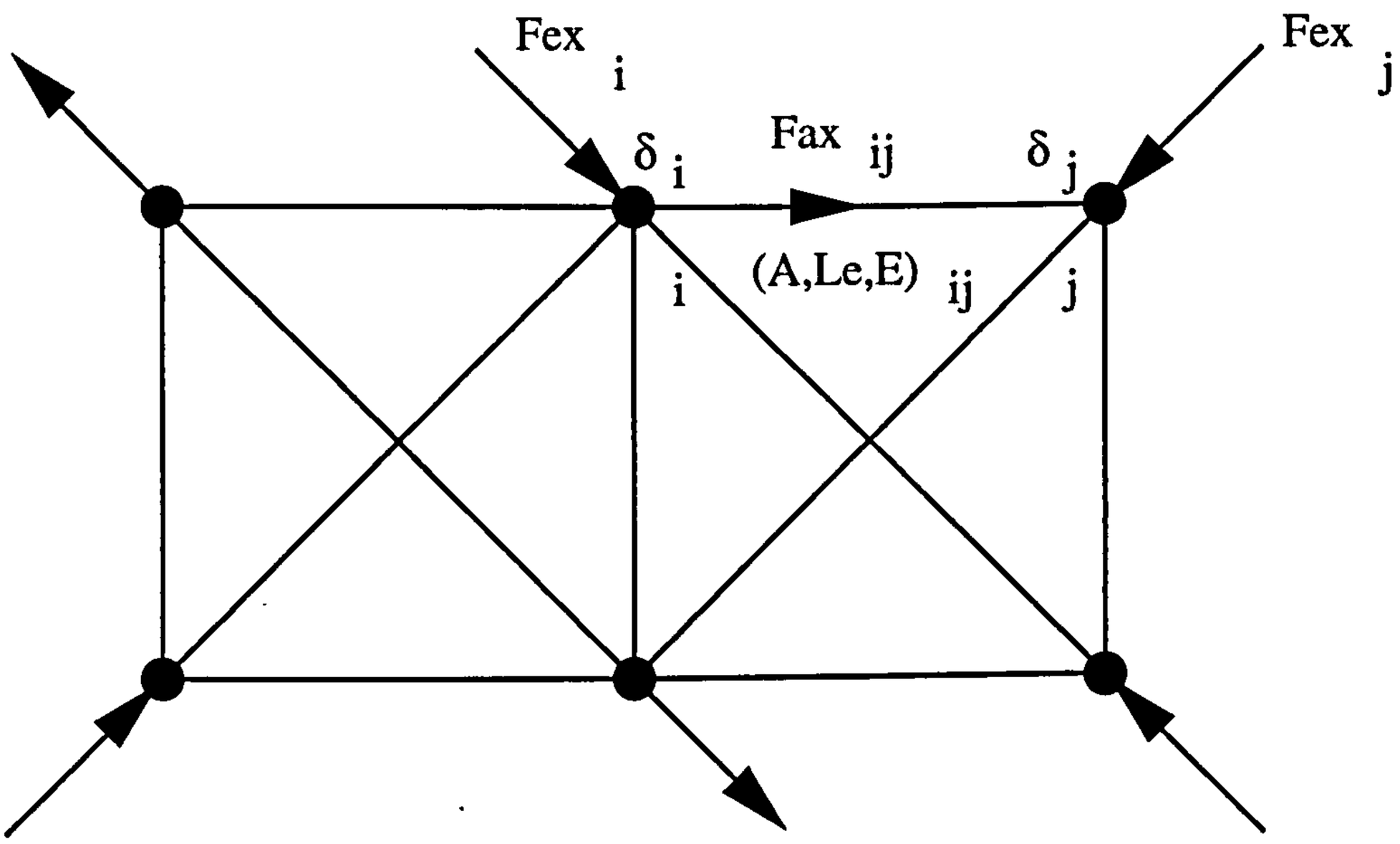

Figure 3.1 Typical structural truss

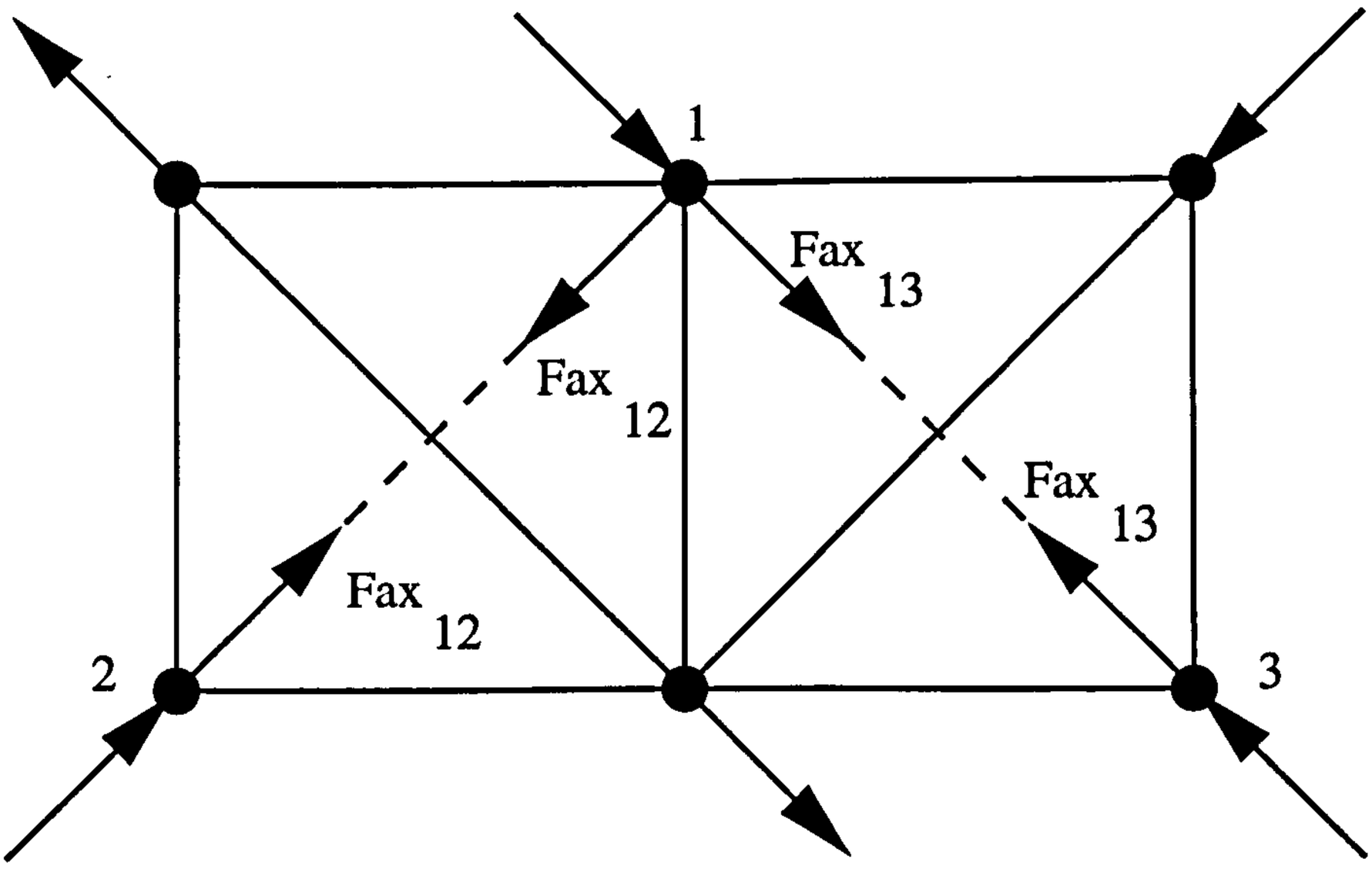

Figure 3.2 Truss with redundant bars replaced by external applied loads

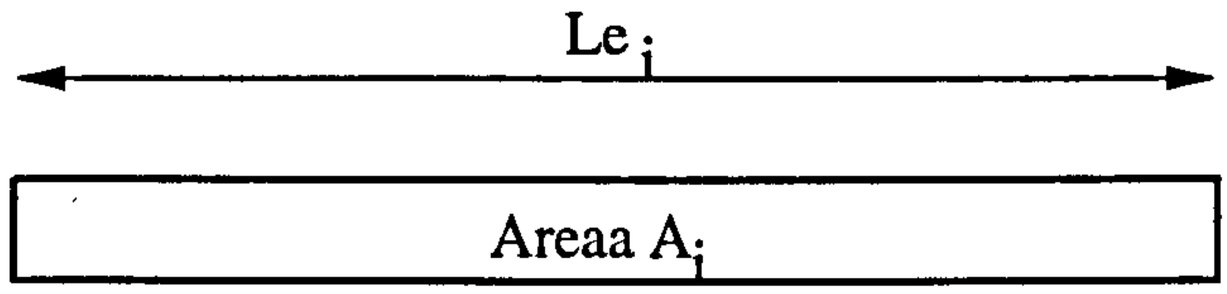

Conventional Member

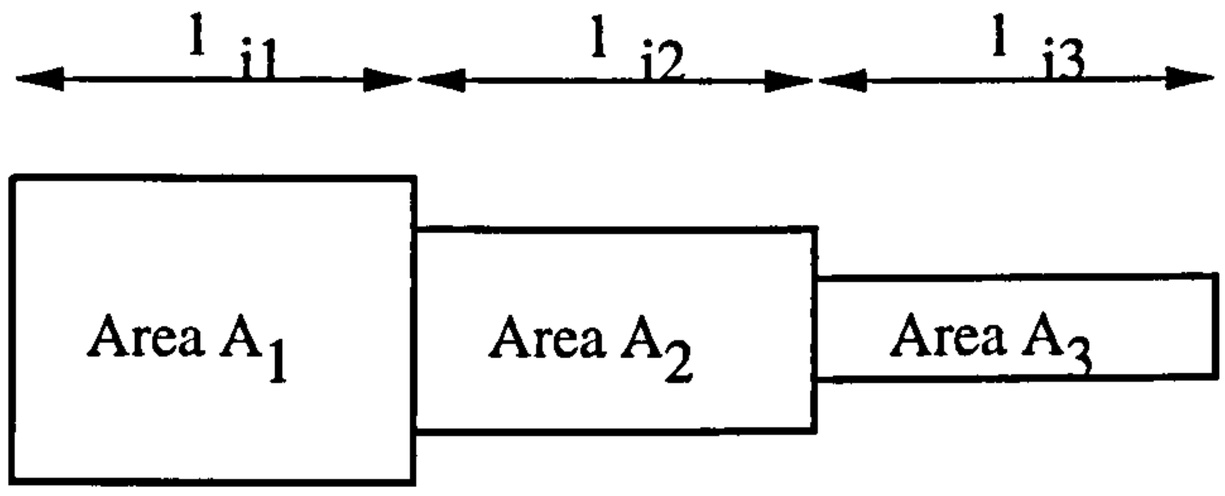

Segmental Member

Figure 3.3 Conventional and segmental axial force bars

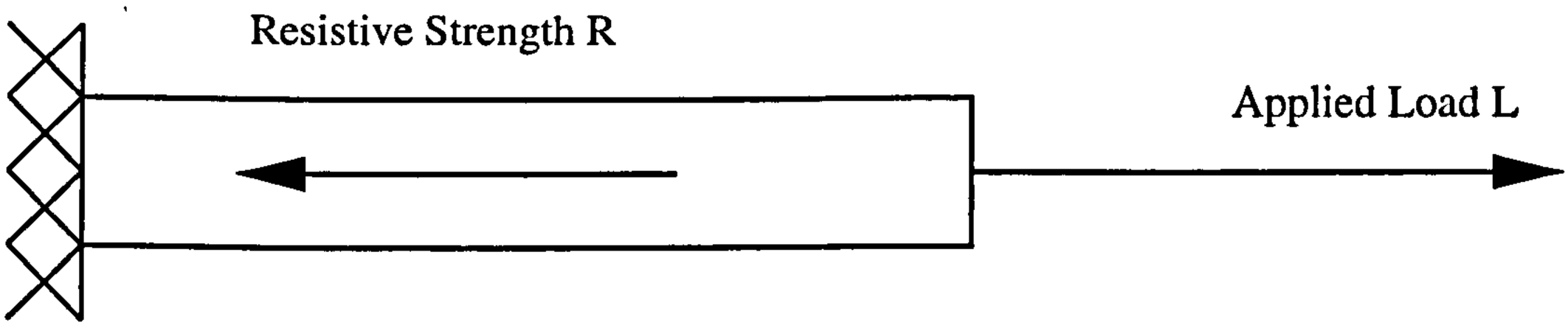

Figure 3.4 The fundamental case

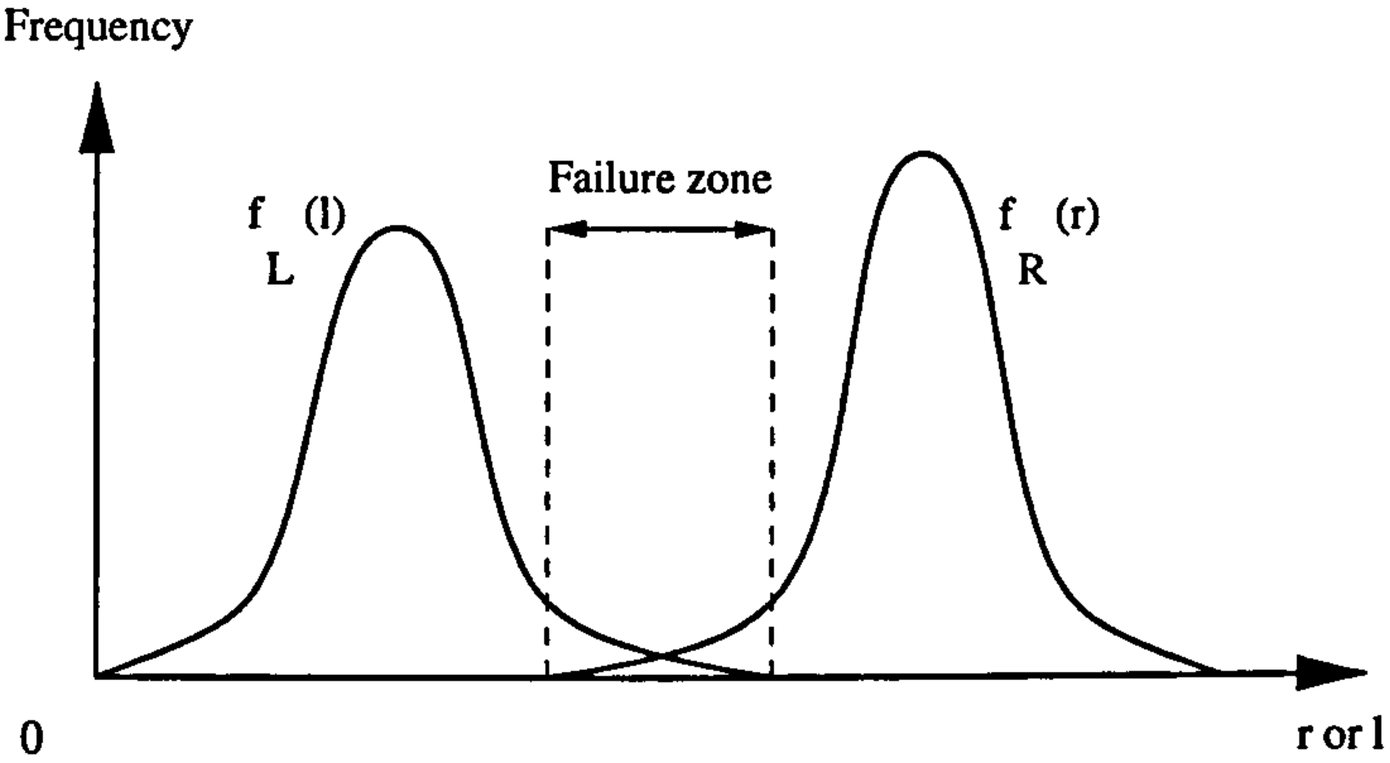

Figure 3.5 Single distribution of strength R for a given load L

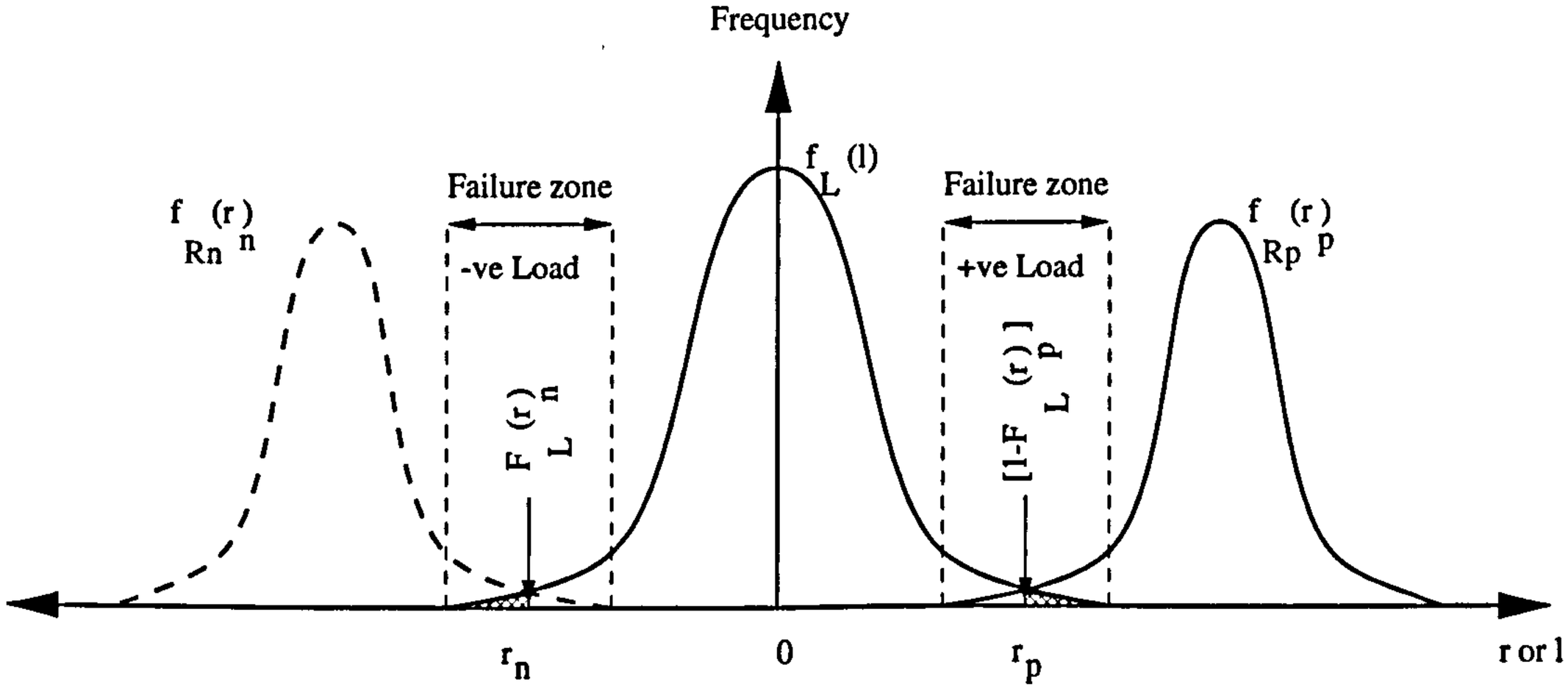

Figure 3.6 Different distributions of strength R for positive and negative load

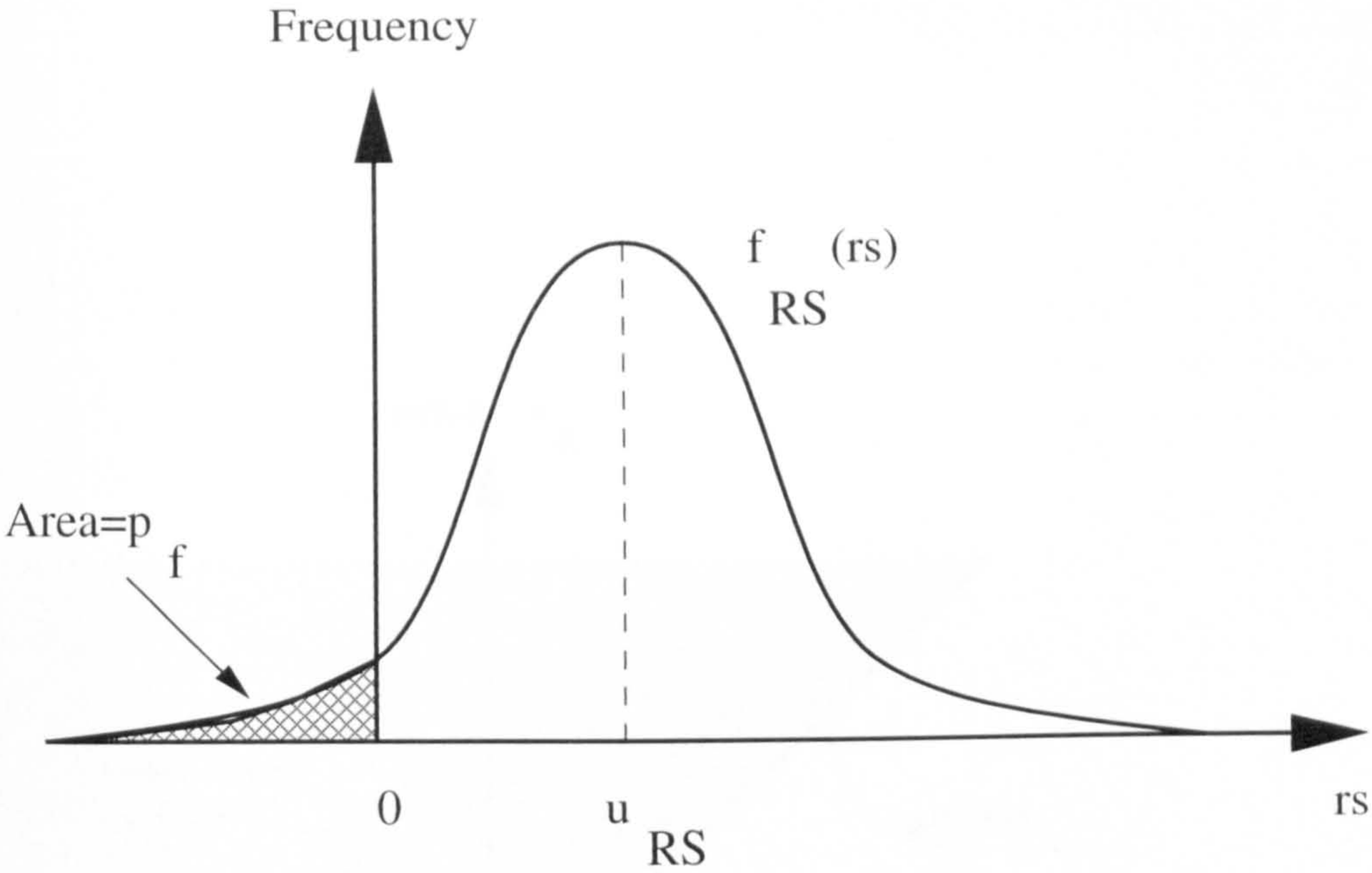

Figure 3.7 Concept of residual strength

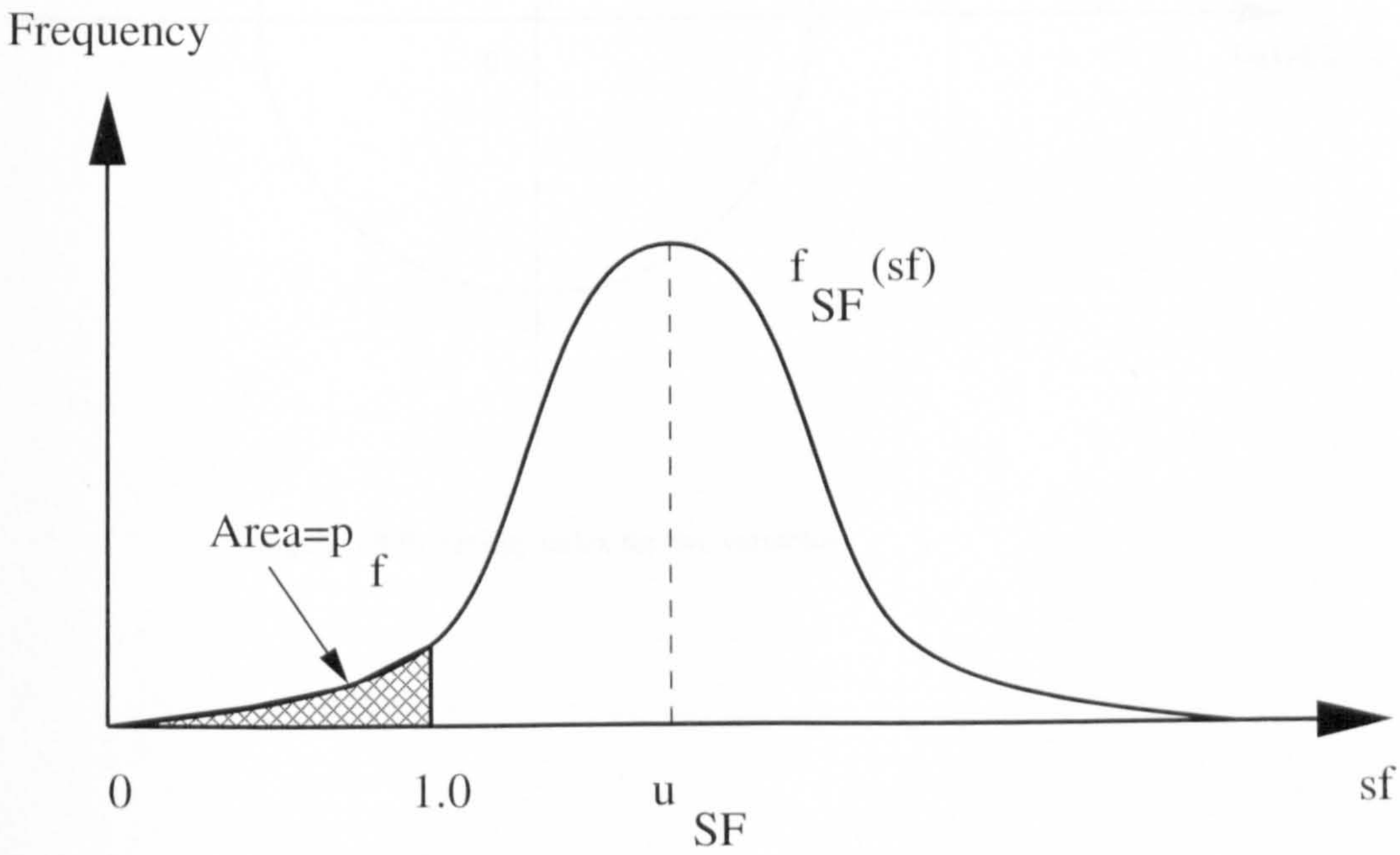

Figure 3.8 Concept of factor of safety

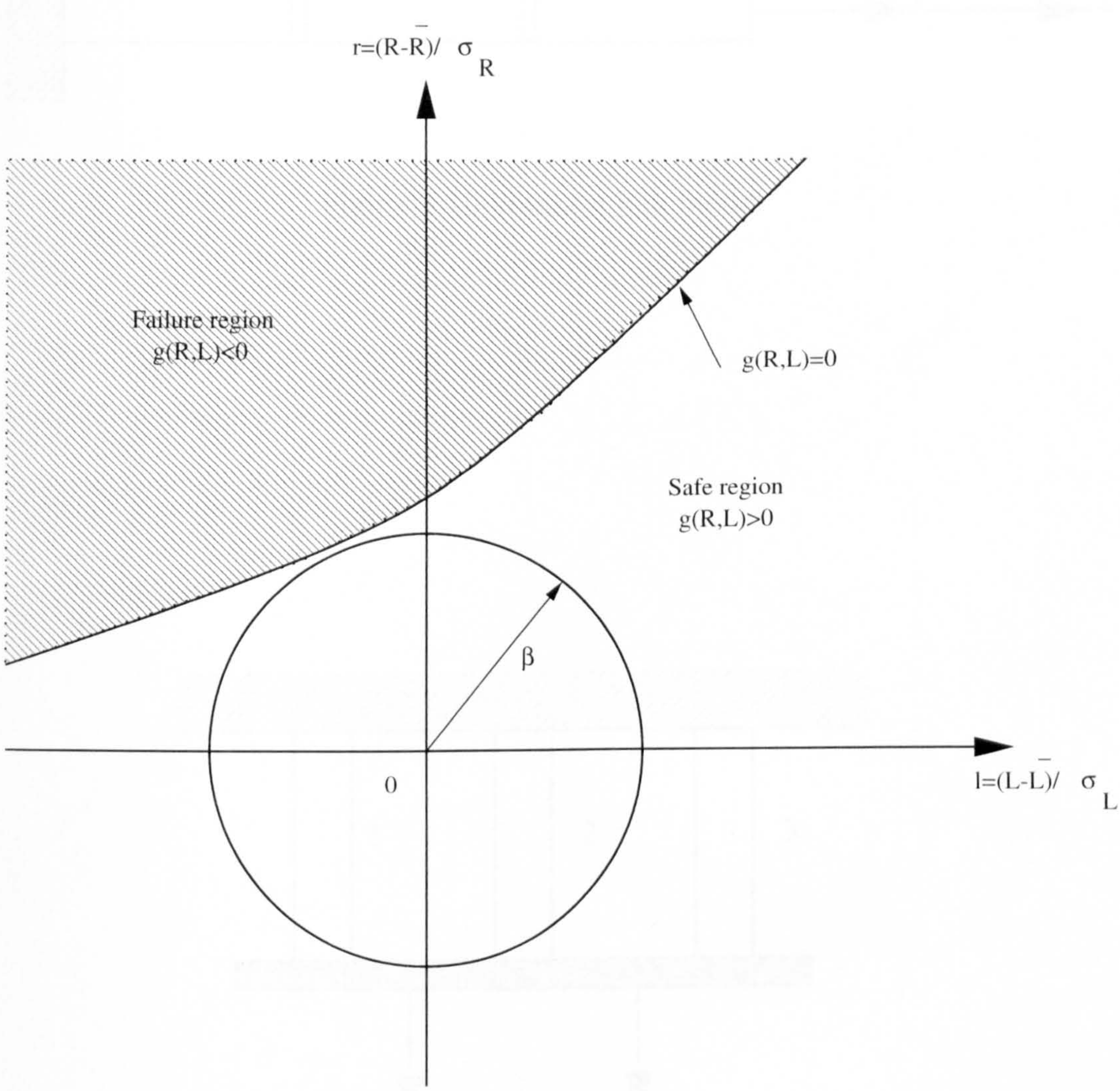

Figure 3.9 Reliability index for two variables

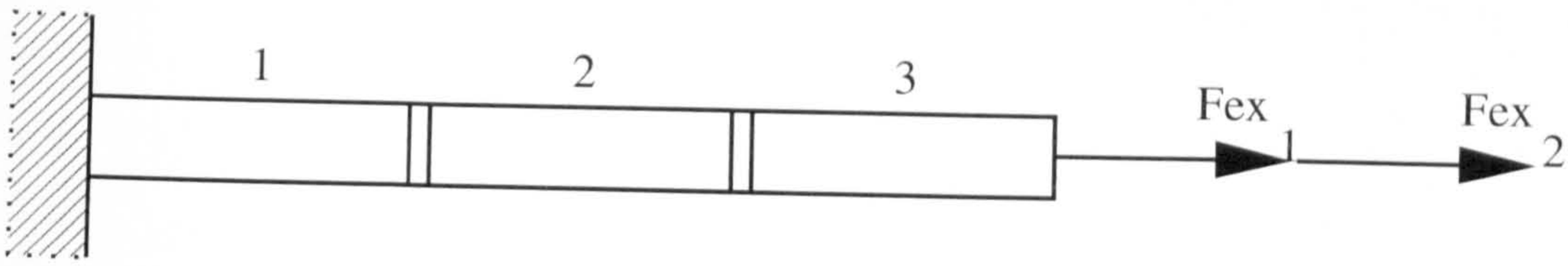

Figure 3.10 Weakest link model

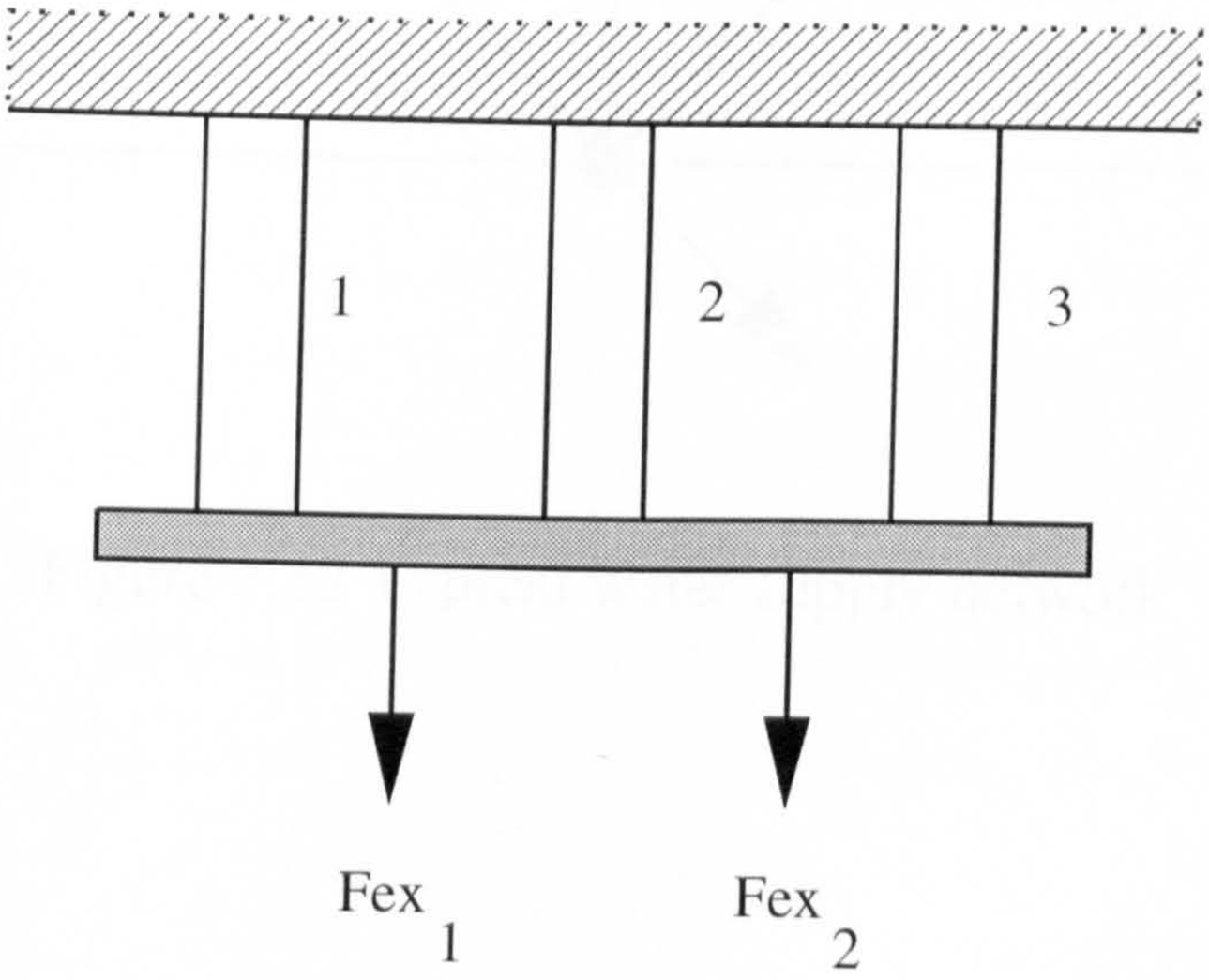

Figure 3.11 Fail safe model

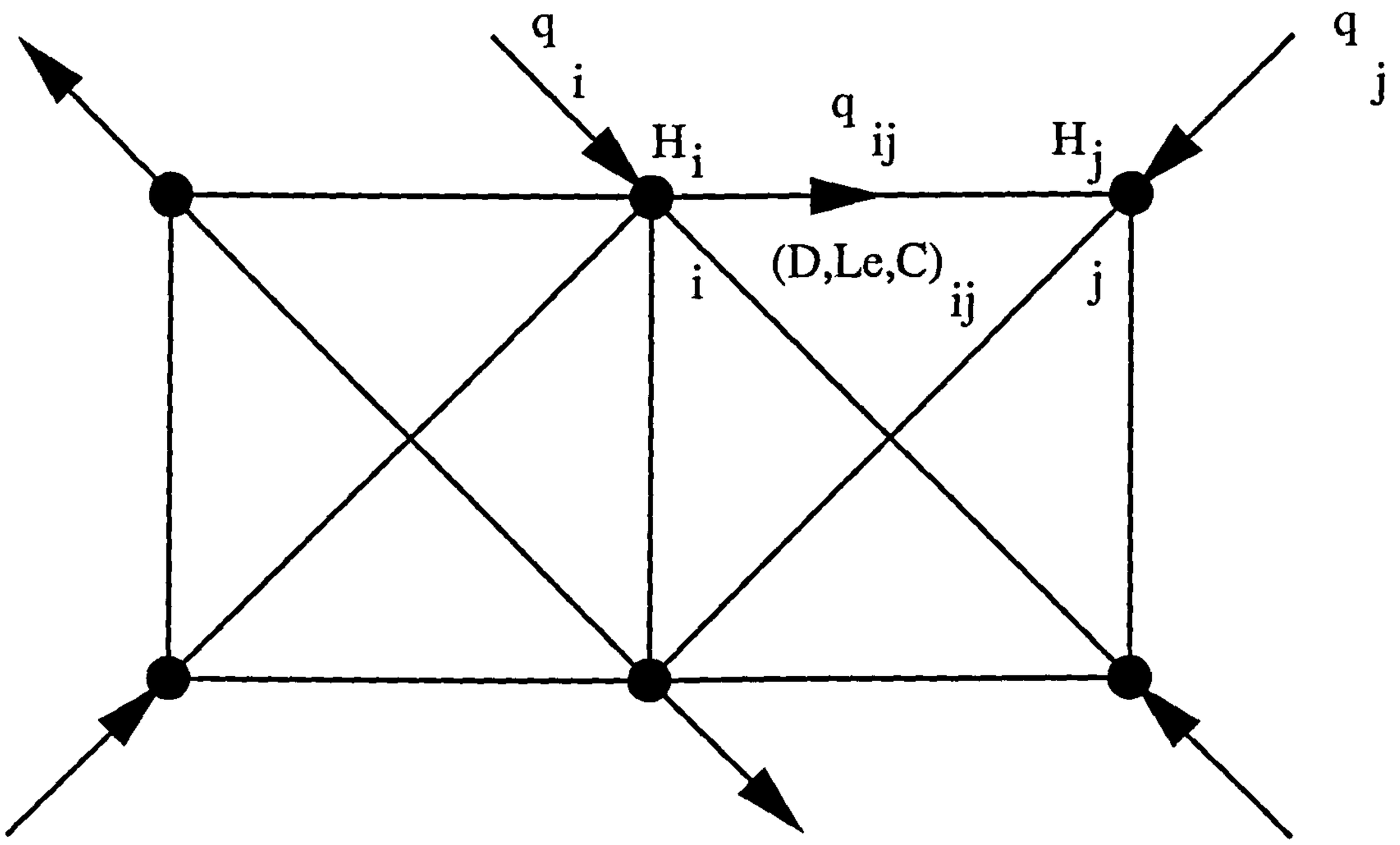

Figure 3.12 Typical water supply network

CHAPTER 4

CALCULATING MAXIMUM ENTROPY FLOWS IN MULTI-SOURCE, MULTI-DEMAND GENERAL NETWORKS

4.1 INTRODUCTION

It has been shown in Chapter 2 how most-likely, or least-biased, flows in water distribution networks can be calculated using the maximum entropy formalism. The key feature of the problem which was presented in Chapter 2 as Problem 3 was that very limited data was assumed to be available: only source flow rates, demand flow rates and the topology of the network with arc flow directions were assumed to be known. Data on arc properties such as lengths, diameters of pipes and roughness properties were assumed not to be available. Because of this very limited data, there was insufficient information to permit an accurate physical analysis of the pipe network to be performed which would generate accurate pipe flow rates and a corresponding pressure regime. Under these circumstances, Shannon's entropy function (Shannon, 1948) and the maximum entropy formalism (Jaynes, 1957) were used to estimate the most-likely, or least-biased, flows in water distribution networks by maximizing the network nodal entropy function presented by Tanyimboh and Templeman (1993a) subject to the available information. (See Problem 3 presented in Chapter 2).

The problem of calculating maximum entropy flows in water supply networks is nonlinear and hence requires nonlinear programming. In an attempt to simplify the problem, Tanyimboh and Templeman (1993b) proposed a different and simpler path-based approach to calculate maximum entropy flows in single-source networks. Their method is not iterative and does not involve linear or nonlinear programming. The

method was described in Chapter 2 by means of three algorithms, a node numbering algorithm, a node weighting algorithm and a flow distribution algorithm. The main idea behind the method is that according to the maximum entropy formalism the demand of any node in the network served by more than one path from the source should be divided equally amongst all paths supplying it if there is no further information about these paths.

The above simple method, however, is not capable of handling general multi-source networks. The super-source approach proposed by Tanyimboh and Templeman (1993b) as an extension of the simple single-source algorithm to multiple sources has been shown to be invalid. Walters (1995) showed how it should correctly be used in a rather unwieldy method. (See Appendix A for more details on his proposed method). A rigorous general method and relatively simple and quick algorithm based on the path approach are proposed in this chapter for calculating maximum entropy flows for multi-source general networks without involving linear or nonlinear programming. Also, the proposed method is not iterative and does not use the super-source idea in any way. Because the method is based on path flows, a path-based network entropy function is developed to facilitate the proposed method. In this chapter, the theory behind the method is introduced along with the network path entropy function. This is followed by a full description of the proposed method and the accompanying algorithms. Illustrative examples and general discussions on the proposed method are left to the next chapter.

4.2 MULTI-PATH FLOWS AND THEIR EQUILIBRIUM EQUATIONS FOR MULTI-SOURCE NETWORKS

Consider the water network shown in Figure 4.1. The network has two sources and three demand nodes. The external inflows and outflows at those source and demand nodes respectively are known. Also, the layout of the network and the flow directions in all the pipes are given but no further information about the network is available. Under these circumstances, the most-likely pipe flows corresponding to the maximum entropy value of the network have to be sought. Instead of maximizing the nodal

entropy function of the network subject to available information (see Problem 3 presented in Chapter 2), the maximum entropy flows are sought in this chapter using the idea of path flows from each source to each demand node.

Considering any demand node in the network of Figure 4.1 served by more than one path from a source, all the paths from that source supplying that demand node should have the same probability of doing so if there is no further information about those paths. This accords with the maximum entropy formalism presented in Chapter 2 as Problem 1. Therefore, flow to a demand node supplied by a source should be distributed equally amongst all the paths supplying that node from that source. However, the proportion of flow for a demand node supplied by each source is unknown, and the relationship between path flows for each demand node supplied by different sources is consequently unknown. Defining $q_{p,ij}$ to be the path flow from source i to demand node j, Figure 4.2 shows the unknown and equal path flows from each source to each demand node reachable from that source. For demand node 5, there are three paths from each source in the network, these being 1-3-5, 1-3-4-5 and 1-4-5 from source node 1 (Figure 4.2a), each carrying one path flow $q_{p,15}$, and 2-5, 2-3-5 and 2-3-4-5 from source node 2 (Figure 4.2b), each carrying one path flow $q_{p,25}$. Demand node 4 receives two paths from source node 1 (Figure 4.2c), each having flow equal to $q_{p,14}$, and one path from source node 2 (Figure 4.2 d) carrying a flow equal to $q_{p,24}$. Finally, only two paths are supplying node 3, one path from each source (Figures 4.2e and 4.2f respectively), where the path from source node 1 carries a flow equal to $q_{p,13}$ and the path from source node 2 carries $q_{p,23}$.

Consequently, there are six unknown path flows for the network of Figure 4.1, two for each demand node. However, three demand equilibrium equations can be constructed, one for each demand node, by equating all the path flows supplying each demand node to the demand of that node. These equations can generally be written as:

$$\sum_{i \in I_{S,j}} NP_{ij}\, q_{p,ij} = q_{j0} \quad \forall j \in I_D \tag{4.1}$$

in which NP_{ij} is the number of paths from source i, $\forall i \in I_{S,j}$, to demand node j, $\forall j \in I_D$; $I_{S,j}$ and I_D being respectively the set of all source nodes supplying node j and the set of all demand nodes in the network; and q_{j0} is the demand at node j.

Also, referring again to Figure 4.1, two source equilibrium equations can be set up, one for each source node, by equating all the path flows for all demand nodes supplied by each source node to the supply of that node. These equations can generally be expressed as:

$$\sum_{j \in I_{D,i}} NP_{ij}\, q_{p,ij} = q_{0i} \quad \forall i \in I_S \tag{4.2}$$

where $I_{D,i}$ is the set of all demand nodes reachable from source node i; q_{0i} is the supply of source node i.

It should be noted that one of the equations in Eqs. (4.1) and (4.2), that is one out of five equations for the network of Figure 4.1, is not usable since it will automatically be satisfied provided that all the source supplies balance the demands in the network. Therefore, for the network of Figure 4.1 there are six unknown path flows and four usable equilibrium equations. Note that this difficulty is not encountered in single-source networks since the number of unknown path flows is equal to the number of demand nodes. (See Tanyimboh and Templeman, 1993b). How can maximum entropy pipe flows be calculated for multi-source general networks using the path-based approach?

This chapter investigates closely the multiple path flows for the two-source network of Figure 4.1. The probabilities of these path flows are needed in this investigation. Therefore, path flow probabilities are defined next accompanied by presentation of a new form of network entropy function based on those probabilities of path flows.

4.3 PATH FLOW PROBABILITIES AND PATH ENTROPY FUNCTION OF WATER NETWORKS

The probability of an event in a repeated experiment can be interpreted in terms of the relative frequency as the frequency or number of occurrences of that event divided by the sum of the frequencies of all the events in the experiment. Following that relative frequency interpretation, the probabilities of path flows in water distribution networks can be obtained by normalising each path flow by its individual source flow as follows:

$$p_{p,ij} = \frac{q_{p,ij}}{q_{0i}} \quad \forall i \in I_S \; ; \; \forall j \in I_{D,i} \tag{4.3}$$

in which $p_{p,ij}$ is the probability that path flow $q_{p,ij}$ supplied by source node i reaches demand node j. Substituting Eqs. (4.3) into Eqs. (4.2) gives the following normality condition equations at the source nodes:

$$\sum_{j \in I_{D,i}} NP_{ij}\, p_{p,ij} = 1 \quad \forall i \in I_S \tag{4.4}$$

Note that Eqs. (4.4) are equivalent to Eqs. (4.2) since Eqs. (4.4) can be obtained by dividing Eqs. (4.2) by the corresponding source flow. However, Eqs. (4.4) are used in the present work instead of Eqs. (4.2) as will be seen later.

Eqs. (4.3) represent NS sets of path probabilities, where NS is the number of sources in the network, each set corresponding to a source. For each set, the path probabilities are mutually exclusive and they sum to unity [Eqs. (4.4)]. Therefore, each set of path probabilities represents a finite scheme. However, these finite schemes are not independent. Each scheme is dependent upon the conditions at the corresponding source. There is no path flow from source node i to demand node j if there is no supply at that source. This can be interpreted as follows: each set of path probabilities corresponding to a source is dependent upon the probability representing the fraction of the total supply in the network provided by the corresponding source node. There are NS number of such probabilities in the network, each corresponds to a source node, and they are:

$$P_{0i} = \frac{q_{0i}}{T_0} \quad \forall i \in I_S \tag{4.5}$$

in which T_0 is the total supply or demand in the network, and is given by:

$$T_0 = \sum_{i \in I_S} q_{0i} = \sum_{j \in I_D} q_{j0} \tag{4.6}$$

Clearly, the set of probabilities given by Eqs. (4.5) represents a finite scheme since these probabilities are mutually exclusive and they sum to unity.

To sum up, there are (NS+1) finite schemes which can be identified in a water distribution network. One of these schemes is the set of all source flow probabilities given by Eqs. (4.5), and each of the remaining NS finite schemes of path probabilities corresponds to a flow from a source and depends upon the flow probability of that source.

Having defined general water supply networks in terms of finite schemes, some of which are dependent upon others, the network entropy in the context of path flows can now be introduced using the concept of entropy of a compound scheme presented in Chapter 2 and defined by the notion of conditional entropy. This can be done by summing the entropy of the set of source flow probabilities to the conditional entropy of each set of path flow probabilities. First, the entropy of the set of source flow probabilities, setting the constant K to unity, can be written as (see Shannon, 1948):

$$S_0^s = -\sum_{i \in I_S} P_{0i} \ln P_{0i} \tag{4.7}$$

in which S_0^s represents the entropy of the distribution of total supply T_0 amongst the sources; and P_{0i} is given by Eq. (4.5). Second, the conditional entropy of each set of path flow probabilities can be written as (see Khinchin, 1953):

$$S_i^p = - P_{0i} \sum_{j \in I_{D,i}} NP_{ij}\, p_{p,ij} \ln p_{p,ij} \quad \forall i \in I_S \tag{4.8}$$

where S_i^p is the conditional entropy of path flow corresponding to source node i.

Consequently, the path entropy function of the network will have the form:

$$S^p = S_0^s + \sum_{i \in I_s} S_i^p \qquad (4.9)$$

in which S^p is the network entropy based on path flows; S_0^s is the entropy of the distribution of the total supply amongst all sources and is given by Eq. (4.7); and S_i^p is the conditional entropy of path flows supplied by source node i and is given by Eq. (4.8).

To demonstrate the above path entropy function, Eq. (4.9) is now applied to the two-source network of Figure 4.1. To do so, the probabilities of all the path flows shown in Figure 4.2 are needed. Assume that the maximum entropy link flows in the network are available. These can be obtained by maximizing the nodal entropy function of the network subject to available information (see Problem 3 presented in Chapter 2). The resulting maximum entropy flows are shown in Figure 4.3 and have a maximum entropy value of 2.3885315. At this stage, the sum of all path flows passing through a link can be equated to the maximum entropy flow of that link. Therefore, the following equations can be obtained:

$2\ q_{p,15} + q_{p,14} + q_{p,13} = 20.\ 061912$ (for link 1-3)

$q_{p,15} + q_{p,14} = 9.938088$ (for link 1-4)

$2\ q_{p,25} + q_{p,24} + q_{p,23} = 16.268405$ (for link 2-3)

$q_{p,25} = 3.731595$ (for link 2-5)

$q_{p,25} + q_{p,15} + q_{p,24} + q_{p,14} = 17.996982$ (for link 3-4)

$q_{p,25} + q_{p,15} = 8.333335$ (for link 3-5)

$q_{p,25} + 2\ q_{p,15} = 12.935070$ (for link 4-5)

Solving six of these equations with six unknown path flows gives: ($q_{p,13}$, $q_{p,14}$, $q_{p,15}$, $q_{p,23}$, $q_{p,24}$, $q_{p,25}$) = (5.522086, 5.336350, 4.601738, 4.477916, 4.327299, 3.731595). The unused equation provides a numerical check for the above path flows which were found to be correct. Using Eqs. (4.3), the path flow probabilities are: ($p_{p,13}$, $p_{p,14}$, $p_{p,15}$, $p_{p,23}$, $p_{p,24}$, $p_{p,25}$) = (0.1840695, 0.1778783, 0.1533913, 0.2238958, 0.2163650,

0.1865798). These path probabilities form two finite schemes, each corresponding to a source. Also, the probabilities of source flows can be obtained using Eqs. (4.5) as: $(P_{01}, P_{02}) = (0.6, 0.4)$, which also form a finite scheme. Having defined the (NS+1=3) finite schemes in the network, the network path entropy value can now be evaluated using Eq. (4.9) as:

$$S^p = S_0^s + \sum_{i=1}^{2} S_i^p$$

$$= - P_{01} \ln P_{01} - P_{02} \ln P_{02}$$
$$- P_{01} \{p_{p,13} \ln p_{p,13} + 2\, p_{p,14} \ln p_{p,14} + 3\, p_{p,15} \ln p_{p,15}\}$$
$$- P_{02} \{p_{p,23} \ln p_{p,23} + p_{p,24} \ln p_{p,24} + 3\, p_{p,25} \ln p_{p,25}\}$$
$$= 2.3885317$$

which compares exactly with the nodal entropy value calculated earlier by maximizing the nodal entropy function of the network. This confirms the general correctness of the path-based approach which assumes equal path flows from each source to each demand node reachable to that source leading to the maximum entropy flows in the network.

It should be noted that the path flow probabilities of the network of Figure 4.1 have been calculated using the maximum entropy flows obtained by maximizing the nodal entropy function of the network. In the next section, these path probabilities are studied so they can be calculated in a relatively simple method which will be called the alfa method. The method does not involve linear, nonlinear programming or iterative processes.

4.4 ALFA METHOD

Consider the two-source network of Figure 4.1. The path flows and their probabilities corresponding to the maximum entropy value of the network (S^*=2.3885315) are shown in Table 4.1 for further study. Several features can be observed when examining Table 4.1. First, the path flows values from each source contributing to a

demand node have different values; $q_{p,13} \neq q_{p,23}$, $q_{p,14} \neq q_{p,24}$ and $q_{p,15} \neq q_{p,25}$. Also, the corresponding probabilities are not equal; $p_{p,13} \neq p_{p,23}$, $p_{p,14} \neq p_{p,24}$ and $p_{p,15} \neq p_{p,25}$, nor does the ratioing of these probabilities according to source flow proportions lead to equality either, $(p_{p,13}/q_{01}) \neq (p_{p,23}/q_{02})$, $(p_{p,14}/q_{01}) \neq (p_{p,24}/q_{02})$ and $(p_{p,15}/q_{01}) \neq (p_{p,25}/q_{02})$.

Table 4.1 The maximum entropy path flows and their probabilities for the two-source network of Figure 4.1 with S^*=2.3885315.

Source node i	q_{0i}	Demand node j	q_{j0}	Path i-j	NP_U	$q_{p,U}$	$p_{p,U}$
1	30	3	10	1-3	1	5.522086	0.1840695
		4	15	1-4	2	5.336350	0.1778783
		5	25	1-5	3	4.601738	0.1533913
2	20	3	10	2-3	1	4.477916	0.2238958
		4	15	2-4	1	4.327299	0.2163650
		5	25	2-5	3	3.731595	0.1865798

Examining the proportions of demand at a node from each source leads to the following: node 3 receives $q_{p,13}$=5.522086 units of flow from source 1 and $q_{p,23}$=4.477916 units of flow from source 2. This means that node 3 gets $(q_{p,13}/q_{30})$=55.22% of its demand from source 1 and $(q_{p,23}/q_{30})$=44.78% from source 2. The same proportions of demand from each source is found at node 5 which receives $(3q_{p,15}/q_{50})$=55.22% of its demand from source 1 and $(3q_{p,25}/q_{50})$=44.78% from source 2. However, node 4 receives different proportions of demand from each source. It gets $(2q_{p,14}/q_{40})$=71.15% of its demand from source 1 and $(q_{p,24}/q_{40})$=28.85% from source 2. It should be noted that node 4 differs from nodes 3 and 5 in that node 4 receives different numbers of paths from the two sources compared with nodes 3 and 5, each of which receives equal number of paths from the sources.

Finally, the path probabilities from each source at a demand node are examined next regardless of the number of paths from each source to that demand node. The following ratios are obtained:

$(p_{p,13}/p_{p,23}) = 0.822121$

$(p_{p,14}/p_{p,24}) = 0.822121$

$(p_{p,15}/p_{p,25}) = 0.822121$

It can obviously be noted that the ratio of the probabilities of path flows from each source to a demand node corresponding to the maximum entropy flows is the same for every demand node.

The above interesting result is now examined for the three-source network shown in Figure 4.4. The maximum entropy flows obtained by solving Problem 3 presented in Chapter 2 are also shown in the figure and have $S^*=2.594634$. The corresponding path flows and their probabilities can respectively be obtained by equating all the path flows passing through a link to the maximum entropy flow of that link and then normalising the resulting path flow by its individual source flow. The resulting path flows and their probabilities are shown in Table 4.2.

Table 4.2 The maximum entropy path flows and their probabilities for the three-source network of Figure 4.4 with $S^*=2.594634$.

Source node i	q_{i0}	Demand node j	q_{j0}	Path i-j	NP_{ij}	$q_{p,ij}$	$p_{p,ij}$
1	20	4	15	1-4	3	2.372647	0.1186324
		5	30	1-5	5	2.576412	0.1288206
2	15	4	15	2-4	1	4.729236	0.3152823
		5	30	2-5	2	5.135382	0.3423588
3	10	4	15	3-4	1	3.152822	0.3152823
		5	30	3-5	2	3.423588	0.3423588

Examining the ratios of the path probabilities from each pair of sources at a demand node shows that:

$$(p_{p,14}/p_{p,24}) = (p_{p,15}/p_{p,25}) = 0.376274$$

$$(p_{p,24}/p_{p,34}) = (p_{p,25}/p_{p,35}) = 1$$

which obviously lead to the equality: $(p_{p,14}/p_{p,34}) = (p_{p,15}/p_{p,35})$.

The above two examples and others examined in the same manner show that the equal path probabilities hold for any pair of sources and all demand nodes reachable from the corresponding pair of sources. This leads to the following important conjecture:

Conjecture A

"The maximum entropy flows in multi-source, multi-demand general networks are such that the ratio of the probabilities of path flows from each pair of sources to a demand node reachable from the corresponding pair of sources is the same for every demand node supplied by this pair of sources in the network".

The above conjecture is the basis of the proposed path-based method for calculating maximum entropy flows in general networks. If the ratios mentioned in Conjecture A can be found, they would provide a very simple means of calculating maximum entropy path flows for multi-source networks. The proposed method therefore aims to determine these ratios which enable maximum entropy path flow probabilities and hence the corresponding path flows to be directly calculated as will be seen very shortly.

The two-source network of Figure 4.1 is now used to demonstrate the proposed method which will be called the alfa method. First, the equilibrium equations at the demand nodes can be written using Eqs. (4.1) as:

$$q_{p,13} + q_{p,23} = 10$$
$$2q_{p,14} + q_{p,24} = 15$$
$$3q_{p,15} + 3q_{p,25} = 25$$

Note that constructing these equations requires the number of paths from each source to each demand node to be determined. Next, the above equations are expressed in terms of probabilities using Eqs. (4.3) as follows:

$$30p_{p,13} + 20p_{p,23} = 10$$
$$60p_{p,14} + 20p_{p,24} = 15$$
$$90p_{p,15} + 60p_{p,25} = 25$$

According to Conjecture A, the following ratios can be identified: $(p_{p,13}/p_{p,23}) = (p_{p,14}/p_{p,24}) = (p_{p,15}/p_{p,25}) = \alpha$, which are substituted into the above probability equilibrium equations to yield the following equations:

$$30\alpha p_{p,23} + 20p_{p,23} = 10$$
$$60\alpha p_{p,24} + 20p_{p,24} = 15$$
$$90\alpha p_{p,25} + 60p_{p,25} = 25$$

These equations can be solved to give:

$p_{p,23} = 10/(20+30\alpha)$, and hence, $p_{p,13} = \alpha p_{p,23} = 10\alpha/(20+30\alpha)$

$p_{p,24} = 15/(20+60\alpha)$, and hence, $p_{p,14} = \alpha p_{p,24} = 15\alpha/(20+60\alpha)$

$p_{p,25} = 25/(60+90\alpha)$, and hence, $p_{p,15} = \alpha p_{p,25} = 25\alpha/(60+90\alpha)$

At this stage, the normality condition equations at the source nodes can be set up using Eqs. (4.4) as:

$$p_{p,13} + 2p_{p,14} + 3p_{p,15} = 1$$
$$p_{p,23} + p_{p,24} + 3p_{p,25} = 1$$

Substituting the path probabilities expressed in terms of α into the second of the above normality condition equations gives: $[10/(20+30\alpha)] + [15/(20+60\alpha)] + 3[25/(60+90\alpha)] = 1$, which is solved to yield: α=0.822121. Back-substituting α into path flow probability expressions gives: $(p_{p,13}, p_{p,14}, p_{p,15}, p_{p,23}, p_{p,24}, p_{p,25})$ = (0.1840695, 0.1778783, 0.1533913, 0.2238958, 0.2163650, 0.1865798). Note that the unused normality condition equation at source node 1 can then be used for checking purposes.

Having calculated all the path flow probabilities in the network, the path network entropy value can now be determined using Eq. (4.9) to give S^p=2.3885315. Also, the path flows corresponding to the above probabilities can be calculated by substituting these probabilities into Eqs. (4.3) to give: $(q_{p,13}, q_{p,14}, q_{p,15}, q_{p,23}, q_{p,24}, q_{p,25})$ = (5.522086, 5.336350, 4.601738, 4.477916, 4.327299, 3.731595). These path flows are now used

to calculate the final link flows in the network by summing all the path flows passing each link in turn. For example, link 3-4 carries four path flows (see Figure 4.2), two path flows serving demand node 4, each path from a source, and the other two path flows serving demand node 5, each path from a source. i.e. $q_{34} = q_{p,14} + q_{p,24} + q_{p,15} + q_{p,25} = 17.996982$. Treating all the links in the network similarly gives the following link flows: $(q_{13}, q_{14}, q_{23}, q_{25}, q_{34}, q_{35}, q_{45})$ = (20.061912, 9.938088, 16.268405, 3.731595, 17.996982, 8.333335, 12.935070).

It can be noted that the above results including α value, path flow probabilities, network entropy value, path flows and final link flows are found to match all the respective results calculated earlier by maximizing the nodal entropy function of the network. (See Figure 4.3 and Table 4.1).

4.5 PATH-BASED ALGORITHMS FOR CALCULATING MAXIMUM ENTROPY FLOWS IN GENERAL WATER NETWORKS

The alfa method presented in the previous section for calculating maximum entropy flows for general multi-source networks requires the set of demand nodes reachable from each source to be identified and the number of paths from each source to each node reachable from that source to be determined. The alfa method has been formalised and cast into algorithms reflecting these requirements. An overview of the algorithms describing the procedures by means of an example is presented next followed by a full list of the proposed algorithms.

The two-source network of Figure 4.5 is now used to describe the algorithms. All the nodes in the networks are numbered by ascending consecutive positive numbers starting by number 1 for any source in the network, then the rest of the source nodes followed by the rest of the nodes chosen in a random order as shown in Figure 4.5a. Therefore, numbering the two sources is arbitrary and may be interchanged. Also, numbering of nodes 3, 4 and 5 may be interchanged.

The next step is to identify the set of nodes reachable from each source in the network. Considering source i, all the links immediately downstream of that source are considered and the immediate downstream nodes of those links are stored in a set $I_{D,i}$. The nodes in the set $I_{D,i}$ are now considered and all their immediate downstream links are obtained. The immediate downstream nodes of those links are checked to determine if they already exist in the set before they are added to that set to avoid double counting of the nodes. The process continues until all the new batch of nodes added to the set are terminal nodes which do not have any link outflows. The set $I_{D,i}$ now contains all the nodes reachable from source node i. The same procedure is repeated for every source in the network until all the sources have been processed and the set of nodes reachable from each source has been obtained. The nodes 3, 4 and 5 in Figure 4.5a are all reachable from both sources. Neither source is reachable from the other. The process of identifying the reachable nodes from each source is terminated when reaching node 5 which is a terminal node. Note that the sets $I_{D,i}$, $\forall i \in I_S$, which are used in Eqs. (4.2) or Eqs. (4.4) can lead to the sets $I_{S,j}$, $\forall j \in I_D$, which are used in Eqs. (4.1). This can be explained as follows. For every demand node j in the network, $\forall j \in I_D$, if node j belongs to $I_{D,i}$, $\forall i \in I_S$, therefore, the source i belongs to the set of sources $I_{S,j}$ supplying node j.

Having identified the set of nodes reachable from each source in the network, the number of paths from each source to each node reachable from it can now be determined by constructing sub-networks, each corresponding to a source and its reachable nodes, and then using the node numbering and node weighting algorithms proposed by Tanyimboh and Templeman (1993b) for single-source networks. Figures 4.5b and 4.5c show the two sub-networks of the network of Figure 4.5a, each corresponding to a source and its reachable nodes. For each sub-network, the nodes are renumbered locally starting with the source which is given the number 1, then the rest of the nodes are numbered in a way that each node is numbered after all nodes immediately upstream of it have been numbered. The resulting local node numbers for each sub-network are enclosed in circles next to the nodes, while the global node numbers matching the original numbers in Figure 4.5a are maintained for convenience. At this stage, the number of paths from the source of each sub-network to each node

in the corresponding sub-network can now be determined. Figures 4.5b and 4.5c show the number of paths from each source to each reachable node as a weight enclosed in a box next to the corresponding node. This is done by assigning the source of each sub-network a weight 1. Then, in ascending local node numbering sequence, the weight of each reachable node is calculated as the sum of the weights assigned to all nodes immediately upstream of it. For example, consider Figure 4.5b. Source node 1 is assigned a weight 1. Then, the ascending local numbering sequence (numbers enclosed in circles) requires nodes 3, 4 and 5 to be weighted consecutively. The weight of node 3 is equal to the weight of node 1, and the weight of node 4 is the sum of the weights of nodes 1 and 3, these being the immediate upstream nodes of node 4. The resulting weight of node 4 is 2. Finally, the weight of node 5 equals the weight of node 3 plus the weight of node 4, that is 3. Similarly, the number of paths from source node 2 to each reachable node can be determined. The resulting number of paths are shown in Figure 4.5c. Note that the local node numbering scheme is used to determine the sequence of nodes to be weighted ensuring that the nodes immediately upstream of the node being weighted have all been weighted.

At this stage, the alfa method presented in the previous section can now be used to determine the path flow probabilities and hence the corresponding path flows from each source to each reachable demand node. Path flow equilibrium equations at the demand nodes are constructed using Eqs. (4.1), and are then expressed in terms of path flow probabilities by means of Eqs. (4.3) as follows:

$$\sum_{i \in I_{Sj}} NP_{ij}\, q_{0i}\, P_{p,ij} = q_{j0} \quad \forall j \in I_D \tag{4.10}$$

which will be called the probability equilibrium equations at the demand nodes. Identifying the ratios of the path flow probabilities from each pair of sources to a demand node supplied by both sources, and substituting these ratios into the probability equilibrium equations enable path flow probabilities to be expressed as functions of (NS-1) unknown αs. Constructing the normality conditions of Eqs. (4.4) at (NS-1) source nodes and substituting the path flow probabilities expressed in terms of the (NS-1) unknown αs yield (NS-1) equations with (NS-1) unknowns. These

equations can easily be solved to give values of the αs which can then be back-substituted into the path probabilities expressions to give values of path flow probabilities and hence the corresponding path flows which correspond to the maximum entropy flows in the network.

The example solved in the previous section by the alfa method has all the demand nodes reachable from all the sources in the network. Generally, some demand nodes may not be reachable from some sources. Conjecture A implies that equal ratios of αs hold for any set of demand nodes reachable from any pair of sources in the network. This can be formalised by the following general equation:

$$\frac{p_{p,ij}}{p_{p,kj}} = \frac{\alpha_i}{\alpha_k} \quad \forall i,k \in I_{S_j} \; ; \; \forall j \in I_D \tag{4.11}$$

in which i and k are any pair of sources supplying demand node j, $\forall j \in I_D$. Eqs. (4.11) have NS unknown αs, where NS is the number of sources in the network. However, there should be only (NS-1) unknown αs relating path flow probabilities in a network. For the two-source network of Figure 4.1 solved by the alfa method in the previous section, there was one unknown α in the network. Therefore, one unknown α in Eqs. (4.11) has to be set to unity. The unknown corresponding to source node 1 is set to unity throughout this thesis, i.e. $\alpha_1=1$.

It should be noted that not all of the ratios of Eqs. (4.11) are usable in solving the probability equilibrium equations formalised as Eqs. (4.10). For the probability equilibrium equation at a demand node j, $\forall j \in I_D$, the proposed method chooses any source i from the set I_{S_j} and expresses all the path flow probabilities existing in this equation in terms of the path flow probability corresponding to source i using the respective ratios from Eqs. (4.11). For example, consider the three-source network of Figure 4.4. The probability equilibrium equation at demand node 5 can be written by means of Eqs. (4.10) as follows:

$100\ p_{p,15} + 30\ p_{p,25} + 20\ p_{p,35} = 30$

Choosing, for example, $p_{p,25}$ as the reference of all other probabilities in the equation, the following ratios can be used:

$(p_{p,15}/p_{p,25}) = (\alpha_1/\alpha_2)$ and $(p_{p,35}/p_{p,25}) = (\alpha_3/\alpha_2)$,

which by setting α_1 to unity give:

$p_{p,15} = (1/\alpha_2)\ p_{p,25}$ and $p_{p,35} = (\alpha_3/\alpha_2)\ p_{p,25}$.

Substituting these ratios into the probability equilibrium equation yields:

$(100/\alpha_2)\ p_{p,25} + 30\ p_{p,25} + (20\alpha_3/\alpha_2)\ p_{p,25} = 30$,

which gives: $p_{p,25} = (30\alpha_2)/(100+30\alpha_2+20\alpha_3)$,

and hence: $p_{p,15} = 30/(100+30\alpha_2+20\alpha_3)$ and $p_{p,35} = (30\alpha_3)/(100+30\alpha_2+20\alpha_3)$.

The above path flow probability expressions can therefore be formalised by the following general equation:

$$p_{p,ij} = \frac{q_{j0}\ \alpha_i}{\sum_{i \in I_{Sj}} NP_{ij}\ q_{0i}\ \alpha_i} \quad \forall i \in I_{Sj}\ ;\ \forall j \in I_D \tag{4.12}$$

in which α_i=1 for i=1. If all the path flow probabilities in a network are expressed in terms of αs using Eqs. (4.12) and then substituted in (NS-1) normality conditions of Eqs. (4.4), the resulting (NS-1) equations with (NS-1) unknown αs can be solved to yield the values of αs and hence the path flow probabilities of Eqs. (4.12).

The final stage of the proposed method is to calculate the final link flows which correspond to the maximum entropy value of the network. This is done by handling each sub-network containing a source and its reachable nodes in turn and calculating the flows in the links of the sub-network supplied by the corresponding source. This is described very shortly. The final maximum entropy flow in a link can then be obtained by superposition of all the flows carried by that link in all the sub-networks.

The link flows for a sub-network are calculated as follows. Consider Figures 4.5b and 4.5c which show the two sub-networks corresponding to source 1 and 2 respectively. The demands at the nodes are the flows supplied by the corresponding source, i.e.

$$q_{j0,i} = NP_{ij}\ q_{p,ij} \quad \forall i \in I_S\ ;\ \forall j \in I_{D,i} \tag{4.13}$$

in which $q_{j0,i}$ is the demand at node j supplied by source i. The total outflows at a node in any sub-network is distributed amongst all the immediate upstream links to

that node in proportion with the weight of the upstream node to the corresponding link. The procedure operates from any terminal node in the sub-network in a descending local numbering order to insure that the link outflows at the node being considered have all been calculated. Starting at the terminal node 5 in the sub-network of Figure 4.5b, the total outflow at node 5 equalling 13.805214 units is divided by 3, this being the number of paths from the source to that node. The quotient is then multiplied by 1 and 2 respectively, these being the respective number of paths to nodes 3 and 4 which are the immediate upstream nodes to node 5. The products, respectively, are the flows in links 3-5 and 4-5 supplied by source 1. At this stage, the total outflow at node 4 is known and is equal to 9.203476+10.6727=19.876176 units is shared equally between links 1-4 and 3-4 due to the equality of the weights of the immediate upstream nodes to these two links. Finally, all the outflows at node 3 are carried by link 1-3 since there is only one link upstream to node 3.

The same procedures are applied for the sub-network of Figure 4.5c. The resulting link flows supplied by source 2 are shown in the figure. The final link flows can finally be obtained by summing the flows in Figures 4.5b and 4.5c for each link in turn. The resulting link flows have been shown to match the maximum entropy flows shown in Figure 4.3.

An alternative way of calculating the final link flows in a network knowing all the path flows is by means of a simple equation. If the number of paths from each node in the network to each node reachable from it is available, the following equation can be used to calculate the final maximum entropy link flows in general networks:

$$q_{kl} = \sum_{i \in I_S} [\, NP_{ik} \sum_{j \in I_D} NP_{lj}\, q_{p,ij} \,] \quad \forall kl \in IJ \tag{4.14}$$

in which q_{kl} is the final flow in link kl, $\forall kl \in IJ$, where IJ is the set of all links in the network. Eqs. (4.14) assumes that the number of paths from a node to the same node is 1, and the number of paths from a node to any other node not reachable from it is zero.

The following is a list of simple algorithms proposed to tackle the path-based problem of calculating maximum entropy flows in multi-source, multi-demand general networks. The global node numbering scheme is used throughout the algorithms unless it is stated otherwise.

Global node numbering algorithm

1. Select any source in the network and number it with 1. Set n to 1.
2. Increase n by 1. Select any other source which has not been numbered and number it with n.
3. If n=NS, go to step 4. Otherwise, go to step 2.
4. Increase n by 1. Select any node which has not been numbered and number it with n.
5. If n=NN, exit. Otherwise, go to to step 4.

Source reachability algorithm

1. Set n to 0.
2. Increase n by 1. Select source node n.
3. Select all the nodes immediately downstream of node n and include their node numbers in an empty set $I_{D,n}$.
4. Select all the nodes immediately downstream of the nodes contained in the set $I_{D,n}$. The node number of each node selected, if any, is added to the set $I_{D,n}$ if it does not already exist in the set.
5. If the number of nodes added to the set $I_{D,n}$ in step 4 equals zero, go to step 6. Otherwise, go to step 4.
6. The set $I_{D,n}$ contains all the nodes reachable from source node n. If n=NS, exit. Otherwise, go to step 2.

Demand node reachability algorithm

1. Set n to NS.
2. Increase n by 1. Select demand node n.
3. Set m to 1.
4. If the set $I_{D,m}$ which is identified by the source reachability algorithm contains node

number n, include m in set $I_{S,n}$.

5. Increase m by 1. If m=NS, go to step 6. Otherwise, go to step 4.

6. The set $I_{S,n}$ contains all the source nodes supplying demand node n. If n=NN, exit. Otherwise, go to step 2.

Local node numbering algorithm

1. Set n to 0.

2. Increase n by 1. Select source node n.

3. Construct a sub-network SNK_n containing source node n and all nodes contained in the set $I_{D,n}$.

4. Number the source node n locally with 1. Set m to 1.

5. Increase m by 1. Select any node in the sub-network SNK_n whose immediate upstream nodes have all been locally numbered and number it with m.

6. If m equals the number of nodes contained in the sub-network SNK_n, go to step 7. Otherwise, go to step 5.

7. If n=NS, exit. Otherwise, go to step 2.

Node weighting algorithm

1. Set n to 0.

2. Increase n by 1. Select the sub-network SNK_n corresponding to source node n.

3. Set m to the source local number, 1. Set NP_{nm} to 1.

4. Increase m by 1 and select the node whose local number in the sub-network SNK_n is m. Calculate NP_{nm}:

$$NP_{nm} = \sum_{j \in NU_m \subset SNK_n} NP_{nj}$$

in which $NU_m \sqsubset SNK_n$ represents the set of upstream nodes of inflow links at a node whose local number in the sub-network SNK_n is m, provided that these upstream nodes are in the sub-network SNK_n.

5. If m equals the number of nodes contained in the sub-network SNK_n, go to step 6. Otherwise, go to step 4.

6. If n=NS, exit. Otherwise, go to step 2.

Alfa algorithm

1. Set n to NS.

2. Increase n by 1. Select demand node n.

3. Define the probabilities of path flows supplying demand node n from each source reachable to it as follows:

$$p_{p,in} = \frac{q_{n0}\ \alpha_i}{\sum_{i \in I_{S,n}} NP_{in}\ q_{0i}\ \alpha_i} \quad \forall i \in I_{S,n}$$

4. If n=NN, go to step 5. Otherwise, go to step 2.

5. Set n to 0.

6. Increase n by 1. Select source node n.

7. Construct the normality condition equation at source node n as follows:

$$\sum_{j \in I_{D,n}} NP_{nj}\ p_{p,nj} = 1$$

8. If n=NS-1, go to step 9. Otherwise, go to step 6.

9. Set α_1=1.

10. Solve the equations constructed in steps 3, 7 and 9 to obtain all the unknown values of αs and all the path flow probabilities. Calculate S^p, if necessary.

11. Calculate the path flows as follows:

$$q_{p,ij} = q_{0i}\ p_{p,ij} \quad \forall i \in I_S\ ;\ \forall J \in I_{D,i}$$

12. Exit.

Flow distribution algorithm

1. Set n to 0.

2. Increase n by 1. Select source node n.

3. Set m to the number of nodes in the sub-network SNK_n including the source node n.

4. Calculate $T_{m,n}$:

$$T_{m,n} = NP_{nm}\, p_{p,nm} + \sum_{k \in ND_m \subset SNK_n} q_{mk,n}$$

in which m indicates the node whose local number in the sub-network SNK_n is m; $T_{m,n}$ is the total outflows at node m; (NP_{nm}* $p_{p,nm}$) is the local demand at node m supplied by source n; $ND_m \sqsubset SNK_n$ represents the set of immediate downstream nodes of inflow links at node m, provided that these downstream nodes are in the sub-network SNK_n. Note that the total demand at the node whose local number in the sub-network SNK_n is m is not included in $T_{m,n}$.

5. Calculate $q_{jm,n}$, $\forall jm \in NU_m \sqsubset SNK_n$:

$$q_{jm,n} = T_{m,n} \frac{NP_{nj}}{NP_{nm}}$$

in which $q_{jm,n}$ is the flow in link jm in the sub-network SNK_n, $\forall jm \in NU_m \sqsubset SNK_n$, supplied by source node n.

6. Reduce m by 1. If m=1, go to step 7. Otherwise, go to step 4.

7. If n=NS, go to step 8. Otherwise, go to step 2.

8. Calculate q_{ij}, $\forall ij \in IJ$:

$$q_{ij} = \sum_{n=1}^{NS} q_{ij,n}$$

in which q_{ij} is the final maximum entropy flow in link ij; $q_{ij,n}$ is the flow in the corresponding link calculated in the sub-network SNK_n in which the link ij is a member.

9. Exit.

4.6 SUMMARY AND CONCLUSION

It has been shown in this chapter how maximum entropy flows for multi-source, multi-demand general networks may be calculated using a relatively simple path-based method. The proposed method is based on two principles. First, the demand of any node in the network served by more than one path from any source should be divided equally amongst all paths supplying it from that source if there is no further information about those paths. This accords with the maximum entropy formalism. Second, the ratio of the probabilities of path flows from any pair of sources to a demand node reachable from this pair of sources is the same for every demand node supplied by the pair of sources mentioned above. This has been established by the research presented in this chapter.

The proposed method does not involve any linear or nonlinear programming. Also, it is not iterative and does not use the super-source approach in any way. It only requires solving (NS-1) normality condition equations with (NS-1) unknown αs after expressing all the path flow probabilities in terms of αs using the path equilibrium equations at demand nodes and the equal ratios of the probabilities of path flows from any pair of sources to every demand node supplied by this pair of sources.

Also, the method has been formalised and cast into simple algorithms tackling all the aspects encountered in the method such as identifying the reachable nodes to each source in the network and determining the number of paths from each source to each node reachable from that source. Furthermore, a network path entropy function has been developed to facilitate the proposed method, where (NS+1) finite probability schemes can be identified in a network. The first scheme is the source flow probabilities, and the remaining NS finite schemes represent the sets of path flow probabilities, each corresponds to a source and is conditional upon the flow probability of the corresponding source. The network path entropy function can then be derived by means of the conditional entropy formula for compound probability schemes. The resulting new entropy function enables the maximum value of network entropy to be directly calculated using the path flow probabilities obtained by the proposed method.

In the next chapter, illustrative numerical examples of the present path-based method for calculating maximum entropy flows for different networks chosen carefully to cover all aspects of general real networks are presented to demonstrate the general applicability of the proposed method. Also, a computer programme representing the present method is written in FORTRAN 90 and is checked on the solved examples. Finally, discussions are presented and further conclusions are drawn.

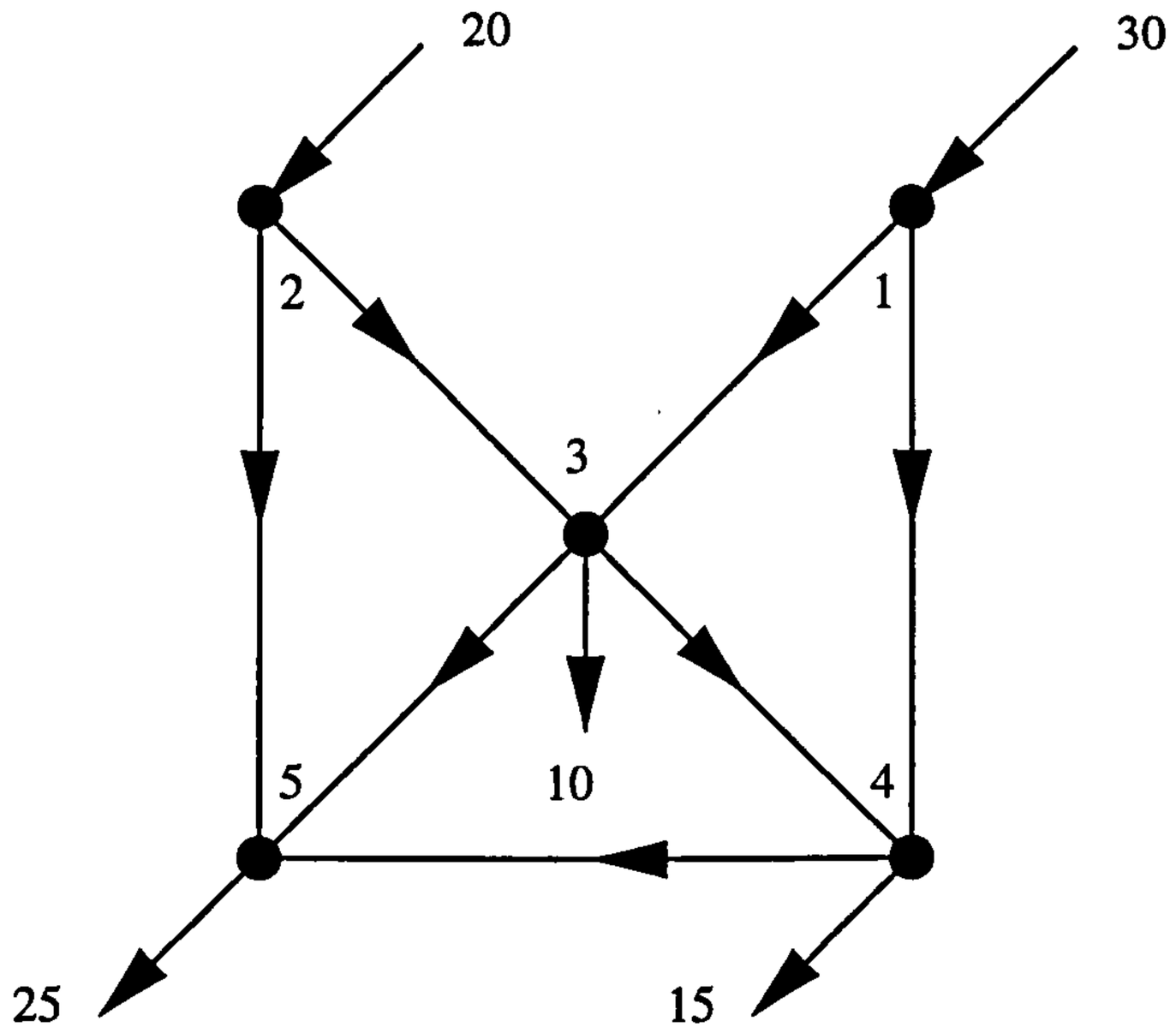

Figure 4.1 Two-source network

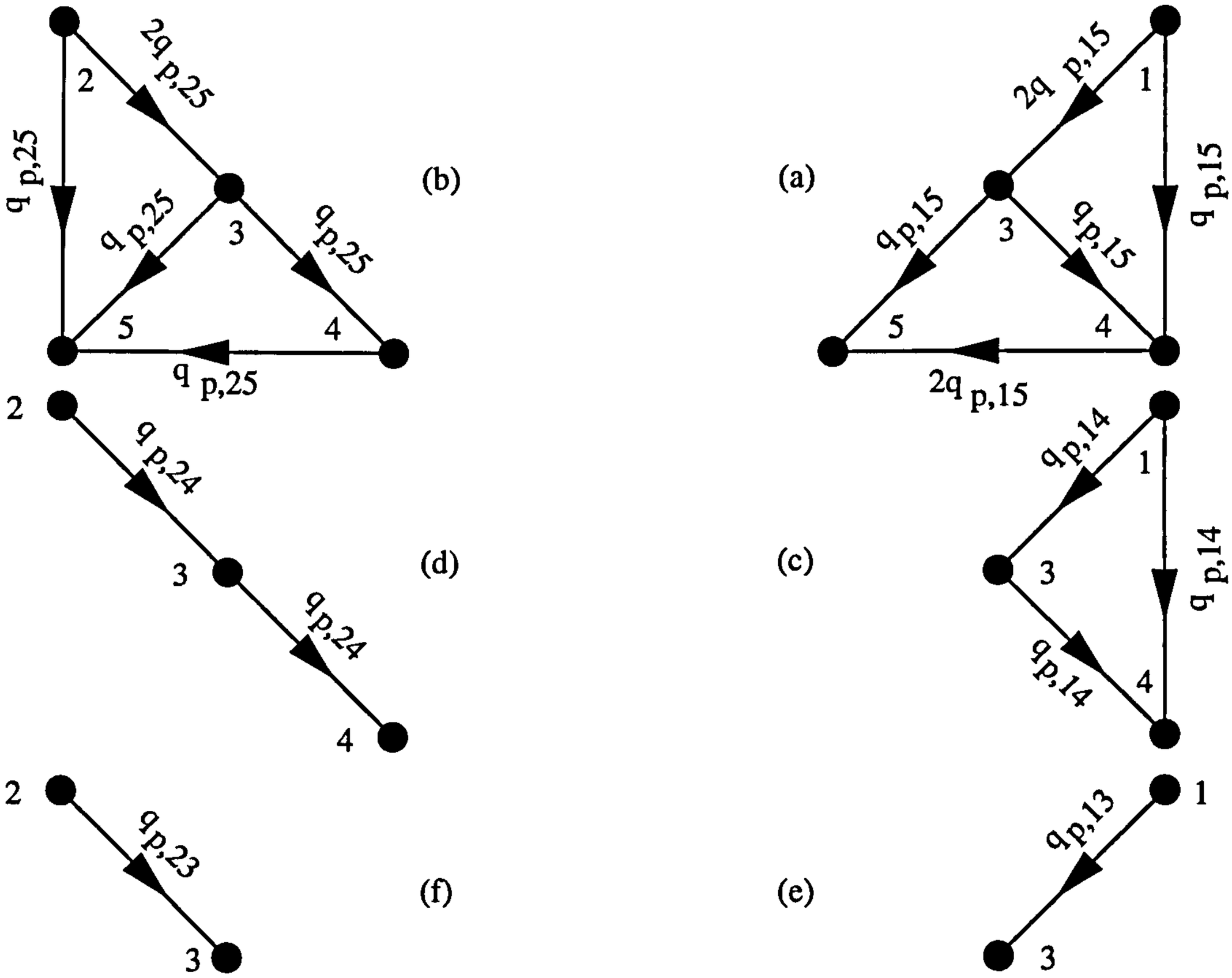

Figure 4.2 Equal path flows from each source to each reachable demand node

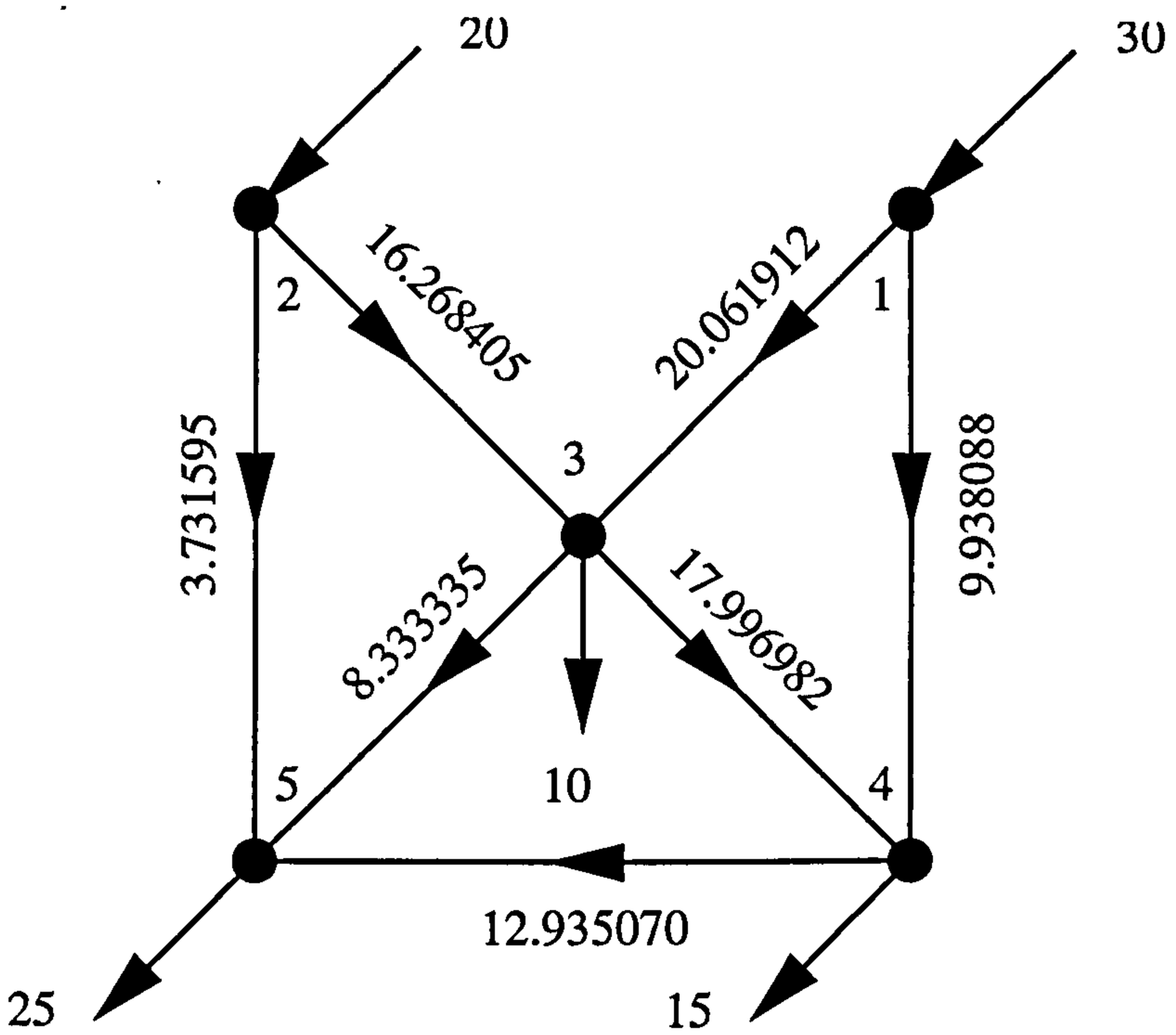

Figure 4.3 Maximum entropy flows for the network of Figure 4.1 obtained by maximizing the nodal entropy function of the network

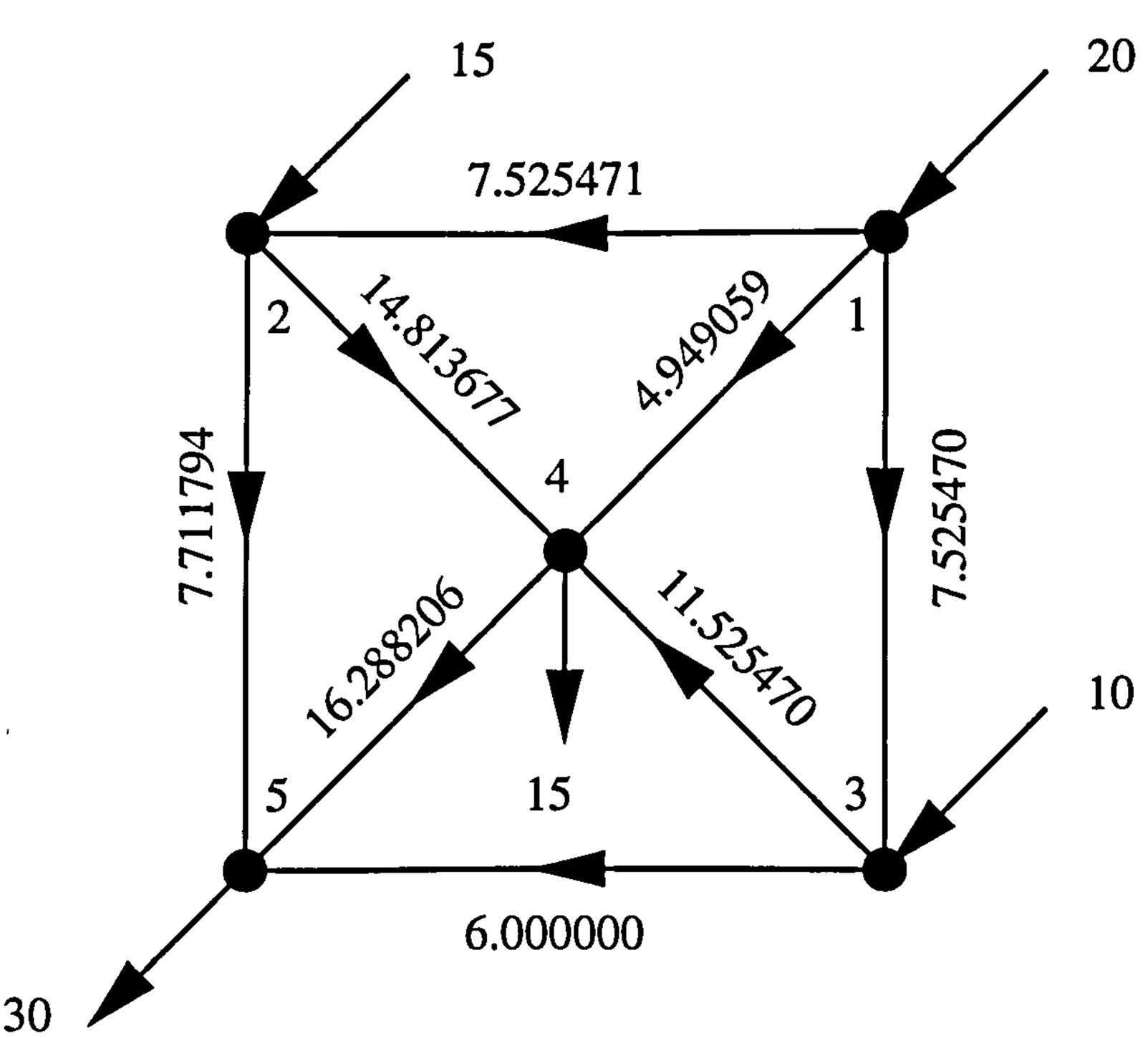

Figure 4.4 Maximum entropy flows for a three-source network obtained by maximizing the nodal entropy function of the network

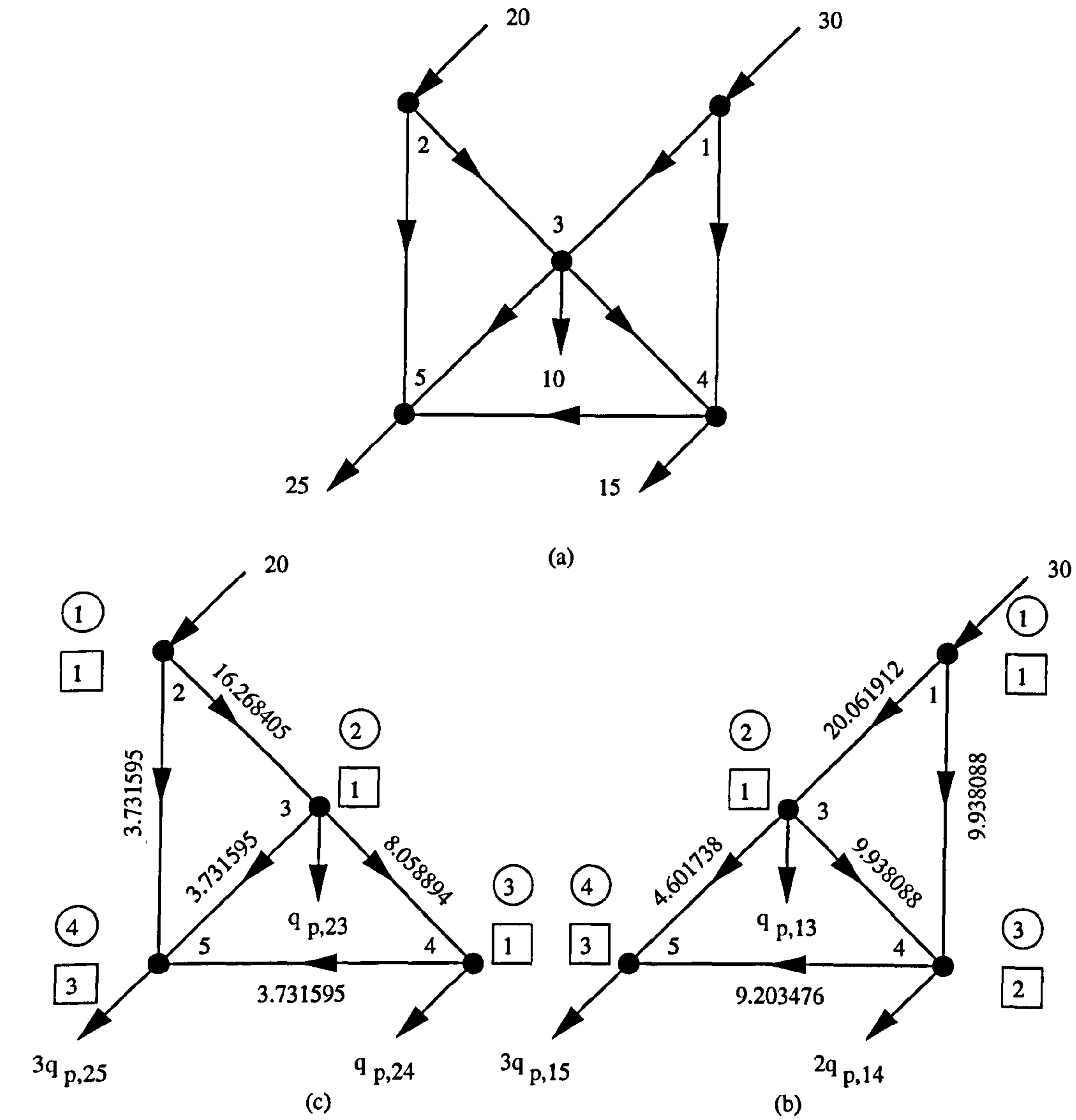

Figure 4.5 Maximum entropy flows for the two-source network of Figure 4.1

(a): Global node numbering
(b): Sub-network SNK 1
(c): Sub-network SNK 2

CHAPTER 5

NUMERICAL APPLICATIONS OF THE ALFA METHOD ALGORITHMS

5.1 INTRODUCTION

This chapter is devoted to demonstrating the path-based method and its algorithms, presented in the previous chapter, for calculating maximum entropy flows in multi-source, multi-demand general water distribution networks. Three major numerical examples were chosen carefully to illustrate the general applicability of the method and to enable several points to be observed and discussed and conclusions to be drawn.

The first major example shown in Figure 5.1 is a two-source network having some demand nodes unreachable from one of the sources. In the second major example which is shown in Figure 5.2, a three-source network has only one source reachable to all demand nodes and the remaining two sources have different sets of demand nodes reachable to each of the sources. The final major example shown in Figure 5.3 is also a three-source network but has no source reachable to all demand nodes. The three different examples exhibit different characteristics when their maximum entropy flows are calculated by the path-based method. The results are discussed and several remarks are observed. A computer programme written in FORTRAN 90 to solve the path-based method, and named the alfa method programme which is given in Appendix B is also run on the three major examples mentioned above.

Also, in this chapter, the super-source approach proposed by Tanyimboh and Templeman (1993b) as an extension of the simple single-source method to multiple sources for calculating maximum entropy flows is studied by means of two simple

examples taken from the above paper. The two examples are resolved by the present path-based alfa method, and the results are discussed and compared with the results quoted in the paper. Several points are observed and conclusions are drawn.

5.2 EXAMPLE 1

A sample two-source network in which some demand nodes are unreachable from one of the sources is shown in Figure 5.1a. The network has 9 nodes 16 links. The supply and demand at the nodes are shown in the figure, and the directions of the link flows are also shown. The path-based algorithms presented in the previous chapter for calculating maximum entropy flows in water supply networks are applied to this example. According to the global node numbering algorithm, the two-sources are numbered first by 1 and 2, then the rest of the nodes are given the numbers 3 to 9 randomly as shown in Figure 5.1a.

The source reachability algorithm is now used to identify the nodes reachable from each source. Consider source node 1. The immediate downstream nodes of node 1 are nodes 3 and 4 which are included in a set $I_{D,1}$, i.e. $I_{D,1}$={3,4,...}. The immediate downstream nodes of nodes 3 and 4 are now found. They are respectively nodes 2 and 5 and nodes 5 and 6. The obtained nodes are included in the set $I_{D,1}$ which now becomes: $I_{D,1}$={3,4,2,5,6,...}. Note that node 5 is included only once although it is an immediate downstream node of both nodes 3 and 4. Now, the new immediate downstream nodes which can be added to the set $I_{D,1}$ and which are not already in the set are nodes 7 and 8. Therefore, the set $I_{D,1}$ becomes: $I_{D,1}$={3,4,2,5,6,7,8,...}. The immediate downstream node of nodes 7 and 8 is node 9 which is the only node which can now be added to the set $I_{D,1}$ to become as follows: $I_{D,1}$={3,4,2,5,6,7,8,9}. At this point , all the nodes immediately downstream to the nodes contained in the set $I_{D,1}$ are already in the set. Therefore, no node can now be added to the set and the process is completed for source node 1 for which all reachable nodes are now included in the set $I_{D,1}$. The same procedure can be applied to source node 2 to give the set: $I_{D,2}$={5,7,6,8,9}, which contains all the nodes reachable from source node 2.

Having defined the sets of nodes reachable from each source, the set of source nodes supplying each demand node can now be obtained using the demand node reachability algorithm. Only the set $I_{D,1}$ contains demand nodes 3 and 4. Therefore, the demand nodes 3 and 4 are supplied by source node 1 only, i.e. $I_{S,3}=I_{S,4}=\{1\}$, while nodes 5 to 9 are contained in the two sets, $I_{D,1}$ and $I_{D,2}$, simultaneously. Therefore, the demand nodes 5 to 9 are supplied by both sources and consequently: $I_{S,i}$, i=5,...,9, $=\{1,2\}$.

At this stage, two sub-networks, each containing a source and its reachable nodes, are constructed as shown in Figures 5.1b and 5.1c. For each sub-network, the nodes are renumbered locally using the local node numbering algorithm, and the number of paths from the source to each node in the sub-network is determined using the node weighting algorithm. This was demonstrated step by step in Chapter 2. For each node in each sub-network of Figures 5.1b and 5.1c, its local number and the number of paths from the source in the corresponding sub-network to the node being considered are respectively enclosed in a circle and a box next to that node. For example, the local numbers of node 9 in the sub-networks corresponding to source node 1 (Figure 5.1b) and source node 2 (Figure 5.1c) are respectively 9 and 6 shown in circles next to it in the two figures. Also, the numbers of paths from source node 1 and source node 2 to demand node 9 are respectively 20 and 6 shown in boxes next to node 9 in Figures 5.1a and 5.1c respectively.

The next step is to calculate the path flow probabilities and the corresponding path flows from each source to each demand node reachable from that source. This is done next using the alfa algorithm. The path flow probabilities are expressed in terms of αs as follows:

$p_{p,13} = (10\alpha_1/60\alpha_1) = 10/60 = 0.1666667$

$p_{p,14} = (10\alpha_1/120\alpha_1) = 10/120 = 0.0833333$

$p_{p,15} = 15\alpha_1/(240\alpha_1+40\alpha_2)$, $p_{p,25} = 15\alpha_2/(240\alpha_1+40\alpha_2)$

$p_{p,16} = 15\alpha_1/(360\alpha_1+40\alpha_2)$, $p_{p,26} = 15\alpha_2/(360\alpha_1+40\alpha_2)$

$p_{p,17} = 15\alpha_1/(300\alpha_1+80\alpha_2)$, $p_{p,27} = 15\alpha_2/(300\alpha_1+80\alpha_2)$

$p_{p,18} = 15\alpha_1/(900\alpha_1+160\alpha_2)$, $p_{p,28} = 15\alpha_2/(900\alpha_1+160\alpha_2)$

$p_{p,19} = 20\alpha_1/(1200\alpha_1+240\alpha_2)$, $p_{p,29} = 20\alpha_2/(1200\alpha_1+240\alpha_2)$.

At this stage, the normality condition equation at source node 1 is constructed as:

$p_{p,13}+2p_{p,14}+4p_{p,15}+6p_{p,16}+5p_{p,17}+15p_{p,18}+20p_{p,19} = 1$

Substituting the path flow probabilities into the above equation yields:

$0.1666667 + 2*0.0833333 + 60\alpha_1/(240\alpha_1+40\alpha_2) + 90\alpha_1/(360\alpha_1+40\alpha_2) + 75\alpha_1/(300\alpha_1+80\alpha_2) + 225\alpha_1/(900\alpha_1+160\alpha_2) + 400\alpha_1/(1200\alpha_1+240\alpha_2) = 1$

which can be solved by setting α_1 to unity to give: α_2=5.5919906. Note that the normality condition equation at source node 2 can be used to check the value of α_2 which was found to be correct.

Having defined the unknown αs, the path flow probabilities calculated earlier in terms of αs can be determined. The resulting values of path flow probabilities are given in Table 5.1. The path entropy value of the network corresponding to those path flow probabilities can be calculated as: S^p=3.748957 which, according to the alfa method, corresponds to the maximum entropy value of the network flows.

Table 5.1 The path flow probabilities and the corresponding path flows for the two-source network of Figure 5.1 calculated by the alfa method with S^p=3.748957.

Source node i	q_{0i}	Demand node j	q_{j0}	Path i-j	NP_{ij}	$p_{p,ij}$	$q_{p,ij}$
1	60	3	10	1-3	1	0.1666667	10.000000
		4	10	1-4	2	0.0833333	5.000000
		5	15	1-5	4	0.0323499	1.940995
		6	15	1-6	6	0.0256990	1.541942
		7	15	1-7	5	0.0200707	1.204240
		8	15	1-8	15	0.0083579	0.501471
		9	20	1-9	20	0.0078676	0.472055
2	40	5	15	2-5	1	0.1809005	7.236019
		6	15	2-6	1	0.1437087	5.748349
		7	15	2-7	2	0.1122350	4.489400
		8	15	2-8	4	0.0467371	1.869482
		9	20	2-9	6	0.0439954	1.759817

Also, the path flows corresponding to the above probabilities can be calculated by multiplying each path flow probability by its individual source flow. The resulting path flows are also given in Table 5.1.

The final stage of the proposed path-based method is to calculate the final link flows in the network. This can be done by using the flow distribution algorithm which calculates the link flows supplied by each source considering each sub-network corresponding to a source in turn. The demands at the nodes used in each sub-network are those supplied by the corresponding source only as shown in Figures 5.1b and 5.1c. For each sub-network, the procedure is carried out in a reverse order starting from the last node considering the local node numbering scheme (numbers in circles next to the nodes). Consider Figure 5.1b. Starting at node 9, the total outflow at that node, $20q_{p,19}$, is distributed between the two links 7-9 and 8-9 proportional to the weights of nodes 7 and 8 respectively. The resulting two link flows are shown in the figure. At node 8, the total outflow is the demand at node 8 supplied by source node 1 added to the flow at link 8-9. The resulting total outflow, $(15q_{p,18}+7.080825)$, is divided by 15, this being the weight of node 8. The quotient is then multiplied by 6, 4 and 5 respectively, these being the respective weight of nodes 6, 5 and 7. The products, respectively, are the flows in links 6-8, 5-8 and 7-8. The process continues until source node 1 is reached. Note that in this sub-network, the supply at node 2 is not considered since this sub-network is concerned with the distribution of the flow supplied by source node 1. Also, note that the demand of node 2 has been set to zero. Therefore, node 2 in the sub-network of Figure 5.1b is used to provide extra paths of flows to all nodes downstream to it. The sub-network corresponding to source node 2 shown in Figure 5.1c is handled in the same way as that of Figure 5.1b. The resulting link flows supplied by source node 2 are shown in Figure 5.1c. Note that calculating the link flows corresponding to source node 1 is independent from calculating the link flows corresponding to source node 2. The sub-network of Figure 5.1c can be solved before the sub-network of Figure 5.1b is solved, and vice versa. This justifies the global node numbering algorithm which enables the source node numbers of Figure 5.1a to be interchanged. Finally, the final link flows in the network can be determined by superposing the link flows of the two sub-networks of Figures

5.1b and 5.1c. The resulting final link flows are shown in Figure 5.1d.

The above example has also been solved by maximizing the nodal entropy function of the network. (See Problem 3 presented in Chapter 2). The resulting maximum entropy flows have been found to match those obtained earlier by hand calculations using the alfa method. Also, the alfa method programme given in Appendix B has been used to solve this example. The input and output files are given in Appendix C.

Commenting on the results of this example, it can be seen that demand nodes 5, 6, 7, 8 and 9 which are reachable from both sources have much larger numbers of paths from source node 1 than from source node 2. This is compensated by having the path flow probabilities corresponding to source node 2 more than five and a half times greater than those corresponding to source node 1. Therefore, the value of α_2 is a way of making the flows supplied by each source to a demand node as uniform as possible subject to the path flow equilibrium equations at the nodes of the network.

Also, the value of α_2 being the same for every demand node reachable from both sources is a bias treatment of these nodes. There is no reason to do otherwise. This is a direct result of the maximum entropy formalism. However, the value of α_2 being other than unity can be justified by the general characteristics of the network being considered. The source flows are not equal. Also, the demand is not the same for every demand node, nor the number of paths from each source to every demand node. The value of α_2 takes into account all the above factors and has the effect of making the path flows in the network more uniform subject to the available information.

It is evident from the above example that the alfa method of calculating maximum entropy flows is computationally very efficient. This is demonstrated by the fact that it is possible to solve the above example by simple hand calculations. Also, the existence of some demand nodes unreachable from source 2 in the example demonstrates the applicability of the method for such a general case. The next two examples, however, examine even more general cases.

5.3 EXAMPLE 2

The three-source network of Figure 5.2a in which source node 2 is the only source in the network reachable to all demand nodes has 9 nodes and 13 links. The network is globally numbered as shown in the figure. The supply and demand at the nodes are also shown along with flow directions in the links. The source reachability algorithm may be applied to give the following sets of nodes: $I_{D,1}$={4,5,6,8}, $I_{D,2}$={7,9,5,8,4,6} and $I_{D,3}$={9,8,6} which represent the nodes reachable from each source in the network. Also, the sets of sources supplying each demand node can be obtained as: $I_{S,4}=I_{S,5}$={1,2}, $I_{S,6}=I_{S,8}$={1,2,3}, $I_{S,7}$={2} and $I_{S,9}$={2,3}. At this stage, three sub-networks, each corresponding to a source and its reachable nodes, can now be constructed as shown in Figures 5.2b, 5.2c and 5.2d. For each sub-network, the local node numbers and the number of paths from the source to each node are shown in the figures where the numbers in circles denote the local node numbers and the numbers in boxes represent the number of paths from the corresponding source to each node in the corresponding sub-network.

The next step is to apply the alfa algorithm. Accordingly, the path flow probabilities can be expressed in terms of αs as follows:

$p_{p,14} = 10\alpha_1/(40\alpha_1+35\alpha_2)$, $p_{p,24} = 10\alpha_2/(40\alpha_1+35\alpha_2)$

$p_{p,15} = 10\alpha_1/(20\alpha_1+35\alpha_2)$, $p_{p,25} = 10\alpha_2/(20\alpha_1+35\alpha_2)$

$p_{p,16} = 15\alpha_1/(60\alpha_1+140\alpha_2+30\alpha_3)$, $p_{p,26} = 15\alpha_2/(60\alpha_1+140\alpha_2+30\alpha_3)$,

$p_{p,36} = 15\alpha_3/(60\alpha_1+140\alpha_2+30\alpha_3)$

$p_{p,27} = 10\alpha_2/35\alpha_2 = 10/35 = 0.2857143$

$p_{p,18} = 15\alpha_1/(20\alpha_1+105\alpha_2+30\alpha_3)$, $p_{p,28} = 15\alpha_2/(20\alpha_1+105\alpha_2+30\alpha_3)$,

$p_{p,38} = 15\alpha_3/(20\alpha_1+105\alpha_2+30\alpha_3)$

$p_{p,29} = 10\alpha_2/(70\alpha_2+15\alpha_3)$, $p_{p,39} = 10\alpha_3/(70\alpha_2+15\alpha_3)$.

The normality condition equations at source nodes 1 and 2 are constructed as:

$2p_{p,14} + p_{p,15} + 3p_{p,16} + p_{p,18} = 1$

$p_{p,24} + p_{p,25} + 4p_{p,26} + p_{p,27} + 3p_{p,28} + 2p_{p,29} = 1$

Substituting the path flow probabilities into the above two equations and solving the resulting two equations by setting α_1 to unity give: α_2=0.4786637 and α_3=1.7134213. These values of αs have been checked using the normality condition equation at source node 3, and they were found to be correct. At this point, the path flow probabilities can be determined by substituting the values of αs into the probability expressions. The resulting path flow probabilities are given in Table 5.2, and the corresponding path entropy value of the network is S^p=3.028466. Also, the corresponding path flows can be calculated by multiplying each path flow probability by its individual source flow. The resulting path flows are also given in Table 5.2.

Table 5.2 The path flow probabilities and the corresponding path flows for the three-source network of Figure 5.2 calculated by the alfa method with S^p=3.028466.

Source node i	q_{0i}	Demand node j	q_{j0}	Path i-j	NP_{ij}	$p_{p,ij}$	$q_{p,ij}$
1	20	4	10	1-4	2	0.1762014	3.524028
		5	10	1-5	1	0.2720849	5.441699
		6	15	1-6	3	0.0840734	1.681468
		8	15	1-8	1	0.1232921	2.465841
2	35	4	10	2-4	1	0.0843412	2.951943
		5	10	2-5	1	0.1302372	4.558301
		6	15	2-6	4	0.0402429	1.408501
		7	10	2-7	1	0.2857143	10.000000
		8	15	2-8	3	0.0590154	2.065540
		9	10	2-9	2	0.0808447	2.829566
3	15	6	15	3-6	2	0.1440531	2.160797
		8	15	3-8	2	0.2112513	3.168769
		9	10	3-9	1	0.2893912	4.340869

Finally, the flow distribution algorithm can now be used to calculate the final link flows in the network. The link flows for each sub-network corresponding to a source are first calculated as shown in Figures 5.2b, 5.2c and 5.2d in which the procedure starts, for each sub-network, at terminal node 6 whose local numbers in SNK_1, SNK_2 and SNK_3 are 5, 7 and 4 respectively. The final link flows can then be obtained by superposition of the three sub-network flow results. The resulting final link flows are shown in Figure 5.2e. They have been found to be corresponding to maximum entropy

flows of the network. Also, the above example has been solved by the alfa method computer programme, and the results are given in Appendix C.

Several remarks can be observed when examining the results of this example. Although demand node 6 has different numbers of paths from each source, its total demand is reasonably distributed amongst the three sources, these being 5.044, 5.634 and 4.322 units of flows from source nodes 1, 2 and 3 respectively. Examining demand node 8 shows that the flow supplied by source node 1 to that demand node is less than half of the flow supplied by each of the remaining sources to that same demand node. However, the values of the αs responsible for the flow distributions can be seen to be justified by considering the group of nodes reachable from each source rather than considering individual nodes. It can be seen that the lowest value of α corresponds to source node 2. This can be appreciated by realizing that source node 2 is forced to supply demand node 7 with the whole 10 units of its demand flow leaving only 25 units of the source flow to supply the five remaining demand nodes. Also, although source node 3 has only 15 units of flows to contribute to the network, its high value of α comes from the fact that source node 3 supplies only three demand nodes in the network.

It should be noted that all the networks solved so far by the alfa method have at least one source supplying all demand nodes in the network. The next example, however, is different in having no source reachable to all demand nodes.

5.4 EXAMPLE 3

Figure 5.3a shows a sample three-source network having 9 nodes and 13 links with no source reachable to all demand nodes. The supply and demand at the nodes and the flow directions in the links are shown in the figure. The nodes are globally numbered and the three sub-networks, each corresponding to a source and its reachable nodes obtained by the source reachability algorithm, are shown in Figures 5.3b, 5.3c and 5.3d respectively. Also, the local node numbers and the number of paths from the source to each node in each sub-network are, respectively, shown in circles and boxes

next to the nodes.

According to the alfa algorithm, the path flow probabilities can be written in terms of αs as follows:

$p_{p,14} = 10\alpha_1/60\alpha_1 = 10/60 = 0.1666667$

$p_{p,15} = 10\alpha_1/30\alpha_1 = 10/30 = 0.3333333$

$p_{p,16} = 20\alpha_1/(90\alpha_1+105\alpha_2+30\alpha_3)$, $p_{p,26} = 20\alpha_2/(90\alpha_1+105\alpha_2+30\alpha_3)$,

$p_{p,36} = 20\alpha_3/(90\alpha_1+105\alpha_2+30\alpha_3)$

$p_{p,27} = 10\alpha_2/35\alpha_2 = 10/35 = 0.2857143$

$p_{p,18} = 20\alpha_1/(30\alpha_1+105\alpha_2+30\alpha_3)$, $p_{p,28} = 20\alpha_2/(30\alpha_1+105\alpha_2+30\alpha_3)$,

$p_{p,38} = 20\alpha_3/(30\alpha_1+105\alpha_2+30\alpha_3)$

$p_{p,29} = 10\alpha_2/(70\alpha_2+15\alpha_3)$, $p_{p,39} = 10\alpha_3/(70\alpha_2+15\alpha_3)$.

Substituting the above path flow probabilities into the following two normality condition equations constructed at source nodes 1 and 2 respectively:

$2p_{p,14} + p_{p,15} + 3p_{p,16} + p_{p,18} = 1$

$3p_{p,26} + p_{p,27} + 3p_{p,28} + 2p_{p,29} = 1$

and solving the resulting equations by setting α_1 to unity gives the following values of αs: α_2=0.9745576 and α_3=2.1945998, which have been checked by the normality condition equation at source node 3 and found to be correct. These values of αs can then be used to determine all the path flow probabilities and hence the corresponding path flows in the network. The results are given in Table 5.3.

Having defined all the path flows in the network, the flow distribution algorithm can now be used to calculate first the link flows for each sub-network supplied by the corresponding source as shown in Figures 5.3b, 5.3c and 5.3d respectively, and then to superpose the resulting sub-network link flows to determine the final link flows in the network as shown in Figure 5.3e. As for the previous examples, the resulting link flows have been found to correspond to maximum entropy flows of the network. Also, the alfa method computer programme has been used to solve this example, and the results are given in Appendix C.

Table 5.3 The path flow probabilities and the corresponding path flows for the three-source network of Figure 5.3 calculated by the alfa method with S^p=2.923974.

Source node i	q_{0i}	Demand node j	q_{j0}	Path i-j	NP_{ij}	$p_{p,ij}$	$q_{p,ij}$
1	30	4	10	1-4	1	0.1666667	5.000000
		5	10	1-5	1	0.3333333	10.000000
		6	20	1-6	3	0.0774694	2.324081
		8	20	1-8	1	0.1009252	3.027756
2	35	6	20	2-6	3	0.0754984	2.642443
		7	10	2-7	1	0.2857143	10.000000
		8	20	2-8	3	0.0983574	3.442510
		9	10	2-9	2	0.0963592	3.372571
3	15	6	20	3-6	2	0.1700143	2.550214
		8	20	3-8	2	0.2214904	3.322357
		9	10	3-9	1	0.2169906	3.254858

Comparing the results of this example with the results of the previous one shows that source node 3 has again the highest value of α. However, the values of path flow probabilities corresponding to source nodes 1 and 2 are almost equal considering demand nodes 6 and 8 which are the only nodes reachable from both sources simultaneously. This can be seen by means of the value of α_2 being equal to 0.975 which is almost twice the corresponding value in the previous example. This can be justified by realizing that source node 2 in this example has fewer nodes reachable from it with higher demands compared with the previous example. The increase of the supply at source node 1, however, has been balanced by the increase of the demands of the two nodes reachable from it, that is nodes 6 and 8.

It is evident from the above three examples used to demonstrate the alfa method that the proposed method and its algorithms presented in the previous chapter are computationally very efficient and applicable for any general network having the supply and demand at the nodes known along with the flow directions in the links. Because the proposed method is based upon the path flows from each source to each reachable demand node in the network, it can be argued that applying the method to a general network would give the same results if the flow directions in the links are all reversed and the supplies become demands and vice versa. The two-source network

of Example 1 has been reversed as shown in Figure 5.4 and solved by the alfa method programme, and the results which are given in Appendix C match the results obtained for Example 1 regarding path flows, the final link flows and the path entropy value of the network.

Also, maximizing the path entropy function of the network presented in the previous chapter subject to the path equilibrium equations at the nodes but excluding the path flow probability ratios in the problem constraints would give exactly the same results as those obtained by the alfa method with path flow probabilities having the expected equal ratios. This can be argued by realizing that the alfa method results always correspond to the maximum entropy flows in the network.

5.5 COMMENTS ON THE SUPER-SOURCE APPROACH

The simple method proposed by Tanyimboh and Templeman (1993b) and described in Chapter 2 for calculating maximum entropy flows in single-source networks may be considered as a special case of the alfa method presented in the previous chapter and demonstrated earlier in this chapter by means of three major examples. This special case of single-source networks has only one α equalling unity and corresponding to the only source in the network.

In their paper, Tanyimboh and Templeman (1993b) extended their single-source method to multiple sources by means of a super-source replacing all the sources in the network. The two-source network used in the paper to demonstrate the super-source approach is shown in Figure 5.5a. The link flows shown in the figure are obtained by the super-source approach as demonstrated in Figure 5.5b. Tanyimboh and Templeman (1993b) suggested replacing the two sources by a super source numbered 0 with 55 units of flows, this being the total supply in the network. Also, the link between sources 1 and 2 has been removed and replaced by a direct link from the super source to each source as shown in Figure 5.5b. The single-source method described in Chapter 2 can then be used to calculate the maximum entropy flows in the network. The resulting link flows are shown in Figure 5.5a with an entropy value of 2.367.

The above example has been resolved by the alfa method, and the resulting link flows are shown in Figure 5.5c with an entropy value of 2.45 which is higher than the corresponding value obtained by the super-source approach, suggesting that the results of Figure 5.5a are not optimal. The results obtained by the alfa method and shown in Figure 5.5c have been found to correspond to the maximum entropy flows in the network, and the network entropy value of 2.45 has been found to be the maximum value the flow entropy can have for the network of Figure 5.5 subject to the available information.

Commenting on the results of Figure 5.5a, the equal flows in links 1-3 and 2-3 is questionable. Link 1-3 carries three path flows from source node 1, one for each demand node in the network. On the other hand, link 2-3 carries six path flows, three of them are the same path flows carried by link 1-3 and the other three path flows are those corresponding to source node 2. Consequently, link 2-3 should carry more flow than link 1-3. The super-source approach seems to disregard some path flows supplied by source node 1 through source node 2.

Finally, Figure 5.6 show the maximum entropy flows for the network of Figure 5.5 having the flow direction in link 1-2 reversed. The results quoted in the paper are shown in Figure 5.6a with an entropy value of 1.947, while the results obtained by the alfa method are shown in Figure 5.6b with a higher entropy value of 2.154. It can be seen from the results of Figure 5.6a that the path flows supplied by source node 2 through source node 1 have all been ignored in the super-source approach by assigning a zero flow for the link 2-1.

It is evident from the above investigation that the super-source approach proposed by Tanyimboh and Templeman (1993b) to extend the single-source method to multiple sources for calculating maximum entropy flows does not produce optimal results, and is therefore invalid. The simple alfa method and its algorithms presented in the previous chapter and illustrated in this chapter by means of three general examples has to be used instead.

5.6 SUMMARY AND CONCLUSION

The alfa method algorithms presented in the previous chapter for calculating maximum entropy flows in multi-source, multi-demand general networks have been illustrated in this chapter by means of three major examples exhibiting different aspects of characteristics which can be expected in general real networks. These general examples demonstrated the general applicability of the algorithms, and showed that the proposed algorithms are very efficient and easy to operate by hand calculations especially for small networks such as those used in the examples. Also, computer implementation of the proposed algorithms has been found to be a straightforward task. This was demonstrated by formalising the algorithms into a computer code written in FORTRAN 90 and solving the illustrative examples of this chapter. The running time of this computer code for solving each of the three example problems was negligible.

Several remarks have been made in this chapter when discussing the results of the illustrative examples solved by the proposed method. First, the α values defined by the method have the effect of making the flows supplied by each source to a demand node as uniform as possible subject to the available information. Also, the requirement of equal ratios of αs amongst all demand nodes reachable from any pair of sources can be interpreted as a direct consequence of the maximum entropy formalism since these equal ratios treat all the corresponding demand nodes equally on a bias scale. The values of αs, however, depend on the supply and demand of the network nodes and are influenced by the layout of the network in terms of the number of paths from each source to each reachable demand node and how many nodes are reachable from each source.

Reversing all directions in a water network should not and does not affect the results obtained by the alfa method as long as the total supply balances the demands in the network. Also, maximizing the path entropy function presented in the previous chapter for a water supply network subject to path equilibrium equations at the network nodes gives the same results obtained by the alfa method with path flow probabilities having

the expected equal ratios. This can simply be deduced from the fact that the alfa method results always correspond to the maximum entropy flows in the network.

It has been shown in this chapter that the super-source approach proposed by Tanyimboh and Templeman (1993b) as an extension of the single-source method to multiple sources for calculating maximum entropy flows is invalid and actually does not lead to optimal results. This was demonstrated by the two simple examples used in the above paper. These examples have been resolved in this chapter by the alfa method, and the results have been found to be optimal. This suggests that using the alfa method instead of the super-source approach is essential for such problems.

Finally, the efficiency and simplicity of the alfa method and its algorithms, taking into consideration the applicability of entropy as a surrogate measure of reliability as concluded in Chapter 2 open up the possibility of developing a simple and quick method for designing reliable general water distribution networks. This can be done by using the flows obtained by the alfa method in one of the simplified optimum design methods presented in Chapters 2 and 3 for water distribution networks such as the linearized method proposed by Alperovits and Shamir (1977).

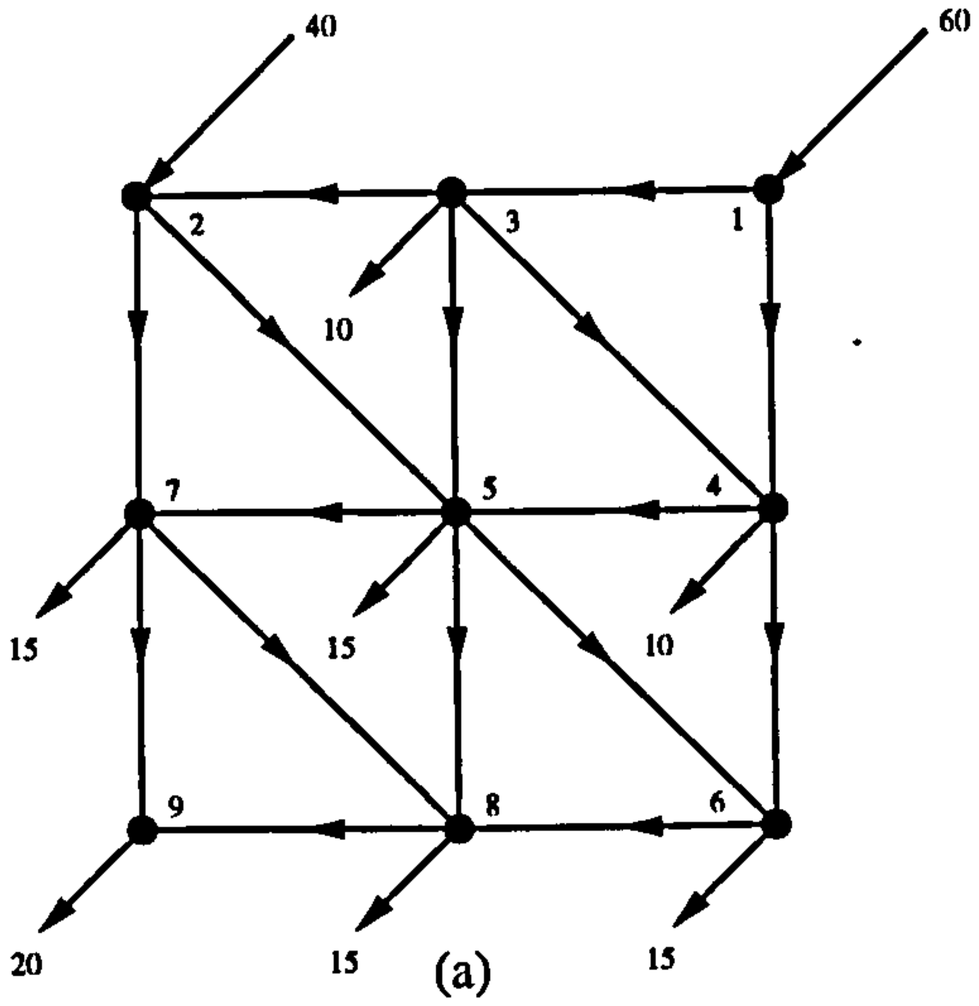

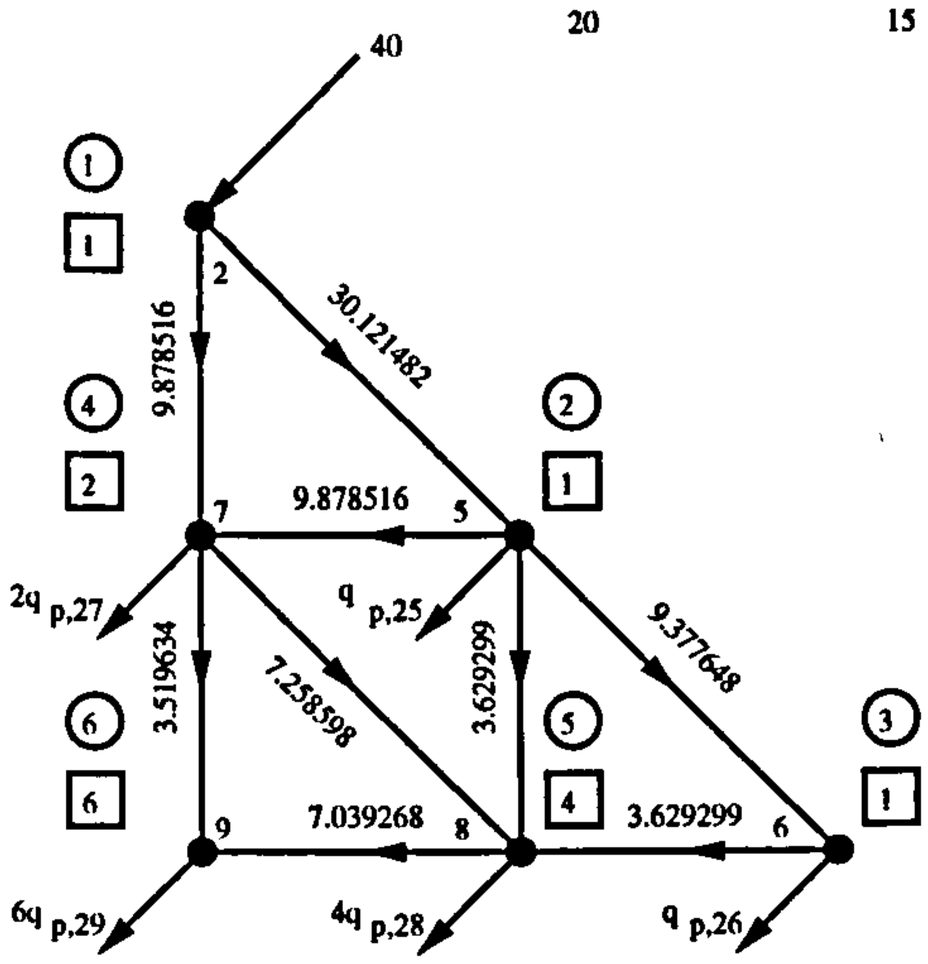

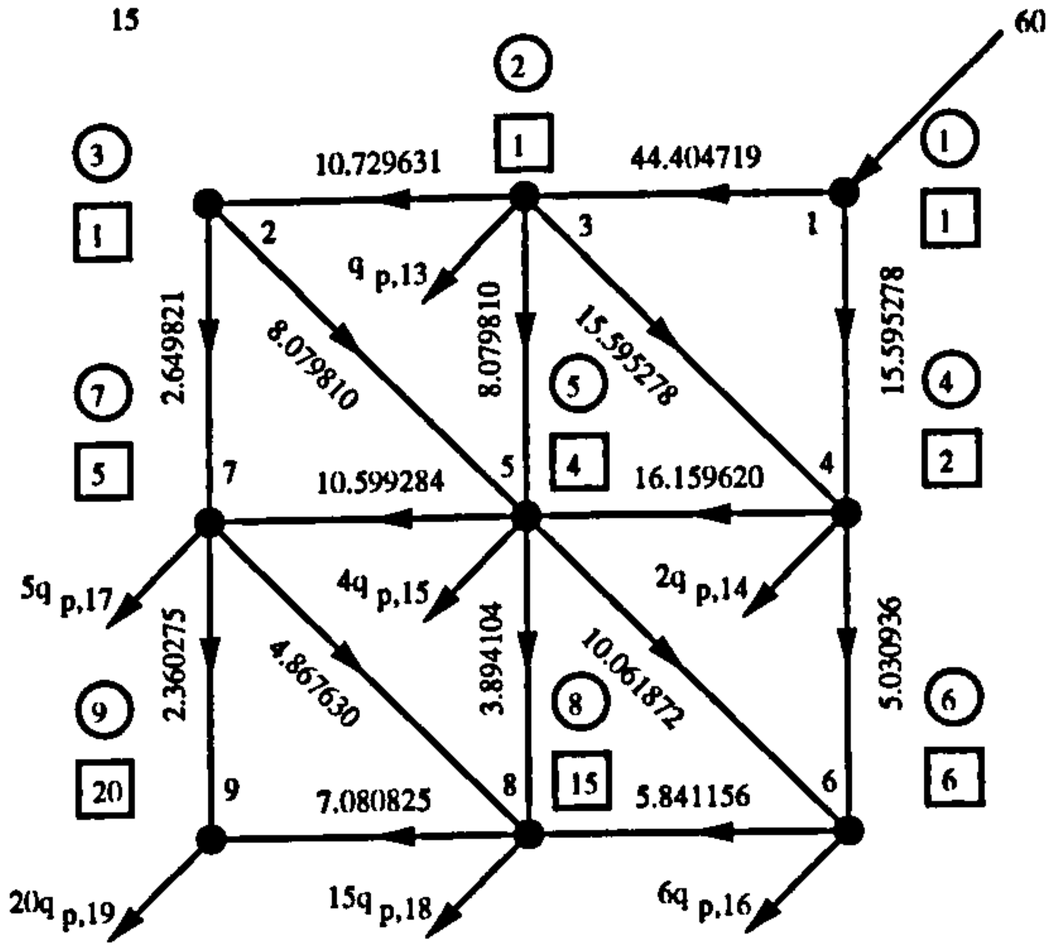

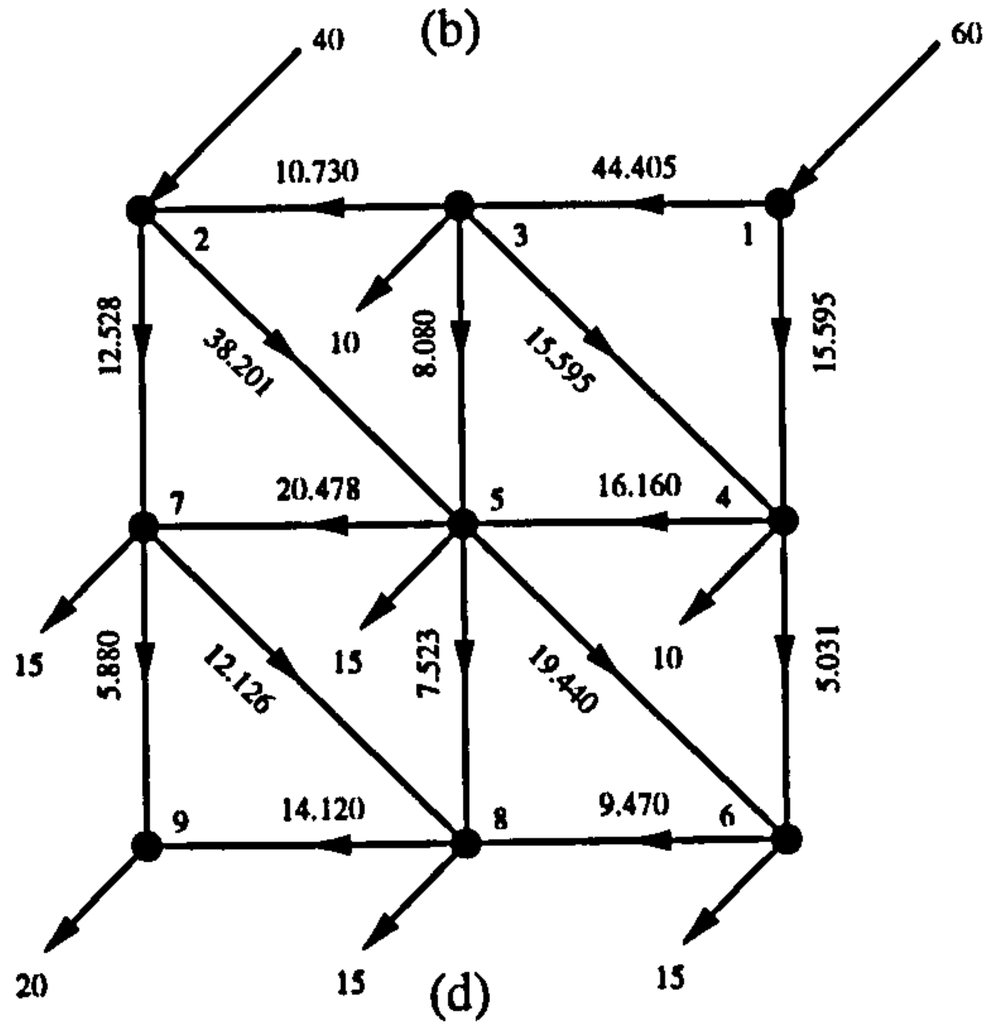

Figure 5.1 Maximum entropy flows for the network of Example 1

(a): Global node numbering
(b): Sub-network SNK 1
(c): Sub-network SNK 2
(d): Final link flows

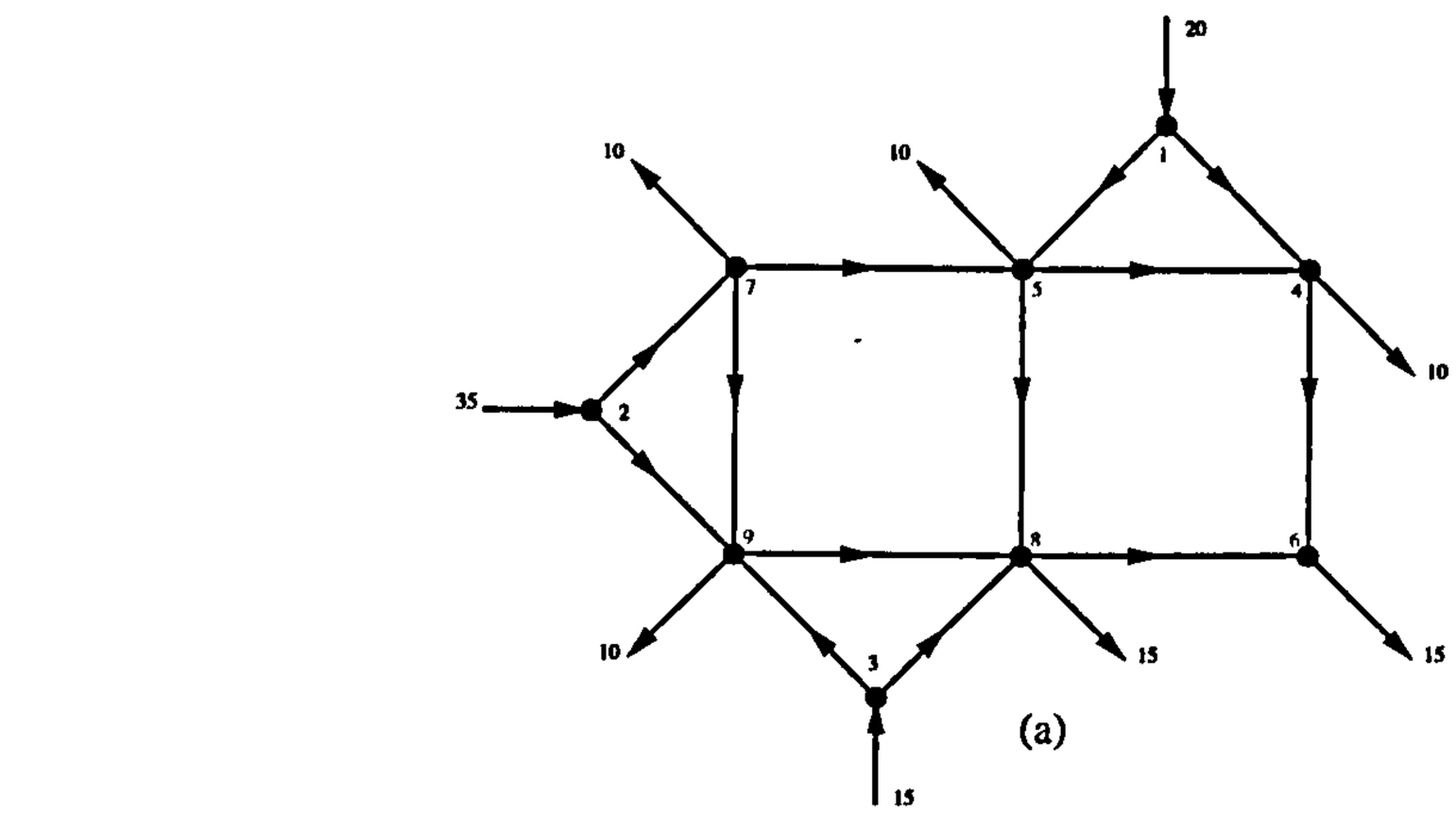

(a)

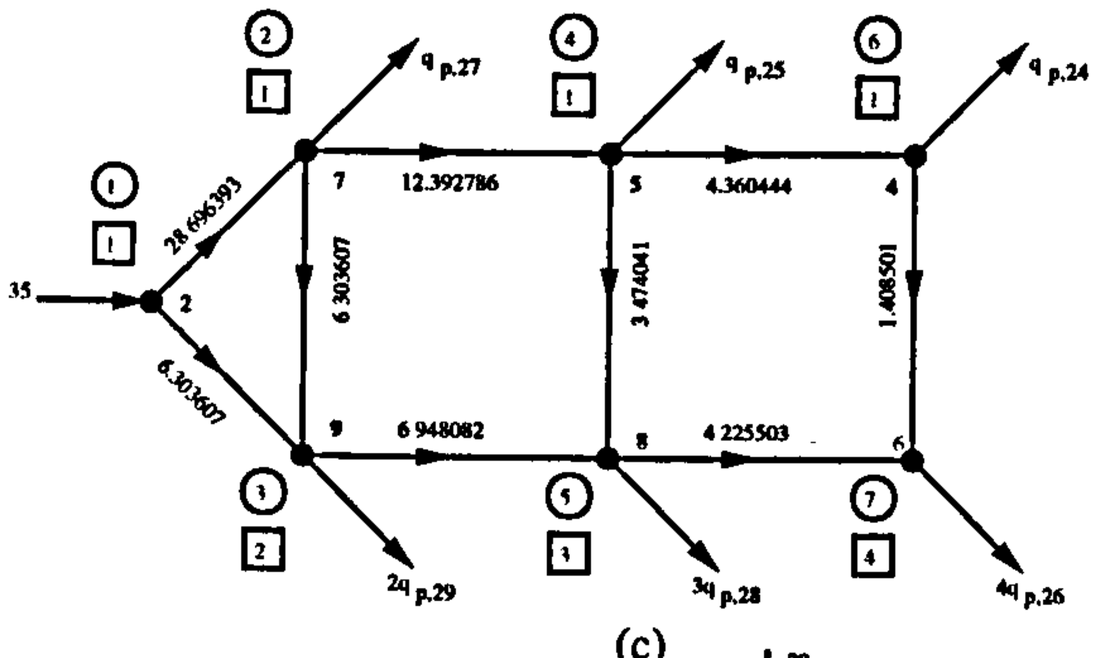

(c)

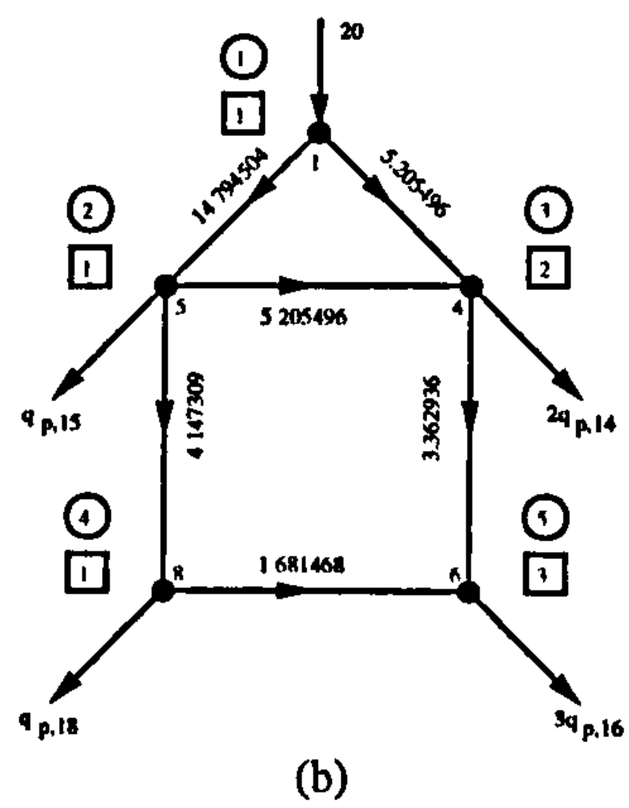

(b)

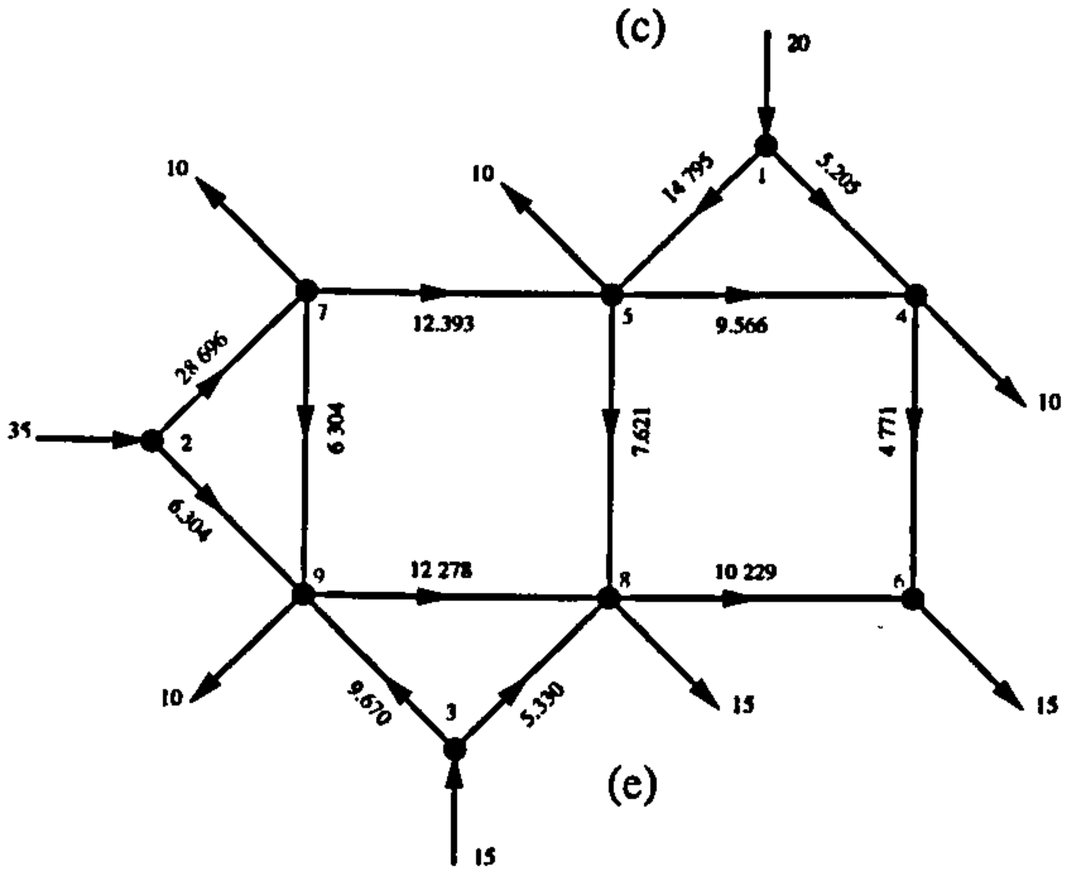

(e)

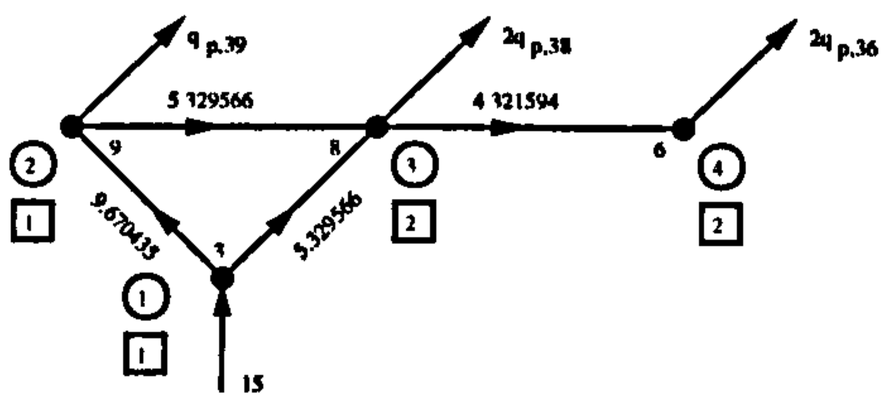

(d)

Figure 5.2 Maximum entropy flows for the network of Example 2

(a): Global node numbering, (b): Sub-network SNK 1
(c): Sub-network SNK 2, (d): Sub-network SNK 3
(e): Final link flows.

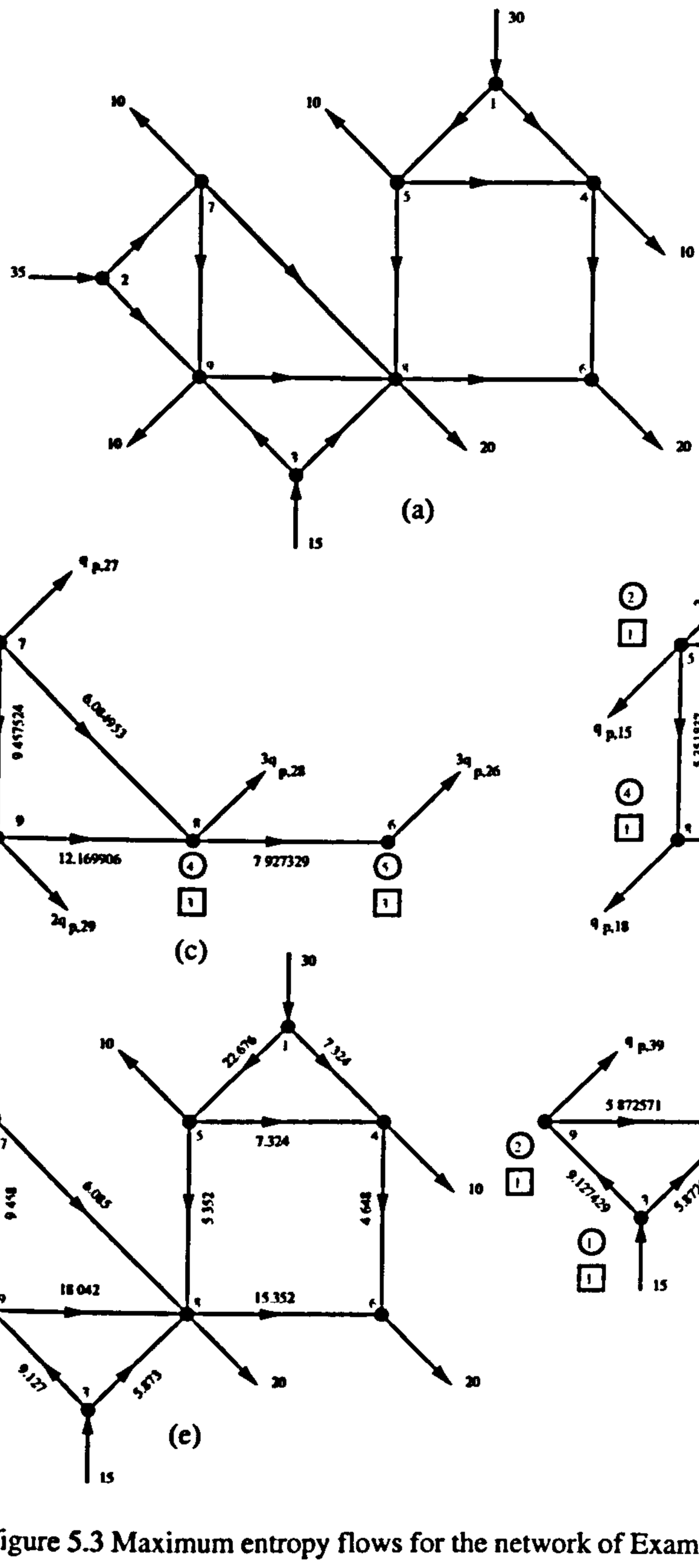

Figure 5.3 Maximum entropy flows for the network of Example 3

(a): Glibal node numbering, (b): Sub-network SNK 1
(c): Sub-network SNK 2, (d): Sub-network SNK 3
(e): Final link flows

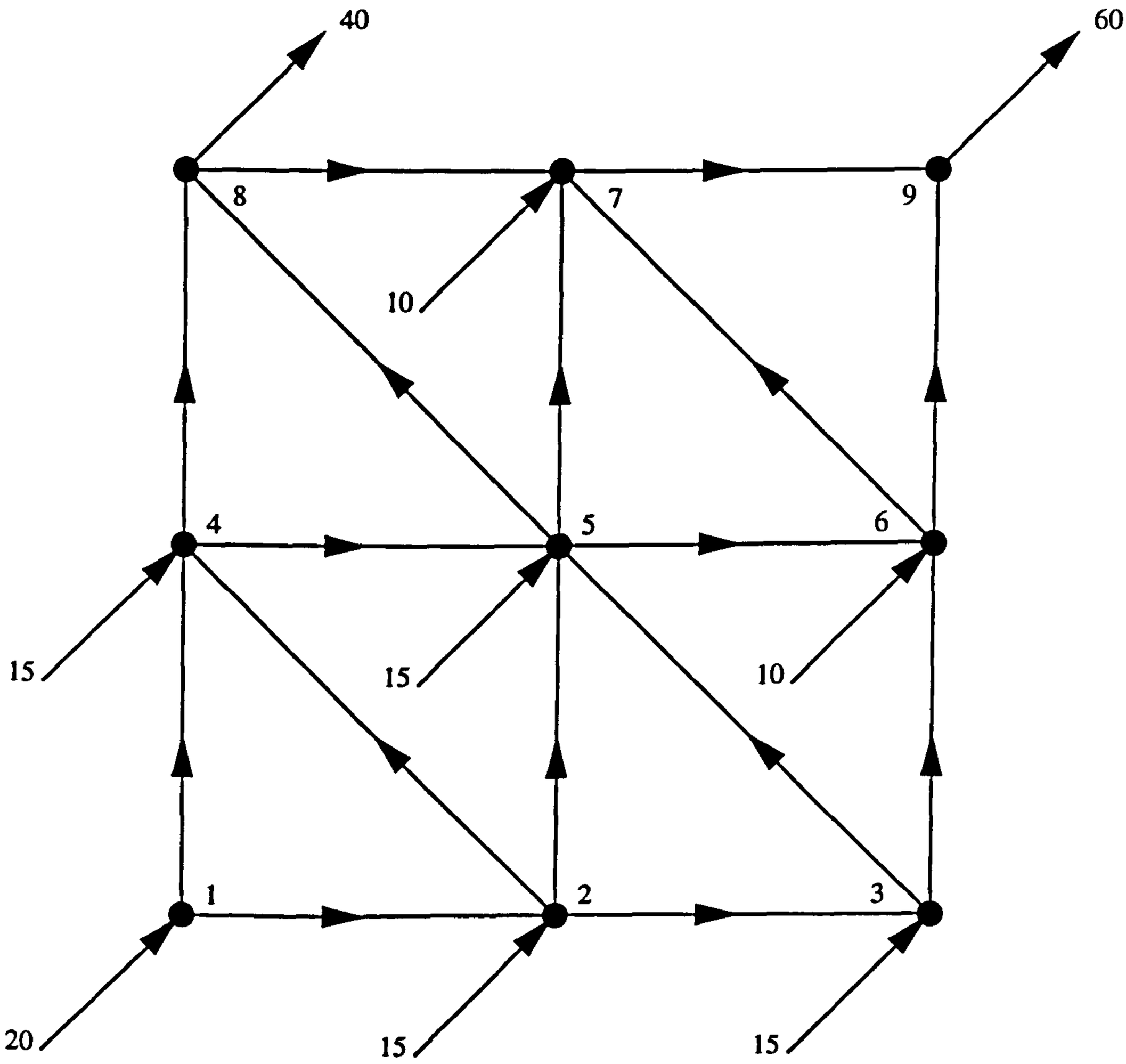

Figure 5.4 The reversed network of the two-source network of Example 1 with a new global node numbering scheme

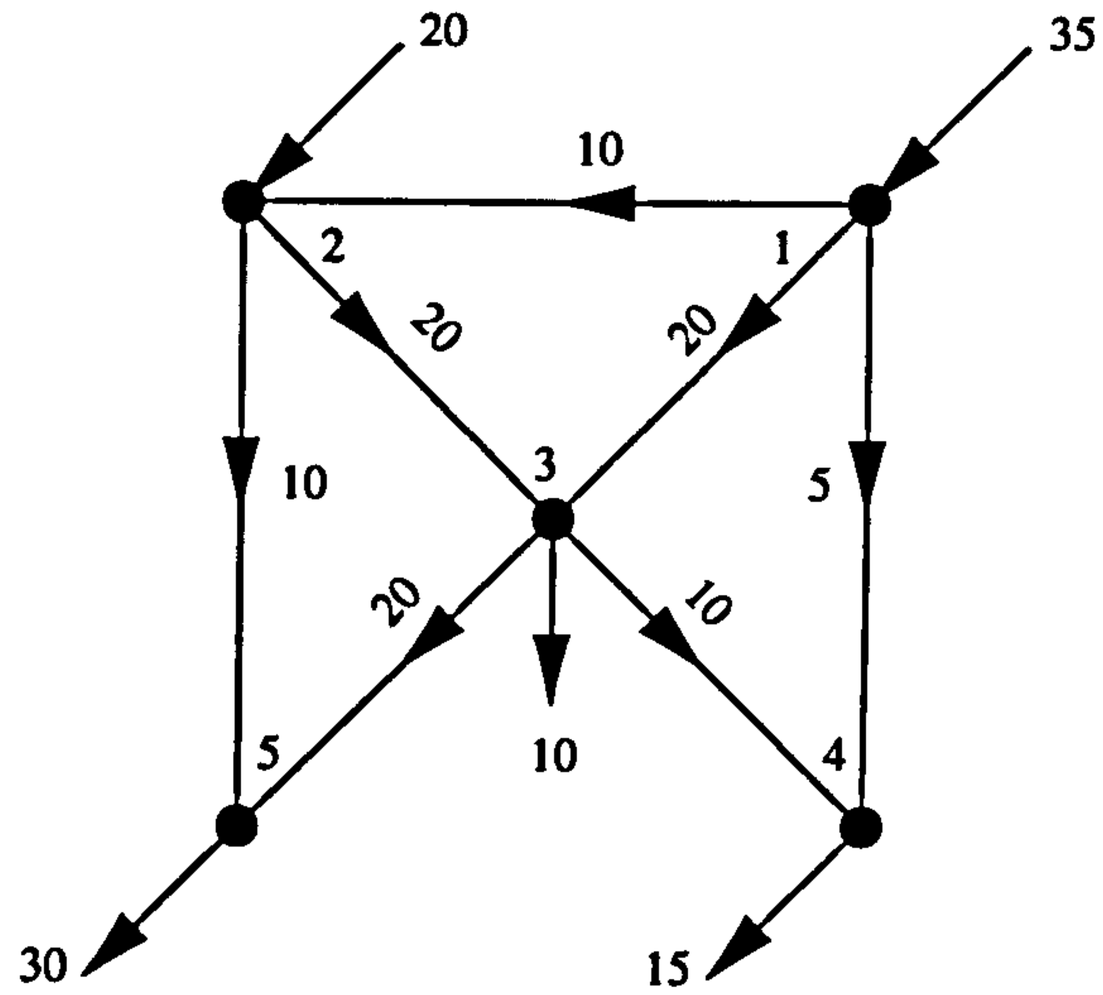

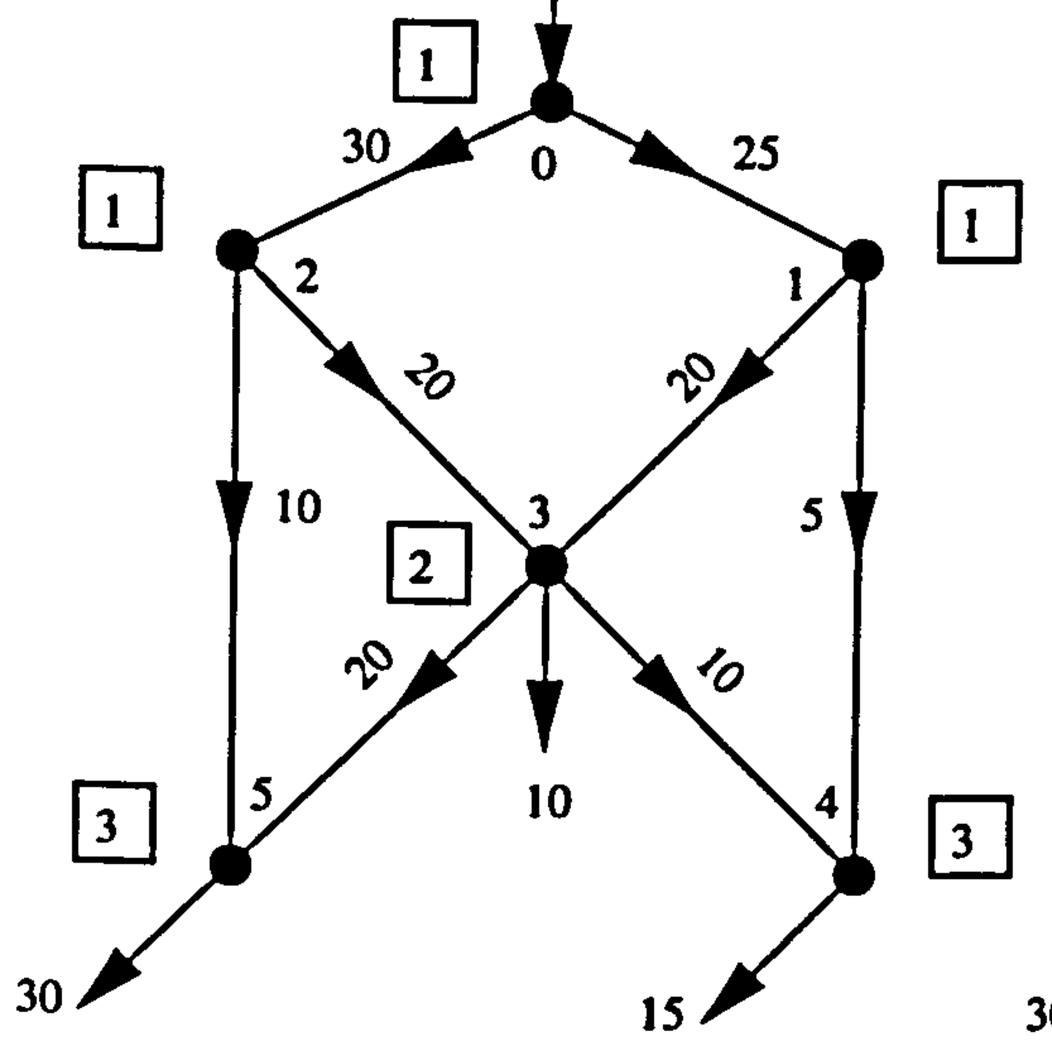

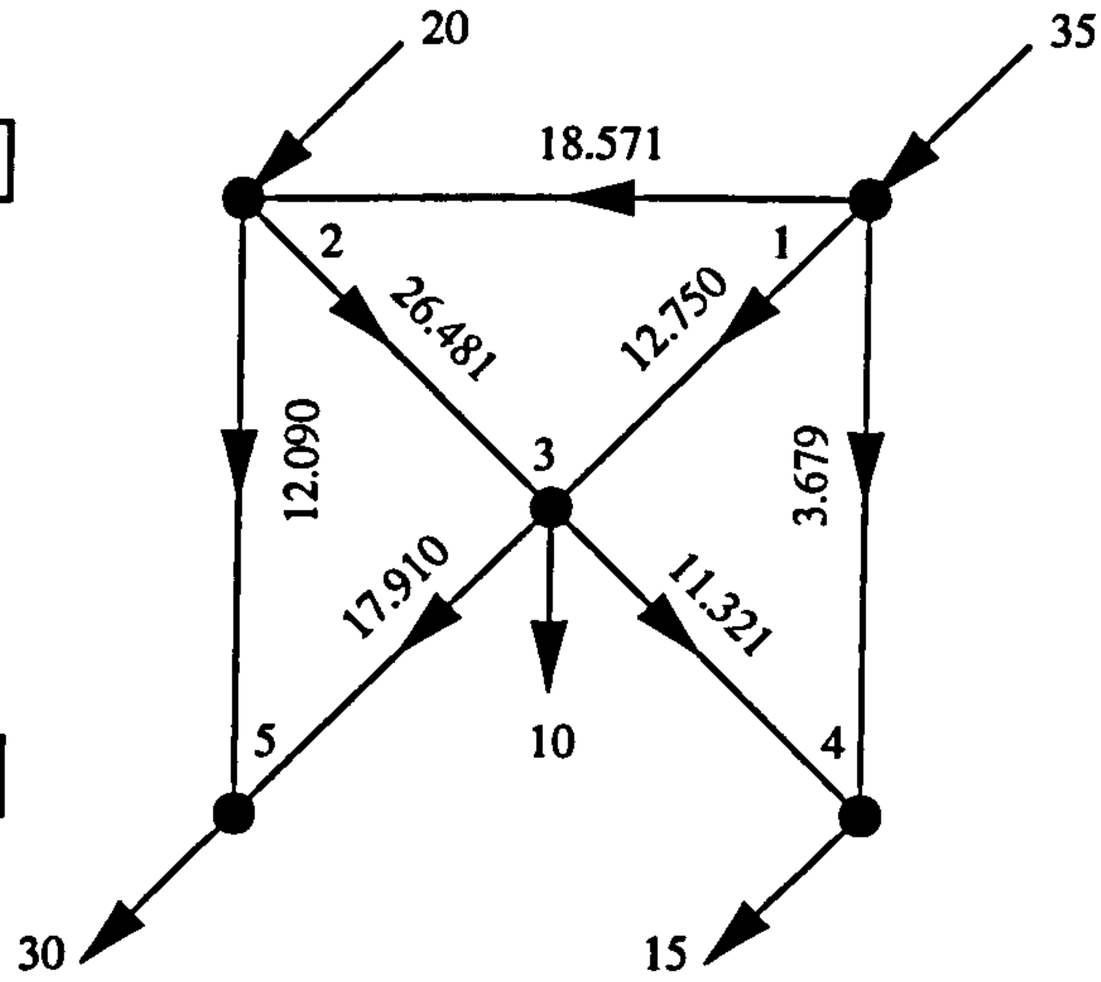

Figure 5.5 Maximum entropy flows for a two-source network adapted from Tanyimboh and Templeman (1993b)

(a): Tanyimboh and Templeman (1993b) results
(b): Super source representation of the network of Figure 5.5a
(c): The alfa method results

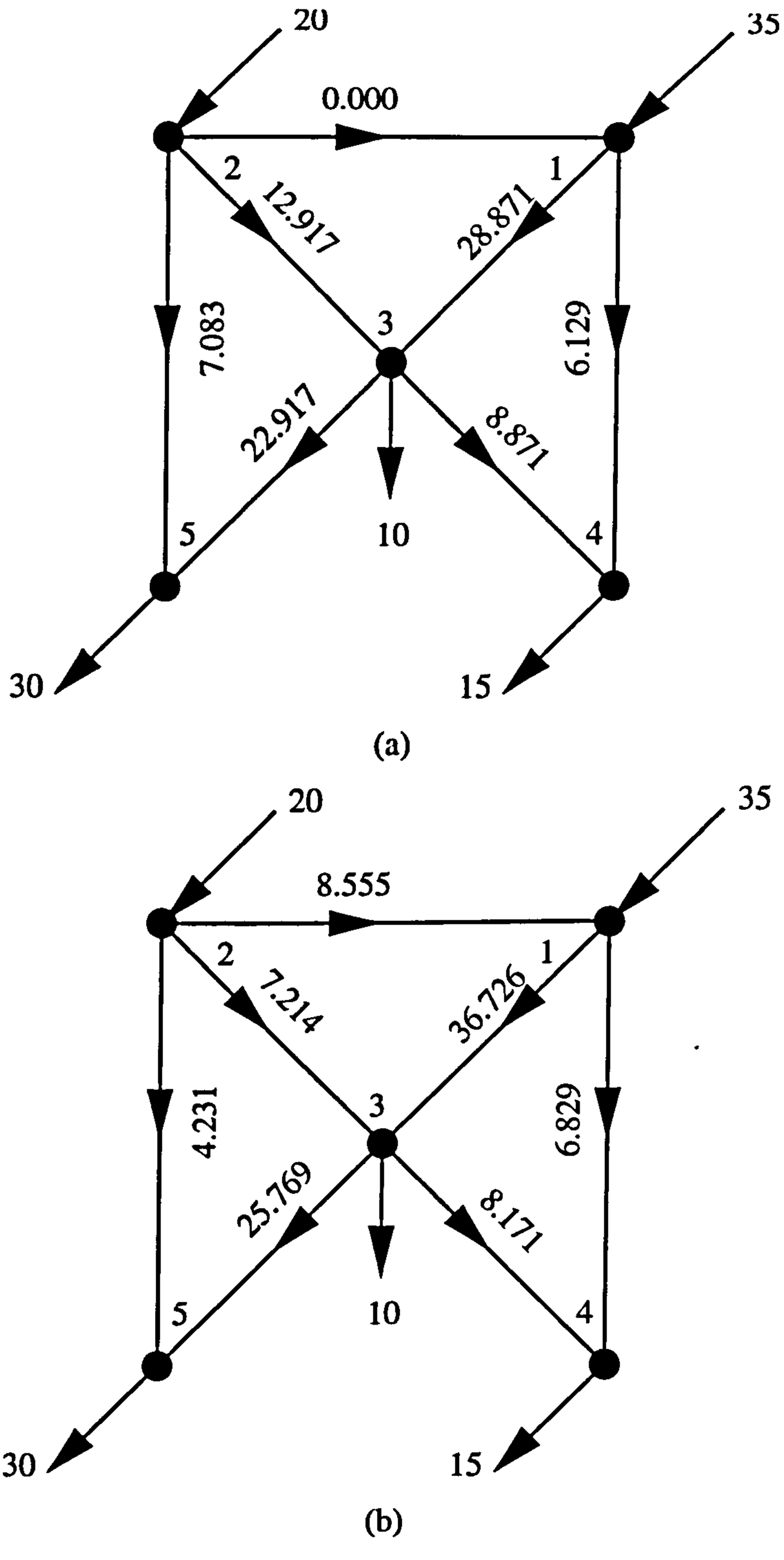

Figure 5.6 Maximum entropy flows for the two-source network of Figure 5.5 having the flow direction in link 1-2 reversed

(a): Tanyimboh and Templeman (1993b) results
(b): The alfa method results

CHAPTER 6

CALIBRATION METHOD FOR GENERAL WATER DISTRIBUTION NETWORKS

6.1 INTRODUCTION

The problem of estimating most-likely, or least-biased, flows in water distribution networks in the presence of incomplete data has fully been investigated in Chapter 2 by means of maximizing the nodal entropy function of the network (see Problem 3), and alternatively and more simply has been solved using the path-based alfa method as shown in Chapter 4 and illustrated in Chapter 5.

In this problem, it has been assumed so far that only source flow rates, demand flow rates and the topology of the network with arc flow directions are known. Other data such as lengths, diameters of pipes and roughness properties were assumed not to be available. Also, some of the physical laws governing water flow in pipe networks have not been considered such as the energy conservation laws presented in Chapter 2. If such extra information can be added to the problem, more accurate flows can be obtained and a more clear understanding of the system behaviour can be visualized.

In practical situations such as old water networks, lengths and diameters of the pipes may be available along with the external flows and the layout of the network. Also, pressure heads at the network nodes can be measured quite easily without any considerable cost or time. Only friction coefficients of the pipes may be missing or may have changed over time. For such cases, an accurate physical analysis of the pipe network cannot be performed to generate accurate pipe flow rates. Also, a physical measurement of these pipe flow rates can be expensive and time consuming. Consequently, a quick method of estimating the pipe flow rates of existing old water

networks and the corresponding unknown pipe characteristics would be most beneficial.

Unfortunately, Problem 3 presented in Chapter 2 and the alfa method presented in Chapter 4 for calculating maximum entropy flows in water distribution networks are not capable of handling such general problems where more information has to be incorporated and added to the formulation. How can such extra information be incorporated in one model capable of estimating pipe flow rates and corresponding pipe characteristics for old water distribution networks?

This chapter addresses the above issues in detail using the maximum entropy formalism. The problem tackled herein is as follows. A water distribution network is given having all the external flows at the sources and demand nodes known. The lengths and diameters of the pipes are also known. Also, the pressure heads at the network nodes may be available. The target is to estimate the most likely pipe flows in the network and the corresponding roughness properties of the pipes. This leads to the possibility of calibrating the already-existing water distribution networks having friction coefficients of the pipes missing or changed with time. Such networks have to be looped, otherwise the pipe flows can be calculated directly from the available flow equilibrium equations, and the pipe roughness properties can then be obtained using the pipe flows and the available pressure heads at the nodes of the network.

There are two sets of variables in the above stated problem, pipe flow variables and pipe roughness characteristic variables. In the pipe flow set of variables, there are NLP number of independent variables in a looped water distribution network as described in Chapter 2, one variable for each loop, where NLP is the number of loops in the network. The number of variables in the pipe roughness characteristic set is equal to the number of links (NLK) in the network, and they are independent. If an entropy function representing the above two sets of variables can be written for general water distribution networks, the problem of inferring the most-likely flows and the corresponding pipe roughness characteristics can be cast as an entropy maximization problem subject to all available information.

To develop such an entropy function for general water distribution networks, pipe flow and pipe characteristic variables have to be cast in a probabilistic way as required by Shannon's informational entropy (Shannon, 1948). It has been shown in Chapter 2 how pipe flows can probabilistically be described at a node (Tanyimboh and Templeman, 1993a) leading to the nodal entropy function of the network. In parallel, an entropy function representing pipe characteristic variables in water distribution networks is introduced in this chapter and is then compounded with the nodal entropy function of the network. The resulting compound entropy function is then maximized subject to all information which can be available in a water distribution network. If such a water distribution network has different patterns of supply and demand flows for different desirable load cases, the above compound problem can then be modified to include all load cases which might be desirable in water distribution networks.

In this chapter, the problem of inferring the least-biased flows and the most-likely pipe characteristics in water distribution networks are individually presented, followed by the compound problem which is then modified to include all desirable load cases which might be available in water distribution networks. The resulting modified general problem, as will be seen later, leads naturally to a model capable of calibrating old general water distribution networks. Illustrative examples of such calibration and others demonstrating the model procedures are left to the next chapter along with general discussions and conclusions.

6.2 PIPE FLOW PROBLEM

The problem of estimating most-likely flows in water distribution networks having source flow rates, demand flow rates and the topology of the network along with pipe flow directions known has been described in Chapter 2 in detail and is briefly restated in this section due to its relevance to the work of this chapter. Before that, the entropy function of network flows developed by Tanyimboh and Templeman (1993a, 1993b, 1993c) and used in the most-likely flow estimation problem is presented.

6.2.1 ENTROPY OF NETWORK FLOWS

It has been shown in Chapter 2 how a flow leaving node n, $\forall$n, in water distribution networks can be cast in a probabilistic way, as required by Shannon's informational entropy function, by normalising it by the total flow reaching or leaving that node, i.e.

$$p_{nk} = \frac{q_{nk}}{T_n} \quad \forall n, \forall k \in ND_n \tag{6.1}$$

in which p_{nk} is the probability that flow, which is destined to pass through node n, $\forall$n, is included in q_{nk}, $\forall k \in ND_n$; q_{nk} is the flow leaving node n, $\forall$n, through link nk, $\forall k \in ND_n$; ND_n is the set of all downstream nodes of link outflows from node n, $\forall$n, including any demand; and T_n represents the total flow reaching or leaving node n, $\forall$n, including any external flow, i.e.

$$T_n = \sum_{j \in NU_n} q_{jn} = \sum_{k \in ND_n} q_{nk} \quad n=1,...,NN \tag{6.2}$$

where NU_n is the set of all upstream nodes of link inflows to node n, $\forall$n, including any supply.

Because the probability p_{nk}, $\forall$n, $\forall k \in ND_n$, given by Eqs. (6.1) is conditional upon the probability that flow has reached node n, $\forall$n, the conditional entropy formula of Khinchin (1953) can be used to obtain the entropy of node n, $\forall$n, as follows:

$$S_n = -P_n \sum_{k \in ND_n} p_{nk} \ln p_{nk} \quad n=1,...,NN \tag{6.3}$$

in which S_n is the entropy of node n, $\forall$n, associated with the outflows from that node n, by setting entropy constant K to unity; P_n is the probability of flow arriving at node n, $\forall$n, which is given by:

$$P_n = \frac{T_n}{T_0} \quad \forall n \tag{6.4}$$

where T_0 is the total supply or demand, i.e.

$$T_0 = \sum_{n \in I_S} q_{0n} = \sum_{n \in I_D} q_{n0} \tag{6.5}$$

in which I_S and I_D respectively are the sets of source nodes and demand nodes in the network; q_{0n} and q_{n0} respectively are the supply and demand of node n,$\forall$n.

Finally, to obtain the total network flow entropy based on the node outflows, the entropy of the distribution of T_0 amongst the sources has to be added to the entropy of all nodes in the network as follows:

$$S_f = S_0^s + \sum_{n=1}^{NN} S_n \tag{6.6}$$

where S_f is the network flow entropy based on the outflows; S_n is the conditional entropy of outflows, including any demand, at node n, $\forall$n, as given by Eq. (6.3); S_0^s is the entropy of the distribution of T_0 amongst the sources and is given by:

$$S_0^s = -\sum_{n \in I_S} P_{0n} \ln P_{0n} \tag{6.7}$$

in which P_{0n} is the fraction of the total supply provided by source node n, $\forall n \in I_S$, and is given by:

$$P_{0n} = \frac{q_{0n}}{T_0} \quad \forall n \in I_S \tag{6.8}$$

It should be noted that a similar nodal entropy function to that of Eq. (6.6) can be obtained based on the inflows to the network nodes rather than the outflows. In this case, the entropy of the distribution of T_0 amongst the sources has to be replaced by an entropy of the distribution of T_0 amongst all the demand nodes in the network. However, the nodal flow entropy function based on the outflows is used throughout this chapter.

Having described the entropy function of network flows, the problem of estimating most-likely flows in water distribution networks excluding any information which might be available about pipe characteristics is presented next.

6.2.2 MAXIMUM ENTROPY FLOWS

To determine most-likely flows in water distribution networks in which only the supplies and demands, and the flow directions in the links are assumed to be available, the network flow entropy given by Eq. (6.6) has to be maximized, according to the maximum entropy formalism, subject to available information which, for this case, are the nodal flow equilibrium equations. If the NLK link flows used in Eq. (6.6), where NLK is the number of links in the network, are substituted in terms of NLP independent link flows, where NLP is the number of loops in the network, to give the following function:

$$S_f = F_s\,(q_s^{ind}) \tag{6.9}$$

in which q_s^{ind} is the vector of all independent flows in the network; one independent flow for each loop; $F_s\,(q_s^{ind})$ is the network entropy of Eq. (6.6) defined in terms of q_i^{ind}, i=1,...,NLP, the nodal flow equilibrium equations can be omitted from the problem as they will be satisfied implicitly in the network entropy objective function. The problem is therefore reduced to maximizing the network flow entropy function of Eq. (6.9) subject to non-negativity of all link flows in the network. The above problem has been introduced in Chapter 2 as Problem 3 and is restated next.

Problem 3

$$\textit{Maximize} \quad S_f = F_s\,(q_s^{ind}) \tag{6.9}$$

Subject to:

$$q_{ij} = Fn_{ij}\,(q_s^{ind}) \geq 0 \quad \forall ij \in IJ \tag{6.10}$$

in which IJ is the set of all the links in the network. Note that Problem 3 can be solved without including the constraints of Eqs. (6.10) since the non-negativity of link flows is implicitly satisfied in the objective function as the logarithmic function is undefined for negative values.

6.3 PIPE CHARACTERISTIC PROBLEM

Having defined the pipe flow problem, the problem of estimating most-likely pipe characteristics in water distribution networks, in which pipe roughness characteristics are assumed not available, can be determined similarly using the maximum entropy formalism. Accordingly, a network entropy formula representing pipe roughness characteristics has to be developed first and is introduced next.

6.3.1 ENTROPY OF NETWORK PIPE CHARACTERISTICS

According to Shannon's informational entropy function, network pipe characteristics have to be described probabilistically if a network pipe characteristic entropy formula is to be defined. Based on the relative frequency interpretation of probability, pipe characteristics can be described in a probabilistic way by normalising each pipe characteristic by the sum of all pipe characteristics in the network as follows:

$$p_{\alpha,ij} = \frac{\alpha_{ij}}{\sum_{ij \in IJ} \alpha_{ij}} \tag{6.11}$$

in which $p_{\alpha,ij}$ is a probability-like quantity representing the contribution of characteristic value α_{ij} of link ij, $\forall ij \in IJ$, to the total; IJ being the set of all links in the network.

Obviously, the set of pipe characteristic probabilities given by Eqs. (6.11) are mutually exclusive and they sum to unity, i.e.

$$\sum_{ij \in IJ} p_{\alpha,ij} = 1 \tag{6.12}$$

Therefore, they represent a finite scheme. Consequently, Shannon's informational entropy can directly be applied to give the following entropy function:

$$S_{\alpha} = - \sum_{ij \in IJ} p_{\alpha,ij} \ln p_{\alpha,ij} \tag{6.13}$$

where S_{α} is the network pipe characteristic entropy for which the constant K of Shannon's informational entropy function is set to unity.

6.3.2 MAXIMUM ENTROPY PIPE CHARACTERISTICS

According to the maximum entropy formalism, the most-likely pipe characteristics in water distribution networks, in which pipe characteristics are assumed not be available, can be estimated by maximizing the network pipe characteristic entropy function given by Eq. (6.13) subject to available information which, for this case, is the normality condition of Eq. (6.12) and non-negativity of all pipe characteristics in the network. Therefore, the above problem can be written as follows:

Problem 6

$$\textit{Maximize} \quad S_{\alpha} = -\sum_{ij \in IJ} p_{\alpha,ij} \ln p_{\alpha,ij} \tag{6.13}$$

Subject to:

$$\sum_{ij \in IJ} p_{\alpha,ij} = 1 \tag{6.12}$$

$$p_{\alpha,ij} \geq 0 \quad \forall ij \in IJ \tag{6.14}$$

Clearly, solving Problem 6 will produce equal pipe characteristic probabilities in the network since there is no reason, or extra information available in this problem, to think otherwise. Therefore, all pipe characteristics in the network would have the same value.

It can be noted that Problems 3 and 6 do not contain information other than external flows and the topology of the network with flow directions in the pipes, which might be available in old water distribution networks. Information such as lengths and diameters of network pipes, energy conservation around each loop and head pressures at the nodes of the network may be available, however. How can such available information be considered and taken into account so that the most-likely flows and the corresponding pipe characteristics in water distribution networks can be estimated more accurately and closer to the actual values which are unique but unknown for the

designer? The answers to this question and others are addressed in the next section.

6.4 COMPOUND PROBLEM

The problem considered in this section is as follows. Find most-likely pipe flows and corresponding pipe characteristics in water distribution networks in which source flow rates, demand flow rates and the topology of the network with pipe flow directions and lengths and diameters of the pipes are known. The pipe flows and pipe characteristics sought in this problem should satisfy the conservation laws of energy around the loops and should match head pressures which might be available at the nodes of the network.

It is recalled from Chapter 2 that conservation laws of energy around the loops in water distribution networks state that the net head loss around each loop should be equal to zero, i.e.

$$\sum_{ij \in IJ_l} h_{ij} = 0 \quad l=1,...,NLP \tag{6.15}$$

in which h_{ij} is the head loss in link ij, $\forall ij \in IJ_l$, l=1,...,NLP; where IJ_l being the set of all links in loop l and NLP is the number of loops in the network.

Also, the total head loss along any path between two nodes whose head pressures are known must equal the head loss of that path which is the difference between the heads of the first and the last node of that path. Therefore:

$$\sum_{ij \in IJ_p} h_{ij} = h_p \quad p=1,...,NP \tag{6.16}$$

in which IJ_p is the set of all links in path p, $\forall p$; h_p is the known path head loss; and NP is the number of independent paths in the network, each of which contains some information which is not already contained in any other path.

In Eqs. (6.15) and (6.16), the head loss h_{ij} may be given by the following Hazen-Williams equation:

$$h_{ij} = \frac{\alpha\ Le_{ij}\ (\frac{q_{ij}}{C_{ij}})^{1.852}}{D_{ij}^{4.87}} \quad \forall ij \in IJ \tag{6.17}$$

in which q_{ij} is the flow rate in pipe ij, $\forall ij \in IJ$, which is positive in the direction of flow; α is a dimensionless conversion factor for units and is equal to 10.67 in S.I. units; Le_{ij}, D_{ij} and C_{ij} are respectively the length, the internal diameter and the Hazen-Williams coefficient of pipe ij, $\forall ij \in IJ$; and IJ is the set of all the links in the network.

Considering Eq. (6.17), the pipe characteristics sought in this chapter may take different values for different cases as follows:

1. Lengths and diameters of the pipes are not available:

$$\alpha_{ij} = \frac{\alpha\ Le_{ij}}{C_{ij}^{1.852}\ D_{ij}^{4.87}} \quad \forall ij \in IJ \tag{6.18}$$

2. Pipe lengths are available:

$$\alpha_{ij} = \frac{\alpha}{C_{ij}^{1.852}\ D_{ij}^{4.87}} \quad \forall ij \in IJ \tag{6.19}$$

3. Lengths and diameters are available:

$$\alpha_{ij} = \frac{\alpha}{C_{ij}^{1.852}} \quad \forall ij \in IJ \tag{6.20}$$

Consequently, Eq. (6.17) can be simplified as follows:

$$h_{ij} = \alpha_{ij}\ q_{ij}^{1.852} \quad \forall ij \in IJ \tag{6.21}$$

in which α_{ij} is the characteristic value of pipe ij, $\forall ij \in IJ$, and is given by Eqs. (6.18), (6.19) or (6.20) depending whether the length and the diameter of pipe ij are available or not available as shown earlier. Finally, substituting Eq. (6.21) into energy conservation equations [Eqs. (6.15) and (6.16)] gives the following equations:

$$\sum_{ij \in IJ_l} \alpha_{ij}\ q_{ij}^{1.852} = 0 \quad l=1,\ldots,NLP \tag{6.22}$$

$$\sum_{ij \in LJ_p} \alpha_{ij} \, q_{ij}^{1.852} = h_p \quad p=1,...,NP \tag{6.23}$$

Eqs. (6.22) and (6.23) can contain all the information which might be available in old water distribution networks. Apart from the equilibrium equations which are implicitly satisfied in the objective function of Problem 3, the conservation of energy around the loops is contained in Eqs. (6.22) and the head pressures at the network nodes may be included by means of Eqs. (6.23). Also, the lengths and the diameters of the pipes can be included in α_{ij} values as required.

Clearly, neither equation Eq. (6.22) and (6.23) can be added as a constraint to Problem 3 or Problem 6 since these equations contain more variables than those contained in either problem individually. The question which needs to be answered here becomes as follows: how can Eqs. (6.22) and (6.23) be incorporated in one single model in conjunction with Problems 3 and 6?

A compound entropy function for water distribution networks is presented next, followed by the problem of estimating maximum entropy flows and corresponding maximum entropy pipe characteristics in water distribution networks.

6.4.1 COMPOUND NETWORK ENTROPY

It is recalled here that the nodal entropy function used in Problem 3 is the entropy of a finite probability scheme representing the distribution of the total supply in the network amongst the sources, plus the sum of the entropies of NN conditional finite probability schemes, each representing the outflows from a node in the network and depending upon the probability of flow arriving at that node. On the other hand, the pipe characteristic entropy function used in Problem 6 is the entropy of one single finite probability scheme representing the probabilities of the network pipes having some characteristic values. Assuming the pipe characteristic finite probability scheme is independent from all the finite probability schemes used in the nodal flow entropy function, the joint entropy of a compound scheme presented in Chapter 2 can be

applied by summing the nodal entropy and the pipe characteristic entropy functions to give the following compound function:

$$S = S_f + S_\alpha = F_s\,(q_s^{ind}) - \sum_{ij \in IJ} p_{\alpha,ij} \ln p_{\alpha,ij} \qquad (6.24)$$

in which S is the compound entropy function of the network; q_s^{ind} is the set of NLP independent flows; and $p_{\alpha,ij}$ is characteristic value for pipe ij, $\forall ij \in IJ$, where there are NLK such characteristic values in the network.

6.4.2 MAXIMUM ENTROPY FLOWS AND CORRESPONDING MAXIMUM ENTROPY PIPE CHARACTERISTICS

Having defined the compound network entropy function in water distribution networks in terms of independent flows and pipe characteristics, the problem of estimating most-likely pipe flows and corresponding least-biased pipe characteristics can be formulated according to the maximum entropy formalism as an entropy maximization problem subject to all available information which is the constraints of Problems 3 and 6 and the extra information given by Eqs. (6.22) and (6.23).

However, the compound network entropy function of Eq. (6.24) has the pipe flows defined in terms of independent flows (q_s^{ind}). Therefore, Eqs. (6.22) and (6.23) defined in terms of pipe flows have to be rewritten in terms of independent pipe flows if they are to be included in the constraint set of the compound problem. Consequently, Eqs. (6.22) and (6.23) can be written as follows:

$$\sum_{ij \in IJ_l} \alpha_{ij}\,[Fn_{ij}\,(q_s^{ind})]^{1.852} = 0 \quad l=1,\ldots,NLP \qquad (6.25)$$

$$\sum_{ij \in IJ_p} \alpha_{ij}\,[Fn_{ij}\,(q_s^{ind})]^{1.852} = h_p \quad p=1,\ldots,NP \qquad (6.26)$$

in which $Fn_{ij}\,(q_s^{ind})$ is the flow in pipe ij, $\forall ij \in IJ$, defined in terms of the unknown independent pipe flows in the network.

Also, because Eqs. (6.25) and (6.26) contain pipe characteristic values $\alpha_{ij}, \forall ij$, rather than pipe characteristic probabilities, the compound network entropy function of Eq. (6.24) is rewritten in terms of $\alpha_{ij}, \forall ij$, by substituting Eq. (6.11) into Eq. (6.24) to give the following function:

$$S = F_s\,(q_s^{ind}) - \sum_{ij \in IJ} \frac{\alpha_{ij}}{\sum_{ij \in IJ} \alpha_{ij}} \ln \frac{\alpha_{ij}}{\sum_{ij \in IJ} \alpha_{ij}} \qquad (6.27)$$

At this stage, Eqs. (6.25) and (6.26) are now compatible with Eq. (6.27) and they are fit to be included in the constraint set of the compound problem. Looking to the other possible constraints which are the constraints of Problems 3 and 6, it can be argued that non-negativity constraints of pipe flows and pipe characteristics can be excluded as they are implicitly satisfied in the objective function of Eq. (6.27) since the logarithmic function is undefined for negative values. Also, the normality condition constraint of Eq. (6.12) in Problem 6 can be omitted from the constraint set of the compound problem as it is implied in the second term of the objective function of Eq. (6.27). Consequently, the problem of estimating maximum entropy flows and corresponding maximum entropy pipe characteristics in water distribution networks can be formulated as follows:

Problem 7

$$\textit{Maximize} \quad S = F_s\,(q_s^{ind}) - \sum_{ij \in IJ} \frac{\alpha_{ij}}{\sum_{ij \in IJ} \alpha_{ij}} \ln \frac{\alpha_{ij}}{\sum_{ij \in IJ} \alpha_{ij}} \qquad (6.27)$$

Subject to:

$$\sum_{ij \in IJ_l} \alpha_{ij}\,[Fn_{ij}\,(q_s^{ind})]^{1.852} = 0 \quad l=1,\ldots,NLP \qquad (6.25)$$

$$\sum_{ij \in IJ_p} \alpha_{ij}\,[Fn_{ij}\,(q_s^{ind})]^{1.852} = h_p \quad p=1,\ldots,NP \qquad (6.26)$$

in which α_{ij}, $\forall ij$, is given by Eqs. (6.18), (6.19) or (6.20) depending whether the length and the diameter of pipe ij are available or not available.

Problem 7 has been formalized as one of non-linear constrained optimization, and it can be solved by any suitable non-linear constrained programming algorithm. Because the problem is non-linear in both the objective and constraint functions, it may be non-convex and it may have several local maxima. Therefore, it is suggested that solving Problem 7 with several different starting points should ensure that the obtained solution is a global rather than a local one.

It should be noted that the equilibrium equations of flow at the network nodes have not been included in the constraint set of Problem 7 as they are implicitly satisfied in the first term of the objective function of Eq. (6.27). The number of variables in Problem 7 is (NLP+NLK) in which the unknown NLP independent flows should be selected so that there is one variable for each loop, while the unknown NLK pipe characteristics represent all the pipes in the network. On the other hand, the number of constraints is (NLP+NP), where NP is the number of chosen independent paths between any two nodes in the network, usually a source and a terminal node, whose head pressures are available, and is generally much lower than the number of links in the network.

Because the term $\Sigma\alpha_{ij}$, $\forall ij \in IJ$, used in the objective function of Problem 7 is unknown, the resulting maximum entropy pipe characteristics may have unbounded and non-unique solutions but always with unique optimal probability values. However, including enough head loss path constraints of Eqs. (6.26) will bound the pipe characteristic values into a unique and meaningful solution.

Finally, Problem 7 has been formulated for one single load case only. However, it is desired to consider multiple load cases in water distribution networks to take into account some emergency demands such as fire fighting demands, or because of changes in demand distribution amongst the demand nodes in the network due to other different reasons. Therefore, Problem 7 is modified so that it can include extra

information which might be available from different desirable load cases which might help identifying more accurate pipe characteristic values in the network. The modified problem is presented next.

6.4.3 MULTIPLE-LOAD CASE

In water distribution networks with multiple-load cases, there should be NLC sets of most-likely flows in the network pipes, where NLC is the number of load cases in the network, each set corresponds to a load case and depends upon the external flows and the flow directions in the pipes for that load case. However, only one set of most-likely pipe characteristics is sought since there is only one set of pipes in the network carrying different flows for different load cases. Consequently, the objective function of Problem 7 has to be modified so that it contains the flow entropy functions of all load cases considered in the network, i.e.

$$S = \sum_{r=1}^{NLC} F_{s,r}\left(q_{s,r}^{ind}\right) - \sum_{ij \in IJ} \frac{\alpha_{ij}}{\sum_{ij \in IJ} \alpha_{ij}} \ln \frac{\alpha_{ij}}{\sum_{ij \in IJ} \alpha_{ij}} \tag{6.28}$$

in which the equilibrium equations for load case r, r=1,...,NLC, are implicitly satisfied in the corresponding flow entropy function $F_{s,r}\left(q_{s,r}^{ind}\right)$.

Also, for each load case a set of constraints similar to Eqs. (6.25) and (6.26) has to be added to the problem. This can be done by generalizing Eqs. (6.25) and (6.26) to include NLC load cases as follows:

$$\sum_{ij \in IJ_{l,r}} \alpha_{ij} \left[Fn_{ij,r}\left(q_{s,r}^{ind}\right)\right]^{1.852} = 0 \quad l=1,...,NLP;\ r=1,...,NLC \tag{6.29}$$

$$\sum_{ij \in IJ_{p,r}} \alpha_{ij} \left[Fn_{ij,r}\left(q_{s,r}^{ind}\right)\right]^{1.852} = h_{p,r} \quad p=1,...,NP_r;\ r=1,...,NLC \tag{6.30}$$

in which $IJ_{l,r}$ is the set of the links in loop l for load case r; $IJ_{p,r}$ is the set of the links in path p, $\forall p$, for load case r; $h_{p,r}$ is the known head loss of path p for load case r; and NP_r is the number of independent paths whose head losses are known for load case

r. The problem becomes as follows: maximize Eq. (6.28) subject to the constraints of Eqs. (6.29) and (6.30). It can be seen that in this problem there is one set of pipe characteristics but NLC sets of flows; consequently objective function (6.28) is biased towards flow entropy. Therefore, the objective function Eq. (6.28) has to be modified so that there will be some balance between the single pipe characteristic entropy and the NLC flow entropies contained in the equation. This can be done either by weighting the pipe characteristic entropy by NLC, or by averaging the NLC flow entropies amongst all the load cases in the network. The second option is used in this thesis to give the following modified objective function:

$$S = \frac{1}{NLC} \sum_{r=1}^{NLC} F_{s,r}\left(q_{s,r}^{ind}\right) - \sum_{ij \in IJ} \frac{\alpha_{ij}}{\sum_{ij \in IJ} \alpha_{ij}} \ln \frac{\alpha_{ij}}{\sum_{ij \in IJ} \alpha_{ij}} \qquad (6.31)$$

Consequently, the final modified general problem can be written as follows:

Problem 8

$$Maximize \quad S = \frac{1}{NLC} \sum_{r=1}^{NLC} F_{s,r}\left(q_{s,r}^{ind}\right) - \sum_{ij \in IJ} \frac{\alpha_{ij}}{\sum_{ij \in IJ} \alpha_{ij}} \ln \frac{\alpha_{ij}}{\sum_{ij \in IJ} \alpha_{ij}} \qquad (6.31)$$

Subject to:

$$\sum_{ij \in IJ_{l,r}} \alpha_{ij} \left[Fn_{ij,r}\left(q_{s,r}^{ind}\right)\right]^{1.852} = 0 \quad l=1,...,NLP;\ r=1,...,NLC \qquad (6.29)$$

$$\sum_{ij \in IJ_{p,r}} \alpha_{ij} \left[Fn_{ij,r}\left(q_{s,r}^{ind}\right)\right]^{1.852} = h_{p,r} \quad p=1,...,NP_r;\ r=1,...,NLC \qquad (6.30)$$

Problem 8, as Problem 7, is a non-linear and non-convex constrained optimization problem. The number of variables, however, has increased from (NLP+NLK) to (NLC*NLP+NLK), and the number of constraints has increased from (NLP+NP) to (NLC*NLP+Σ NP_r). Any suitable non-linear constrained programming algorithm can be used to solve this problem. A computer programme has been written in FORTRAN

77 to solve the above problem for general water distribution networks in conjunction with the NAG library routine E04UCF which uses a sequential quadratic programming method for non-linear constrained optimization. This computer programme is given in Appendix D and is used in the next chapter to solve some numerical examples. The results are discussed and conclusions are drawn.

The real potential benefit of Problem 8 is the possibility of calibrating old water distribution networks in which roughness coefficients of the network pipes have been lost or changed over time. If Problem 8 is applied to such networks, the missing pipe characteristics can be estimated and the corresponding pipe flows, which are unknown due to the loss of those pipe characteristics, can be calculated quite easily and directly without the need for physical measurement of the pipe flows, which might be expensive and time consuming. A simulated water distribution network whose pipe flows and pipe characteristics are known is calibrated in the next chapter by applying Problem 8. The results are compared to the actual values and discussed, and conclusions are drawn.

6.5 SUMMARY

The problem of estimating most-likely flows and corresponding most-likely pipe characteristics in water distribution networks, in which roughness coefficients of the network pipes have been lost or changed with time, has been developed in this chapter using the maximum entropy formalism. Two problems have been introduced in this chapter and then compounded to produce the above problem. The first problem is the pipe flow problem in which the nodal entropy function of the network flows developed by Tanyimboh and Templeman (1993a, 1993b, 1993c) has been maximized subject to equilibrium equations. The second problem is concerned with pipe characteristics, for which entropy of the network pipe characteristics has been defined after normalising each pipe characteristic by the sum of all pipe characteristics in the network, and which is then maximized subject to the normality condition of the pipe characteristic probability scheme in the network.

It has been shown in this chapter that neither of the above two problems is capable of incorporating some basic information which is often available in real water distribution networks, such as the lengths and diameters of the network pipes, and some basic requirements of energy conservation in the network. The compound problem, however, is capable of handling such information, and is applicable to real general water distribution networks in the sense that it is capable of considering all general data which might be available in already-existing water distribution networks in which only pipe characteristics and pipe flows are not available, leading to the possibility of calibrating such networks quite easily and directly without the need for any expensive equipment for measuring the flows in the network pipes, which can also be time consuming.

Moreover, the above developed calibration model for water distribution networks has been modified to include several load cases which might be desirable in water distribution networks due to some emergency requirements or due to some other reasons. The modified model, which has been cast as non-linear constrained optimization, can be applied to general water distribution networks having several desirable load cases, and can be solved by any suitable constrained non-linear programming algorithm. Illustrative examples for this general model are solved in the next chapter demonstrating the calibration procedure on a simulated real water distribution network. The results are discussed and general conclusions are drawn.

CHAPTER 7

NUMERICAL APPLICATIONS OF THE WATER DISTRIBUTION NETWORK CALIBRATION METHOD

7.1 INTRODUCTION

The aim of this chapter is to demonstrate the calibration method presented in the previous chapter as Problem 8 for calculating maximum entropy flows and corresponding maximum entropy pipe characteristics in water distribution networks in which only pipe roughness coefficients and hence the pipe flows are assumed not available.

Two network examples are used in this regard. The first example is a one-source network of Figure 7.1 adapted from Tanyimboh and Templeman (1993c) and designed to carry maximum entropy flows. The second example is a simulated one-source network of Figure 7.2 having multiple load cases and known pipe characteristics and pipe flows for all different load cases.

The computer programme written in FORTRAN 77 for solving Problem 8 in conjunction with the NAG library routine E04UCF for non-linear constrained optimization, and given in Appendix D is referred to in this chapter as CAMONET (CAlibration MOdel for water NETworks) and is used to solve the above two examples for which the available information is added step by step to each problem, so that the effect of each piece of information on the results can be investigated and compared with the actual values. The CAMONET computer programme has been designed to allow for this step-by-step adding of information and is used in this chapter to solve the calibration problem with different piece of information available

as follows:

1. In addition to external flows and the topology of the network with flow directions in the pipes, head losses around the loops are considered but lengths and diameters of the pipes are assumed not available .
2. Head losses around the loops and head losses along some paths are considered but lengths and diameters of the pipe are still not available .
3. Head losses around the loops and head losses along some paths are considered and pipe lengths are known.
4. Head losses around the loops and head losses along some paths are considered, with both pipe lengths and diameters also known.
5. All the above cases can be considered for different load cases which might be desirable in a water distribution network.

In this chapter, the two examples of Figures 7.1 and 7.2 are solved using the CAMONET computer programme for the above different cases. The results are discussed and compared with the actual values, and conclusions are drawn.

7.2 EXAMPLE 1

The one-source network of this example adapted from Tanyimboh and Templeman (1993c) and shown here in Figure 7.1 has six nodes and seven links with two loops. The external inflows and outflows and the flow directions in the pipe are shown in the figure, with units of m^3/sec.

In their paper, Tanyimboh and Templeman (1993c) assumed that each link in the network is 1000m long and has a Hazen-Williams coefficient of 130, and the total head loss along any path between nodes 1 and 6 is 20m. They designed this network to carry maximum entropy flows calculated by solving Problem 3 presented in the previous chapter. The calculated maximum nodal entropy pipe flows and the corresponding designed pipe diameters are given in Table 7.1.

Table 7.1 Pipe data for the one-source network of Figure 7.1 and pipe diameters designed by Tanyimboh and Templeman (1993c) to carry maximum nodal entropy pipe flows with S_f= 1.915.

Link i-j	1-2	2-4	3-4	4-6	5-6	1-3	3-5
Le_{ij} (m)	1000	1000	1000	1000	1000	1000	1000
C_{ij}	130	130	130	130	130	130	130
$\alpha_{ij}=10.67/C_{ij}^{1.852}$	0.0013	0.0013	0.0013	0.0013	0.0013	0.0013	0.0013
$*q_{ij}(m^3/sec)$	0.084	0.056	0.057	0.038	0.018	0.200	0.110
D_{ij} (m)	0.261	0.235	0.234	0.234	0.185	0.367	0.294

* Design maximum nodal entropy pipe flows obtained by solving Problem 3.

The above network is now solved by the CAMONET computer programme assuming that pipe characteristics α_{ij}, $\forall ij \in IJ$, and corresponding design pipe flows q_{ij}, $\forall ij \in IJ$, are not available. The number of variables in this problem is nine, two independent flows in the links 1-3 and 3-5 and seven pipe characteristics. The CAMONET computer programme is run on this example for four different cases, each with an extra piece of information added to the problem. In the first run, only loop head losses are considered assuming that all pipes lengths and diameters are not available. This is done by setting all the lengths and diameters of the pipes to unity in the input file of the CAMONET programme. (see Eqs. (6.18), (6.19) and (6.20) presented in the previous chapter).

The path head loss of 20m between source node 1 and terminal node 6 is added to the problem in the second run with pipe lengths and diameters still assumed not available. The pipe lengths are added in the third run , while the designed pipe diameters shown in Table 7.1 are considered in the fourth and final run.

The input and output files of the CAMONET computer programme for the four runs are given in Appendix E, from which maximum entropy pipe flows and corresponding maximum entropy pipe characteristics and their probabilities along with pipe head losses for the four runs are tabulated in Table 7.2 for convenience.

Table 7.2 Maximum entropy pipe flows and corresponding maximum entropy pipe characteristics and their probabilities along with pipe head losses for the network of Example 1 obtained by the CAMONET computer programme for four different runs.

Link i-j			1-2	2-4	3-4	4-6	5-6	1-3	3-5
run 1	S=3.793	q_{ij} (m^3/sec)	0.100	0.072	0.050	0.047	0.009	0.184	0.101
		α_{ij}	1.3035	1.1770	1.1456	1.1968	1.0356	0.5190	0.5865
		$p_{\alpha,ij}$	0.1872	0.1690	0.1645	0.1719	0.1487	0.0745	0.0842
		h_{ij} (m)	0.0182	0.0089	0.0045	0.0041	0.0002	0.0227	0.0084
run 2	S=3.793	q_{ij} (m^3/sec)	0.100	0.072	0.050	0.047	0.009	0.184	0.101
		α_{ij}	834.02	753.08	732.93	765.71	662.59	332.04	375.25
		$p_{\alpha,ij}$	0.1872	0.1690	0.1645	0.1719	0.1487	0.0745	0.0842
		h_{ij} (m)	11.651	5.711	2.870	2.638	0.112	14.493	5.395
run 3	S=3.793	q_{ij} (m^3/sec)	0.100	0.072	0.050	0.047	0.009	0.184	0.101
		α_{ij}	0.8340	0.7531	0.7329	0.7657	0.6626	0.3320	0.3753
		$p_{\alpha,ij}$	0.1872	0.1690	0.1645	0.1719	0.1487	0.0745	0.0842
		h_{ij} (m)	11.651	5.711	2.870	2.638	0.112	14.493	5.395
run 4	S=3.861	q_{ij} (m^3/sec)	0.084	0.056	0.057	0.038	0.018	0.200	0.110
		α_{ij}	0.0013	0.0013	0.0013	0.0013	0.0013	0.0013	0.0013
		$p_{\alpha,ij}$	0.1428	0.1428	0.1444	0.1436	0.1423	0.1429	0.1412
		h_{ij} (m)	9.184	7.224	7.684	3.592	2.869	8.725	8.407

7.2.1 DISCUSSION

Several interesting points can be observed from the results of Table 7.2. In the first run where the loop head losses are included in the constraint set of the problem without considering the lengths and diameters of the network pipes, the pipe flows are, as expected, different from the maximum entropy flows shown in Table 7.1 as there is more information considered in this run than in the data used to obtain the pipe flows of Table 7.1. Also, the pipe characteristics obtained from this run are far from the actual values since there is much information not yet included in the problem. However, adding the head loss of 20m along the path 1-6 to the constraint set of run 2 followed by adding the pipe lengths to the constraint set of run 3 does not change the resulting pipe flows and the corresponding pipe characteristic probabilities, although different pipe characteristic values are obtained in each run of the three

above runs. This can be justified by arguing that the head loss of path 1-6 added in run 2 does not favour any pipe above the others in assigning different pipe characteristic values. It only adjusts the unbounded pipe characteristic values to meaningful values matching the head loss of 20m assigned to path 1-6. This can be seen by checking the pipe head losses shown in Table 7.2 along all possible paths between nodes 1 and 6.

The same can be said about run 3 where the equal pipe lengths of 1000m added in this run provide no reason to treat the pipes unequally, leaving the pipe flows and pipe characteristic probabilities unchanged but readjusting the pipe characteristic values to match the pipe lengths and, at the same time, the head loss of 20m for each path between nodes 1 and 6. As expected, the new pipe characteristic values are 1000 times less than the previous values as shown in Table 7.2. This ensures producing the same head loss in the pipes to match the unchanged head loss of 20m along path 1-6.

It should be noted that assigning unequal pipe lengths would change all the pipe flows and corresponding pipe characteristic probabilities since there would be a reason to treat the pipes differently. A similar argument can be applied to pipe diameters where equal diameters will not affect the results but will adjust pipe characteristic values to match the new equal diameters, while unequal diameters will influence the whole results of the problem. This can be seen in run 4 where the unequal pipe diameters shown in Table 7.1 and added in this run result in a new set of pipe flows and pipe characteristic values and probabilities as shown in Table 7.2. The interesting thing about this new set of results is that it matches exactly the actual values shown in Table 7.1 and used by Tanyimboh and Templeman (1993c) to design the network of this example (Figure 7.1). This should have been anticipated since maximum entropy flows have been used to design the network to give the pipe diameters which are used in the current calibration model example.

The above demonstration shows how well the calibration model performs for networks designed to carry maximum entropy flows. In the next example, a more realistic and simulated water distribution network having all pipe characteristic values and

corresponding unique pipe flows known is solved by the calibration method using the CAMONET computer programme. Five different load cases are considered in calibrating the network. The results are discussed and compared with the actual values.

7.3 EXAMPLE 2

Most of conclusions drawn in this chapter are based on this example in which the simulated one-source network of Figure 7.2 is analyzed by the Hardy-Cross method, which was presented in Chapter 2, to calculate the real and unique pipe flows and corresponding pipe head losses. The network is then solved by the calibration method using the CAMONET computer programme and assuming that all pipe characteristics and corresponding pipe flows which were calculated by the Hardy-Cross method are not available. The network has one source and four demand nodes connected by seven links which form three loops as shown in the figure. The external flows and the flow directions in the pipes are also shown in the figure, while all the pipe data and pipe flows and head losses calculated by the Hardy-Cross method are given in Table 7.3.

Table 7.3 Pipe data for the network of Figure 7.2 and pipe flows and head losses calculated by the Hardy-Cross method.

Pipe number i	1	2	3	4	5	6	7
Flow direction	1-2	2-3	3-4	4-5	1-3	2-4	3-5
Le_i (m)	800	450	500	600	700	600	500
D_i (m)	0.5	0.25	0.25	0.25	0.5	0.4	0.4
$\alpha\ Le_i/C_i^{1.852}\ D_i^{4.87}$	$7.5*10^{-4}$	$8.0*10^{-4}$	$8.0*10^{-4}$	$7.5*10^{-4}$	$7.0*10^{-4}$	$7.5*10^{-4}$	$7.0*10^{-4}$
$\alpha_i=\alpha/C_i^{1.852}$	$3.21*10^{-8}$	$0.21*10^{-8}$	$0.19*10^{-8}$	0.15*10-8	$3.42*10^{-8}$	$1.44*10^{-8}$	$1.61*10^{-8}$
q_i (ltr/sec)	120.843	24.546	36.036	32.333	129.157	46.297	52.667
h_i (m)	5.387	0.300	0.611	0.469	5.687	0.911	1.080

Five different patterns of demand outflows are considered in this example. Labelling the above original load case by case 1, cases 2 and 3 shown in Figure 7.3 have the same flow directions in the pipes as those for load case 1, while some of the pipe flows in cases 4 and 5 have different directions as shown in Figure 7.4. All pipe flows and corresponding pipe head losses calculated by the Hardy-Cross method for load

cases 2, 3, 4 and 5 are given in Table 7.4.

Table 7.4 Actual pipe flows and corresponding pipe head losses calculated by the Hardy-Cross method for load cases 2, 3, 4 and 5 shown in Figures 7.3 and 7.4.

Pipe number i		1	2	3	4	5	6	7
case 2	direction	1-2	2-3	3-4	4-5	1-3	2-4	3-5
	q_i (ltr/sec)	120.351	27.965	40.621	33.007	129.649	52.386	56.993
	h_i (m)	5.346	0.382	0.763	0.487	5.728	1.146	1.250
case 3	direction	1-2	2-3	3-4	4-5	1-3	2-4	3-5
	q_i (ltr/sec)	119.913	30.664	46.642	35.891	130.087	59.249	64.109
	h_i (m)	5.310	0.453	0.986	0.569	5.764	1.439	1.554
case 4	direction	1-2	3-2	3-4	5-4	1-3	2-4	3-5
	q_i (ltr/sec)	122.693	2.205	48.277	1.825	127.307	49.898	51.825
	h_i (m)	5.541	0.003	1.050	0.002	5.537	1.047	1.048
case 5	direction	1-2	2-3	3-4	5-4	1-3	2-4	3-5
	q_i (ltr/sec)	119.583	32.466	42.858	20.025	130.417	57.117	40.025
	h_i (m)	5.283	0.504	0.843	0.193	5.790	1.345	0.650

It is assumed in this example that all the actual pipe flows for all five load cases and the actual pipe characteristics, which are the same for all load cases, are not available. All the remaining data given in Tables 7.3 and 7.4 are assumed available and are used in the calibration model to estimate the most-likely pipe characteristics and corresponding pipe flows in the network.

The purpose of this example is to investigate how much information is needed to be included in the calibration model in order to obtain pipe characteristics and corresponding pipe flows in the network as close as possible to the actual values. In this example, the CAMONET computer programme is used to solve first the original load case 1. Then, cases 2 and 3 which have the same pipe flow directions as those in load case 1 are added step by step to the original load case 1. Finally, the effect of changing some of the pipe flow directions on the obtained results is studied by considering cases 4 and 5 in the model. The results are discussed and compared to the actual values, and conclusions are drawn.

7.3.1 ORIGINAL LOAD CASE 1

Before the CAMONET computer programme is used to solve this original load case shown in Figure 7.2, the maximum nodal entropy pipe flows have been calculated, for comparison purposes only, using Problem 3 presented in the previous chapter, in which pipe characteristics are not considered in the formulation. The resulting maximum entropy flows are given in Table 7.5.

The CAMONET computer programme is now used to solve the above load case for which seven runs are carried out. In the first run, the loop head loss constraints are considered, followed by adding pipe lengths and pipe diameters in runs 2 and 3 respectively. The head loss along path 1-5 is then included in run 4 followed by adding the head losses along paths 1-4, 1-3 and 1-2 into runs 5, 6 and 7 respectively. The resulting maximum entropy flows and corresponding maximum entropy pipe characteristics along with pipe head losses for the seven runs are given in Tables 7.5, 7.6 and 7.7 respectively. Also, the actual values are included in the respective table for convenience.

Table 7.5 Maximum entropy pipe flows for load case 1 of Example 2, obtained by the CAMONET computer programme for seven different runs.

Pipe number i			1	2	3	4	5	6	7
Actual q_i values			120.843	24.546	36.036	32.333	129.157	46.297	52.667
Pipe flows (Problem 3)			166.833	83.167	67.333	51.000	83.167	33.666	34.000
q_i	run 1	S=4.125	146.803	49.406	41.298	38.695	103.197	47.397	46.305
	run 2	S=4.130	146.621	51.804	42.325	37.142	103.379	44.817	47.858
	run 3	S=3.833	147.935	50.786	19.962	17.111	102.065	47.149	67.889
	run 4	S=3.833	148.024	50.924	19.998	17.098	101.976	47.100	67.902
	run 5	S=3.773	131.725	22.522	20.267	29.471	118.275	59.203	55.529
	run 6	S=3.747	124.972	23.034	43.836	45.774	125.028	51.938	39.226
	run 7	S=3.700	136.854	56.837	67.119	47.137	113.146	30.017	37.863

Table 7.6 Maximum entropy pipe characteristics for load case 1 of Example 2, obtained by the CAMONET computer programme for seven different runs.

Pipe number i			1	2	3	4	5	6	7
Actual α_i values			$3.21*10^{-8}$	$0.21*10^{-8}$	$0.19*10^{-8}$	$0.15*10^{-8}$	$3.42*10^{-8}$	$1.44*10^{-8}$	$1.61*10^{-8}$
α_i	run 1	S=4.125	$5.87*10^{-6}$	$6.96*10^{-6}$	$6.98*10^{-6}$	$8.71*10^{-6}$	$13.1*10^{-6}$	$12.9*10^{-6}$	$11.9*10^{-6}$
	run 2	S=4.130	$5.36*10^{-6}$	$7.40*10^{-6}$	$7.04*10^{-6}$	$8.51*10^{-6}$	$13.0*10^{-6}$	$12.5*10^{-6}$	$12.0*10^{-6}$
	run 3	S=3.833	$6.87*10^{-6}$	$0.50*10^{-6}$	$7.39*10^{-6}$	$10.7*10^{-6}$	$18.2*10^{-6}$	$16.6*10^{-6}$	$17.4*10^{-6}$
	run 4	S=3.833	$1.22*10^{-8}$	$0.09*10^{-8}$	$1.31*10^{-8}$	$1.90*10^{-8}$	$3.23*10^{-8}$	$2.94*10^{-8}$	$3.09*10^{-8}$
	run 5	S=3.773	$1.60*10^{-8}$	$1.28*10^{-8}$	$1.40*10^{-8}$	$0.17*10^{-8}$	$3.35*10^{-8}$	$3.16*10^{-8}$	$2.76*10^{-8}$
	run 6	S=3.747	$2.07*10^{-8}$	$1.54*10^{-8}$	$0.13*10^{-8}$	$0.08*10^{-8}$	$3.63*10^{-8}$	$3.31*10^{-8}$	$2.79*10^{-8}$
	run 7	S=3.700	$2.55*10^{-8}$	$0.04*10^{-8}$	$0.06*10^{-8}$	$0.07*10^{-8}$	$4.37*10^{-8}$	$3.22*10^{-8}$	$2.98*10^{-8}$

Table 7.7 Maximum entropy pipe head losses for load case 1 of Example 2, obtained by the CAMONET computer programme for seven different runs.

Pipe number i			1	2	3	4	5	6	7
Actual h_i values			5.387	0.300	0.611	0.469	5.687	0.911	1.080
h_i	run 1	S=4.125	0.0604	0.0095	0.0069	0.0076	0.0700	0.0164	0.0145
	run 2	S=4.130	44.069	4.986	3.622	4.124	49.055	8.608	7.746
	run 3	S=3.833	1679.5	279.0	807.9	1056.3	1958.6	1086.9	1864.2
	run 4	S=3.833	2.976	0.487	1.434	1.870	3.463	1.921	3.304
	run 5	S=3.773	3.152	1.577	1.570	0.469	4.728	3.147	2.039
	run 6	S=3.747	3.707	1.980	0.611	0.469	5.687	2.592	1.080
	run 7	S=3.700	5.387	0.300	0.611	0.469	5.687	0.911	1.080

7.3.2 MULTIPLE LOAD CASE WITH UNCHANGED PIPE FLOW DIRECTIONS

In this multiple load case, cases 1, 2 and 3 which all have the same flow directions in the pipes are considered by including first cases 1 and 2 in the model followed by the three load case compound problem.

7.3.2.1 MULTIPLE LOAD CASE (1+2)

In this section, the external flows of load case 2 and its pipe flow directions along with the loop head loss constraints are added to runs 4, 5, 6 and 7 to produce runs 8, 9, 10 and 11 respectively whose results are tabulated in Tables 7.8, 7.9 and 7.10. No path head losses related to case 2 are considered in these runs. However, the head loss of path 1-5 for load case 2 is used in run 12 which is obtained by adding this head loss to run 8. The results of run 12 are also included in the above three tables.

Table 7.8 Maximum entropy pipe flows for multiple load case (1+2) of Example 2, obtained by the CAMONET computer programme for runs 8-12.

Pipe number i			1	2	3	4	5	6	7
Actual $q_{i,1}$ values			120.843	24.546	36.036	32.333	129.157	46.297	52.667
Actual $q_{i,2}$ values			120.351	27.965	40.621	33.007	129.649	52.386	56.993
run 8	S=3.847	$q_{i,1}$	146.335	49.650	20.884	17.569	103.665	46.686	67.431
		$q_{i,2}$	145.747	52.569	24.422	17.600	104.253	53.178	72.400
run 9	S=3.787	$q_{i,1}$	131.487	22.469	21.476	30.494	118.513	59.018	54.506
		$q_{i,2}$	129.570	24.185	24.463	29.848	120.430	65.386	60.152
run 10	S=3.771	$q_{i,1}$	124.793	23.255	44.636	46.174	125.207	51.538	38.826
		$q_{i,2}$	122.284	25.415	50.737	47.606	127.716	56.868	42.394
run 11	S=3.728	$q_{i,1}$	136.018	55.897	67.134	47.255	113.982	30.121	37.745
		$q_{i,2}$	135.637	61.968	75.341	49.010	114.363	33.669	40.990
run 12	S=3.768	$q_{i,1}$	133.566	66.236	51.960	19.291	116.434	17.330	65.709
		$q_{i,2}$	133.550	73.518	60.179	20.212	116.450	20.032	69.788

Table 7.9 Maximum entropy pipe characteristics for multiple load case (1+2) of Example 2, obtained by the CAMONET computer programme for runs 8-12.

Pipe number i			1	2	3	4	5	6	7
Actual α_i values ($*10^{-8}$)			3.21	0.21	0.19	0.15	3.42	1.44	1.61
α_i ($*10^{-8}$)	run 8	S=3.847	1.25	0.10	1.13	1.84	3.17	2.92	3.08
	run 9	S=3.787	1.62	1.28	1.23	0.16	3.35	3.14	2.83
	run 10	S=3.771	2.09	1.50	0.13	0.08	3.62	3.34	2.84
	run 11	S=3.728	2.58	0.05	0.06	0.07	4.31	3.20	2.99
	run 12	S=3.768	2.46	0.001	0.03	1.26	3.64	2.28	1.76

Table 7.10 Maximum entropy pipe head losses for multiple load case (1+2) of Example 2, obtained by the CAMONET computer programme for runs 8-12.

Pipe number i			1	2	3	4	5	6	7
Actual $h_{i,1}$ values			5.387	0.300	0.611	0.469	5.687	0.911	1.080
Actual $h_{i,2}$ values			5.346	0.382	0.763	0.487	5.728	1.146	1.250
run 8	S=3.847	$h_{i,1}$	2.983	0.530	1.344	1.911	3.512	1.874	3.255
		$h_{i,2}$	2.960	0.589	1.796	1.917	3.549	2.385	3.713
run 9	S=3.787	$h_{i,1}$	3.185	1.567	1.546	0.469	4.752	3.113	2.015
		$h_{i,2}$	3.100	1.796	1.968	0.451	4.895	3.763	2.418
run 10	S=3.771	$h_{i,1}$	3.727	1.960	0.611	0.469	5.687	2.571	1.080
		$h_{i,2}$	3.590	2.310	0.775	0.496	5.900	3.085	1.271
run 11	S=3.728	$h_{i,1}$	5.387	0.300	0.611	0.469	5.687	0.911	1.080
		$h_{i,2}$	5.359	0.363	0.757	0.501	5.722	1.120	1.258
run 12	S=3.768	$h_{i,1}$	4.978	0.011	0.222	1.556	4.989	0.233	1.778
		$h_{i,2}$	4.977	0.014	0.292	1.696	4.990	0.305	1.988

7.3.2.2 MULTIPLE LOAD CASE (1+2+3)

Five runs are performed on the CAMONET computer programme for this multiple load case. Runs 13-16 are formulated by adding the external flows of load case 3 and its pipe flow directions along with the loop head loss requirements to runs 8-11 respectively. The last run, which is run 17, is obtained by adding the head losses of path 1-5 corresponding to cases 2 and 3 to run 13. The results of the five runs are given in Tables 7.11, 7.12 and 7.13.

Table 7.11 Maximum entropy pipe flows for multiple load case (1+2+3) of Example 2, obtained by the CAMONET computer programme for runs 13-17.

Pipe number i			1	2	3	4	5	6	7
Actual $q_{i,1}$ values			120.843	24.546	36.036	32.333	129.157	46.297	52.667
Actual $q_{i,2}$ values			120.351	27.965	40.621	33.007	129.649	52.386	56.993
Actual $q_{i,3}$ values			119.913	30.664	46.642	35.891	130.087	59.249	64.109
run 13	S=3.856	$q_{i,1}$	145.129	49.940	22.949	18.138	104.871	45.189	66.862
		$q_{i,2}$	144.535	53.070	26.815	18.281	105.465	51.465	71.719
		$q_{i,3}$	144.042	55.559	31.249	19.732	105.958	58.483	80.268
run 14	S=3.797	$q_{i,1}$	130.932	22.447	23.640	32.125	119.068	58.485	52.875
		$q_{i,2}$	128.979	24.204	26.899	31.674	121.021	64.775	58.326
		$q_{i,3}$	127.474	25.491	31.327	33.310	122.526	71.983	66.690
run 15	S=3.792	$q_{i,1}$	124.689	23.460	45.329	46.558	125.311	51.229	38.442
		$q_{i,2}$	122.191	25.651	51.491	48.032	127.809	56.540	41.968
		$q_{i,3}$	119.802	27.612	60.094	52.285	130.198	62.190	47.715
run 16	S=3.750	$q_{i,1}$	135.258	55.026	67.111	47.343	114.742	30.232	37.657
		$q_{i,2}$	134.873	61.071	75.304	49.106	115.127	33.802	40.894
		$q_{i,3}$	134.498	66.482	85.976	53.993	115.502	38.017	46.007
run 17	S=3.766	$q_{i,1}$	130.251	49.044	66.505	47.712	119.749	31.207	37.288
		$q_{i,2}$	129.100	54.439	75.820	50.481	120.900	34.661	39.519
		$q_{i,3}$	127.866	59.764	87.961	56.063	122.134	38.102	43.937

Table 7.12 Maximum entropy pipe characteristics for multiple load case (1+2+3) of Example 2, obtained by the CAMONET computer programme for runs 13-17.

Pipe number i			1	2	3	4	5	6	7
Actual α_i values ($*10^{-8}$)			3.21	0.21	0.19	0.15	3.42	1.44	1.61
α_i ($*10^{-8}$)	run 13	S=3.856	1.29	0.09	0.88	1.79	3.13	2.91	3.10
	run 14	S=3.797	1.66	1.29	0.99	0.15	3.36	3.14	2.90
	run 15	S=3.792	2.10	1.46	0.12	0.07	3.62	3.35	2.89
	run 16	S=3.750	2.60	0.05	0.06	0.07	4.26	3.17	3.01
	run 17	S=3.766	2.57	0.17	0.002	0.14	4.03	2.92	2.67

Table 7.13 Maximum entropy pipe head losses for multiple load case (1+2+3) of Example 2, obtained by the CAMONET computer programme for runs 13-17.

Pipe number i			1	2	3	4	5	6	7
Actual $h_{i,1}$ values			5.387	0.300	0.611	0.469	5.687	0.911	1.080
Actual $h_{i,2}$ values			5.346	0.382	0.763	0.487	5.728	1.146	1.250
Actual $h_{i,3}$ values			5.310	0.453	0.986	0.569	5.764	1.439	1.554
run 13	S=3.856	$h_{i,1}$	3.038	0.505	1.252	1.972	3.543	1.757	3.224
		$h_{i,2}$	3.015	0.566	1.670	2.001	3.581	2.236	3.671
		$h_{i,3}$	2.996	0.616	2.217	2.305	3.612	2.833	4.522
run 14	S=3.797	$h_{i,1}$	3.234	1.576	1.488	0.469	4.810	3.064	1.957
		$h_{i,2}$	3.146	1.812	1.890	0.457	4.957	3.702	2.347
		$h_{i,3}$	3.078	1.994	2.507	0.501	5.072	4.501	3.008
run 15	S=3.792	$h_{i,1}$	3.743	1.944	0.611	0.469	5.687	2.556	1.080
		$h_{i,2}$	3.605	2.293	0.774	0.497	5.899	3.067	1.271
		$h_{i,3}$	3.476	2.629	1.030	0.581	6.105	3.659	1.611
run 16	S=3.750	$h_{i,1}$	5.387	0.300	0.611	0.469	5.687	0.911	1.080
		$h_{i,2}$	5.358	0.364	0.757	0.502	5.722	1.121	1.258
		$h_{i,3}$	5.331	0.426	0.967	0.598	5.757	1.393	1.565
run 17	S=3.766	$h_{i,1}$	4.958	0.868	0.020	0.921	5.826	0.888	0.941
		$h_{i,2}$	4.878	1.053	0.025	1.022	5.930	1.078	1.048
		$h_{i,3}$	4.792	1.251	0.033	1.242	6.043	1.285	1.275

7.3.3 MULTIPLE LOAD CASE WITH CHANGING PIPE FLOW DIRECTIONS

The case of changing some pipe flow directions between the load cases included in the calibration model is now considered by including cases 1 and 4 first in the model followed by three load cases incorporating load cases 1, 4 and 5.

7.3.3.1 MULTIPLE LOAD CASE (1+4)

For this multiple load case, the CAMONET computer programme is used five times by adding the external flows of load case 4 and its pipe flow directions along with the loop head loss constraints to runs 4-7 to produce runs 18-21 respectively, and then by adding the head loss of path 1-4 related to load case 4, where node 4 is a terminal node for that load case, to run 18 giving the final run for this multiple load case, which is run 22. The results of the five runs are given in Tables 7.14, 7.15 and 7.16.

Table 7.14 Maximum entropy pipe flows for multiple load case (1+4) of Example 2, obtained by the CAMONET computer programme for runs 18-22.

Pipe number i			1	2	3	4	5	6	7
Actual $q_{i,1}$ values			120.843	24.546	36.036	32.333	129.157	46.297	52.667
Actual $q_{i,4}$ values			122.693	2.205	48.277	1.825	127.307	49.898	51.825
run 18	S=3.756	$q_{i,1}$	111.483	11.612	15.303	15.174	138.517	49.871	69.826
		$q_{i,4}$	122.693	13.281	26.139	12.887	127.307	60.973	62.887
run 19	S=3.708	$q_{i,1}$	105.790	11.389	13.949	8.350	144.210	44.401	76.650
		$q_{i,4}$	116.359	14.441	24.281	19.920	133.641	55.799	69.920
run 20	S=3.671	$q_{i,1}$	112.451	14.649	9.923	7.725	137.549	47.802	77.275
		$q_{i,4}$	122.950	11.001	23.432	17.617	127.050	58.951	67.617
run 21	S=3.625	$q_{i,1}$	106.144	8.350	10.134	7.928	143.856	47.794	77.072
		$q_{i,4}$	116.069	18.993	22.902	17.035	133.931	60.063	67.035
run 22	S=3.755	$q_{i,1}$	112.425	11.808	15.371	15.988	137.575	50.618	69.012
		$q_{i,4}$	123.630	13.083	26.486	11.800	126.370	61.714	61.800

Table 7.15 Maximum entropy pipe characteristics for multiple load case (1+4) of Example 2, obtained by the CAMONET computer programme for runs 18-22.

Pipe number i			1	2	3	4	5	6	7
Actual α_i values ($*10^{-5}$)			3.21	0.21	0.19	0.15	3.42	1.44	1.61
α_i ($*10^{-5}$)	run 18	S=3.756	2.43	1.54	1.83	1.86	2.15	2.46	2.39
	run 19	S=3.708	3.28	1.66	2.50	1.79	2.40	3.39	1.40
	run 20	S=3.671	3.17	1.83	2.04	2.07	3.04	2.43	0.79
	run 21	S=3.625	4.08	1.53	1.96	1.97	2.80	1.36	0.80
	run 22	S=3.755	2.34	1.51	1.71	1.84	2.14	2.31	2.50

Table 7.16 Maximum entropy pipe head losses for multiple load case (1+4) of Example 2, obtained by the CAMONET computer programme for runs 18-22.

Pipe number i			1	2	3	4	5	6	7
Actual $h_{i,1}$ values			5.387	0.300	0.611	0.469	5.687	0.911	1.080
Actual $h_{i,4}$ values			5.541	0.003	1.050	0.002	5.537	1.047	1.048
run 18	S=3.756	$h_{i,1}$	3.518	0.558	1.225	1.467	4.075	1.782	2.692
		$h_{i,4}$	4.201	0.715	3.301	1.084	3.486	2.586	2.217
run 19	S=3.708	$h_{i,1}$	4.313	0.578	1.407	0.469	4.891	1.985	1.876
		$h_{i,4}$	5.145	0.897	3.928	2.346	4.248	3.031	1.582
run 20	S=3.671	$h_{i,1}$	4.669	1.018	0.611	0.469	5.687	1.629	1.080
		$h_{i,4}$	5.508	0.599	3.001	2.158	4.909	2.402	0.843
run 21	S=3.625	$h_{i,1}$	5.387	0.300	0.611	0.469	5.687	0.911	1.080
		$h_{i,4}$	6.357	1.375	2.766	1.932	4.982	1.391	0.834
run 22	S=3.755	$h_{i,1}$	3.444	0.564	1.155	1.604	4.008	1.719	2.759
		$h_{i,4}$	4.107	0.682	3.163	0.914	3.425	2.481	2.249

7.3.3.2 MULTIPLE LOAD CASE (1+4+5)

The external flows for load case 5 and its pipe flow directions along with the loop head loss constraints are added to runs 18-21 in order to solve this multiple load case by the CAMONET computer programme, giving runs 23-26 respectively whose results are given in Tables 7.17, 7.18 and 7.19. The final run performed on this multiple load case is run 27 which is obtained by adding the head losses of path 1-4 corresponding to cases 4 and 5 to run 23. The results of this final run are also given in the above tables.

Table 7.17 Maximum entropy pipe flows for multiple load case (1+4+5) of Example 2, obtained by the CAMONET computer programme for runs 23-27.

Pipe number i			1	2	3	4	5	6	7
Actual $q_{i,1}$ values			120.843	24.546	36.036	32.333	129.157	46.297	52.667
Actual $q_{i,4}$ values			122.693	2.205	48.277	1.825	127.307	49.898	51.825
Actual $q_{i,5}$ values			119.583	32.466	42.858	20.025	130.417	57.117	40.025
run 23	S=3.743	$q_{i,1}$	114.654	14.935	15.641	15.361	135.346	49.719	69.639
		$q_{i,4}$	125.365	9.439	26.781	13.415	124.635	59.804	63.415
		$q_{i,5}$	115.770	13.693	27.244	20.678	134.230	72.077	40.678
run 24	S=3.703	$q_{i,1}$	109.822	14.676	14.344	9.490	140.178	45.146	75.510
		$q_{i,4}$	119.451	10.430	24.355	20.764	130.549	54.881	70.764
		$q_{i,5}$	110.898	13.268	25.569	26.800	139.102	67.631	46.800
run 25	S=3.672	$q_{i,1}$	114.750	17.022	10.386	8.114	135.250	47.728	76.886
		$q_{i,4}$	125.274	7.168	24.345	18.212	124.726	57.442	68.212
		$q_{i,5}$	117.137	14.338	25.542	21.659	132.863	72.799	41.659
run 26	S=3.567	$q_{i,1}$	107.653	9.710	12.438	10.381	142.347	47.943	74.619
		$q_{i,4}$	114.841	17.625	24.714	17.820	135.159	57.466	67.820
		$q_{i,5}$	109.131	3.827	23.905	20.791	140.869	75.304	40.791
run 27	S=3.678	$q_{i,1}$	114.392	7.667	18.270	24.995	135.608	56.725	60.005
		$q_{i,4}$	124.178	13.317	26.421	11.084	125.822	62.496	61.084
		$q_{i,5}$	112.930	9.754	23.632	23.192	137.070	73.176	43.192

Table 7.18 Maximum entropy pipe characteristics for multiple load case (1+4+5) of Example 2, obtained by the CAMONET computer programme for runs 23-27.

Pipe number i			1	2	3	4	5	6	7
Actual α_i values ($*10^{-8}$)			3.21	0.21	0.19	0.15	3.42	1.44	1.61
α_i ($*10^{-8}$)	run 23	S=3.743	2.21	1.46	1.71	1.70	2.32	2.81	2.28
	run 24	S=3.703	2.91	1.52	2.29	1.42	2.55	3.66	1.40
	run 25	S=3.672	2.87	1.78	1.87	1.89	3.14	2.86	0.80
	run 26	S=3.567	3.97	1.16	1.34	1.20	2.86	1.35	0.85
	run 27	S=3.678	2.48	1.81	1.66	0.58	2.24	2.00	3.17

Table 7.19 Maximum entropy pipe head losses for multiple load case (1+4+5) of Example 2, obtained by the CAMONET computer programme for runs 23-27.

Pipe number i			1	2	3	4	5	6	7
Actual $h_{i,1}$ values			5.387	0.300	0.611	0.469	5.687	0.911	1.080
Actual $h_{i,4}$ values			5.541	0.003	1.050	0.002	5.537	1.047	1.048
Actual $h_{i,5}$ values			5.283	0.504	0.843	0.193	5.790	1.345	0.650
run 23	S=3.743	$h_{i,1}$	3.366	0.842	1.189	1.370	4.208	2.030	2.559
		$h_{i,4}$	3.972	0.360	3.218	1.066	3.612	2.858	2.152
		$h_{i,5}$	3.427	0.717	3.322	2.376	4.144	4.039	0.945
run 24	S=3.703	$h_{i,1}$	4.093	0.849	1.357	0.469	4.941	2.206	1.826
		$h_{i,4}$	4.782	0.451	3.618	1.998	4.331	3.167	1.619
		$h_{i,5}$	4.167	0.704	3.959	3.206	4.871	4.663	0.753
run 25	S=3.672	$h_{i,1}$	4.384	1.303	0.611	0.469	5.687	1.914	1.080
		$h_{i,4}$	5.157	0.263	2.961	2.095	4.895	2.698	0.865
		$h_{i,5}$	4.554	0.948	3.236	2.889	5.503	4.184	0.347
run 26	S=3.567	$h_{i,1}$	5.387	0.300	0.611	0.469	5.687	0.911	1.080
		$h_{i,4}$	6.072	0.905	2.180	1.275	5.167	1.275	0.905
		$h_{i,5}$	5.525	0.054	2.049	1.697	5.578	2.103	0.353
run 27	S=3.678	$h_{i,1}$	3.767	0.303	1.538	1.160	4.070	1.841	2.697
		$h_{i,4}$	4.385	0.843	3.045	0.257	3.542	2.202	2.788
		$h_{i,5}$	3.678	0.473	2.477	1.009	4.151	2.950	1.467

7.3.4 DISCUSSION

The results of the 27 runs performed on Example 2 are now investigated and compared with the actual values in order to study the influence of information added in each run on the calibration model solution. The main concern for the calibration model is to see how close are the pipe characteristics values of the network being considered to the actual values. Obviously, the closer the estimate of the pipe characteristic values are to the real values, the more realistic pipe flows for all load cases can be generated. Consequently, the discussion will be concentrated on the sensitivity of the resulting pipe characteristic values to the information included in each run. However, pipe head losses and pipe flow results are also discussed but briefly and under various headings.

7.3.4.1 ORIGINAL LOAD CASE 1

The results of the seven runs performed on this load case and given in Table 7.5, 7.6 and 7.7 are discussed in this section. First, it can be seen from Table 7.5 that the maximum nodal entropy pipe flows obtained by solving Problem 3 are far away from the actual flows. This is due to the fact that only the external flows and the topology of the network along with pipe flow directions have been considered. Neither pipe data nor loop head loss requirements have been accounted for.

Adding the loop head loss constraints to the problem in run 1, however, leads to a radical change in the pipe flows towards the actual values although neither pipe length nor pipe diameters have been included in those loop constraints. In runs 2 and 3 where respectively the pipe lengths and pipe diameters were considered in the loop equations, it is evident that pipe flows are more sensitive to information about pipe diameters than to the lengths. Only a very little change in the pipe flows can be seen in run 2, while the flows corresponding to run 3 in links 3, 4 and 7 (all belonging to one loop) have changed quite remarkably although no improvement on their values toward the actual values has been achieved. This different influence of pipe lengths and pipe diameters on pipe flows can be justified by the different exponential powers of pipe

lengths and pipe diameters in the loop equations. The effect of considering nodal heads on the pipe flows can be studied by investigating runs 4-7 in which the head losses along paths 1-5, 1-4, 1-3 and 1-2 have been included respectively. Hardly any change can be seen in the pipe flows of run 4 since the head loss along path 1-5 added in this run is only a way of bounding pipe characteristics and hence pipe head losses to meaningful values as will be seen later. However, an interesting improvement in the pipe flows can be seen in runs 5, 6, and 7 where a new path head loss has been included in each run. Special attention should be made to run 6 where the best estimation of pipe flows for the seven runs has been obtained. Although all pipe head losses in run 7 are restricted to their actual values, the pipe flows have been unexpectedly diverted away from their real values. This may suggest that the head loss along path 1-2 added in run 7 is extra information which is not necessary and gives the problem a small range of freedom for choosing the pipe flows and pipe characteristic values to fit the restricted head losses in all the pipes, taking into account that those values are the most-likely values rather than the actual values.

Referring to Table 7.6, the pipe characteristic values for the first three runs are unbounded and have meaningless values since there are infinite numbers of values which fit the resulting maximum entropy pipe characteristic probabilities for each run. However, the head loss of path 1-5 added in run 4 directs the unbounded pipe characteristic values to a unique solution which is a much more realistic one than the previous solutions. Adding extra information about path head losses in runs 5, 6 and 7 has remarkably improved the estimation of characteristic values of the network pipes. In these last three runs, the characteristic values of some pipes have been improved on the expense of the other pipes. The best estimated values, however, are shared between runs 6 and 7 with a little favour towards run 7 in which the restricted head losses in all pipes force pipe flows to accommodate inaccurate characteristic values of some pipes as mentioned earlier.

Finally, some remarks have to be stated about the pipe head losses which are given in Table 7.7. Following pipe characteristic values, the pipe head losses in the first three runs represent unbounded values which are then restricted in run 4 by adding the

head loss of path 1-5. As expected, these pipe head losses are driven towards their actual values by adding extra information about different path head losses until all the pipe head losses reach the actual values in run 7. The path head losses included in this run are sufficient to determine the head losses in all pipes in the network.

7.3.4.2 MULTIPLE LOAD CASE WITH UNCHANGED PIPE FLOW DIRECTIONS

It can be seen from Tables 7.8 and 7.9 that adding information about load case 2 to original load case 1 without considering any path head loss related to case 2 gives only a slight improvement on the pipe flows concerning load case 1 and pipe characteristics for runs 8-11 compared with the results of runs 4-7 respectively. This may be due to the fact that the information about load case 2 added to the formulation is balanced by increasing the number of variables in the problem by the extra pipe flow variables which are related to that extra load case. Similar to the original load case, pipe flows related to case 1 divert away from the actual values in run 11 by adding the head loss of path 1-2 for case 1 to the formulation, while, as expected, pipe characteristics get closer to the actual values in this run. Similar improvement to pipe flows for load case 1 can be noticed in the pipe flows for load case 2 in runs 8-11 although no path head losses related to load case 2 have been considered in these runs. In run 12, however, where the head loss of path 1-5 related to load case 2 has been included, all the results have improved quite remarkably, especially pipe characteristic values which have the best estimated values so far in the 12 runs.

Referring to Table 7.10, pipe head losses for load case 1 have also improved slightly by adding load case 2 to the formulation until convergence to the actual values has been completed as expected in run 11. The interesting thing about the results of Table 7.10 is that although no path head losses related to load case 2 have been included in runs 8-11, the pipe head losses for load case 2 have improved quite remarkably until a very good estimation was obtained in run 11 which is even better than the estimation of run 12 where the head loss along path 1-5 for load case 2 has been considered but only with its counterpart in load case 1.

Exactly the same thing can be said about the compound problem of cases 1,2 and 3 whose results are shown in Tables 7.11, 7.12 and 7.13. There is a slight improvement on pipe flows and pipe characteristics when load case 3 has been added to the compound problem of cases 1 and 2. Also, the pipe characteristics improve by restricting all the pipe head losses for load case 1 to the actual values as shown in run 16, while the pipe flows, as previously, are slightly worse in this case. In run 17 where the head losses of path 1-5 for the three load cases have been only considered, a slight improvement in all pipe flows and pipe characteristics can be observed. Moreover, the pipe head losses for load cases 2 and 3 improve quite remarkably up to run 16 although no path head losses related to these two load cases have been considered. They are even better than the respective results of run 17 where the head losses of path 1-5 related to the two cases along with the respective head loss in case 1 have been considered in the formulation.

To sum up, including information up to loop head loss requirements in the calibration model for extra load cases having the same pipe flow directions as those for the original load case leads only to a slight improvement in the pipe flows and pipe characteristics, and is a much smaller improvement than that which can be obtained by adding extra path head losses related to the original load case.

7.3.4.3 MULTIPLE LOAD CASE WITH CHANGING PIPE FLOW DIRECTIONS

The results of multiple load case (1+4) shown in Tables 7.14, 7.15 and 7.16 are investigated in this section to determine the effect of changing some pipe flow directions between the load cases being considered on the calibration model results. No regular changes in the pipe flows related to case 1 can be observed when the results of runs 18-21 are compared to the respective results of runs 4-7 for the original load case although some pipe flow results such as the results of runs 18 and 21 are better than the respective results of runs 8 and 11 related to the multiple load case (1+2). Even in the runs 18-22 themselves, the pipe flows do not improve regularly as a new path head loss related to case 1 has been included through the above mentioned

runs.

However, all pipe characteristic results in runs 18-22 are worse than the results of respective runs related to the original load case or the multiple load case (1+2) as will be seen later. On the other hand, pipe head losses related to case 1 are remarkably improved in runs 18-21 compared with the respective results of the runs related to the original load case and the multiple load case (1+2). Only in run 22 where a path head loss related to case 4 has been included, pipe head losses concerning case 1 are worsened comparing to the results of the respective run 12 of the multiple load case (1+2). This suggests that information about extra load cases having different pipe flow directions may sometimes divert the results of the original load case away from the actual values.

The irregularity in pipe flow changes observed in the above multiple load case can also be noticed in the multiple load case (1+4+5) whose results are shown in Tables 7.17, 7.18 and 7.19. Although the pipe flow results are slightly improved in this multiple load case. Compared with the respective results of the multiple load case (1+4), they are still less accurate than the results of the two previous sections. Also, a slight improvement in the pipe characteristics can be seen in Table 7.18 compared with the results of the multiple load case (1+4). However, they are not as good as the results of the original load case or the multiple load case with unchanged pipe flow directions. Considering the pipe head losses shown in Table 7.19, they are noticeably improved towards run 26 although no regular improvement can be observed when the results of Table 7.19 are compared with the respective results of Table 7.16 which are related to the multiple load case (1+4).

To sum up, no improvement on the results of the calibration model can be achieved when extra information about extra load cases having different flow directions in some pipes are included in the model. Moreover, the results sometimes worsen by adding such load cases into the calibration model.

Finally, to conclude the discussion of Example 2, a confirmation of the above results can be seen clearly in Table 7.20 where the deviations of pipe characteristic results of runs 4-27 from the actual values are tabulated and the sums of the square errors of all runs are determined. The results of runs 1-3, however, are not included in the table since they are unbounded and have no meaningful values.

Table 7.20 Deviations of pipe characteristic results from the actual values for the network of Example 2 along with the sums of the square errors for runs 4-27.

Pipe number i		**1**	**2**	**3**	**4**	**5**	**6**	**7**	**$\Sigma\Delta_i^2$ ($*10^{-16}$)**
Actual α_i values ($*10^{-8}$)		**3.21**	**0.21**	**0.19**	**0.15**	**3.42**	**1.44**	**1.61**	
Δ_i	**run 4**	-1.99	-0.12	+1.12	+1.75	-0.19	+1.50	+1.48	**12.8**
	run 5	-1.61	+1.07	+1.21	+0.02	-0.07	+1.72	+1.15	**9.5**
	run 6	-1.14	+1.33	-0.06	-0.07	+0.21	+1.87	+1.18	**8.0**
	run 7	-0.66	-0.17	-0.13	-0.08	+0.95	+1.78	+1.37	**6.4**
	run 8	-1.96	-0.11	+0.94	+1.69	-0.25	+1.48	+1.47	**12.0**
	run 9	-1.59	+1.07	+1.04	+0.01	-0.07	+1.70	+1.22	**9.1**
	run 10	-1.12	+1.29	-0.06	-0.07	+0.20	+1.90	+1.23	**8.1**
	run 11	-0.63	-0.16	-0.13	-0.08	+0.89	+1.76	+1.38	**6.2**
	run 12	-0.75	-0.21	-0.16	+1.11	+0.22	+0.84	+0.15	**2.6**
	run 13	-1.92	-0.12	+0.69	+1.64	-0.29	+1.47	+1.49	**11.3**
	run 14	-1.55	+1.08	+0.80	0.00	-0.06	+1.70	+1.29	**8.8**
	run 15	-1.11	+1.25	-0.07	-0.08	+0.20	+0.91	+1.28	**5.3**
	run 16	-0.61	-0.16	-0.13	-0.08	+0.84	+1.73	+1.40	**6.1**
	run 17	-0.64	-0.04	-0.19	-0.01	+0.61	+1.48	+1.06	**4.1**
	run 18	-0.78	+1.33	+1.64	+1.71	-1.27	+1.02	+0.78	**11.3**
	run 19	+0.07	+1.45	+2.31	+1.64	-1.02	+1.95	-0.21	**15.0**
	run 20	-0.04	+1.62	+1.85	+1.92	-0.38	+0.99	-0.82	**10.9**
	run 21	+0.87	+1.32	+1.77	+1.82	-0.62	-0.08	-0.81	**10.0**
	run 22	-0.87	+1.30	+1.52	+1.69	-1.28	+0.87	+0.89	**10.8**
	run 23	-1.00	+1.25	+1.52	+1.55	-1.10	+1.37	+0.67	**10.8**
	run 24	-0.30	+1.31	+2.10	+1.27	-0.87	+2.22	-0.21	**13.6**
	run 25	-0.34	+1.57	+1.68	+1.74	-0.28	+1.42	-0.81	**11.2**
	run 26	+0.76	+0.95	+1.15	+1.05	-0.56	-0.09	-0.76	**4.8**
	run 27	-0.73	+1.60	+1.47	+0.43	-1.18	+0.56	+1.56	**9.6**

It is evident from the results of the last column in Table 7.20 that pipe characteristics improved smoothly and as expected in load case 1, multiple load case (1+2) and multiple load case (1+2+3) through runs 4-7, 8-12 and 13-17 respectively. Also, the results of runs 13-17 corresponding to load case (1+2+3) are better than the respective results of runs 8-12 corresponding to load case (1+2) which in turn are better than the respective results of runs 4-7 which are related to load case 1. However, although the results are generally improved in runs 23-27 of load case (1+4+5) compared to runs 18-22 of load case (1+4), there is some irregularity in pipe characteristic changes in these two sets of runs, and their results are generally less accurate than the results of runs 4-7, 8-12 and 13-17 which correspond to case 1, (1+2), and (1+2+3) respectively.

In conclusions, a radical improvement towards the actual values can be achieved in the results of the calibration model when the loop head requirements for the original load case are included in the model. The results are remarkably improved when extra path head losses are constrained and added to the formulation. However, only a slight improvement on the results can be obtained by adding extra load cases having the same pipe flow directions as those for the original load case. Any information about other load cases which have different flow directions in some pipes may divert the results away from the actual values.

7.4 SUMMARY AND CONCLUSION

The calibration method presented in the previous chapter as Problem 8 for calculating most-likely pipe flows and corresponding pipe characteristics in water distribution networks has been demonstrated in this chapter by calibrating two network examples for which pipe characteristics and hence pipe flows are assumed not available. The first example is a one-source network with one load case. The network has seven links designed by Tanyimboh and Templeman (1993c) to carry maximum entropy flows. The second example is a simulated one-source network with three loops and seven links analyzed by the Hardy-Cross method to calculate the unique flows in the network pipes for five different load cases with all information needed for the analysis known. The computer programme CAMONET which is written in FORTRAN 77 in

conjunction with the NAG library routine E04UCF for non-linear constrained optimization has been used in this chapter to calibrate the two examples assuming that pipe characteristics and corresponding pipe flows are not available. This computer programme CAMONET has been designed in a way that it can incorporate any piece of information which might individually be available in the network being considered. Consequently, 4 runs and 27 runs respectively have been performed on the above two examples with extra information added in each run in order to investigate the influence of that information on the model results.

It has been shown from Example 1 how well and accurately the calibration model performs for water distribution networks designed to carry maximum entropy flows. It has been conjectured (Tanyimboh and Templeman, 1993c) that designing water networks to carry maximum entropy flows would give a good compromise between cost and reliability in water distribution networks. If the calibration model is used for such reliable networks, it will generate exactly the same actual pipe characteristics and corresponding design pipe flows in the network for the case where roughness coefficients of some or all pipes have been lost.

In Example 2, however, from which the main conclusions have been drawn, it is evident that the results of the calibration model improve radically towards the actual values by adding the loop head loss requirements into the formulation. The results are more sensitive to pipe diameters than to pipe lengths due to the higher power of the pipe diameters in the head loss equations. Also, a significant improvement on the results can be achieved by adding extra path head losses to the formulation. However, the results can be slightly improved further by considering extra load cases which have the same pipe flow directions as those for the original load case. Any extra information concerning other load cases which may have different flow directions in some pipes may divert the results away from the actual values. Consequently, in real water distribution networks in which pipe flow directions for different load cases are not guaranteed to be the same, the information about one load case is enough to calibrate the missing pipe characteristics and hence the corresponding pipe flows. Any other load cases which might be available for such networks appear to add little extra

useful information.

It should be noted that although the results of Example 2 are much better than those obtained by the maximum entropy flow model, they are less satisfactory and less accurate than had been hoped for. Discrepancies between actual and estimated network values are still relatively too large to be practically useful. The assumption of independence used in the calibration model between the pipe characteristic finite probability scheme and the finite probability schemes used in the nodal flow entropy function may be the main reason behind these unsatisfactory discrepancies. Further work in this regard based on the present calibration model is necessary to determine in what form extra information must be added to get better accuracy.

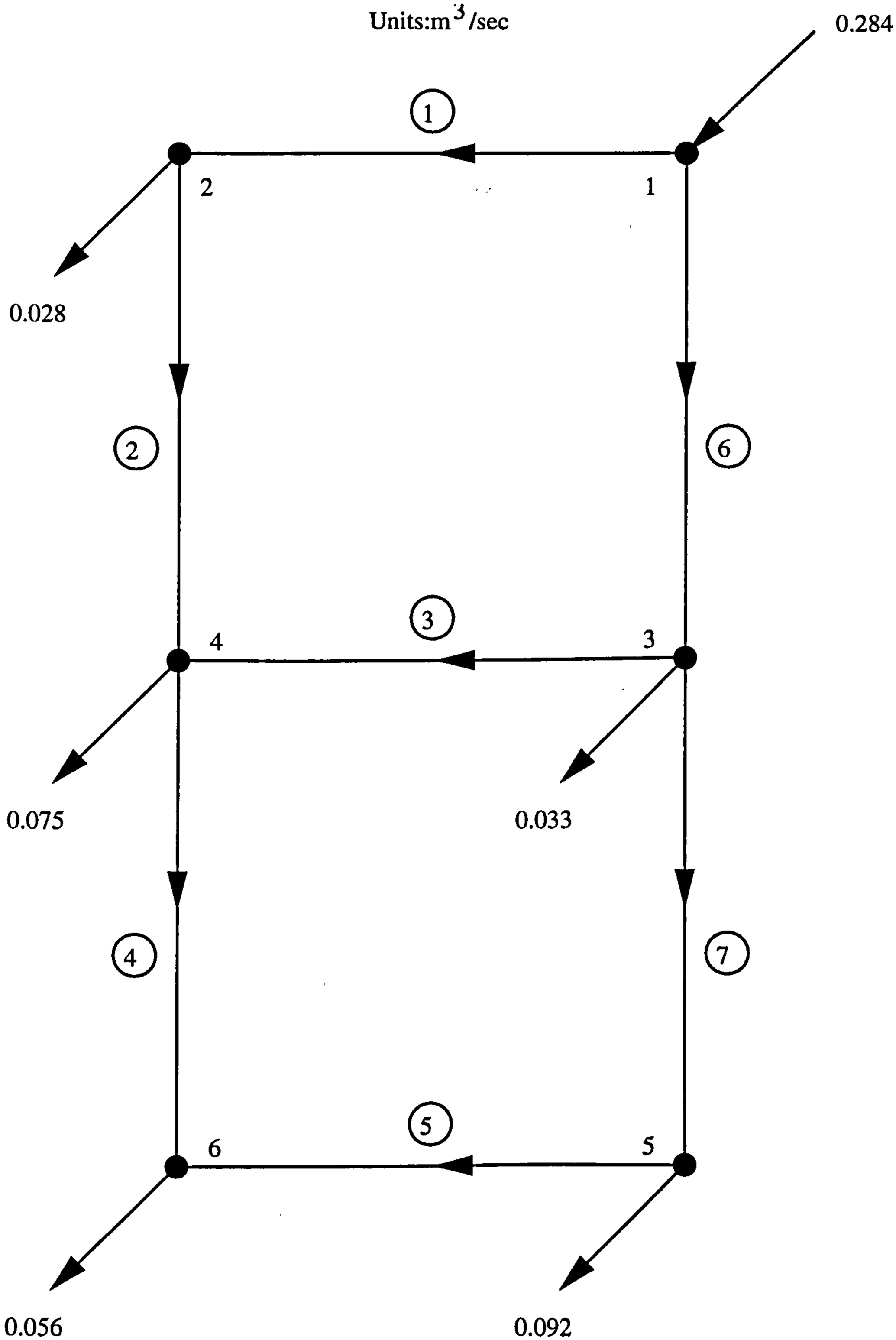

Figure 7.1 The one-source network of Example 1 adapted from Tanyimboh and Templeman (1993c)

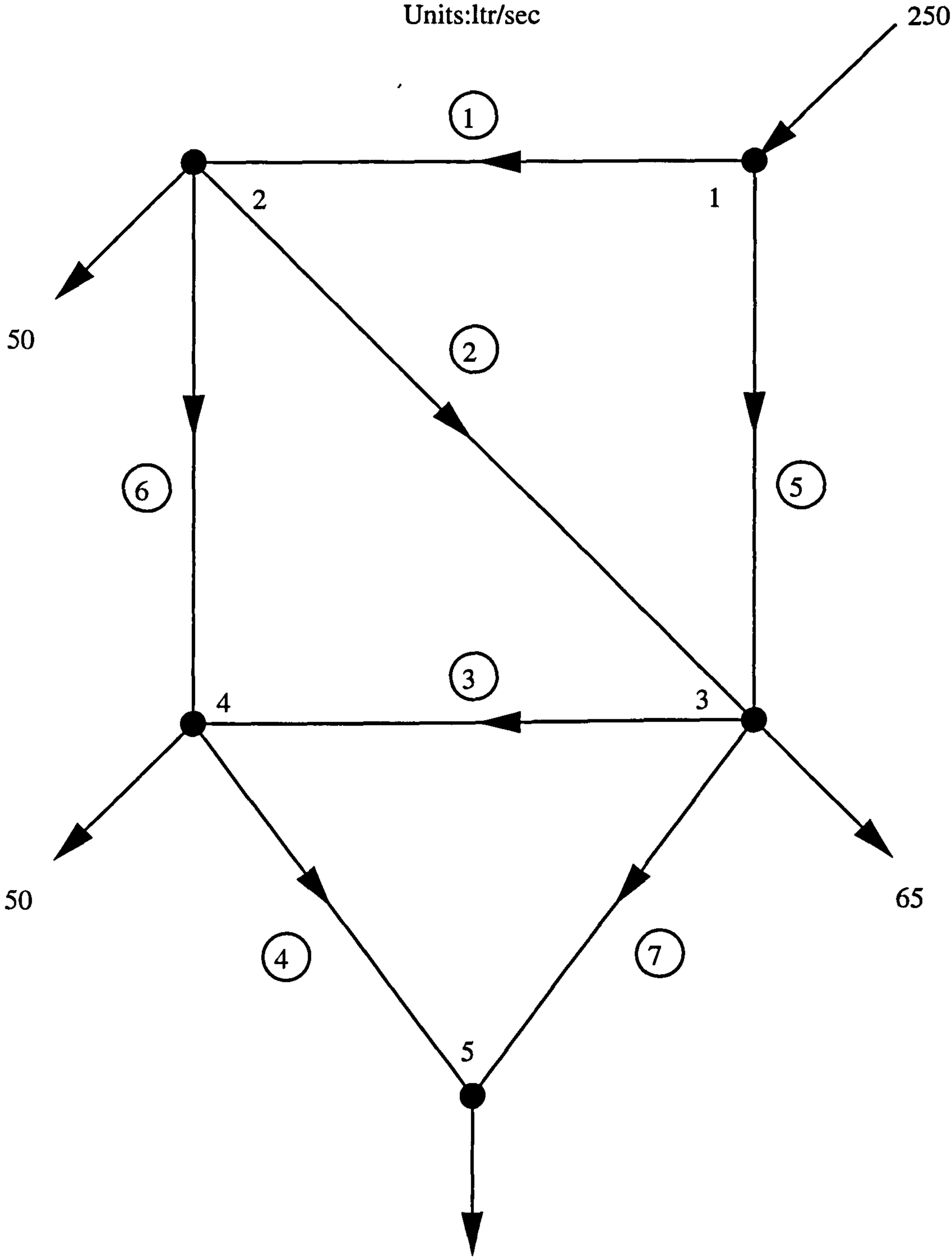

Figure 7.2 The one-source network of the original load case of Example 1

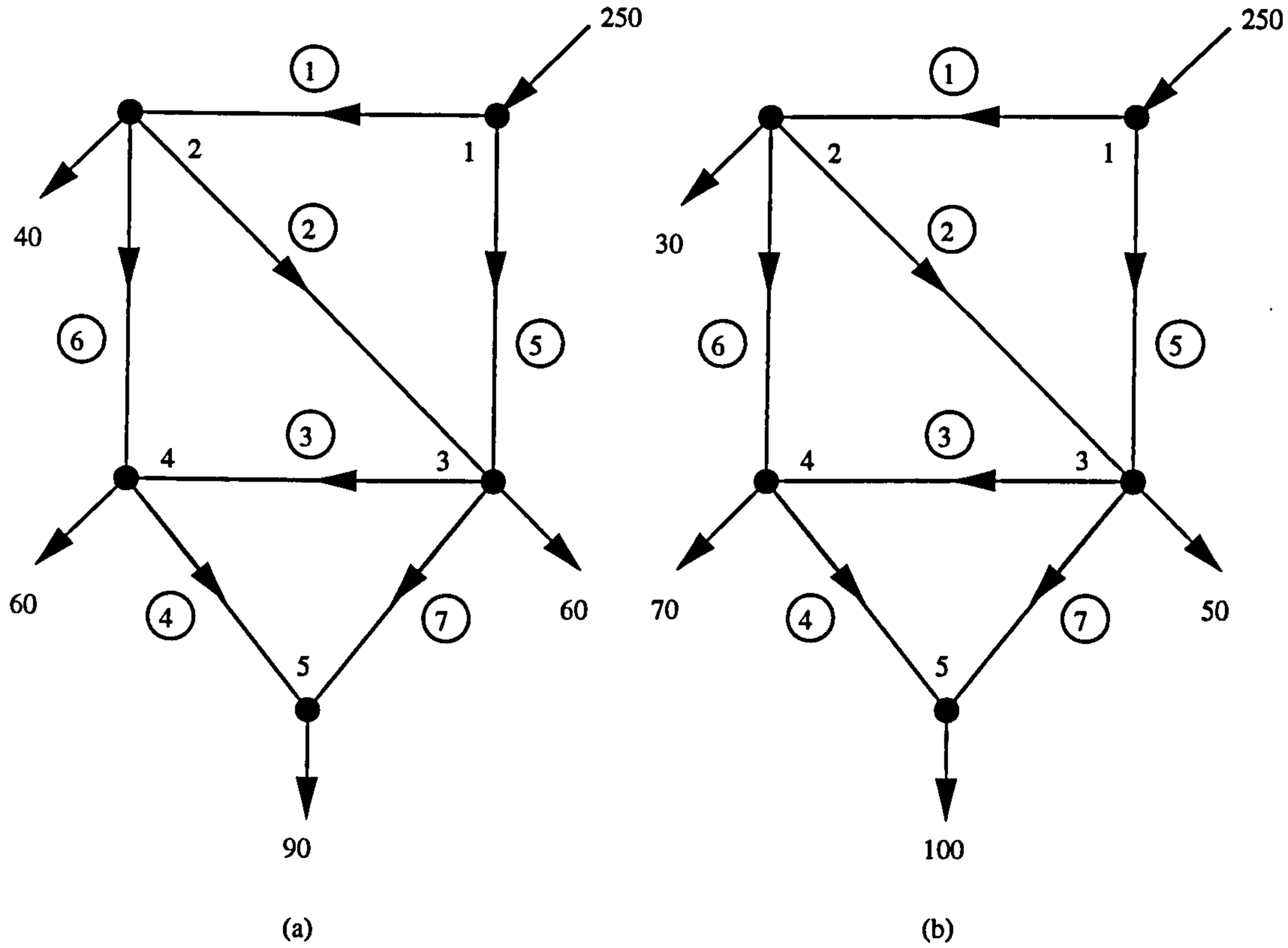

Figure 7.3 Two load cases of Example 2 with unchanged pipe flow directions comparing with the original load case of Figure 7.2

(a): Load case 2

(b): Load case 3

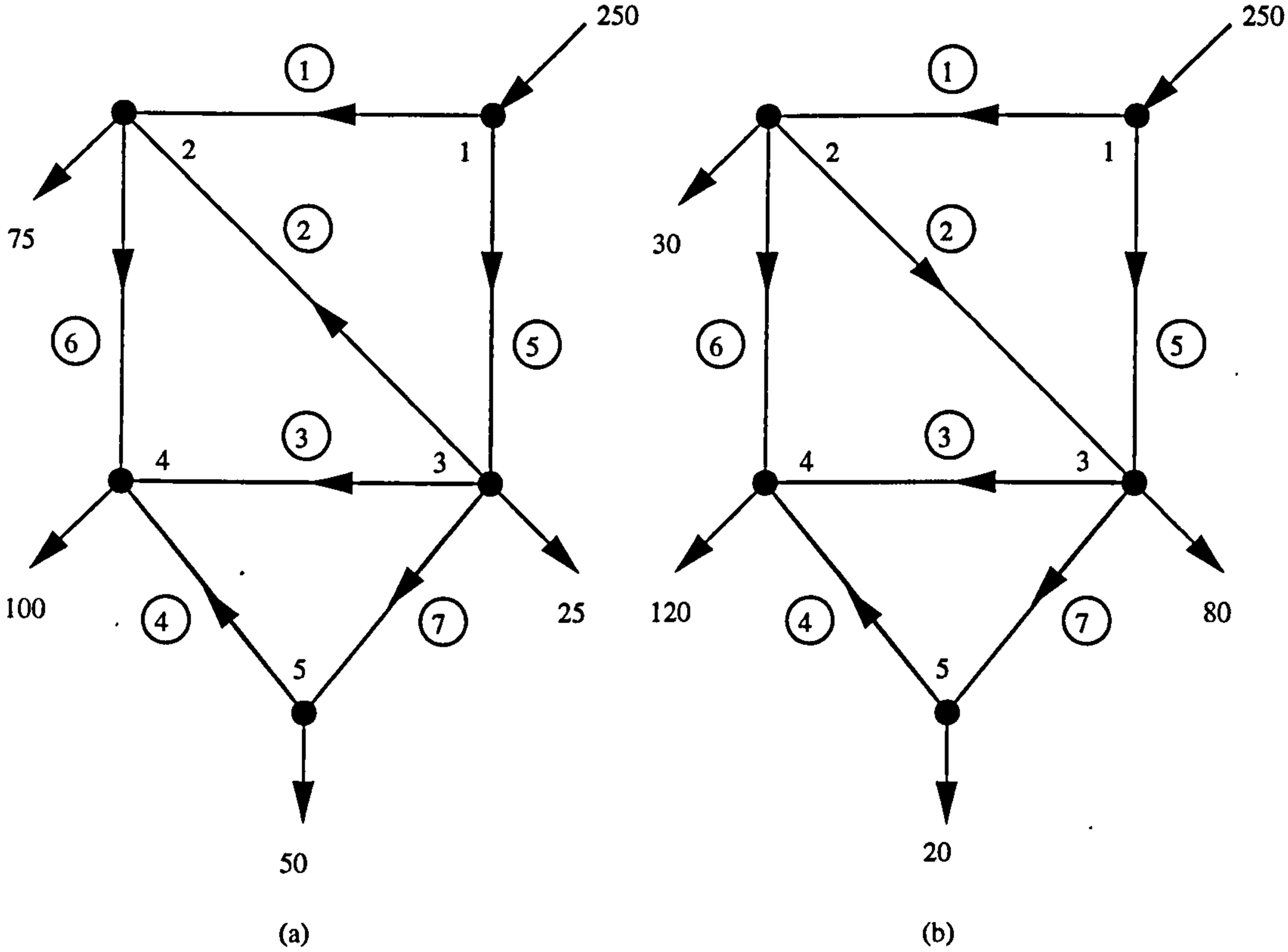

Figure 7.4 Two load cases of Example 2 with changing flow directions in some pipes comparing with the original load case of Figure 7.2

(a): Load case 4

(b): Load case 5

CHAPTER 8

ENTROPY-BASED STRUCTURAL APPLICATIONS

8.1 INTRODUCTION

It has been demonstrated in Chapter 3 that structural trusses and water supply networks share many aspects of similarity which can be extended almost fully to include terms such as physical quantities, constitutive equations, methods of analysis and design and even some reliability approaches, enabling both structural trusses and water supply networks to be included in the same general class of potentiated networks.

Most of the analysis and design methods used in water distribution networks have been shown to have counterparts in structural trusses and vice versa. Consequently, any approach or method used in either system and not explored in the other has the potential to be used in this other system. It has been shown in Chapter 4 how maximum entropy flows can be calculated in water distribution networks. Tanyimboh and Templeman (1993c) showed that designing water networks to carry those maximum entropy flows leads to a very good compromise between cost and reliability which is desired in urban water distribution networks. If bar axial forces in structural trusses can be considered as bar axial force flows and external loads as demands or supplies in a similar way to pipe water network flows, as described in Chapter 3, maximum entropy bar axial forces can be determined using the alfa method presented in Chapter 4, and structural trusses can consequently be designed to carry those calculated axial forces.

Force flows, however, differ from water flows in their vectorial nature. Each force in two dimensional structural trusses has two components, vertical and horizontal, as mentioned in Chapter 3. This difference can be overcome by treating each component at a time as will be seen later. Moreover, structural trusses have to be also treated as three dimensional rather than two, increasing the number of force flow components to three. However, this three dimensional truss case is beyond the scope of this thesis, and is left to future work.

It should be noted that structural trusses have to be indeterminate if maximum entropy force flows are to be determined since, similarly to branched water networks, the equilibrium equations are sufficient to calculate unique bar axial forces in the case of determinate structural trusses.

In this chapter, the force flow diagram for two dimensional structural trusses is developed in a similar fashion to water supply networks, followed by a method for calculating maximum entropy bar axial forces corresponding to those for water networks. A sample two dimensional indeterminate structural truss is presented and solved to demonstrate the above procedure, and then designed to carry the resulting maximum entropy bar axial forces. Finally, the maximum entropy truss design is tested and compared to a conventional design of the same truss by considering the removal of each bar in turn, and then by increasing the external load at each joint in the truss at a time. The results are discussed and conclusions are drawn.

8.2 STRUCTURAL FORCE FLOW DIAGRAM

To calculate maximum entropy bar axial force flows for indeterminate structural trusses, force flow diagrams for such trusses have to be developed first. External loads and the topology of the truss, along with bar force flow directions are assumed to be available, thus paralleling water distribution networks. This is described next by means of an example.

Consider the two dimensional truss of Figure 8.1. The external loads including support reactions are shown in the figure, while bar lengths needed to calculate these support reactions are given in Table 8.1. Because the truss has five joints and nine members, it is therefore indeterminate with two redundant bars. Bars 1-4 and 2-3 are arbitrarily chosen as the two redundant bars. Consequently, all axial forces in the truss bars can be calculated in terms of these two redundant bar axial forces, Fax_{14} and Fax_{23}, using bar force equilibrium equations only and assuming compressive forces are positive and tensile forces are negative as shown in Figure 8.2 and Table 8.1.

Table 8.1 Bar axial forces of the truss of Figure 8.1, calculated by bar force equilibrium equations in terms of redundant axial bar forces Fax_{14} and Fax_{23}.

Member i-j		Length Le_{ij} (mm)	*Bar axial force Fax_{ij} (KN)
1	1-3	2000	126.037 - 0.577 Fax_{14}
2	2-4	2000	76.036 - 0.577 Fax_{23}
3	1-4	3464	Fax_{14}
4	2-3	3464	Fax_{23}
5	3-5	2000	- 68.301 + 0.577 Fax_{14} - 0.577 Fax_{23}
6	4-5	2000	- 18.301 - 0.577 Fax_{14} + 0.577 Fax_{23}
7	3-4	2000	97.169 - 0.577 Fax_{14} - 0.577 Fax_{23}
8	1-5	2000	- 13.018 - 0.577 Fax_{14}
9	2-5	2000	- 38.018 - 0.577 Fax_{23}

*compressive force +ve, tensile force -ve.

Looking at the layout of the truss and the directions of external loads applied to it (Figure 8.1), it can be expected that both redundant bars are in compression, i.e. Fax_{14} and Fax_{23} are positive. Consequently, it can be deduced from Table 8.1 that members 1-5, 2-5, 3-5 and 4-5 are in tension and members 1-3, 1-4, 2-3 and 2-4 are in compression, while member 3-4 could be either in tension or compression depending on the values of Fax_{14} and Fax_{23}. These states of the truss members are needed in developing a force flow diagram for the truss being considered, as will be seen later.

It can be seen from Table 8.1 that bar force equilibrium equations are not sufficient to determine uniquely the bar axial forces of the indeterminate truss of Figure 8.1. It is recalled here from Chapter 3 that bar cross-sectional areas are required to calculate

these forces for such indeterminate cases. In the maximum entropy approach, however, these areas are not required for calculating the most likely axial forces in the truss bars, making the design procedure non-iterative and quicker than the conventional routine, as will be seen later.

In developing a force flow diagram for the truss of Figure 8.1, it is obvious that the vectorial nature of the problem makes it more complicated than that corresponding to water supply networks. However, this can be overcome by investigating only one component of force flows which, when determined, leads to the other component and hence to the final bar axial forces in the truss, as will be described later.

8.2.1 VERTICAL COMPONENT OF FORCE FLOW DIAGRAM

Figure 8.3 shows the vertical component of force flow diagram for the truss of Figure 8.1 assuming that bar axial compressive forces and external inflows are upwards and bar axial tensile forces and external outflows are downwards as shown in the figure. At joints 1 and 2, the upwards vertical support reactions of 109.151 and 65.849 respectively are considered as external inflows and all upwards compressive forces in the bars connected to these two joints are considered as force flows leaving joints 1 and 2 as shown in the figure. On the other hand, the downwards vertical external loads at joints 3, 4 and 5 are treated as external outflows and the downwards tensile force in bars 3-5 and 4-5 are treated as force flows leaving joints 3 and 4 respectively and both reaching joint 5 as shown in Figure 8.3.

8.2.2 HORIZONTAL COMPONENT OF FORCE FLOW DIAGRAM

Figure 8.4 shows the horizontal components of both bar axial forces and the external loads including support reactions, assuming that bar axial compressive forces and external inflows are rightwards and bar axial tensile forces and external outflows are leftwards. In this diagram, there is only one source (joint 1) and one demand (joint 4), and the force flow directions comply with the convention defined. Note that member 3-4 has been assumed to be in compression although it may be in tension as

mentioned earlier.

Having defined the two components of force flow diagrams, maximum entropy bar axial forces are calculated next using the alfa method programme described in Chapter 4 and 5 and given in Appendix B.

8.3 MAXIMUM ENTROPY BAR AXIAL FORCES

The alfa method programme is used in this section to calculate maximum entropy bar axial forces for the truss of Figure 8.1 with the external flows and the topology of the truss along with force flow directions in the bars for the two components of force flow diagram as shown in Figures 8.3 and 8.4. Obviously, solving one component diagram by the alfa method programme is sufficient to determine the axial forces in all bars since any force component which does not exist in the solved component diagram can be determined by bar equilibrium equations at the joints related to that force component.

Consider the vertical component of force flow diagram shown in Figure 8.3. All the requirements of the alfa method programme are satisfied in this diagram which can therefore be solved by that computer programme to yield all vertical components of the bar axial forces shown in figure 8.3, which can easily be used to give the axial forces in the corresponding bars. Three axial forces in bars 1-5, 2-5 and 3-4 have not been determined since they are horizontal and therefore have no vertical components to be included in the vertical component diagram of Figure 8.3. However, they can be calculated by bar force equilibrium equations at joints 1, 2 and 3 respectively. The results of maximum entropy axial forces in all bars are given in Table 8.2. Note that members in tension are assigned negative values while positive values are given to members in compression.

Table 8.2 Maximum entropy bar axial forces of the truss of Figure 8.1, calculated by solving the vertical component of force flow diagram (Figure 8.3) using the alfa method programme.

Member i-j		$Fax_{ij,v}$ (KN)	*Final maximum entropy Fax_{ij} (KN)
1	1-3	54.5755	+ 63.018
2	2-4	32.9245	+ 38.018
3	1-4	54.5755	+ 109.151
4	2-3	32.9245	+ 65.849
5	3-5	37.5000	- 43.301
6	4-5	37.5000	- 43.301
7	3-4	0.0000	- 3.867
8	1-5	0.0000	- 76.036
9	2-5	0.0000	- 76.036

*compressive force +ve, tensile force -ve.

Alternatively, the axial forces in the truss bars can theoretically be calculated by solving the horizontal component of force flow diagram shown in Figure 8.4. However, a close examination of the diagram shows that there is no terminal node in this force flow component diagram. Also, the flows in loops 3-4-5 and 3-2-5 circulate the loops infinitely so no conservation of energy around these two loops can be satisfied. Even reversing the flow in member 3-4, i.e. considering tensile force rather than compressive force in that member does not solve the problem. Consequently, the horizontal component of force flow diagram shown in figure 8.4 is unsolvable by the alfa method programme and its maximum entropy force flow component cannot be determined. It can then be concluded that maximum entropy bar axial forces for indeterminate structural trusses cannot be guaranteed to be calculatable for all types of trusses. Certain logical requirements for force flow diagrams are required to match those corresponding to water supply networks.

Considering the truss of Figure 8.1, solving its horizontal component of force flow diagram shown in Figure 8.4 is, however, not needed, at least for this particular truss example, since maximum entropy axial forces in the truss bars have been calculated by solving the vertical force flow component as shown earlier. In the remainder of this chapter, the truss of Figure 8.1 is designed to carry those maximum entropy bar axial forces. The resulting design is tested and compared to a conventional design of the

same truss.

8.4 MAXIMUM ENTROPY OPTIMUM STRUCTURAL DESIGN

Having calculated maximum entropy bar axial forces for the truss of Figure 8.1 as shown in Table 8.2, the segmental optimum design method presented in Chapter 3 as Problem 5 is used in this section to design the truss to carry those maximum entropy bar axial forces. It is recalled from Chapter 3 that the segmental optimum design formulation is one of linear programming and produces optimum bar sizes for structural trusses with some members composed of several segments which need to be rounded up to the size of the largest segment in each multi-segment member. For indeterminate trusses, the analysis, optimization and rounding up phases of the method should be made iteratively until the convergence of bar sizes between iterations is achieved.

In this section, however, only one iteration of the segmental optimum design is performed since the axial forces designed in the bars are the maximum entropy forces which are fixed and need not to be altered. Therefore, special arrangements are required to ensure that axial forces induced in the resulting optimum design bars are equal to the desirable maximum entropy forces, as will be seen later.

Assuming the set A_D of bar sizes available is 500, 1100, 1400, 1900, 2400, 3200 and 3500 mm^2 with round cross-sectional areas of steel grade 43 with elastic modulus equal to 210 KN/mm^2 and density equal to 7850Kg/m^3, Problem 5 can then be applied to design the truss of Figure 8.1 by assigning different sets of sizes to each member without violating stress limits and minimum gauge desired which is 500 mm^2 for this example as shown in Table 8.3. Maximum entropy bar axial virtual forces in the truss associated with virtual unit downwards load at node 5 needed in Problem 5 formulation to constrain the vertical deflection at that node to 2 mm and calculated by solving the vertical component of the respective force flow diagram using the alfa method programme are also shown in Table 8.3.

Table 8.3 Input data of Problem 5 for maximum entropy optimum design of the truss of Figure 8.1.

Member i-j		*Virtual maximum entropy $Fax_{ij,s}$ (KN)	Discrete bar sizes A_{ij} (mm^2)
1	1-3	+ 0.289	1400, 1900, 2400, 3200, 3500
2	2-4	+ 0.289	1100, 1400, 1900, 2400, 3200, 3500
3	1-4	+ 0.500	3200, 3500
4	2-3	+ 0.500	2400, 3200, 3500
5	3-5	- 0.577	500, 1100, 1400, 1900, 2400, 3200, 3500
6	4-5	- 0.577	500, 1100, 1400, 1900, 2400, 3200, 3500
7	3-4	$-5 * 10^{-11}$	500, 1100, 1400, 1900, 2400, 3200, 3500
8	1-5	- 0.577	500, 1100, 1400, 1900, 2400, 3200, 3500
9	2-5	- 0.577	500, 1100, 1400, 1900, 2400, 3200, 3500

*compressive force +ve, tensile force -ve.

A linear programming algorithm called EZLP and designed by Professor A. B. Templeman in the Department of Civil Engineering of Liverpool University has been used to solve Problem 5 for which data are shown in Table 8.3. The input and output files of this EZLP run are given in Appendix F from which the resulting segmental optimum design is summarized in Table 8.4.

The maximum entropy segmental optimum design shown in Table 8.4 has one multi-segment member (member 4-5) which can be rounded up to give the maximum entropy discrete optimum design without significant increase in the truss weight as shown in the table.

Table 8.4 Maximum entropy optimum design of the truss of Figure 8.1, obtained by solving Problem 5 using the EZLP linear programming algorithm.

Member i-j		Maximum entropy member area (mm^2)	
		Segmental optimum design	Discrete optimum design
1	1-3	1400	1400
2	2-4	1100	1100
3	1-4	3200	3200
4	2-3	2400	2400
5	3-5	1100	1100
6	4-5	624.127mm @ 500mm^2 ; 1375.873mm @ 1100mm^2	1100
7	3-4	500	500
8	1-5	1100	1100
9	2-5	1100	1100
Weight W (Kg)		265.518	268.457

Because the truss being considered is redundant, the resulting initial axial forces in the maximum entropy discrete optimum design bars would differ from the desirable maximum entropy bar axial forces shown in Table 8.2. A computer programme called TRUSS2D and given in Appendix G is used to calculate these initial bar axial forces and corresponding horizontal and vertical deflections at the truss joints. The results are summarized in Table 8.5.

Table 8.5 Initial bar axial forces and joint deflection components for the maximum entropy discrete optimum design of the truss of Figure 8.1, calculated by the TRUSS2D programme.

Member i-j		*Fax_{ij} (KN)	Joint i	**δ_{ih} (mm)	**δ_{iv} (mm)
1	1-3	+ 81.610	1	0	0
2	2-4	+ 53.559	2	+ 1.021	0
3	1-4	+ 76.951	3	+ 0.720	- 1.057
4	2-3	+ 38.935	4	+ 0.144	- 1.042
5	3-5	- 46.353	5	+ 0.497	- 1.649
6	4-5	- 40.250			
7	3-4	+ 30.264			
8	1-5	- 57.448			
9	2-5	- 60.499			

*compressive force +ve, tensile force -ve.
**upwards and rightwards deflection +ve, downwards and leftwards deflection -ve.

As expected, it can be seen from Table 8.5 that the initial axial forces in the truss bars are not the desirable maximum entropy bar axial forces shown in Table 8.2. To achieve that, the two redundant bars 1-4 and 2-3 have to be precompressed by the differences between the maximum entropy bar axial forces in these two bars and their initial force values respectively, i.e. 32.200 and 26.914 KN respectively as shown in Figure 8.5. This can practically be done by enlarging these two bars by two extra lengths which can be calculated by the characteristic force-strain relationship equations presented in Chapter 3 as follows:

$\Delta_{14} = 32.200 * (3464.076 + \Delta_{14}) / (3200 * 210) = 0.166$ mm.

$\Delta_{23} = 26.914 * (3464.076 + \Delta_{23}) / (2400 * 210) = 0.185$ mm.

These two extra lengths ensure inducing extra axial forces of 32.200 and 26.914 KN in bars 1-4 and 2-3 respectively when these two bars are precompressed to fit their original places in the truss. The extra axial forces induced in bars 1-4 and 2-3 obviously generate extra axial forces in the remaining bars in the truss, which can be determined by analysing the truss of Figure 8.6 and then can be added to the initial bar axial forces induced by the external applied loads to generate the desirable maximum entropy bar axial forces as demonstrated in Table 8.6. The final joint deflections in the maximum entropy design can be obtained by adding the extra deflections induced by enlarging bars 1-4 and 2-3 to the initial deflections shown in Table 8.5. The results are given in Table 8.7.

Table 8.6 Maximum entropy bar axial forces in the truss of Figure 8.1, generated by adding the extra bar axial forces induced by precompressing of bars 1-4 and 2-3 by forces 32.200 and 26.914 KN respectively to the initial bar axial forces induced by the external applied loads.

Member i-j		*Initial Fax_{ij} (KN)	*Extra Fax_{ij} (KN)	*Final Fax_{ij} (KN)
1	1-3	+ 81.610	- 18.592	+ 63.018
2	2-4	+ 53.559	- 15.541	+ 38.018
3	1-4	+ 76.951	+ 32.200	+ 109.151
4	2-3	+ 38.935	+ 26.914	+ 65.849
5	3-5	- 46.353	+ 3.052	- 43.301
6	4-5	- 40.250	- 3.051	- 43.301
7	3-4	+ 30.264	- 34.131	- 3.867
8	1-5	- 57.448	- 18.588	- 76.036
9	2-5	- 60.499	- 15.537	- 76.036

*compressive force +ve, tensile force -ve.

Table 8.7 Final joint deflection components in the maximum entropy design of the truss of Figure 8.1, generated by adding the extra joint deflection components caused by precompressing of bars 1-4 and 2-3 to the initial deflection components caused by the external applied loads.

Joint i	Initial deflection components		Extra deflection components		Final deflection components	
	*δ_{ih} (mm)	*δ_{iv} (mm)	*δ_{ih} (mm)	*δ_{iv} (mm)	*δ_{ih} (mm)	*δ_{iv} (mm)
1	0	0	0	0	0	0
2	+ 1.021	0	+ 0.295	0	+ 1.316	0
3	+ 0.720	- 1.057	- 0.148	+ 0.232	+ 0.572	- 0.825
4	+ 0.144	- 1.042	+ 0.502	+ 0.274	+ 0.646	- 0.768
5	+ 0.497	- 1.649	+ 0.161	+ 0.441	+ 0.658	- 1.208

*upwards and rightwards deflection +ve, downwards and leftwards deflection -ve.

Having designed the truss of Figure 8.1 to carry maximum entropy bar axial forces calculated by solving the vertical component of force flow diagram using the alfa method computer programme, the truss is conventionally designed next and then compared from reliability point of view with the maximum entropy discrete optimum design obtained in this section.

8.5 CONVENTIONAL OPTIMUM STRUCTURAL DESIGN

In this section, the segmental optimum design method presented in Chapter 3 as Problem 5 is used to design the truss of Figure 8.1 in a conventional way in which the analysis, optimization and rounding up phases are carried out iteratively until the converged discrete optimum design is achieved. The TRUSS2D computer programme is used to solve the analysis phase of the method for each iteration needed for convergence, while the EZLP algorithm is used for optimization.

Using the same set of available bar sizes A_D used in the maximum entropy design, five iterations of analysis, optimization and rounding up of the segmental optimum structural design method were needed to obtain the converged conventional optimum design of the truss of the Figure 8.1, with the maximum entropy discrete optimum design shown in Table 8.4 being used as an initial design for the procedure. In each iteration, different sets of bar sizes chosen from the set A_D have been assigned to each member of the truss in such a way that no stress limit or minimum gauge limit has been violated. The resulting conventional discrete optimum design for the last iteration along with its corresponding bar axial forces and joint deflection components is given in Table 8.8.

Obviously, the above conventional optimum design of the truss of Figure 8.1 differs from the maximum entropy design of the same truss in many aspects such as weight, bar axial forces distribution, bar cross-sectional areas and joint deflection components. The reliability of the two designs is tested next by means of two major reliability approaches, those being damage tolerance, and resilience or flexibility approaches.

Table 8.8 Last iteration results of the conventional discrete optimum design of the truss of Figure 8.1, obtained by five iterations of analysis, optimization and rounding up process of the segmental optimum structural design method using TRUSS2D and EZLP computer programmes.

Member i-j		A_{ij} (mm^2)	*Fax_{ij} (KN)	Joint i	**δ_{ih} (mm)	**δ_{iv} (mm)
1	1-3	1900	+ 106.850	1	0	0
2	2-4	1900	+ 77.082	2	+ 1.318	0
3	1-4	1900	+ 33.235	3	+ 0.669	- 1.005
4	2-3	500	- 1.809	4	+ 0.273	- 1.050
5	3-5	500	- 48.068	5	+ 0.613	- 2.000
6	4-5	500	- 38.535			
7	3-4	1900	+ 79.027			
8	1-5	500	- 32.208			
9	2-5	500	- 36.975			
Weight W (Kg)		186.152				

*compressive force +ve, tensile force -ve.
**upwards and rightwards deflection +ve, downwards and leftwards deflection -ve.

8.6 MAXIMUM ENTROPY DESIGN AND CONVENTIONAL DESIGN RELIABILITY COMPARISON

It is recalled from Chapter 3 that the damage tolerance of a structural truss is the capability of the truss to sustain partial damage (failure of one bar or more) without leading to a complete failure. Also, the flexibility or the resilience of a truss is its capability to withstand extra applied loads which are not specifically designed for. In this section, the damage tolerance of the maximum entropy design and the conventional design of the truss of Figure 8.1 is examined by considering the removal of each bar in the truss in turn and analysing the resulting nine reduced truss cases for each design using the TRUSS2D computer programme. Also in this section, the resilience of both designs is investigated by analysing the two designs using the TRUSS2D computer programme with each external load component applied to the truss is increased to 150 KN in turn. Therefore, there are four cases of resilience analysis to be considered for each design.

Because the final analysis results for the maximum entropy design are a combination of initial results and their corresponding results obtained by precompressing of bars 1-4 and 2-3 as shown in Tables 8.6 and 8.7, damage tolerance and resilience analysis results for that design have been respectively calculated by adding the final maximum entropy results of Tables 8.6 and 8.7 to the results obtained by considering each reduced truss having external applied loads equal and opposite to axial forces in the removed bar as shown in Figure 8.7 for the case of bar 1-3 being removed for an example, and by adding the final maximum entropy results to the results obtained by analysing the truss to sustain the extra load applied to each external load component as shown in Figure 8.8 for the case of increasing the vertical load component of the external applied load at joint 5 as an example. All the final damage tolerance and resilience analysis results for the maximum entropy design are given in Tables 8.9-8.12.

Table 8.9 Bar axial force results of damage tolerance analysis for the maximum entropy design of the truss of Figure 8.1.

Member i-j		1-3	2-4	1-4	2-3	3-5	4-5	3-4	1-5	2-5
*Capacity (KN)		+63.289	+42.757	+114.809	+66.885	+42.757	+42.757	+9.147	+42.757	+42.757
		-369.964	-292.681	-822.581	-623.777	-292.681	-292.681	-135.577	-292.681	-292.681
*Fax_{ij} (KN)	case 1	failed	+39.488	+218.302	+63.304	+21.187	-107.789	-65.416	-139.056	-74.567
	case 2	+63.997	failed	+107.456	+131.700	-82.299	-4.303	-40.907	-75.057	-114.056
	case 3	+126.036	+36.549	failed	+68.395	-107.788	+21.186	+57.682	-13.017	-77.506
	case 4	+62.040	+76.035	+110.847	failed	-4.305	-82.297	+33.172	-77.015	-38.018
	case 5	+75.942	+72.592	+124.268	+86.766	failed	-86.603	+21.980	-154.74	-111.438
	case 6	+85.715	+17.413	+69.838	+101.537	-86.603	failed	-1.774	-53.339	-96.641
	case 7	+65.050	+39.853	+105.632	+62.670	-43.497	-43.105	failed	-74.004	-74.201
	case 8	+139.052	+36.245	-22.549	+68.920	-121.109	+34.507	+70.396	failed	-77.809
	case 9	+61.060	+114.052	+112.542	-65.851	+34.691	-121.293	+70.211	-77.994	failed

*compressive force +ve, tensile force -ve.

Table 8.10 Joint deflection component results of damage tolerance analysis for the maximum entropy design of the truss of Figure 8.1.

Case number	$*\delta_{2h}$ (mm)	$*\delta_{3h}$ (mm)	$*\delta_{3v}$ (mm)	$*\delta_{4h}$ (mm)	$*\delta_{4v}$ (mm)	$*\delta_{5h}$ (mm)	$*\delta_{5v}$ (mm)
case 1	+1.849	-0.948	-4.346	+0.298	-1.291	+1.204	-2.892
case 2	+1.637	+1.201	-1.196	+1.981	-3.062	+0.650	-2.337
case 3	+0.783	-0.027	-0.974	-1.125	-1.468	+0.112	-1.971
case 4	+0.995	+1.354	-1.269	+0.723	-0.919	+0.666	-1.709
case 5	+2.304	+1.394	-1.401	+0.975	-1.494	+1.339	-2.570
case 6	+1.298	+0.694	-1.074	+0.728	-0.504	+0.461	-2.073
case 7	+1.283	+0.521	-0.812	+0.661	-0.758	+0.640	-1.177
case 8	+5.786	+3.684	-3.219	+2.344	-2.351	+5.113	-3.605
case 9	+6.321	+3.548	-2.528	+2.211	-3.514	+0.675	-3.840

*upwards and rightwards deflection +ve, downwards and leftwards deflection -ve.

Table 8.11 Bar axial force results of resilience analysis for the maximum entropy design of the truss of Figure 8.1.

Member i-j		1-3	2-4	1-4	2-3	3-5	4-5	3-4	1-5	2-5
*Capacity (KN)		+63.289	+42.757	+114.809	+66.885	+42.757	+42.757	+9.147	+42.757	+42.757
		-369.964	-292.681	-822.581	-623.777	-292.681	-292.681	-135.577	-292.681	-292.681
$*Fax_{ij}$ (KN)	case 1	+146.100	+51.158	+115.251	+93.091	-26.640	-59.962	+5.751	-122.860	-106.199
	case 2	+71.222	-9.259	+181.542	+61.135	-48.784	-37.818	+7.059	-42.832	-48.314
	case 3	+75.362	+119.288	+137.772	+75.087	-60.978	-25.624	+3.144	-106.995	-124.672
	case 4	+92.813	+68.011	+132.546	+88.901	-86.405	-86.800	+12.619	-111.194	-110.997

*compressive force +ve, tensile force -ve.

Table 8.12 Joint deflection component results of resilience analysis for the maximum entropy design of the truss of Figure 8.1.

Case number	$*\delta_{2h}$ (mm)	$*\delta_{3h}$ (mm)	$*\delta_{3v}$ (mm)	$*\delta_{4h}$ (mm)	$*\delta_{4v}$ (mm)	$*\delta_{5h}$ (mm)	$*\delta_{5v}$ (mm)
case 1	+1.983	+0.951	-1.697	+0.842	-1.171	+1.063	-1.898
case 2	+0.788	+0.120	-0.629	-0.014	-0.372	+0.371	-0.972
case 3	+2.005	+1.102	-1.228	+1.042	-1.750	+0.926	-1.939
case 4	+1.923	+1.063	-1.343	+0.823	-1.316	+0.962	-2.264

*upwards and rightwards deflection +ve, downwards and leftwards deflection -ve.

For the conventional design, however, the results of all damage tolerance and resilience analysis cases have been respectively calculated by analysing each reduced truss in turn (see Figure 8.9 for the case of bar 1-3 being removed as an example), and by considering the whole truss subjected to all applied loads with each load

component increased to 150 KN in turn (see Figure 8.10 for the case of increasing the vertical component of the external load applied to joint 5 to 150 KN, as an example). All the damage tolerance and resilience analysis results for the conventional design are given in Tables 8.13-8.16.

Table 8.13 Bar axial force results of damage tolerance analysis for the conventional design of the truss of Figure 8.1.

Member i-j		1-3	2-4	1-4	2-3	3-5	4-5	3-4	1-5	2-5
*Capacity (KN)		+112.877	+112.877	+41.475	+0.000	+9.147	+9.147	+112.877	+9.147	+9.147
		-497.683	-497.683	-497.683	-135.577	-135.577	-135.577	-497.683	-135.577	-135.577
*Fax_{ij} (KN)	case 1	failed	+55.807	+218.300	+35.041	+37.505	-124.110	-49.099	-139.060	-58.250
	case 2	+79.492	failed	+80.619	+131.700	-97.794	+11.191	-25.414	-59.565	-114.060
	case 3	+126.040	+80.903	failed	-8.427	-63.436	-23.167	+102.040	-13.020	-33.154
	case 4	+106.480	+76.038	+33.877	failed	-48.742	-37.861	+77.612	-32.579	-38.020
	case 5	+73.741	+92.044	+90.579	-27.724	failed	-86.603	+60.881	-65.316	-22.013
	case 6	+133.390	+65.088	-12.735	+18.965	-86.603	failed	+93.574	-5.667	-48.969
	case 7	+58.483	+46.422	+117.010	+51.297	-30.363	-56..240	failed	-80.574	-67.636
	case 8	+139.060	+83.495	-22.551	-12.917	-73.863	-12.740	+117.650	failed	-30.562
	case 9	+119.970	+114.060	+10.507	-65.851	-24.216	-62.387	+129.120	-19.086	failed

*compressive force +ve, tensile force -ve.

Table 8.14 Joint deflection component results of damage tolerance analysis for the conventional design of the truss of Figure 8.1.

Case number	*δ_{2h} (mm)	*δ_{3h} (mm)	*δ_{3v} (mm)	*δ_{4h} (mm)	*δ_{4v} (mm)	*δ_{5h} (mm)	*δ_{5v} (mm)
case 1	+3.758	-0.808	-10.221	-0.562	-2.817	+2.649	-7.401
case 2	+3.307	+6.044	-3.950	+6.171	-12.089	+1.135	-8.935
case 3	+0.880	+0.103	-0.789	-0.408	-1.212	+0.248	-2.100
case 4	+1.345	+0.661	-0.998	+0.272	-1.059	+0.621	-2.093
case 5	+1.663	+0.271	-0.583	-0.035	-1.513	+1.244	-4.156
case 6	+1.041	+0.988	-1.343	+0.519	-0.678	+0.108	-3.755
case 7	+2.823	+3.436	-2.323	-0.058	-1.932	+1.535	-4.088
case 8	+3.372	+1.812	-1.851	+1.222	-1.725	+2.790	-2.910
case 9	+6.072	+2.372	-2.064	+1.725	-3.170	+0.364	-3.756

*upwards and rightwards deflection +ve, downwards and leftwards deflection -ve.

Table 8.15 Bar axial force results of resilience analysis for the conventional design of the truss of Figure 8.1.

Member i-j		1-3	2-4	1-4	2-3	3-5	4-5	3-4	1-5	2-5
*Capacity (KN)		+112.877	+112.877	+41.475	+0.000	+9.147	+9.147	+112.877	+9.147	+9.147
		-497.683	-497.683	-497.683	-135.577	-135.577	-135.577	-497.683	-135.577	-135.577
*Fax_{ij} (KN)	case 1	+206.430	+101.830	+10.764	+5.332	-36.297	-50.306	+116.750	-62.537	-55.532
	case 2	+115.870	+27.521	+104.220	-2.568	-56.648	-29.955	+88.482	+1.810	-11.537
	case 3	+125.950	+169.840	+50.155	-12.470	-61.013	-25.590	+104.280	-56.411	-74.123
	case 4	+149.850	+120.190	+33.755	-1.480	-91.260	-81.946	+121.840	-54.160	-58.817

*compressive force +ve, tensile force -ve.

Table 8.16 Joint deflection component results of resilience analysis for the conventional design of the truss of Figure 8.1.

Case number	*δ_{2h} (mm)	*δ_{3h} (mm)	*δ_{3v} (mm)	*δ_{4h} (mm)	*δ_{4v} (mm)	*δ_{5h} (mm)	*δ_{5v} (mm)
case 1	+2.249	+1.322	-1.958	+0.737	-1.463	+1.191	-2.832
case 2	+0.185	-0.225	-0.541	-0 668	-0.652	-0.034	-1.677
case 3	+2.486	+1.193	-1.418	+0.670	-2.032	+1.075	-2.828
case 4	+2.152	+1.196	-1.558	+0.585	-1.600	+1.032	-3.660

*upwards and rightwards deflection +ve, downwards and leftwards deflection -ve.

Finally, the compressive and tensile strength capacities of each bar for both designs have been calculated according to British Standard Code of Practice for steel design BS 5950 and included in the tables of bar axial force results. This forms a convenient way of establishing the behaviour of the truss under the severe circumstances being considered.

8.7 DISCUSSION

Before discussing the reliability analysis results for both maximum entropy and conventional designs of the truss of Figure 8.1, a brief comparison between the two designs is presented next in terms of weight, bar axial force distribution, bar cross-sectional areas and joint deflection components.

Table 8.17 shows a summary of the two designs with some statistical measures of mean and spread for the above-mentioned results. It can be seen from the table that

the conventional design is about 30% lighter than the maximum entropy design. Most of the extra weight used in the maximum entropy design is consumed by the two long and thick bars 1-4 and 2-3 which provide the main strength to the truss. Bar 2-3 in the conventional design is hardly used as can be seen from its very small axial force. Also, the coefficients of variation of bar cross-sectional areas, bar axial forces and joint deflection components for both designs show that the maximum entropy design results are more uniform than the corresponding conventional design results. This accords with the maximum entropy formalism which assigns the most uniform values to a system subject to available information.

Table 8.17 Maximum entropy design and conventional design results for the truss of Figure 8.1 with some statistical comparison.

Member i-j		Maximum entropy design		Conventional design		**Joint deflection component	Maximum entropy design	Conventional design
		A_{ij} (mm^2)	*Fax_{ij} (KN)	A_{ij} (mm^2)	*Fax_{ij} (KN)	δ_{ik}	0	0
1	1-3	1400	+63.018	1900	+106.850	δ_{ik}	0	0
2	2-4	1100	+38.018	1900	+77.082	δ_{ik}	+1.316	+1.318
3	1-4	3200	+109.151	1900	+33.235	δ_{ik}	0	0
4	2-3	2400	+65.849	500	-1.809	δ_{ik}	+0.572	+0.669
5	3-5	1100	-43.301	500	-48.068	δ_{ik}	-0.825	-1.005
6	4-5	1100	-43.301	500	-38.535	δ_{ik}	+0.646	+0.273
7	3-4	500	-3.867	1900	+79.027	δ_{ik}	-0.768	-1.050
8	1-5	1100	-76.036	500	-32.208	δ_{ik}	+0.658	+0.613
9	2-5	1100	-76.036	500	-36.975	δ_{ik}	-1.208	-2.000
Mean		1444.444	59.410	1122.222	50.421	Mean	0.856	0.990
σ_{n-1}		827.815	31.359	737.865	31.684	σ_{n-1}	0.291	0.561
σ_{n-1}/mean		0.573	0.528	0.658	0.628	σ_{n-1}/mean	0.340	0.567
Weight (Kg)		268.457		186.152				

*compressive force +ve, tensile force -ve.
**upwards and rightwards deflection +ve, downwards and leftwards -ve.

The general uniformity of the maximum entropy design results may be considered as an advantage from a reliability point of view. For a truss with uniform bar cross-sectional areas, for example, there would be more possible alternate load paths in some emergency circumstances such as the case of unexpected extra load applied to the truss or the case of a partial damage to the truss. The same can be said about bar

axial forces as they follow their corresponding bar cross-sectional areas. However, the small force in bar 3-4 in the maximum entropy design may be due to the fact that only the vertical component of force flow diagram of the truss being considered has been solved, for which the horizontal bar 3-4 is not a member. In contrast, this bar in the conventional design is a main bar with high compressive axial force as shown in Table 8.17, while the long cross bar 2-3 is redundant as it carries very small tensile axial force. It cannot be usable for alternate load paths as it has minimum cross-sectional area. Finally, looking at joint deflection results for both designs shown in Table 8.17, it can be seen that deflection values for the maximum entropy design are relatively smaller than the corresponding values for the conventional design as indicated by the mean values. Obviously, this can be expected as the maximum entropy design is heavier than the conventional design. Also, the coefficients of variation for the deflection results for both designs show that these deflection results corresponding to the maximum entropy design are less spread than those corresponding to the conventional design for which the maximum deflection value is up to the limit (2 mm).

Returning to the reliability analysis results given in Tables 8.9-8.16, it can be deduced that neither design is damage tolerant nor flexible enough to sustain the extra load applied to the truss. Failure of any member in the maximum entropy design, for example, leads to a failure of at least one other member leading to a progressive failure as can be seen from Table 8.9 by comparing the bar axial forces in each reduced truss case to their respective capacities. Because bar 3-4 in the maximum entropy design carries very small axial force, case 7 which is the case of removing that bar is the safest case amongst the nine cases. Only bar 1-3 is just above the limit capacity as shown in the table. This can be confirmed by the deflection results given in Table 8.10 where the deflection results of case 7 are the smallest. All the other deflection results in the table have no meaning since their corresponding truss cases have progressively been failed. Also, the resilience analysis results given in Table 8.11 for the maximum entropy design show that increasing any external load component applied to the truss leads inevitably to a complete failure of the truss by progressive bar failures. Again, this leads to disregarding the deflection results of all four

resilience analysis cases shown in Table 8.12.

The same can be said about the conventional design analysis results. Apart from case 4 of damage tolerance analysis where, as expected, removing the redundant and unusable bar 2-3 leaves the truss perfectly safe, Tables 8.13 and 8.15 show respectively that the conventional design is neither damage tolerant nor flexible in sustaining extra load applied to it. Also, the deflection results of Tables 8.14 and 8.16 can be disregarded due to the failure of the respective truss cases. Only the deflection results of case 4 of damage tolerance analysis are valid with the vertical component of the deflection at joint 5 just above the limit of 2 mm as shown in Table 8.14.

The non-damage tolerance of the maximum entropy design and the conventional design can be justified as there are special ways of designing damage tolerant structures by designing those structures to have some residual strengths, as described in Chapter 3. However, the non-flexibility of both designs is valid only for the extra loads specified in the example. Because both designs behaved similarly in damage tolerance and flexibility analyses, the two designs are compared next by determining their probabilities of failure and survival analytically as described in Chapter 3.

It is recalled from Chapter 3 that the failure probability of a system can be calculated from the following equation:

$$p_f(system) = 1 - \prod_{i=1}^{NM} [1 - p(FM_i)] \tag{8.1}$$

in which p_f (system) is the probability of the system failure; $p(FM_i)$ is the probability of failure mode i, i=1,...,NM; where NM being the number of failure modes.

The non-damage tolerance of the maximum entropy and conventional designs of the truss of Figure 8.1 as shown earlier suggests considering failure of each bar in the truss as a failure mode. Consequently, to calculate the probability of failure of each design , the probability of failure of each bar in each design has to be calculated first. Assuming both strength and load for each bar are normally distributed, the following

first order approximation of probability of failure can be used:

$$p_f = \Phi(-\beta) = 1-\Phi(\beta) \tag{8.2}$$

in which p_f is the failure probability of a component; Φ is the cumulative normal distribution function; and β is the safety index which for the fundamental case, e.g. the case of a truss bar, can be calculated as:

$$\beta = \frac{\overline{R} - \overline{L}}{\sqrt{\sigma_R^2 + \sigma_L^2}} \tag{8.3}$$

in which $\overline{R}$ and $\overline{L}$ are the mean values of strength and load respectively; σ_R and σ_L are respectively the standard deviations of strength and load.

Once the system probability of failure is calculated using Eq. (8.1), the reliability of the system or its probability of survival p_s (system) can be calculated from the following equation:

$$p_s\ (system) = 1 - p_f\ (system) \tag{8.4}$$

Applying the above four equations to the maximum entropy and conventional designs and assuming that the mean values of strength and load for each bar in both designs have respectively the same values of capacities and bar axial forces calculated earlier for the respective bar in the respective design,with σ_R taken as 10% of $\overline{R}$ and σ_L taken as 15% of $\overline{L}$ for each bar, Tables 8.18 and 8.19 show the safety index of each bar and its probability of failure for the maximum entropy design and the conventional design respectively, along with their system probabilities of failure and survival.

Table 8.18 Reliability analysis for the maximum entropy design of the truss of Figure 8.1.

Member i-j		*$\overline{R}_{ij}$ (KN)	*$\sigma_{R,ij}$ (KN)	*$\overline{L}_{ij}$ (KN)	*$\sigma_{L,ij}$ (KN)	**β_{ij}	$p_{f,ij}$
1	1-3	+63.289	+6.3289	+63.018	+9.4527	0.024	0.4904
2	2-4	+42.757	+4.2757	+38.018	+5.7027	0.665	0.2530
3	1-4	+114.809	+11.4809	+109.151	+16.3727	0.283	0.3886
4	2-3	+66.885	+6.6885	+65.849	+9.8774	0.087	0.4653
5	3-5	-292.681	-29.2681	-43.301	-6.4952	8.318	0.0000
6	4-5	-292.681	-29.2681	-43.301	-6.4952	8.318	0.0000
7	3-4	-135.577	-13.5577	-3.867	-0.5801	9.706	0.0000
8	1-5	-292.681	-29.2681	-76.036	-11.4054	6.897	0.0000
9	2-5	-292.681	-29.2681	-76.036	-11.4054	6.897	0.0000
p_f (system)		0.87555					
p_s (system)		0.12445					

*compressive force +ve, tensile force -ve.
**β_{ij} takes its absolute values for tension bars.

Table 8.19 Reliability analysis for the conventional design of the truss of Figure 8.1.

Member i-j		*$\overline{R}_{ij}$ (KN)	*$\sigma_{R,ij}$ (KN)	*$\overline{L}_{ij}$ (KN)	*$\sigma_{L,ij}$ (KN)	**β_{ij}	$p_{f,ij}$
1	1-3	+122.877	+11.2877	+106.850	+16.0275	0.307	0.3794
2	2-4	+112.877	+11.2877	+77.082	+11.5623	2.215	0.0134
3	1-4	+41.475	+4.1475	+33.235	+4.9853	1.271	0.1018
4	2-3	-135.577	-13.5577	-1.809	-0.2714	9.865	0.0000
5	3-5	-135.577	-13.5577	-48.068	-7.2102	5.699	0.0000
6	4-5	-135.577	-13.5577	-38.535	-5.7803	6.584	0.0000
7	3-4	+112.877	+11.2877	+79.027	+11.8541	2.068	0.0193
8	1-5	-135.577	-13.5577	-32.208	-4.8312	7.182	0.0000
9	2-5	-135.577	-13.5577	-36.975	-5.5463	6.731	0.0000
p_f (system)		0.46066					
p_s (system)		0.53934					

*compressive force +ve, tensile force -ve.
**β_{ij} takes its absolute values for tension bars.

Firstly, the relatively small system reliabilities of both designs as shown in Tables 8.18 and 8.19 are due to the fact that both designs have been designed deterministically using the mean values of strengths and loads. Also, the highest safety

index values are, as expected, those for bars 2-3 and 3-4 for the conventional design and the maximum entropy design respectively, since these two bars are almost unused in their respective designs. All high safety indices which have almost zero probabilities of failure are those for tension members whose bar sizes have been bounded by minimum gauge of 500 mm^2 taking into account the very high tensile strength of steel, or by the minimum vertical deflection of 2 mm at joint 5 taking into account the very high elasticity of steel.

Secondly, it can be seen from Tables 8.18 and 8.19 that the conventional design is more reliable than the maximum entropy design although the former is lighter than the latter. This can be argued by realizing that the larger bar sizes of the maximum entropy design have been used to sustain larger bar axial forces compared with the conventional design. These larger bar axial forces are due to the extra forces induced by precompressing bars 1-4 and 2-3 in the maximum entropy design. Therefore, the reliabilities of a stronger truss sustaining larger loads and a weaker truss sustaining smaller loads depend on the differences between bar capacities and bar loads for both designs. Accidently, the available bar sizes used in the two designs have strength capacities much closer to the maximum entropy bar axial forces than to those corresponding to the conventional design, making the latter design more reliable than the former design. Choosing another set of available bar sizes may produce a maximum entropy design which is more reliable than its corresponding conventional design. The above arguments justify the case being studied, but also lead to the conclusion that the current method of designing maximum entropy structural trusses does not produce the desirable and reliable trusses which are sought in this chapter. This may be due to the vectorial nature of bar axial forces compared with pipe water flows as demonstrated earlier by the difficulties encountered in solving the horizontal component of force flow diagram for the truss of Figure 8.1.

8.8 SUMMARY AND CONCLUSION

The alfa method of calculating maximum entropy pipe flows presented in Chapter 4 and illustrated in Chapter 5 for water distribution networks has been used in this chapter to calculate maximum entropy bar axial forces for a sample indeterminate structural truss in an attempt to obtain a reliable truss by designing it to carry maximum entropy bar axial forces. This parallels the results for reliable water distribution networks obtained by Tanyimboh and Templeman (1993c) by designing them to carry maximum entropy pipe flows. The motivation for this application was the striking similarities between structural trusses and water distribution networks in almost every aspect, as demonstrated in Chapter 3.

Because of the vectorial nature of the axial forces in the truss bars, force flow diagrams for two components (horizontal and vertical) are needed instead of a single pipe flow diagram. Solving either component by the alfa method should lead to the other, which together with the first component results gives the final maximum entropy bar axial forces in the truss. For the truss under research, the vertical component has been solved by the alfa method, and its results have been used to determine the horizontal component of the force flow diagram leading to the sought maximum entropy bar axial forces in the truss. These final maximum entropy bar axial forces have been used to design the truss being considered by applying the segmental optimum design method presented in Chapter 3 as Problem 5 by means of the linear programming algorithm EZLP which is available in the Department of Civil Engineering of Liverpool University. Because the sample truss is indeterminate with two redundant bars, the bar axial forces induced by the applied loads in the resulting maximum entropy design were different from the desirable maximum entropy bar axial forces which the truss has been designed for. Therefore, the two redundant bars have been precompressed in such a way that final bar axial forces in the truss have been converted towards the desirable maximum entropy values.

Also in this chapter, the truss under investigation has been conventionally designed using the segmental optimum design in which five iterations were needed for

convergence. The resulting conventional design was about 30% lighter than the maximum entropy design. Moreover, the two designs of the truss being considered have been compared from a reliability point of view by means of two major approaches, those being damage tolerance and resilience or flexibility approaches. The damage tolerance of both designs has been tested by considering the removal of each bar in the truss in turn and analysing the resulting reduced truss cases for each design. The resilience or the flexibility of both designs, however, has been studied by analysing the two designs with each external load component applied to the truss increased to 150 KN in turn. It has been shown that neither design is damage tolerant nor flexible to sustain the extra load applied to the truss. The stronger strengths used in the maximum entropy design bars (larger bar sizes) have been cancelled out by the larger bar axial forces which are due to the extra forces induced by precompressing the two redundant bars in the maximum entropy design.

Finally, because both designs exhibited similar behaviour against damage tolerance and flexibility analysis approaches, a probabilistic reliability analysis has been carried out on both designs in order to calculate their probabilities of failure and survival for comparison reasons. For this purpose, all strength and load values used for both design bars have been assumed to be the mean values with standard deviations of 10% and 15% of each bar strength and bar load respectively. The analysis showed that the conventional design was more reliable than the maximum entropy design. This was due to the fact that the probability of failure and hence the probability of survival depends on the gap between the strength and load of each individual bar, and accidently the strengths of available bar sizes used in both designs were closer to the maximum entropy bar axial forces than to those corresponding to the conventional design taking into account the above observation of the simultaneous increase of strengths and loads in the maximum entropy design bars compared with those corresponding to the conventional design.

Armed with the above results, it can be concluded that the entropy-based approach to designing structural trusses does not produce reliable trusses as had been hoped for. The vectorial nature of bar axial forces in structural trusses in general and the inability

of solving the horizontal component of force flow diagram for the truss used in this chapter in particular may be the main reason for failing to obtain reliable maximum entropy designs. Because of that, it is unknown whether the maximum entropy force results of one component would lead to the maximum entropy force results of the other, or which component would give the final maximum entropy results in the case of each component giving different final results. Also, the extra axial forces induced in the maximum entropy design bars by precompressing the redundant bars in order to bring the bar axial forces up to the desirable maximum entropy results would undervalue the extra strengths achieved in the maximum entropy design.

Clearly, the research described in this chapter must be regarded as unsuccessful and inconclusive. It has generated many more questions than answers, but has also brought to light some unsuspected difficulties in extending the scalar methodologies developed for water networks to the vectorial domain of structural trusses. Much further research is needed in this area.

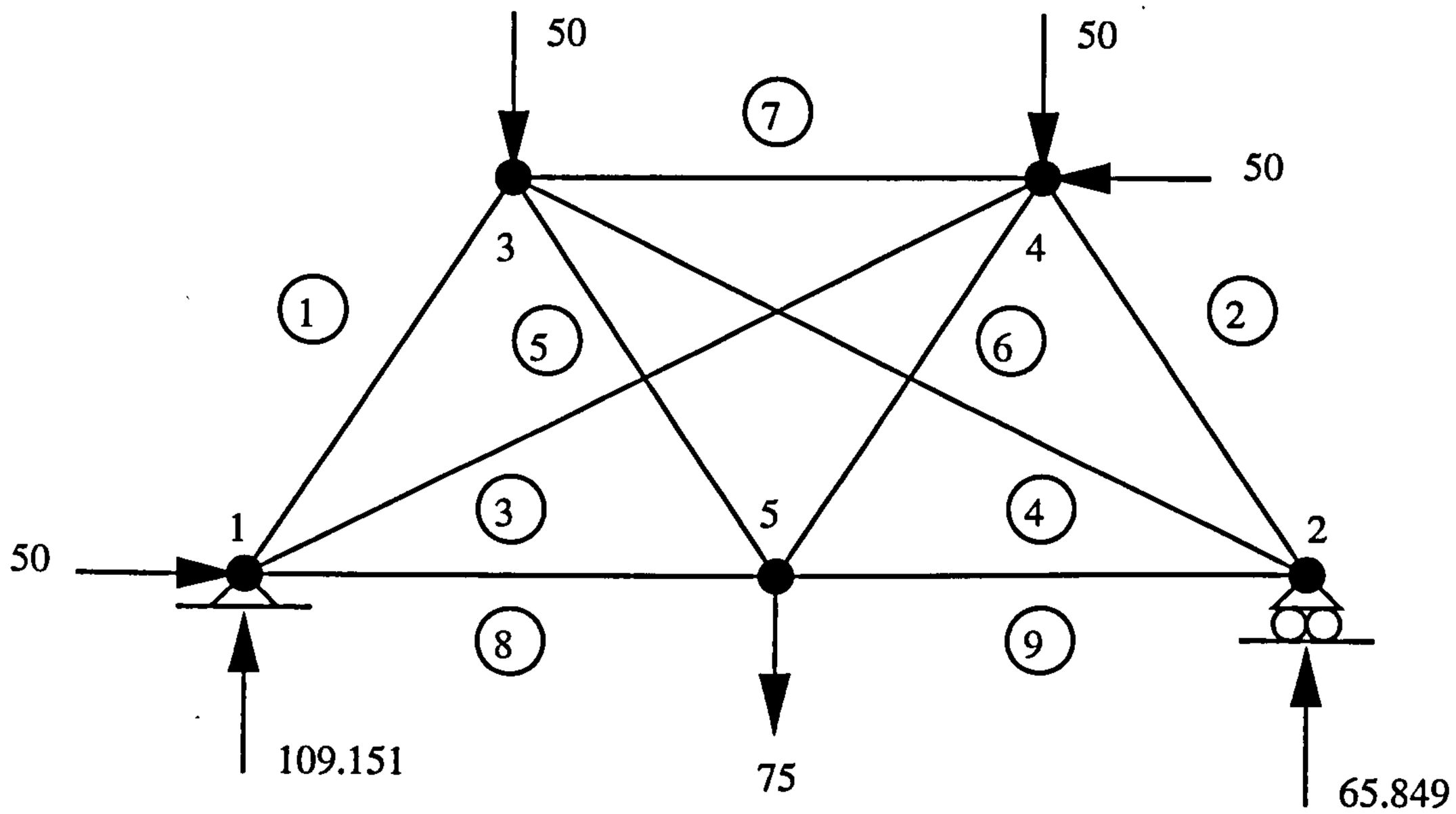

Figure 8.1 A sample indeterminate structural truss

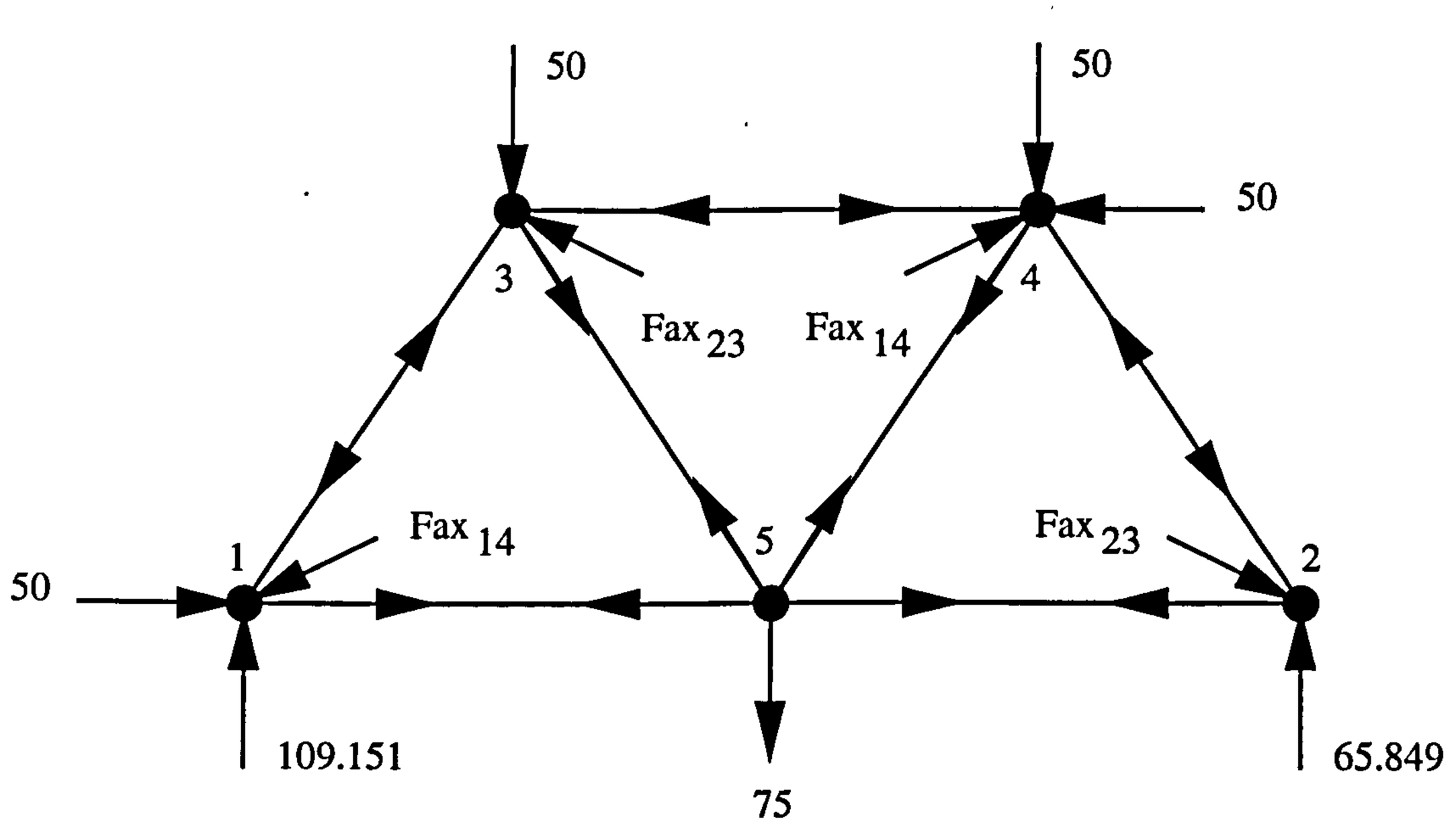

Figure 8.2 The truss of Figure 8.1 with the two redundant bars replaced by their bar axial forces

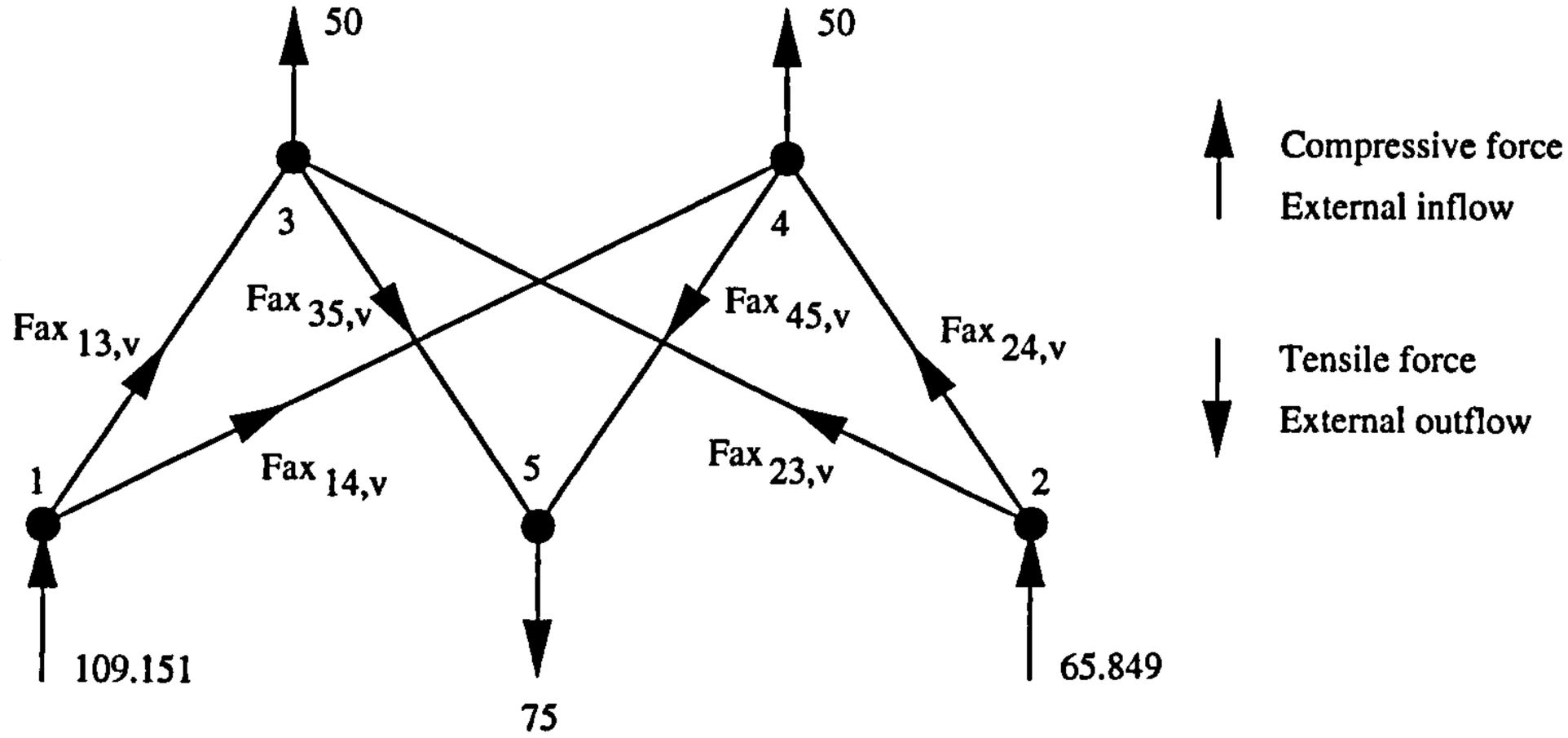

Figure 8.3 The vertical component of force flow diagram
of the truss of Figure 8.1

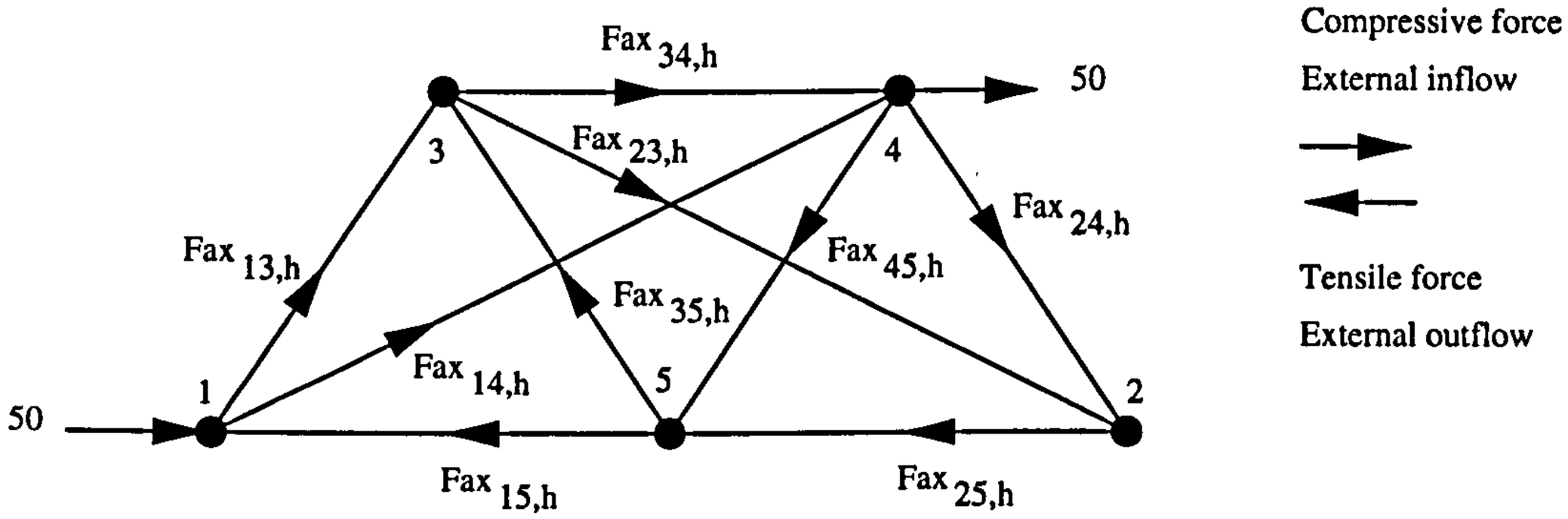

Figure 8.4 The horizontal component of force flow diagram
of the truss of Figure 8.1

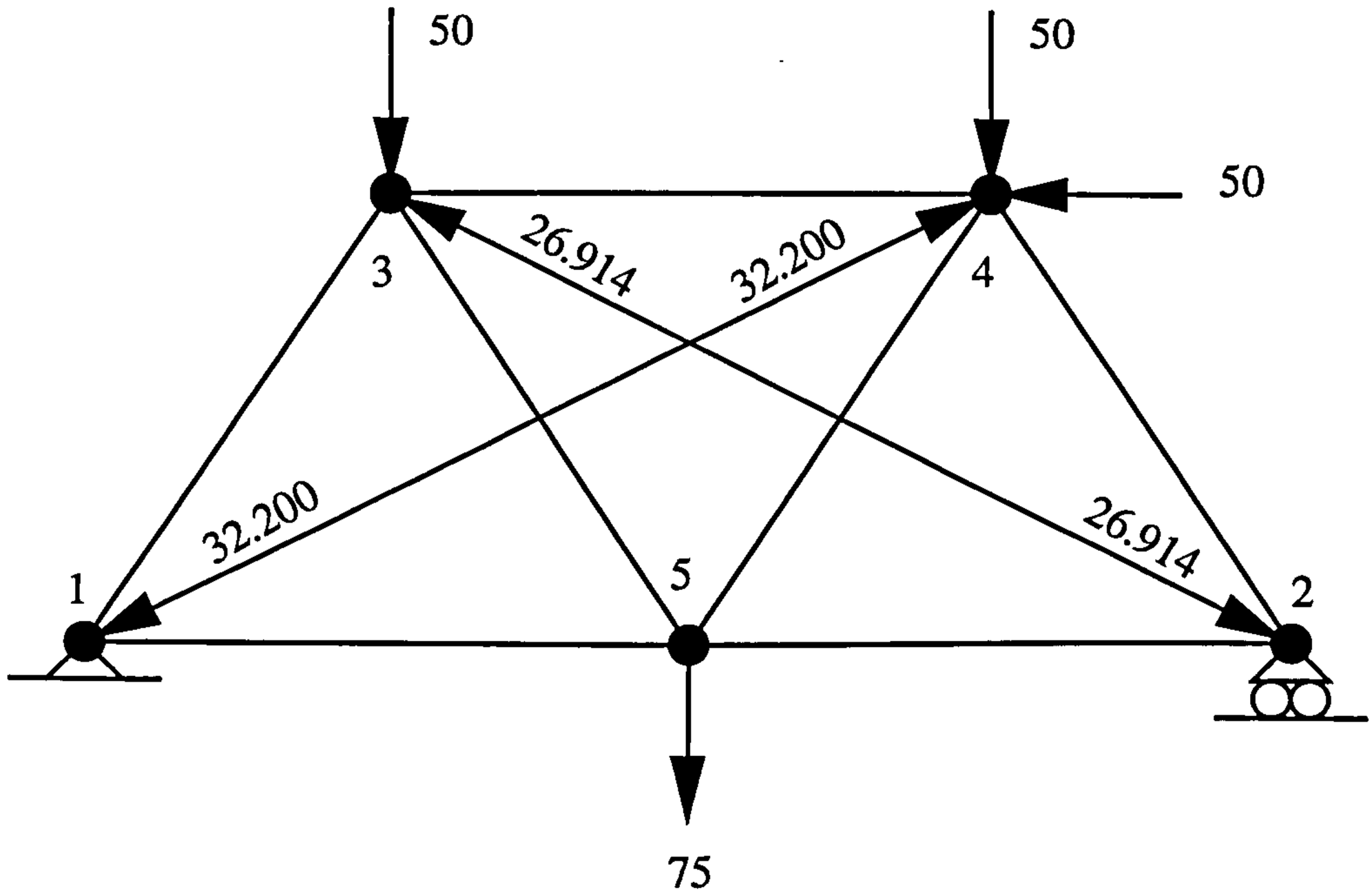

Figure 8.5 Precompressing of bars 1-4 and 2-3 in the maximum entropy design of the truss of Figure 8.1

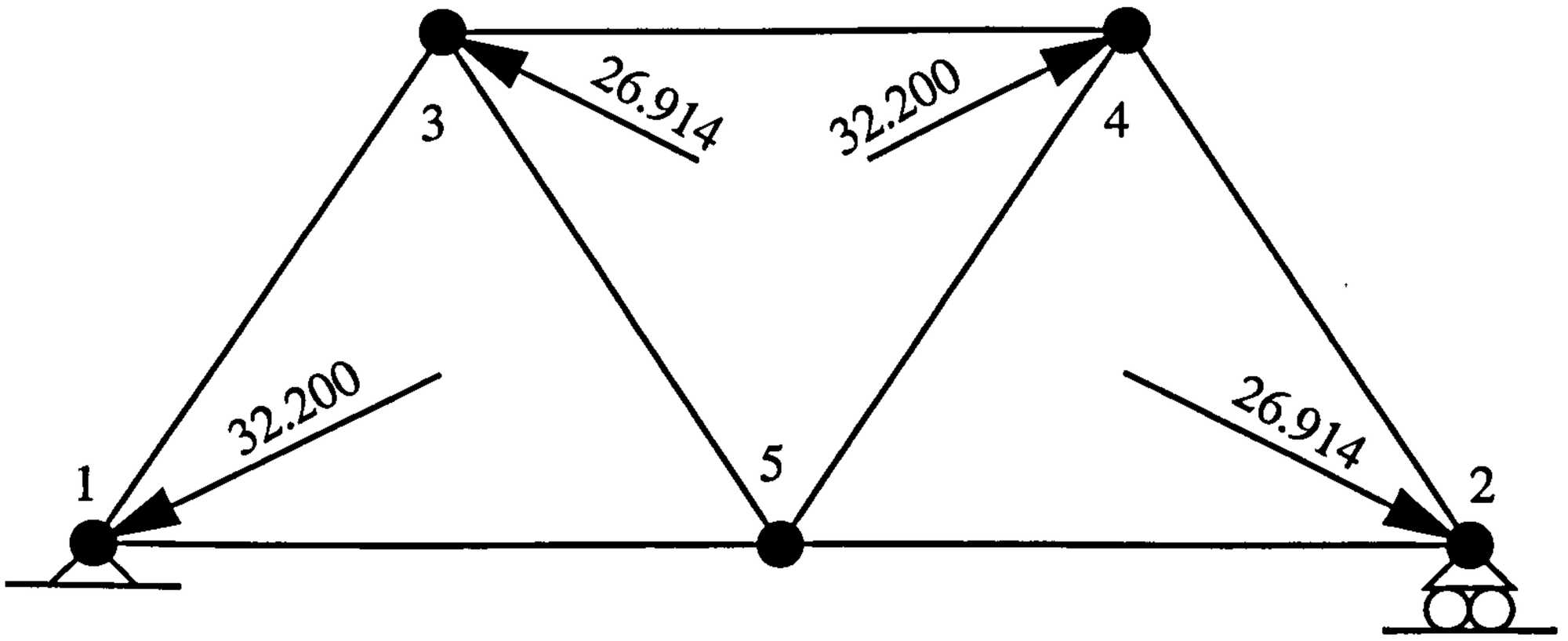

Figure 8.6 The maximum entropy design of the truss of Figure 8.1 under precompressing applied loads

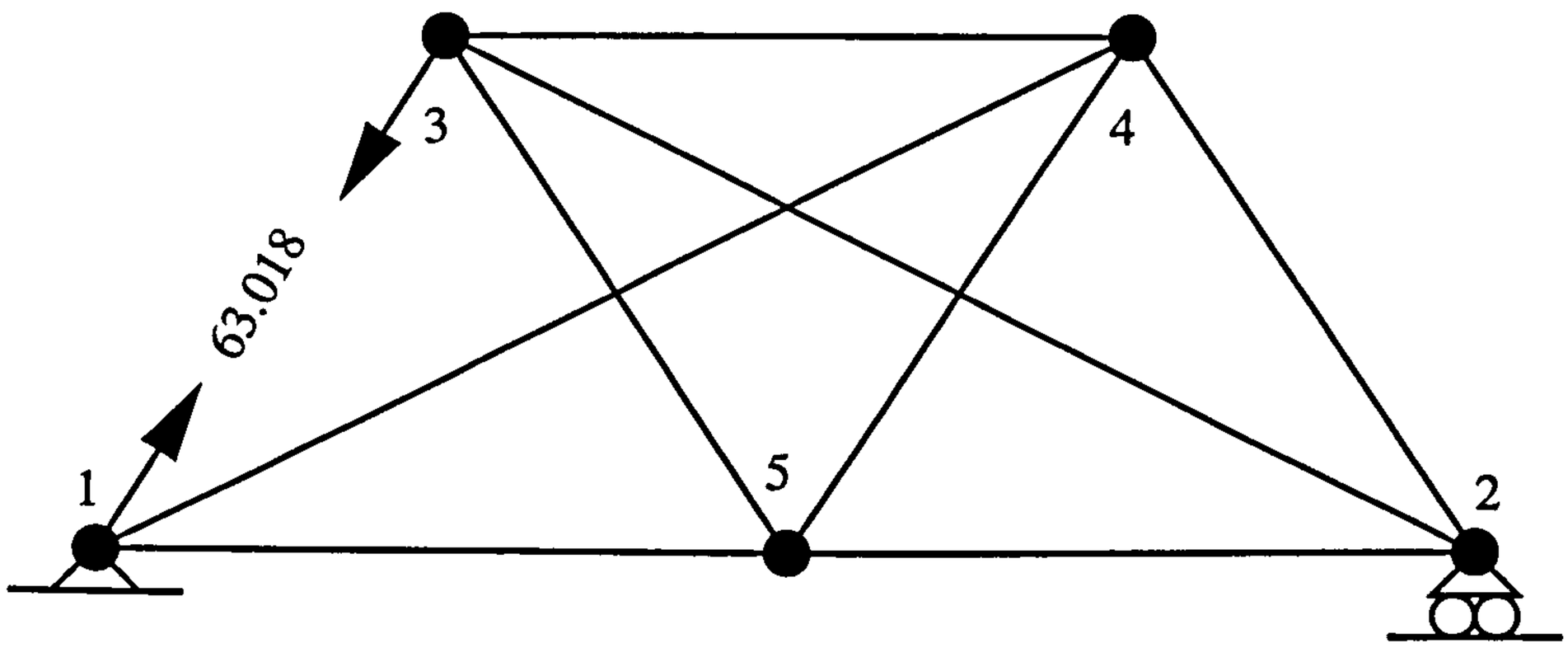

Figure 8.7 Removing of bar 1-3 case which has to be added to the maximum entropy design results to give case 1 of damage tolerance analysis

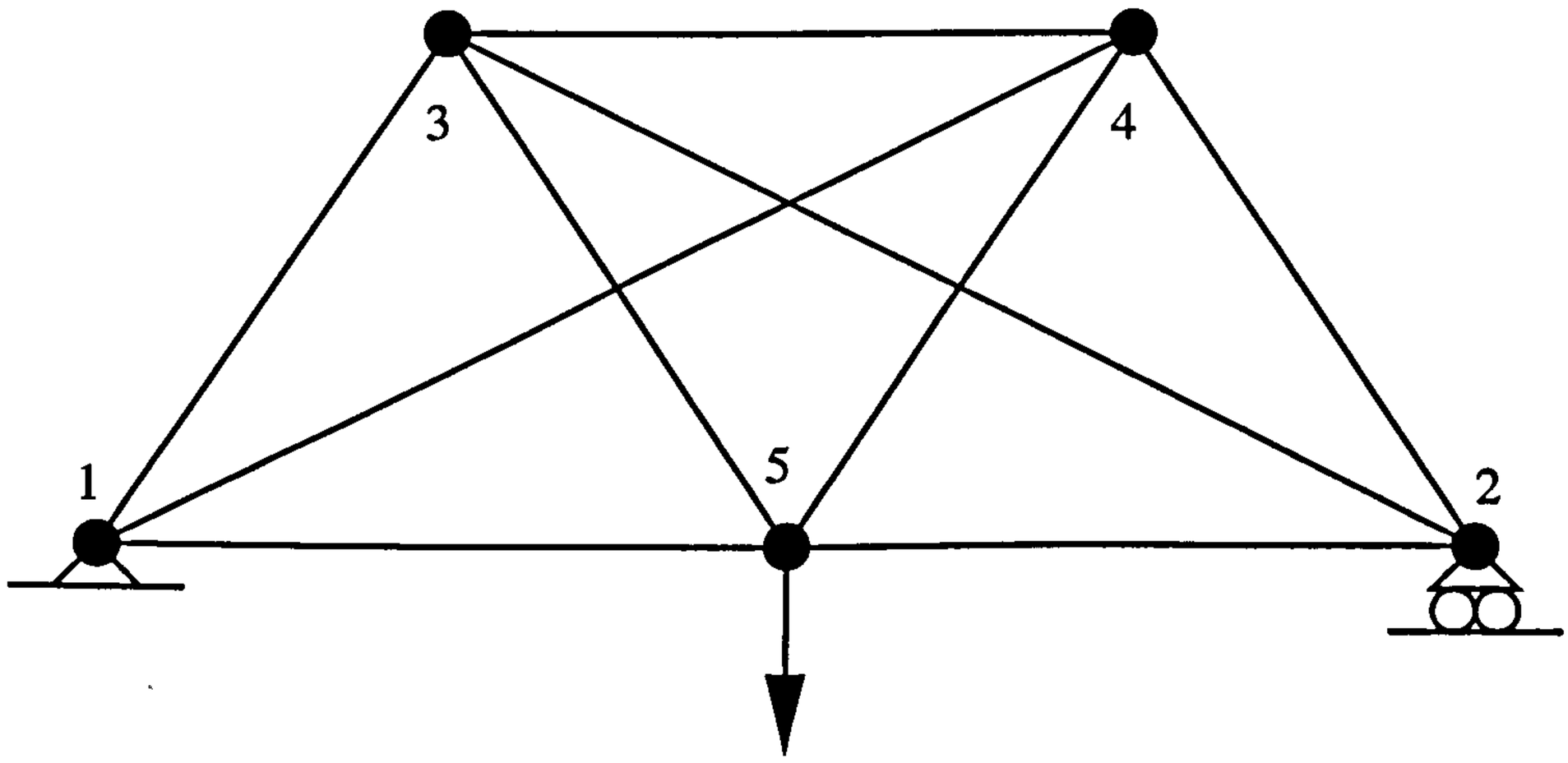

150-75=75

Figure 8.8 Increasing the load at joint 5 case which has to be added to the maximum entropy design results to give case 4 of resilience analysis

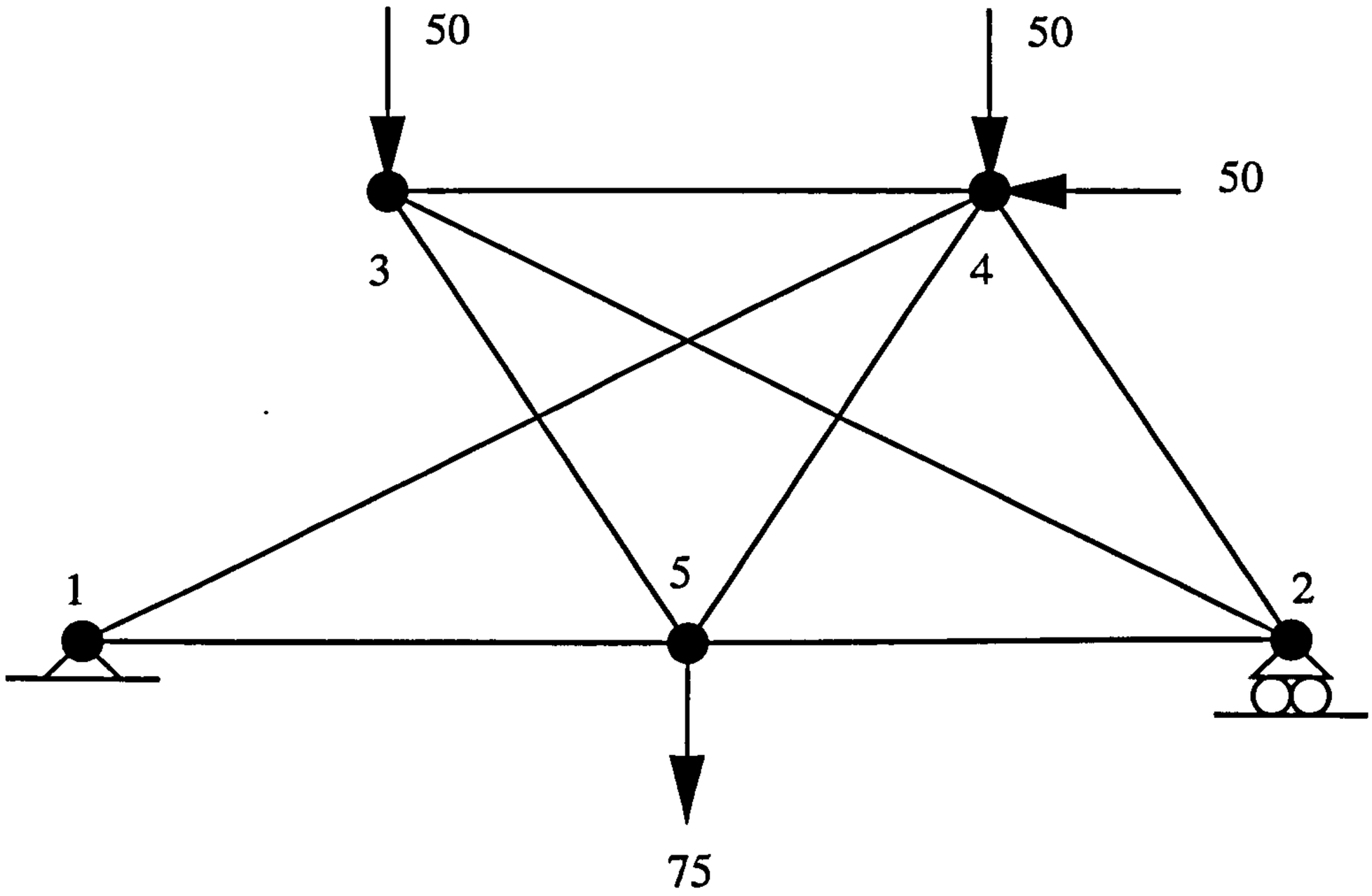

Figure 8.9 Case 1 of damage tolerance analysis for the conventional design with bar 1-3 being removed

Figure 8.10 Case 4 of resilience analysis for the conventional design with the external load at joint 5 being increased

CHAPTER 9

SUMMARY, CONCLUSIONS AND RECOMMENDATIONS FOR FUTURE WORK

9.1 INTRODUCTION

In recent years, Jaynes' maximum entropy formalism, based on Shannon's informational entropy measure of uncertainty, has been used in the literature to generate solutions to a wide range of civil engineering problems under uncertainty. By casting in probabilistic terms the missing or uncertain information of the system being considered, as required by Shannon's informational entropy, so that an entropy function measuring the information can be developed, and by maximizing the resulting entropy function subject to any available information, the most-likely, or least-biased, performance estimates of the missing information can be inferred. In this thesis, methods of logical inference based on the maximum entropy formalism have been developed for two different civil engineering system models under uncertainty; those being water distribution networks and structural trusses.

The first point tackled in the present research was the problem of estimating most-likely flows in old and inaccessible water distribution networks in which only source flow rates, demand flow rates and the topology of the networks with arc flow directions were assumed to be available. Other data such as pipe lengths, pipe diameters and roughness properties, which may have been lost or may have changed over time, were assumed not be available. This problem of incomplete information, causing uncertainty surrounding the multiplicity of the possible ways of routing flows in the network, has already been investigated by Tanyimboh and Templeman (1993a) using Shannon's informational entropy and the maximum entropy formalism. In this regard, they rigorously derived a nodal entropy function representing the network

flows by casting them probabilistically using the relative frequency interpretation of probabilities and then by applying the conditional entropy formula of Khinchin (Khinchin, 1953) for the entropy of compound probability schemes. By maximizing the resulting nodal entropy function of the network flows subject to the equilibrium equations at the network nodes, Tanyimboh and Templeman (1993a) produced a model for calculating maximum entropy flows in water distribution networks, which flows can be regarded as the most-likely flows in this case of incomplete information.

The above model for calculating maximum entropy flows in water networks produced by Tanyimboh and Templeman (1993a) is non-linear, and hence requires non-linear programming. However, the present research has developed a simple and quick method for calculating maximum entropy flows in multi-source, multi-demand general networks based on path flows supplying each demand node from all the sources serving that demand node. Neither mathematical programming techniques nor iterative processes are needed in the proposed path-based method. The motivation behind developing such a simple method was the applicability of network flow entropy as a surrogate measure of reliability which is desirable in urban water distribution networks, a conjecture which has been established by Awumah et al. (1990, 1991, 1992) and rigorously confirmed later by Tanyimboh and Templeman (1993c) who showed that designing a water network to carry maximum entropy flows improves the network reliability very significantly. Therefore, simplifying the maximum entropy flow problem would be very useful if it is to be incorporated into a linearized least-cost optimum design formulation for water distribution networks such as the linear programming method of Alperovits and Shamir (1977) without introducing any extra complexity into the formulation.

The second problem raised in the present research concerning water distribution networks was the possibility of using Shannon's entropy measure of uncertainty for calibrating computer models of existing water distribution networks, in which pipe characteristics, and hence pipe flows, are not known, without the need for physical measurement of the network pipe flows. The idea behind developing such a calibration model arose in the present research on the realization that the maximum entropy flow

problem mentioned earlier does not consider other obvious information which might be available in old water distribution networks. Data such as pipe lengths, pipe diameters and pressure heads at some nodes of the network can sometimes easily be measured and are often available. Also, the conservation laws of energy around the network loops must be satisfied in the estimated pipe flows. Additionally, similar information regarding other patterns of external flows which might be experienced in the network being considered should be taken into account. Only pipe characteristics, and hence pipe flows, may be assumed not to be available. The question was how the above extra information, along with the already considered information, can be incorporated in one single model. The present research has developed such a single model capable of estimating most-likely pipe flows and corresponding pipe characteristics in water distribution networks, opening up the possibility of calibrating old and inaccessible real water distribution networks.

Turning to structural trusses, the work presented in this thesis has examined the possibility of extending some of the entropy-based inference methods developed for water supply networks to the optimum design of structural trusses. This has been encouraged by the research carried out by Templeman (1992b) who showed that structural trusses and water supply networks share similar characteristics in almost every aspect such as physical quantities, constitutive equations, methods of analysis and design and even some reliability approaches. He demonstrated that almost every method of analysis and design used in water supply networks has a counterpart in structural trusses, suggesting that other methods used in one of the two systems which have not yet been explored in the other system have the potential to be used in that other system. In the present research, an attempt has been made to design a reliable structural truss to carry maximum entropy bar axial forces as a parallel to that used in water distribution networks (Tanyimboh and Templeman, 1993c).

A summary of the work carried out in the present research is presented next along with its main conclusions. This is followed by some suggestions and recommendations for future work which have been raised in the present work and have not been explored.

9.2 SUMMARY OF THE PRESENT WORK AND ITS MAIN CONCLUSIONS

The simple method presented in Chapter 4 and illustrated in Chapter 5 for calculating maximum entropy flows for multi-source, multi-demand general networks has been developed using the idea of path flows. By visualizing the network flows as a set of path flows supplying demand nodes by all possible routes, it has been argued that according to Laplace's principle of insufficient reason, which is a direct consequence of the maximum entropy formalism, the demand of any node in the network served by more than one path from any source should be distributed equally amongst all the paths supplying that node from that source. Treating all demand nodes in a network in this way is sufficient to generate the final pipe flows in water networks having only one source supplying all demand nodes in the networks (Tanyimboh and Templeman, 1993b). In general networks, however, the amount of flow supplying a demand node from each source serving it is unknown. It has been shown in the present research that the maximum entropy flows in multi-source, multi-demand general networks are such that the ratio of the probabilities of path flows from each pair of sources to a demand node reachable from the corresponding pair of sources is the same for every demand node supplied by this pair of sources in the network. This conjecture can be also interpreted as a consequence of the maximum entropy formalism since the equal ratios of path flow probabilities treat all the corresponding demand nodes equally on a bias scale. The values of these probability ratios, however, depend on the external inflows and outflows in the network and are influenced by the network layout. They are, therefore, a simple means of making the flows supplied by each source to a demand node as uniform as possible subject to available information.

The proposed method has been derived using the above conjecture. Accordingly, there are (NS-1) unknown ratios of path flow probabilities in a water network, where NS is the number of sources in the network. Calculating these (NS-1) unknown ratios yields a very simple means of calculating the final maximum entropy flows in water distribution networks. It has been shown that calculating such ratios only requires solving (NS-1) linear equations (the normality conditions) at (NS-1) source nodes in the network with (NS-1) unknown ratios. The remaining calculations through to the

final maximum entropy flows have been shown to be straightforward.

The above path-based method is very simple and efficient. Neither mathematical programming techniques nor iterative processes are needed in the method. Its simplicity and efficiency have been demonstrated by formalising it into simple algorithms tackling all the aspects encountered in the method such as identifying the reachability of the network nodes from each source in the network and determining the number of paths from each source to each node reachable from that source. Also, coding these simple algorithms by means of a computer programme written in FORTRAN 90 has been shown to be straightforward.

To facilitate the proposed method, a path entropy function representing the uncertainty associated with the path flows in a water distribution network has been developed. In this regard, (NS+1) finite probability schemes have been identified in a network. The first scheme is related to the source flow probabilities, and the remaining NS finite schemes represent the NS sets of path flow probabilities; each corresponds to a source and is conditional upon the flow probability of the corresponding source. The sought path entropy function has then been derived using the conditional entropy formula of Khinchin (Khinchin, 1953) for compound probability schemes. The derived path entropy function has the advantage of calculating the maximum entropy value of a water network directly from the path flow probabilities which have already been obtained by the proposed method without the need to maximize it.

Finally, the general applicability of the proposed algorithms and their coded computer programme has been demonstrated in Chapter 5 by means of three network examples exhibiting different aspects of complexity which can be expected in general real water distribution networks. It has been shown that the proposed algorithms are easy to operate by hand calculations especially for small networks similar to those used in the examples. Also, the running time of the computer programme for solving these examples was trivial.

It should be noted that although the proposed algorithms have been developed for multi-source networks, they can be used for single-source networks for which no unknown ratios of path flow probabilities exist. This special case matches exactly the simple algorithm proposed by Tanyimboh and Templeman (1993b) for calculating maximum entropy flows in single-source networks. However, their super-source approach, developed as an extension of the single-source method to multiple sources, has been shown in this thesis to be invalid and not to lead to optimal results. This suggests that the algorithms developed in this thesis should be used instead of the super-source approach for calculating maximum entropy flows for multi-source, multi-demand general networks.

The possibility of calibrating computer models of old and inaccessible water distribution networks, addressed in the present research by using the maximum entropy formalism, has been investigated in Chapters 6 and 7 of this thesis. In order to calibrate water networks models, their pipe characteristics along with pipe flows have to be estimated as close as possible to the actual values. According to the maximum entropy formalism, all the sought missing information has to be cast probabilistically so that an entropy function representing it can be derived. Tanyimboh and Templeman (1993a) showed how this can be done for network flows by developing a nodal flow entropy formula containing (NN+1) entropy functions, where NN is the number of nodes in the network. The first entropy function is the entropy of a finite probability scheme representing the distribution of the total supply amongst the sources, and the remaining NN entropy functions are the entropies of NN conditional finite probability schemes, each representing the outflows from a node in the network and depending upon the probability of flow arriving at that node.

In the present research, pipe characteristics in water distribution networks have been considered. By normalising the characteristic value of each pipe in the network by the sum of the characteristics values of all the network pipes, a finite probability scheme representing the probabilities of the network pipes having some characteristic values has been identified and an entropy function representing this finite probability scheme has been derived. In a compound problem, the joint entropy of a compound scheme

has been used to develop an entropy formula representing pipe flows and pipe characteristics in water distribution networks. Accordingly, the pipe characteristic entropy formula derived in the present research has been added to the (NN+1) flow entropy functions of Tanyimboh and Templeman (1993a) assuming that the pipe characteristic finite probability scheme is independent from all the finite probability schemes used in the (NN+1) flow entropy functions.

It has been shown in Chapter 6 that maximizing the compound entropy function enables most-likely pipe characteristics and corresponding pipe flows to be estimated in water distribution networks using information which might be available such as multiple external flow patterns, pipe lengths and diameters, nodal pressure heads and nodal equilibrium equations along with conservation laws of energy around the network loops.

The above calibration model has been coded in FORTRAN 77 in conjunction with the NAG library routine E04UCF for nonlinear constrained optimization. The resulting computer programme has been used in Chapter 7 to calibrate two network examples for which the available information has been considered step-by-step in order to investigate the influence of each new piece of information on the model results. The first example is a one-source network with one load case designed by Tanyimboh and Templeman (1993c) to carry maximum entropy flows. The second example is a simulated one-source network with five load cases. It has been shown from the first example that the calibration model generates the exact pipe characteristics and corresponding pipe flows in water distribution networks designed to carry maximum entropy flows for the case where roughness coefficients of some or all pipes have been lost. For real water networks such as the simulated network used in the second example, it has been demonstrated that the calibration model results improve remarkably for a single load case towards the actual values by adding step-by-step the available information about that load case. A slight improvement on the results can be obtained by adding information about extra load cases which share the same pipe flow directions with the original load case. However, changing flow directions in some pipes for any load case considered in the calibration model may cause the results to

move away from the actual values, suggesting that information about one load case is enough for the current calibration model to calibrate real water distribution networks.

It can be seen that the calibration model developed in this thesis estimates most-likely characteristics and corresponding pipe flows in water networks. The objective of this calibration model, however, is to calibrate real water networks. Although the model generates the exact results for networks designed to carry maximum entropy flows, its results for the second example are not accurate enough to be practically useful for calibrating real water networks. This may be due to the assumption of independence used in developing the model between the pipe characteristic finite probability scheme and those representing the network pipe flows. However, the present calibration model is the first of its kind in the sense that it does nor require any physical measurement of the network pipe flows which might be expensive and time consuming. A suggestion which might improve this model in getting better accuracy is discussed in the next section.

The last part of the present research is an attempt to extend network flow entropy concept to structural trusses following the striking similarities between the two systems. By handling axial forces of structural truss bars as bar axial force flows and external applied loads as demand and supplies, as described in Chapter 3, the path-based method derived in this thesis for calculating maximum entropy flows in water networks has been used in Chapter 8 to calculate maximum entropy bar axial forces for a sample indeterminate and two-dimensional structural truss which has been designed to carry these maximum entropy bar axial forces in an attempt to obtain a reliable truss paralleling reliable water networks designed to carry maximum entropy flows (Tanyimboh and Templeman, 1993c).

Force flow diagrams for horizontal and vertical components were needed for calculating maximum entropy bar axial forces in the two-dimensional sample truss, instead of a single pipe flow diagram, due to the vectorial nature of the axial bar forces in the truss bars. Because the truss is indeterminate with two redundant bars,

the bar axial forces induced by the applied loads in the resulting maximum entropy design were different from the desirable maximum entropy bar axial forces. Therefore, the two redundant bars have been precompressed in such a way that the final bar axial forces in the truss induced by both the applied loads and the precompressing forces in the redundant bars match the maximum entropy results.

For comparison reasons, the same truss has been conventionally designed and, along with the maximum entropy design, has been tested against damage tolerance and resilience reliability approaches. It has been shown that neither design is damage tolerant against removing any bar in the corresponding design nor resilient to sustain extra load which has not been designed for. Also, a probabilistic reliability analysis of both designs for calculating their probabilities of failure and survival has shown that the entropy-based approach to designing structural trusses does not lead to the sought reliable truss. This may be due to the vectorial nature of bar axial forces in structural trusses compared with the scalar pipe flows in water networks. Also, the difference between the well-established structural reliability concepts and their counterparts in water networks may play an important part in the failure to obtain reliable maximum entropy truss designs. This can be appreciated by realizing that the extra strengths achieved in the maximum entropy design have been largely cancelled by the extra bar axial forces induced by precompressing the two redundant bars. More fundamental research is needed in this area.

To sum up, the main conclusions which can be drawn from the present research are:

1. The path-based method developed in this thesis for calculating maximum entropy flows in water distribution networks provides further confirmation of the general correctness of the network flow entropy approach. By appreciating the applicability of network flow entropy as a surrogate measure of reliability, there would be a very simple means of designing least-cost and reliable water networks by incorporating the simple path-based method into one of the simplified optimum design methods such as the linearized method of Alperovits and Shamir (1977).
2. The calibration model presented in this thesis can be considered as a possible way of calibrating existing water distribution networks in the sense that it does not require a physical measurement of the network pipe flows which might be expensive and time consuming. It produces very accurate results for networks designed to carry maximum entropy flows. For conventionally designed networks, however, the results are not accurate enough to be practically useful. Further work based on the present model is necessary to determine in what form available information must be added to get better accuracy.
3. Using flow entropy as a surrogate measure of reliability in water distribution networks seems to have no direct parallel in the reliability of structural trusses due to two main factors. The first factor is related to the unsuspected difficulties brought to light in the present research regarding extending the scalar methodologies developed in water distribution networks to the vectorial domain of structural trusses. The second factor is the difference between reliability concepts in structural trusses and water networks. Any future research regarding this area should appreciate the above two factors.
4. In general, the present research confirms the broad applicability of the maximum entropy formalism based on Shannon's entropy measure of uncertainty in generating solutions to a wide range of civil engineering problems which are not directly or obviously related to probabilities.

9.3 RECOMMENDATIONS FOR FUTURE WORK

The research carried out in this thesis has raised several points which have not been explored herein. Some proposals regarding these aspects are suggested next for future research.

1. A linear programming method for designing optimum and reliable water distribution networks:

The least-cost optimum design problem of water distribution networks is one of nonlinear optimization and hence requires nonlinear programming. It is very difficult to solve for networks of realistic sizes especially if the network pipes have to be chosen from a discrete set of commercially available sizes. Also, the desirability of water distribution networks being reliable under operation requires incorporating some measure of reliability in the least-cost optimum design formulation, making the problem more difficult to solve.

Many attempts have been made in the literature to simplify the least-cost optimum design formulation. The Linear Programming Gradient approach of Alperovits and Shamir (1977) is the most widely-used simplified approach in which two phases, the linear programming phase and the gradient phase, are solved in an iterative scheme. In the linear programming phase, a set of pipe flows is specified and the least-cost optimum design formulation is linearized by replacing each pipe in the network by several segments of known diameters and unknown lengths, bearing in mind that for known pipe flows the formulation is nonlinear with respect to pipe diameters but linear with respect to pipe lengths. The resulting linear programming formulation is then used to obtain least-cost optimum design for the specified set of flows. In the gradient phase, however, the pipe flows used in the first phase are modified to further reduce the total cost of pipes. The resulting new set of pipe flows is then used in the linear programming phase to obtain a new design. The process continues iteratively between the two phases until convergence of network cost is achieved.

Taking into account reliability considerations, there is some evidence in the literature that network flow entropy is a good measure of reliability. It has been shown that the path-based method developed in this thesis for calculating maximum entropy flows for general water networks requires only solving (NS-1) linear equations with (NS-1) unknowns. Consequently, if the maximum entropy flows calculated by this simple path-method are used in the linear programming phase of the method of Alperovits and Shamir (1977), the gradient phase will not be needed and the problem of designing optimum and reliable water distribution networks becomes non-iterative and requires only linear programming.

2. Calibrating existing water distribution networks:

Although the calibration model developed in the present research produces very accurate results for networks designed to carry maximum entropy flows, its results are not accurate enough to be practically useful for conventionally designed real networks. An improvement of the present model is therefore needed.

In developing the present calibration model, an entropy function representing the pipe characteristic finite probability scheme is added to (NN+1) flow entropy functions derived by Tanyimboh and Templeman (1993a) in order to develop a compound entropy formula representing pipe characteristics and pipe flows in water distribution networks assuming that the pipe characteristic finite probability scheme is independent from all the finite probability schemes used in the (NN+1) flow entropy functions. In the (NN+1) flow entropy functions, there are NN flow entropy functions representing the entropies of NN conditional finite probability schemes, each representing the outflows from a node in the network and depending upon the probability of flow arriving at that node. However, by adding pipe characteristic variables into the problem, the above NN conditional finite probability schemes will also depend upon the characteristic value of the corresponding pipe. This has not been considered in deriving the present calibration model. Considering this new extra dependence, new NN flow entropy functions can be derived using the conditional entropy formula of Khinchin (Khinchin, 1953) of compound probability schemes. The new NN flow

entropy functions will then replace the old NN functions to produce a new compound network entropy formula which can be used as before to produce a new calibration model. This new model needs to be tested for calibrating real water distribution networks.

3. Entropy-based structural truss applications:

The attempt made in the present research for designing reliable maximum entropy structural trusses paralleling designing reliable maximum entropy water networks (Tanyimboh and Templeman, 1993c) has raised many questions and problems regarding two main issues, these being the vectorial nature of bar axial forces as opposed to scalar pipe flows and the difference between reliability concepts in structural trusses and water networks.

Regarding the vectorial issue, which has led to two components of force flow diagrams for the sample truss used in the present research, the inability to solve the horizontal component because the flows contradicted the behaviour of pipe flows in water networks has led to doubt about whether the maximum entropy force results of the two components would be identical and, if they are not the same, which one would be correct. Choosing carefully a truss in which both components of force flow diagrams are solvable by the path-based maximum entropy method, for example, would help in clarifying some points regarding these matters.

On the other hand, the reliability concepts in structural trusses differ fundamentally from their counterparts in water networks. The well-established probabilistic reliability analysis for calculating failure probability in structural trusses has no counterpart in water distribution networks. The greater strengths generated in the maximum entropy design of the truss example by using larger bar sizes have been cancelled out by the larger bar axial forces induced by precompressing the two redundant bars in the maximum entropy design. This issue, which does not directly involve network reliability, may be the main reason behind flow entropy failing to improve reliability in structural trusses. Any future work regarding entropy-based structural reliability

must consider this point very closely.

In conclusion, fundamental research directed towards overcoming the difficulties regarding the above two main issues is needed in developing an entropy-based optimum and reliable structural truss design method. The three-dimensional case of trusses should be also considered in such research.

REFERENCES

Al-Harthy, A. S. and Frangopol, D. M. (1994) Reliability assessment of prestressed concrete beams. *ASCE J. Str. Eng.*, **120,** (1), 180-199.

Alperovits, E. and Shamir, U. (1977) Design of optimal water distribution systems. *Water Resources Research*, **13**, (6), 885-900.

Ang, A. H. S. and Amin, M. (1968) Reliability of structures and structural system. *ASCE J. Eng. Mech. Div.*, **94**, (EM2), 671-691.

Ang, A. H. S. and Cornell, C. A. (1974) Reliability bases of structural safety and design. *ASCE J. Str. Div.*, **100,** (ST9), 1755-1769.

Ang, A. H. S. and Tang, W. H. (1975) **Probability Concepts in Engineering Planning and Design, Vol. I: Basic Principles**, John Wiley & Sons, New York.

Ang, A. H. S. and Tang, W. H. (1984) **Probability Concepts in Engineering Planning and Design, Vol. II: Decision, Risk and Reliability**, John Wiley, New York.

Arora, J. S., Haskell, D. F. and Govil, A. K. (1980) Optimal design of large structures for damage tolerance. *AIAA J.*, **118,** 563-570.

Awumah, K. and Goulter, I. (1992) Maximizing entropy-defined reliability of water distribution network. *Eng. Opt.*, **20**, (1), 57-80.

Awumah, K., Goulter, I. and Bhatt, S. K. (1990) Assessment of reliability in water distribution networks using entropy-based measures. *Stochastic Hydrology and Hydraulics*, **4**, (4), 325-336.

Awumah, K., Goulter, I. and Bhatt, S. K. (1991) Entropy-based redundancy measures in water distribution network design. *ASCE J. Hyd. Eng.*, **117**, (5), 595-614.

Bao, Y. and Mays, L. W. (1990) Model for water distribution system reliability. *ASCE J. Hyd. Eng.*, **116**, (9), 1119-1137.

Basu, P. C. (1981) **Optimum Design of Structures Using Deflection Based Method in Deterministic and Reliability Formats,** Ph.D. Thesis, Department of Civil Engineering, University of Liverpool, U.K.

Basu, P. C. and Templeman, A. B. (1984) An efficient algorithm to generate maximum entropy distributions. *International J. Numerical Methods in Engineering*, **20**, 1039-1055.

Basu, P. C. and Templeman, A. B. (1985) Structural reliability and its sensitivity. *Civ. Eng. Syst.*, **2**, (1), 3-11.

Bell, M. G. H. (1983) The estimation of an origin-destination matrix from traffic counts. *Transportation Science*, **17**, (2), 198-217.

Bjerager, P. (1990) On computation methods for structural reliability analysis. *Structural Safety*, **9**, 79-96.

Borri, A. and Speranzini, E. (1997) A numerical procedure for optimal design subjected to prefixed reliability requirements. **Reliability and Optimization of Structural Systems,** Frangopol, D. M., Corotis, R. B. and Rackwitz, R. (Eds.), Pergamon, 101-108.

Breitung, K. (1984) Asymptotic approximations for multinormal integrals. *ASCE J. Eng. Mech.*, **100,** (3), 357-366.

Bruneau, M. (1992) Evaluation of system-reliability methods for cable-stayed bridge design. *ASCE J. Str. Eng.*, **118,** (4), 1106-1120.

Chang, C. C., Ger, J. F. and Cheng, F. Y. (1994) Reliability-based optimum design for UBC and nondeterministic seismic spectra. *ASCE J. Str. Eng.*, **120,** (1), 139-160.

Cheng, G. D. and Ma, H. T. (1989) Optimal design of water distribution systems. *Civ. Eng. Syst.*, **6,** (3), 111-121.

Chiu, C.-L. (1987) Entropy and probability concepts in hydraulics. *ASCE J. Hyd. Eng.*, **113**, (5), 583-600.

Chiu, C.-L. (1988) Entropy 2-D velocity distribution in open channels. *ASCE J. Hyd. Eng.*, **114**, (7), 738-756.

Chiu, C.-L. (1989) Velocity distribution in open channel flow. *ASCE J. Hyd. Eng.*, **115**, (5), 576-594.

Chiu, C.-L. (1991) Application of entropy concept in open channel flow study. *ASCE J. Hyd. Eng.*, **117**, (5), 615-628.

Coates, R. C., Coutie, M. G. and Kong, F. K. (1994) **Structural Analysis**, 3rd edition, Chapman & Hall, London.

Cornell, C. A. (1967) Bounds on the reliability of structural systems. *ASCE J. Str. Div.*, **93,** (ST1), 171-200.

Cornell, C. A. (1969) A probability based structural code. *J. Am. Concr. Inst*, **66**, 974-985.

Cui, W. and Blockley, D. I. (1991) On the bounds for structural system reliability. *Structural Safety,* **9,** 247-259.

Cullinane, M. J., Lansey, K. E. and Mays, L. W. (1992) Optimization-availability-based design of water distribution networks. *ASCE J. Hyd. Eng.*, **118**, (3), 420-441.

Ditlevsen, O. (1979) Narrow reliability bounds for structural systems. *J. Str. Mech.*, **7,** (4), 453-472.

Ditlevsen, O. and Madsen, H. O. (1989) Proposal for a code for the direct use of reliability methods in structural design, (working document). Zurich, *JCSS-IABSE.*

Ellingwood, B. R. (1994) Probability-based codified design: past accomplishments and future challenges. *Structural Safety,* **13,** 159-176.

Ellingwood, B. R. and Ang, A. H. S. (1974) Risk-based evaluation of design criteria. *ASCE J. Str. Div.,* **100,** (ST9), 1771-1788.

Erlander, S. (1977) Accessibility, entropy and the distribution and assignment of traffic. *Transportation Research*, **11**, 149-153.

Frangopol, D. M., Klisinski, M. and Iizuka, M. (1991) Optimization of damage-tolerant structural systems. *Computers & Structures,* **40,** (5), 1085-1095.

Freudenthal, A. M. (1956) Safety and probability of structural failure. Paper No. 2843, *Trans. of ASCE,* **121,** 1337-1397.

Freudenthal, A. M., Garrelts, J. M., and Shinozuka, M. (1966) The analysis of structural safety. *ASCE J. Str. Div.*, **92**, (ST1), 267-325.

Fujiwara, O. and De Silva, A. U. (1990) Algorithm for reliability-based optimal design of water networks. *ASCE J. Env. Eng.*, **116**, (3), 575-587.

Galambos, T. V. (1990) Systems reliability and structural design. *Structural Safety,* **7,** 101-108.

Garfinkel, R. and Nemhauser, G. (1972) **Integer Programming**, Wiley, New York.

Goulter, I. C. and Coals, A. V. (1986) Quantitative approaches to reliability assessment in pipe networks. *ASCE J. Trans. Eng.*, **112**, (3), 287-301.

Grandhi, R. V. and Wang, L. (1997) Structural failure probability calculation using nonlinear approximations. **Reliability and Optimization of Structural Systems,** Frangopol, D. M., Corotis, R. B. and Rackwitz, R. (Eds.), Pergamon, 165-172

Guiasu, S. (1977) **Information Theory with Applications**, McGraw-Hill Inc.

Hasofer, A. M. and Lind, N. C. (1974) Exact and invariant second-moment code format. *ASCE J. Eng. Mech. Div.*, **100,** (EM1), 111-121.

Hilton, H. H. and Feigen, M. (1960) Minimum weight analysis based on structural reliability. *J. Aerospace Sciences.* **27,** (9), 641-652.

Hong, H. P. and Lind, N. C. (1996) Approximate reliability analysis using normal polynomial and simulation results. *Structural Safety,* **18,** (4), 329-339.

Ignizio, J. P. (1982) **Linear Programming in Single and Multiple Objective Systems,** Prentice-Hall.

Jaynes, E. T. (1957) Information theory and statistical mechanics. *Phys. Rev.*, **106,** 620-630 and **108**, 171-190.

Jaynes, E. T. (1979) Where do we stand on maximum entropy? **The Maximum Entropy Formalism,** Levine, R. D. and Tribus, M. (Eds.), M.I.T. Press, 15-118.

Jeppson, R. W. (1976) **Analysis of Flow in Pipe Networks,** Ann Arbor Science, Ann Arbor (Mich.).

Jones, D. S. (1979) **Elementary Information Theory,** Clarendon Press, Oxford.

Kalaba, R. (1962) Design of minimal-weight structures for given reliability and cost. *J. Aerospace Sciences,* **29,** (3), 355-356.

Kapur, J. N. (1989) **Maximum Entropy Models in Science and Engineering,** John Wiley and Sons.

Kapur, J. N. and Kesavan, H. K. (1987) **The Generalized Maximum Entropy Principle with Applications,** Sandford Educational Press, Waterloo (Ont.).

Karamchandani, A. (1990) Limitations of some of the approximate structural analysis methods that are used in structural system reliability. *Structural Safety,* **7,** 115-127.

Katsuki, S., Frangopol, D. M. and Ishikawa, N. (1993a) Holonomic elastoplastic reliability analysis of truss systems. I: Theory. *ASCE J. Str. Eng.,* **119,** (6), 1778-1791.

Katsuki, S., Frangopol, D. M. and Ishikawa, N. (1993b) Holonomic elastoplastic reliability analysis of truss systems. II: Applications. *ASCE J. Str. Eng.,* **119,** (6), 1792-1806.

Kaya, A. and Simon, A. L. (1974) An optimization method to design hydraulic networks. *Eng. Opt.,* **1,** 71-78.

Khinchin, A. I. (1953) The entropy concept in probability theory. *Uspekhi Matematicheskikh Nauk,* **8,** (3), 3-20. Translation in Khinchin, A. I. (1957) **Mathematical Foundations of Information Theory,** Dover, New York, 1-28.

Kjerengtroen, L. and Wirsching, P. H. (1984) Structural reliability analysis of series systems. *ASCE J. Str. Eng.,* **110,** (7), 1495-1511.

Koyluoglu, H. U. and Nielsen, S. R. K. (1994) New approximations for SORM integrals. *Structural Safety,* **13,** 235-246.

Kwak, B. M. and Lee, T. W. (1987) Sensitivity analysis for reliability-based optimization using an AFOSM method. *Computers & Structures,* **27,** (3), 399-406.

Lai, D. and Schaake, J. (1969) Linear programming and dynamic programming applications to water distribution network design. *Report 116,* Dept. of Civil Engineering, MIT, Cambridge, Mass.

Levine, R. D. and Tribus, M. (Eds.) (1979) **The Maximum Entropy Formalism,** M.I.T. Press.

Li, X. (1987) **Entropy and Optimization,** Ph.D. Thesis, Department of Civil Engineering, University of Liverpool, U.K.

Li, X. and Templeman, A. B. (1988) Entropy-based optimum sizing of trusses. *Civ. Eng. Syst.*, **5**, 121-128.

Liu, Y. W. and Moses, F. (1992) Truss optimization including reserve and residual reliability constraints. *Computers & structures,* **42,** (3), 355-363.

Martin, D. W. and Peters, G. (1963) The application of Newton's method to network analysis by digital computer. *J. Institution of Water Engineers*, **17**, 115-129.

McKeown, J. J. (1977) Optimal composite structures by deflection-variable programming. *Comp. Meth. App. Mech. Eng.*, **12,** 155-179.

McKeown, J. J. (1989) The design of optimal trusses via sequences of optimal fixed displacement structures. *Eng. Opt.*, **14,** (3), 159-178.

Mebarki, A., Lorrain, M. and Bertin, J. (1990) Structural reliability analysis by a new level-2 method: The hypercone method. *Structural Safety,* **9,** 31-40.

Mebarki, A., Lorrain, M. and Bertin, J. (1991) The hypercone method for structural reliability analysis: Its theoretical principles. *Reliability Engineering and System Safety,* **31,** 239-253.

Melchers, R. E. (1987) **Structural Reliability Analysis and Prediction**, Ellis Horwood, New York.

Mistree, F. (1983) Design of damage tolerant structural systems. *Eng. Opt.*, **6**, 141-144.

Moses, F. (1974) Reliability of structural systems. *ASCE J. Str. Div.*, **100**, (ST9), 1813-1820.

Moses, F. and Kinser, D. E. (1967) Optimum structural design with failure probability constraints. *AIAA J.*, **5**, (6), 1152-1158

Moses, F. and Stevenson, J. D. (1970) Reliability-based structural design. *ASCE J. Str. Div.*, **96**, (ST2), 221-244.

Mountain, L., Maher, M. and Maher, S. (1986a) The estimation of turning flows from traffic counts. 1. At four-arm intersections. *Traffic Engineering and Control*, **27**, (10), 501-507.

Mountain, L., Maher, M. and Maher, S. (1986b) The estimation of turning flows from traffic counts. 2. At five-arm intersections. *Traffic Engineering and Control*, **27**, (11), 566-569.

Mountain, L. and Steele, D. (1983a) Prior information and the accuracy of turning flow estimates. *Traffic Engineering and Control*, **24**, (12), 582-588.

Mountain, L. J. and Westwell, P. M. (1983b) The accuracy of estimation of turning flows from traffic counts. *Traffic Engineering and Control*, **24**, (1), 3-7.

Mrazik, A. and Krizma, M. (1997) Probability-based design standards of structures. *Structural Safety,* **19,** (2), 219-234.

Munro, J. and Jowitt, P. W. (1978) Decision analysis in the ready-mixed concrete industry. *Proceeding of The Institution of Civil Engineers, Part 2,* **65,** 41-52.

Murotsu, Y., Shao, S. and Watanabe, A. (1994) An approach to reliability-based optimization of redundant structures. *Structural Safety,* **16,** 133-143.

Provan, J. S. and Ball, M. O. (1983) The complexity of counting cuts and of computing the probability that a graph is connected. *SIAM J. Comput.*, **12,** (4), 777-788.

Quindry, G. E., Brill, E. D. and Liebman J. C. (1981) Optimization of looped water distribution systems. *ASCE J. Env. Eng. Div.*, **107,** (4), 665-679.

Rackwitz, R. and Fiessler, B. (1978) Structural reliability under combined random load sequences. *Computers & Structures,* **9,** 489-494.

Ravindra, M. K., Lind, N. C. and Siu, W. (1974) Illustrations of reliability-based design. *ASCE J. Str. Div.*, **100,** (ST9), 1789-1811.

Robinstein, R. Y. (1981) **Simulation and the Monte Carlo Method,** John Wiley & Sons, New York.

Rowell, W. F. and Barnes, J. (1982) Obtaining layout of water distribution systems. *ASCE J. Hyd. Div.*, **108,** (1), 137-148.

Shamir, U. and Howard, C. D. D. (1968) Water distribution systems analysis. *ASCE J. Hyd. Div.*, **94**, (1), 219-234.

Shannon, C. E. (1948) A mathematical theory of communication. *Bell System Technical J.*, **27**, (3), 379-428.

Shupe, J. A. and Mistree, F. (1987) Compromise: An effective approach for the design of damage tolerant structural systems. *Computers & Structures,* **27,** (3), 407-415.

Spillers, W. R. (1972) **Automated Structural Analysis**, Pergamon Press Inc., New York.

Stevenson, J. and Moses, F. (1970) Reliability analysis of frame structures. *ASCE J. Str. Div.*, **96,** (ST11), 2409-2427.

Su, Y., Mays, L. W., Duan, N. and Lansey, K. E. (1987) Reliability-based optimization model for water distribution systems. *ASCE J. Hyd. Eng.*, **114**, (12), 1539-1556.

Switsky, H. (1964) Minimum weight design with structural reliability. *AIAA 5th Annual Structures and Materials Conference,* 316-322.

Takada, T., Kohama, Y. and Miyamura, A. (1994) Reliability-based minimum weight design of space truss: A case under constraint of system reliability. **Structural Safety and Reliability, Vol. 1,** Schueller, G. I., Shinozuka, M. and Yao, J. T. P. (Eds.), Balkema, Rotterdam, 677-683.

Tang, K. and Melchers, R. E. (1988) Incremental formulation for structural reliability analysis. *Civ. Eng. Syst.*, **5,** 153-158.

Tanyimboh, T. T. (1993) **An Entropy-Based Approach to the Optimum Design of Reliable Water Distribution Networks,** Ph.D. Thesis, Department of Civil Engineering, University of Liverpool, U.K.

Tanyimboh, T. T. and Templeman, A. B. (1993a) Calculating maximum entropy flows in networks. *J. Operational Research Soc.*, **44**, (4), 383-396.

Tanyimboh, T. T. and Templeman, A. B. (1993b) Maximum entropy flows for single-source networks. *Eng. Opt.*, **22**, (1), 49-63.

Tanyimboh, T. T. and Templeman, A. B. (1993c) Optimum design of flexible water distribution networks. *Civ. Eng. Syst.*, **10**, (3), 243-258.

Templeman, A. B. (1982) Discussion of "Optimization of looped water distribution systems." *ASCE J. Env. Eng. Div.*, **108**, (3), 599-602.

Templeman, A. B. (1987) Computer aided optimum structural design under uncertainty. *Eng. Opt.*, **11,** 281-288.

Templeman, A. B. (1988a) Discrete optimum structural design. *Computers & Structures,* **30,** (3), 511-518.

Templeman, A. B. (1988b) Some reservations about reliability-based design. **New Directions in Structural System Reliability,** Frangopol, D. M. (Ed.), University of Colorado Press, Boulder, Colorado, 265-275.

Templeman, A. B. (1992a) Entropy and civil engineering optimization. **Optimization and Artificial Intelligence in Civil and Structural Engineering. Vol. 1: Optimization in Civil and Structural Engineering,** Topping, B. H. V. (Ed.), Kluwer Academic Publishers, *NATO ASI Series, Series E: Applied Sciences*, **Vol. 221,** 87-105.

Templeman, A. B. (1992b) The optimization of civil engineering networks. **Optimization and Artificial Intelligence in Civil and Structural Engineering. Vol. 1: Optimization in Civil and Structural Engineering,** Topping, B. H. V. (Ed.), Kluwer Academic Publishers, *NATO ASI Series, Series E: Applied Sciences*, **Vol. 221,** 1-18.

Templeman, A. B. (1993) Entropy-based optimization methods for engineering design. **Advanced Techniques in the Optimum Design of Structures. Vol. 12: Topics in Engineering,** Hernandez, S. (Ed.), Computational Mechanics Publications, Southampton U.K. and Boston U.S.A. 109-139.

Templeman, A. B. and Li, X. (1985) Entropy duals. *Eng. Opt.*, **9**, (2), 107-119.

Templeman, A. B. and Li, X. (1987) A maximum entropy approach to constrained non-linear programming. *Eng. Opt.*, **12**, (2), 191-205.

Templeman, A. B. and Li, X. (1989) Maximum entropy and constrained optimization. **Maximum Entropy and Bayesian Methods,** Skilling, J. (Ed.), Kluwer Academic Publishers, 447-454.

Templeman, A. B. and Yates, D. F. (1983) A segmental method for the discrete optimum design of structures. *Eng. Opt.*, **6**, (3), 145-155.

Templeman, A. B. and Yates, D. F. (1984) Mathematical similarities in engineering network analysis. *Civ. Eng. Syst.*, **1**, 114-122.

Trautner, J. J. and Frangopol, D. M. (1990) Computer modelling and reliability evaluation of steel through truss bridges. *Structural Safety,* **7,** 255-267.

Tung, Y.-K. (1985) Evaluation of water distribution network reliability. *Proc. ASCE Hyd. Div. Spec. Conf.,* Orlando, Fl., 359-364.

Tvedt, L. (1983) Two second-order approximations to the failure probability. *Veritas Report RDIV/ 20-004-83, Det Norske Veritas,* Oslo, Norway.

Val. D., Bljuger, F. and Yankelevsky, D. (1997) Reliability evaluation in nonlinear analysis of reinforced concrete structures. *Structural Safety,* **19,** (2), 203-217.

Valliant, L. G. (1979) The complexity of enumeration and reliability problems. *SIAM J. Comput.*, **8**, (3), 410-421.

Van Zuylen, H. J. and Willumsen, L. G. (1980) The most likely trip matrix estimated from traffic counts. *Transportation Research*, **14B**, (3), 281-293.

Wagner, J. M., Shamir, U. and Marks, D. H. (1988a) Water distribution reliability: analytical methods. *ASCE J. Water Resources Planning and Management*, **114**, (3), 253-275.

Wagner, J. M., Shamir, U. and Marks, D. H. (1988b) Water distribution reliability: simulation methods. *ASCE J. Water Resources Planning and Management*, **114**, (3), 276-294.

Walters, G. A. (1988) Optimal design of pipe networks: a review. **Proceedings of the 1st International Conference in Africa on Computer Methods and Water Resources**, 21-31.

Walters, G. A. (1995) Discussion on: Maximum entropy flows in single-source networks. *Eng. Opt.*, **25**, (2), 155-163.

Wang, L. and Grandhi, R. V. (1994) Efficient safety index calculation for structural reliability analysis. *Computers & Structures,* **52**, (1), 103-111.

Wang, L. and Grandhi, R. V. (1996) Safety index calculation using intervening variables for structural reliability analysis. *Computers & Structures,* **59**, (6), 1139-1148.

Wood, D. J. and Charles, C. O. A. (1972) Hydraulic network analysis using linear theory. *ASCE J. Hyd. Div.*, **98**, (HY7), 1157-1170.

Wu, X., Blockley, D. I. and Woodman, N. J. (1993a) Vulnerability of structural systems, Part 1: Rings and clusters. *Civ. Eng. Syst.*, **10**, 301-317.

Wu, X., Blockley, D. I. and Woodman, N. J. (1993b) Vulnerability of structural systems, Part 2: Failure scenarios. *Civ. Eng. Syst.*, **10**, 319-333.

Xiao, Q. and Mahadevan, S. (1994) Fast failure mode identification for ductile structural system reliability. *Structural Safety,* **13**, (4), 207-226.

Yates, D. F., Templeman, A. B. and Boffey, T. B. (1982) The complexity of procedures for determining minimum weight trusses with discrete member sizes. *Int. J. Solids and Structures*, **18**, (6), 487-495.

Yates, D. F., Templeman, A. B. and Boffey, T. B. (1984) The computational complexity of determining least capital cost designs for water supply networks. *Eng. Opt.*, **7**, (2), 143-155.

Zimmerman, J. J., Ellis, H. and Corotis, R. B. (1993) Stochastic optimization models for structural- reliability analysis. *ASCE J. Str. Eng.*, **119,** (1), 223-239.

APPENDIX A

WALTERS' APPROACH FOR CALCULATING MAXIMUM ENTROPY FLOWS IN GENERAL WATER SUPPLY NETWORKS

Eng. Opt., 1995, Vol. 25, pp. 155–163
Reprints available directly from the publisher
Photocopying permitted by license only

DISCUSSION ON: MAXIMUM ENTROPY FLOWS IN SINGLE SOURCE NETWORKS[3]

G. A. WALTERS

School of Engineering, University of Exeter, North Park Road, Exeter EX4 4QF, U.K.

(Received 27 July 1994)

NOTATION

I	set of all source nodes
K	arbitrary positive constant
N	number of nodes
ND_n	set of all links or nodes immediately downstream of node n
p_{oi}	q_{oi}/T_o
p_{nj}	q_{nj}/T_n
P_n	probability of event n
q_{io}	external outflow at node i
q_{nj}	flow from node n to node j
q_{oi}	external inflow at node i
S	Shannon's entropy
S_n	entropy of outflows at node n
S_o	entropy of external inflows
T_n	total outflow from node n
T_o	total supply or demand
r_{ij}	q_{ij}/T_o
R_n	T_n/T_o
L	set of all positive flow links, including outflow links
M	L + inflow links

The authors are to be congratulated on the presentation of their very interesting and stimulating work on flow entropy, and on their earlier papers[1,2] which combine with this to form the definitive work on the subject.

The theoretical derivation for Eqs. (1) to (6) which define flow entropy for a general network has been rigorously established[1]. However, it is interesting to take the analysis a few steps further, as detailed in the Appendix to this discussion, to give a value of Shannon's entropy for a distribution network as:

$$\frac{S}{K} = -\sum_{ij\epsilon m} r_{ij}\ln(r_{ij}) + \sum_{n=1}^{N} R_n \ln(R_n) \qquad \text{(A1)}$$

The above equation is perhaps easier to apply than the authors' equations, and does allow two interesting properties to be clearly seen. First Eq. (A1) does not distinguish between inflows and outflows, and so by inspection, a network in which all flows are reversed will have the same numerical value of flow entropy.

Second, if there is a single inflow (or outflow) to a node, the term $r \ln(r)$ for the pipe flow entering (or leaving) the node cancels with the term $R \ln(R)$ for the node, since $r = R$. For any non-looped section of a network each node has a single inflow, and it therefore follows that all link flow and nodal flow terms in (A1) cancel out, leaving only the external outflows contributing to the entropy. This is equally true for a network which is entirely tree structured, the flow entropy being determined only by the pattern of external flows at the demand nodes. Although no proof is offered here, it can be shown that a tree forms a minimum flow entropy network for supplying a given set of nodal demands, and from the above discussion any tree that connects the demand nodes will have the same minimum entropy value.

Furthermore, it can be argued that a tree network is a special case of a looped network, in which the flows along some of the pipes are zero. Therefore when considering the flow entropy of a looped network as a function of flow distribution, there will be multiple global minima for the entropy, each corresponding to a tree-like flow distribution. The present of multiple minima suggests the probability of multiple local maxima of the entropy function, and hence possible problems with the use of conventional optimization algorithms in the identification of the global maximum entropy. In this context it is interesting that both the two-source examples in the paper appear not to be global maximum entropy solutions, as shown below.

Whereas the authors' algorithm for determining maximum entropy flows for single source networks is rigorous and can be applied very readily, its application to multiple source networks by the super-source method proposed in the paper leads to inconsistencies. However, multiple sources can be correctly converted to equivalent single sources by the addition of a 'super-source network' with multiple flow paths from the super-source to each supply node. For example, Figure A1 is based on the authors' Figure 6 with the addition of the super-source network shown in dashed lines. Application of the authors' flow distribution algorithm to this network gives the flows indicated on the figure, and it can be seen that the inflows at nodes 1 and 2 are very close to the required values of 35 and 20 for the original two source problem. The resulting flow entropy, calculated over the original network and therefore directly comparable to the authors' results, has a numerical value of 2.154 compared to the authors' value of 1.947 for a significantly different pattern of flows, indicating that the authors' result was in fact a local rather than a global maximum.

Unfortunately, it is not easy to determine the super-source network configuration that will give the correct set of inflows to the original network at the maximum entropy state. The super-source network used above was initially determined by trial and error until the ratio of paths between super-source and the two supply nodes gave approximately the correct inflows. A more analytical approach was tried for the example of Figure 5a, reproduced here as Figure A2, with x paths being assumed from super-source to node 1 and 1 path from super-source to node 2. Applications of the authors' algorithm then leads to path numbers and flows being

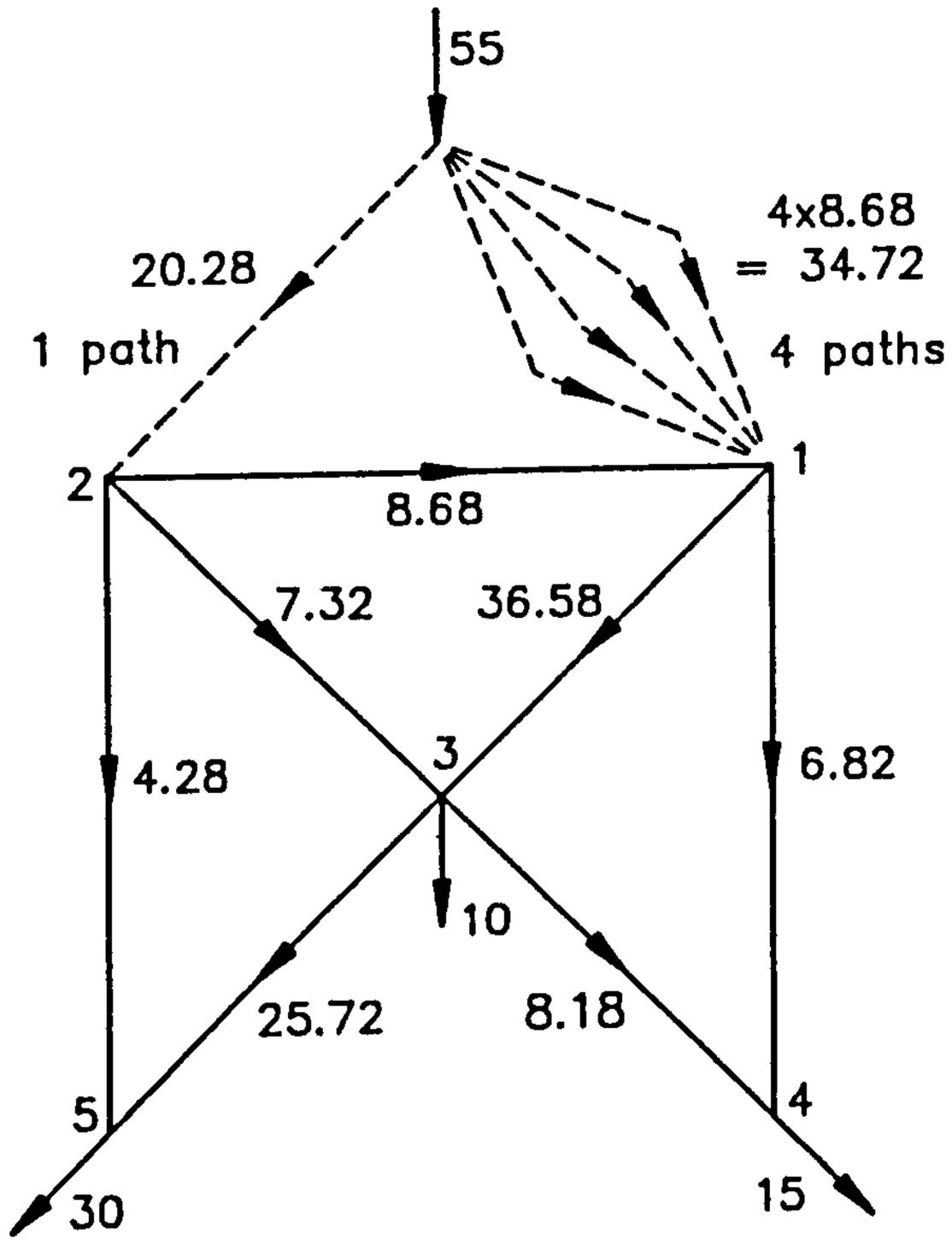

Figure A1 Maximum entropy flows.

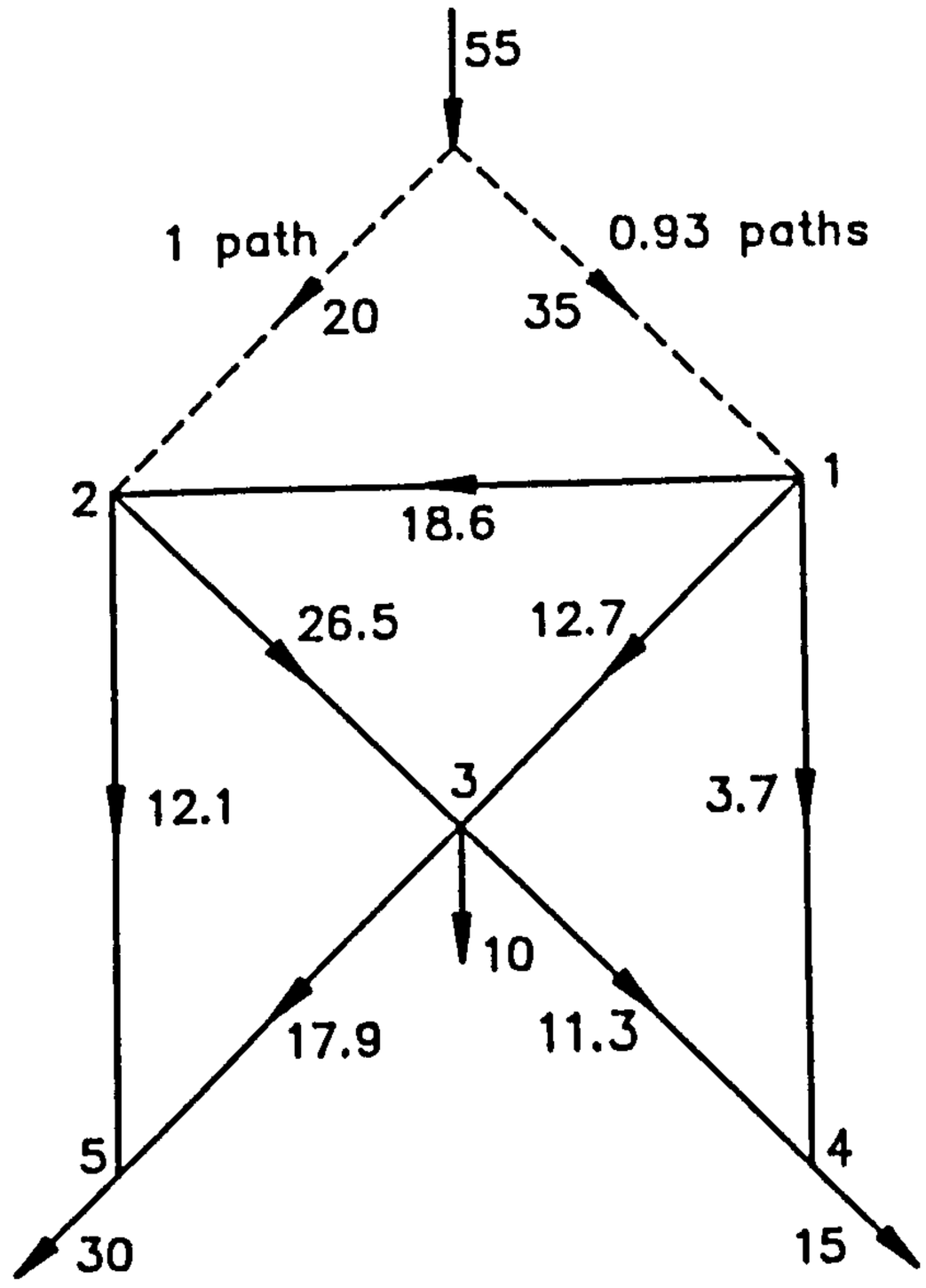

Figure A2 Maximum entropy flows.

determined in terms of the unknown variable x by straightforward, but tedious, algebra. Equating an expression for one of the inflows to a known value determines x, which in this example is approximately 0.93, giving the flows indicated on the figure. The entropy for this flow arrangement is 2.45, which is again higher than the authors' result.

In the above procedure it is assumed that the maximum entropy flow solution for the total network (with super-source sub-network included) gives the maximum entropy flow set for the original system. Without giving a formal proof, this can be deduced either from the definition of flow entropy derived by the authors or from the form of Eq. (A1).

The use of flow entropy as a surrogate measure for distribution system reliability is certainly an interesting topic, and the methodology of the paper for deriving maximum entropy flow distributions could well prove very useful in the context of designing reliable systems. However, it should be remembered that maximum entropy flow distribution is based only on the numbers of paths. A cluster of numerous short paths in one region of the network can produce illogical flow distributions, as can be seen when a small 3×3 grid is added to the network of Figure A3a, thereby changing the maximum entropy flow distribution radically to that shown in Figure A3b. The reliability of supply to the demand node is likely to

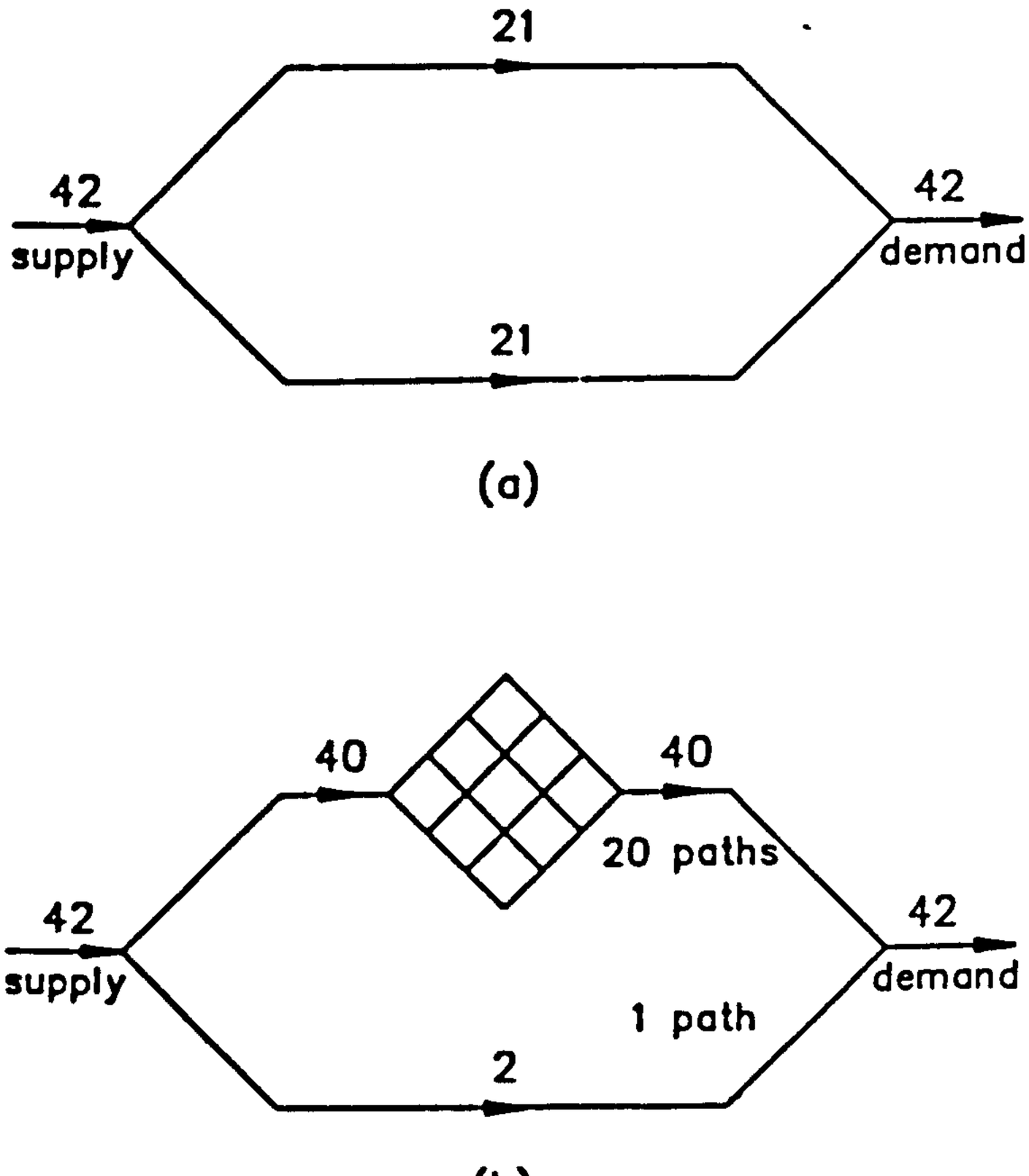

Figure A3 Maximum entropy flows.

be significantly smaller with the latter flow pattern, thereby illustrating the difficulty of trying to relate flow entropy directly to reliability.

References

1. Tanyimboh, T. T. and Templeman, A. B. (1993) Calculating maximum entropy flows in networks. *J. Operational Research Soc.*, **44**, (4), 383–396.
2. Tanyimboh, T. T. and Templeman, A. B. (1993) Optimum design of flexible water distribution networks. *Civil Engineering Systems*, **10**, (3), 243–258.
3. Tanyimboh, T. T. and Templeman, A. B. (1993) Maximum entropy flows in single source networks. *Engineering Optimization*, **22**, (1), 49–63.

APPENDIX

Defining $r_{nj} = \dfrac{q_{nj}}{T_o}$ and $R_n = \dfrac{T_n}{T_o}$

Eq. (4), $S_n = -\sum_{nj \in ND_n} p_{nj} \ln(p_{nj})$

becomes $S_n = -\sum_{nj \in ND_n} \dfrac{r_{nj}}{R_n} \ln\left(\dfrac{r_{nj}}{R_n}\right)$

$$= -\frac{1}{R_n}\left[\sum_{nj \in ND_n} r_{nj} \ln(r_{nj}) - \sum_{nj \in ND_n} r_{nj} \ln(R_n)\right]$$

But $\sum_{nj \in ND_n} r_{nj} \ln(R_n) = R_n \ln(R_n)$

Therefore $S_n = \dfrac{-1}{R_n} \sum_{nj \in ND_n} r_{nj} \ln(r_{nj}) + \ln(R_n)$

From Eq. (6) $P_n = \dfrac{T_n}{T_o} = R_n$

Therefore Eq. (1) $\dfrac{S}{K} = S_o + \sum_{n=1}^{N} P_n S_n$

becomes $\dfrac{S}{K} = S_o + \sum_{n=1}^{N} R_n \left(\dfrac{-1}{R_n} \sum_{nj \in ND_n} r_{nj} \ln(r_{nj}) + \ln(R_n)\right)$

$$= S_o - \sum_{n=1}^{N} \left(\sum_{nj \in ND_n} r_{nj} \ln(r_{nj}) - R_n \ln(R_n)\right)$$

Defining L = set of all positive flow links ij in the network, including outflow links io

$$\frac{S}{K} = S_o - \sum_{ij \in L} r_{ij} \ln(r_{ij}) + \sum_{n=1}^{N} R_n \ln(R_n)$$

From Eq. (2) $S_o = -\sum_{i \in I} p_{oi} \ln(p_{oi}) = -\sum_{i \in I} r_{oi} \ln(r_{oi})$

Therefore $\frac{S}{K} = -\sum_{i \in I} r_{oi} \ln(r_{oi}) - \sum_{ij \in L} r_{ij} \ln(r_{ij}) + \sum_{n=1}^{N} R_n \ln(R_n)$

Defining M = set of all positive flow links ij in the network, including inflow links oj and outflow links io,

$$\frac{S}{K} = -\sum_{ij \in M} r_{ij} \ln(r_{ij}) + \sum_{n=1}^{N} R_n \ln(R_n) \tag{A1}$$

Reply by A. B. Templeman and T. T. Tanyimboh

The authors thank the writer for a most helpful and interesting discussion and for the opportunity to correct some aspects of the paper.

Eq. (A1) extends the entropy expressions developed in the paper and transforms them from probability variables to network flow variables. This provides added insight on network flow entropy and a very convenient way of demonstrating the invariance of the entropy with respect to variable transformation (e.g. reversal of flow directions), an essential feature of a valid entropy measure and one which the authors had verified only numerically hitherto. The proof of Eq. (A1) given in the Appendix is most helpful.

That all spanning tree networks chosen from a prescribed, looped network will have the same (minimum) value of entropy which can be calculated solely from the external flows at the demand nodes is an interesting result. However, it applies only to single-source trees. For multiple-source trees it is possible for a node to have more than one inflow and the entropy value turns out to be dependent upon the tree layout. As an example, Figure A4(a) shows the permissible pipes, flow directions, supplies and demands in a two-source, four-demand system. Figures A4(b), (c) and (d) show three possible spanning tree networks which could be chosen from this system and their associated entropy values. Figures A4(b) and A4(c) both have the same entropy value but the tree layout of Figure A4(d) has a smaller entropy value and represents the minimum entropy configuration.

The authors do not agree that the presence of multiple minima necessarily suggests that multiple maxima may exist. There is no logical link between the two. On the contrary, all the features of the maximum entropy network flow problem suggest that it is convex and consequently has a single global maximum. One of the authors has made this conjecture in Ref. [4] although a formal proof is not available. However, the lines of such a proof are evident from Eq. (A1). The form $x\ln(x)$ is a convex function for $0 \leqslant x \leqslant 1$ and so, in Eq. (A1), the first negative summation is concave and the second positive summation is convex. Since the first summation is larger than the second, S/K is a concave function. Maximizing a concave function subject only to nodal flow equilibrium constraints which are linear is a convex problem which cannot possess local optima. There has never been any hint of local optima in any of the many examples which the authors have studied.

DISCUSSION

The fact that the writer has found different and better solutions to the two examples presented in Section 4 of the paper should not be interpreted as implying that the various solutions found must be local optima of a non-convex problem. In fact, the results quoted in the paper are quite simply incorrect and invalid. The authors are most grateful to the writer for pointing out that better solutions can be found. As a consequence the authors have re-examined Section 4 of the paper in detail and have found that the entire Section 4 is theoretically invalid and should be deleted from the paper.

The main thrust of the paper was towards the development of a quick method for calculating maximum entropy flows for single-source networks. The method and the algorithms developed in the paper remain valid for all single-source networks. However, in Section 4 of the paper the authors attempted to extend this method to multiple-source networks by providing a single super-source to supply all the multiple sources. This super-source approach appeared to give sensible results and to be intuitively defensible. It now transpires that the super-source extension of the method as described in Section 4 of the paper was a step too far and is, in fact, completely wrong. In his discussion the writer has shown how the super-source idea

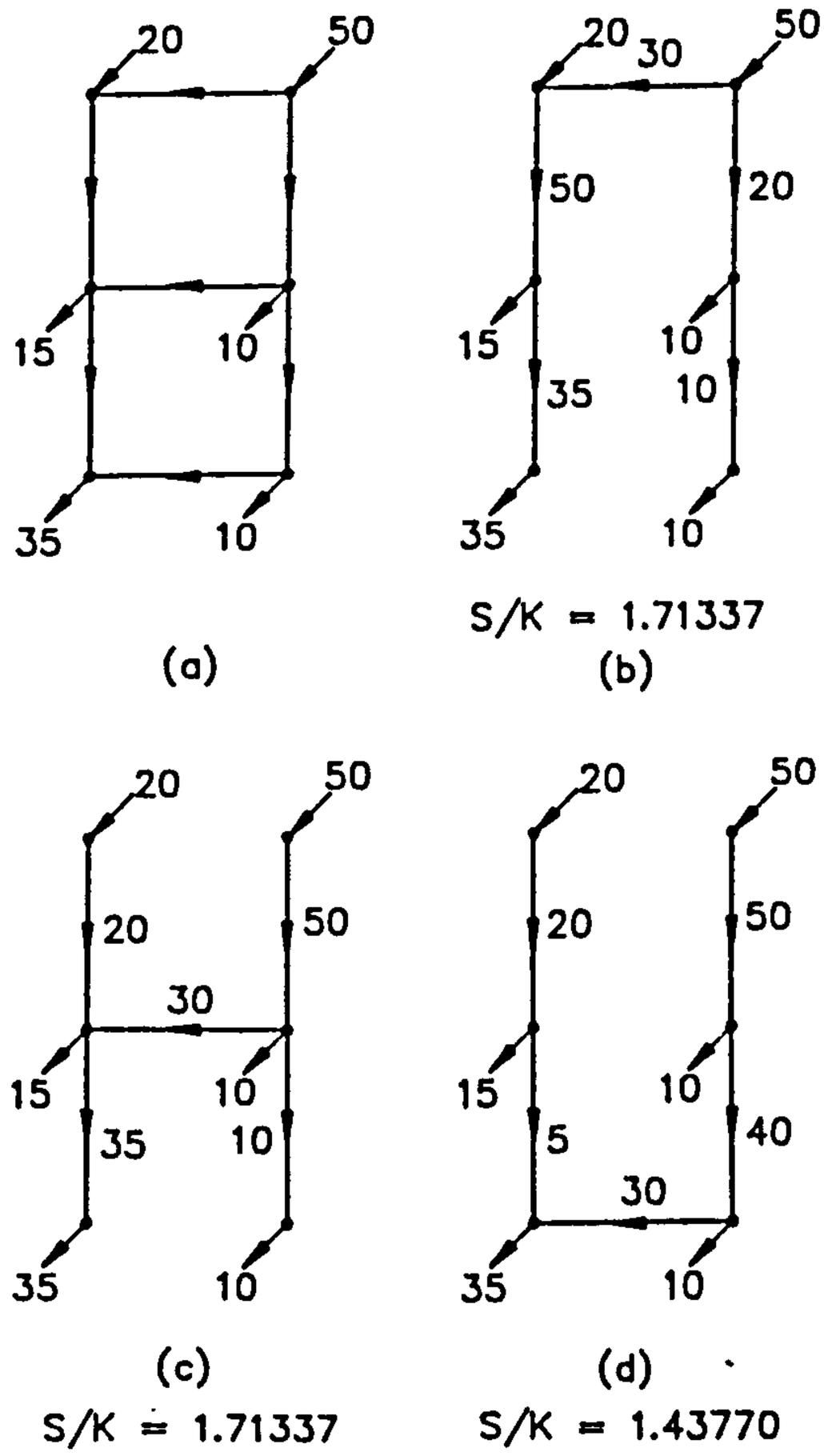

Figure A4 Entropies of different tree layouts.

can be manipulated to give correct results for multiple source networks but, as he has pointed out, it is not easy to operate this approach for anything but the simplest of networks. In the general case of a large network with many sources a more rigorous approach is still required. The authors have developed a rigorous general method and quick algorithm for general multi-source networks which does not use the super-source idea. This is the subject of a further paper currently in preparation. However, the method has been applied to the example networks in Section 4 of the paper and it has confirmed that the results shown in Figures A1 and A2 of the discussion are approximately correct to the accuracy claimed by the writer. Tables 1 and 2 list what are now believed to be the exact results for pipe flows and entropy values for the two example networks in Section 4 of the paper.

The writer's final point concerns Figures A3a and A3b and questions the ability of the flow entropy approach to provide intuitively-reliable flow distributions in the two networks shown. Clearly the flow distribution of Figure A3b, as suggested by maximum flow entropy, looks somewhat odd. However, the entropy measure depends only upon paths, inflows and demands and is independent of any factors such as length or scale. Consequently, in Figure A3b, the flow entropy measure cannot account for the fact that the 3×3 grid is defined by the writer to be "small". If it actually is "small" then the flows suggested in Figure A3b may look odd; but if it is actually "large" as shown in Figure A5, which has exactly the same topology, then the same maximum entropy flows no longer look as anomalous.

Figure A3b is obviously a carefully contrived example but it is worth examining further. If, as the writer suggests, the 3×3 grid of pipes is small it can be noted that the grid does not have any nodal demands and is therefore simply a throughflow system. It represents a most peculiar feature of a network design and it is hard to imagine why any rational designer would wish to include such a feature. In the network modelling of real distribution networks a certain amount of lumping

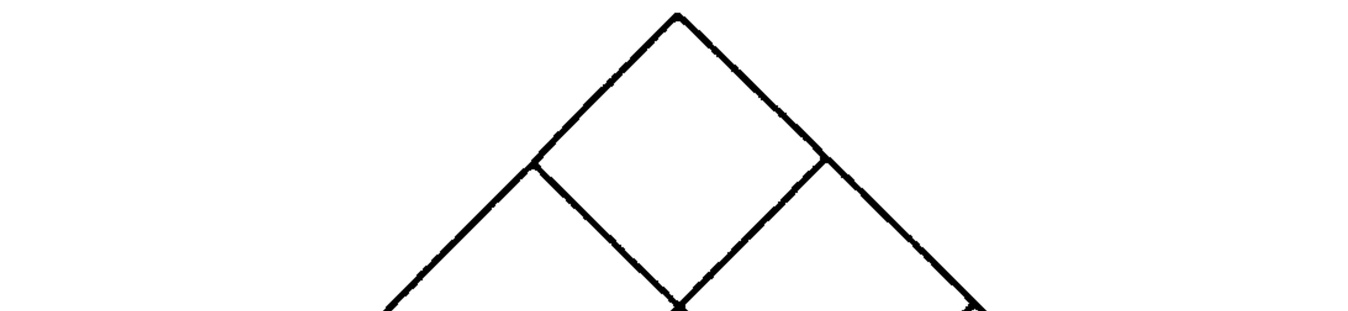

Figure A5 Maximum entropy flows.

Table 1 Correct results for Figure 6 in the paper and A1

Pipe	*Flow*
2–1	8.55537
2–3	7.21392
2–5	4.23071
1–3	36.72609
1–4	6.82928
3–4	8.17072
3–5	25.76929
S/K	2.15383

Table 2 Correct results for Figure 5a in the paper and A2

Pipe	*Flow*
1–2	18.57080
2–3	26.48121
2–5	12.08959
1–3	12.74999
1–4	3.67921
3–4	11.32079
3–5	17.91041
S/K	2.45001

and aggregation is usually necessary. A small throughflow grid such as that in Figure A3b would probably be eliminated entirely from an overall network model so that main flows would be determined for the system of Figure A3a. The 3 × 3 grid would then be examined separately, if necessary, using the main inflows and outflows of Figure A3a.

Given the simplicity of Eq. (A1) and the minimal information required to calculate the flow entropy, it would be over-optimistic to expect a great deal more than a reasonable correlation between entropy and reliability. Carefully contrived hypothetical examples can demonstrate the fallibility of most existing measures of network reliability. Fortunately most practical networks are not hypothetically contrived and the authors have yet to encounter any practical networks in which the correlation between entropy and reliability is not very good.

References

4. Tanyimboh, T. T. (1993) An entropy-based approach to the optimum design of reliable water distribution networks. *Ph.D Thesis*, University of Liverpool, 128.

APPENDIX B

THE ALFA METHOD
COMPUTER PROGRAMME

```
MODULE ALFA_MODULE
 IMPLICIT NONE
 INTEGER :: NN, NL, NS, I, J, K, L, KK, IK, N, LWA, IFAIL
 REAL(KIND=2) :: FNORM, TOL, S
 INTEGER , DIMENSION (:) , ALLOCATABLE :: UN, DN
 INTEGER , DIMENSION (:,:) , ALLOCATABLE :: A, B, NP
 REAL(KIND=2) , DIMENSION (:) , ALLOCATABLE :: FVEC, WA, Q, D, SP
 REAL(KIND=2) , DIMENSION (:,:) , ALLOCATABLE :: X, PF, TQ, TP
 REAL(KIND=2) :: F06EJF, X02AJF
 CHARACTER (LEN=72) :: INPUT, OUTPUT
 EXTERNAL F06EJF, X02AJF
 EXTERNAL C05NBF
CONTAINS
 SUBROUTINE FCN(N, X, FVEC, IFLAG)
  ! SET UP THE EQUATIONS TO BE SOLVED IN THE FORM F(X)=0:
  INTEGER :: N, IFLAG, NE
REAL(KIND=2) , DIMENSION (:,:) , ALLOCATABLE :: C
REAL(KIND=2) :: FVEC(1:N), X(1:NS,0:NN)
ALLOCATE (C(1:NS,0:NN))
IFLAG=1
DO I=1,NS
   C(I,0:NN)=NP(I,0:NN)*(-D(I))
END DO
NE=0
DO I=NS+1,NN
   NE=NE+1
   FVEC(NE)=DOT_PRODUCT(C(1:NS,I),X(1:NS,I))-D(I)
END DO
NE=NE+1
FVEC(NE)=X(1,1)-1.0_2
DO I=1,NS
   DO J=0,NS
      IF (I/=J) THEN
         NE=NE+1
         FVEC(NE)=X(I,J)
      END IF
   END DO
END DO
DO I=1,NS
   DO J=NS+1,NN
      IF (C(I,J)==0) THEN
         NE=NE+1
```

```
          FVEC(NE)=X(I,J)
        END IF
      END DO
    END DO
  END DO
  DO I=NS+1,NN
    DO J=1,NS-1
      IF (C(J,I)/=0) THEN
        DO L=J+1,NS
          IF (C(L,I)/=0) THEN
            NE=NE+1
            FVEC(NE)=X(J,I)*X(L,L)-X(L,I)*X(J,J)
          END IF
        END DO
        EXIT
      END IF
    END DO
  END DO
  DO I=1,NS-1
    NE=NE+1
    FVEC(NE)=DOT_PRODUCT(NP(I,NS+1:NN),X(I,NS+1:NN))-1.0_2
  END DO
  DEALLOCATE (C)
 END SUBROUTINE
END MODULE ALFA_MODULE
PROGRAM ALFA_METHOD
 USE ALFA_MODULE
 PRINT*, 'ENTER THE NAME OF DATA FILE WITH PATH:'
 READ '(A)', INPUT
 PRINT*, 'ENTER THE NAME OF OUTPUT FILE WITH PATH:'
 READ '(A)', OUTPUT
 OPEN (5, FILE=INPUT, FORM='FORMATTED', STATUS='OLD')
 OPEN (6, FILE=OUTPUT, FORM='FORMATTED', STATUS='UNKNOWN')
 ! INPUT DATA:
 ! ALL NODES SHOULD BE NUMBERED BY POSITIVE CONSECUTIVE
 ! NUMBERS STARTING BY NUMBER ONE FOR ANY SOURCE IN THE
 ! NETWORK, THEN THE  REST OF THE SOURCES, AND THEN THE
 ! REST OF THE NODES RANDOMLY.
 PRINT*, 'NN?'
 READ*, NN ! READ NUMBER OF NODES
 PRINT*, '# NODES =', NN
 PRINT*, 'NL?'
 READ*, NL ! READ NUMBER OF LINKS
 PRINT*, '# LINKS =', NL
 PRINT*, 'NS?'
 READ*, NS ! READ NUMBER OF SOURCES
 PRINT*, '# SOURCES =', NS
 N=NS*(NN+1) ! NUMBER OF EQUATIONS TO BE SOLVED
 LWA=(N*(3*N+13))/2 ! THE DIMENSION OF THE WORKSPACE ARRAY WA
 ALLOCATE (UN(1:NL))
 ALLOCATE (DN(1:NL))
 ALLOCATE (D(1:NN))
 ALLOCATE (A(1:NN,1:NN))
 ALLOCATE (B(1:NN,1:NN))
 ALLOCATE (NP(1:NN,0:NN))
 ALLOCATE (X(1:NS,0:NN))
 ALLOCATE (FVEC(1:N))
```

```
ALLOCATE (WA(1:LWA))
ALLOCATE (PF(1:NS,0:NN))
ALLOCATE (TQ(1:NL,1:NS))
ALLOCATE (Q(1:NL))
ALLOCATE (TP(1:NS,0:NN))
ALLOCATE (SP(1:NS))
PRINT*, 'FOR EACH LINK INPUT UN, DN'
DO I=1,NL ! READ UPSTREAM AND DOWNSTREAM NODES FOR EACH LINK
  READ*, UN(I), DN(I)
END DO
PRINT*, 'FOR EACH NODE INPUT D, (SOURCE -VE)'
DO I=1,NN ! READ INFLOWS AND OUTFLOWS FOR EACH NODE (SOURCE -VE)
  READ*, D(I)
END DO
! PROGRAM TERMINATION AND ERROR MESSAGES:
IF (COUNT(D<0.0_2)/=NS) THEN
  PRINT*, 'INCORRECT INPUT FLOWS'
  PRINT*, 'PROGRAM TERMINATED'
  STOP
END IF
IF (ABS(SUM(D(1:NS)))/=SUM(D(NS+1:NN))) THEN
  PRINT*, 'INFLOWS ARE NOT EQUAL OUTFLOWS'
  PRINT*, 'PROGRAM TERMINATED'
  STOP
END IF
! FIND OUT THE NODES REACHABLE TO EACH NODE:
DO I=1,NN
  A(1,I)=I
  K=1
  IK=1
  DO J=1,NL
    IF (UN(J)==A(1,I)) THEN
      A(K+1,I)=DN(J)
      K=K+1
      IK=IK+1
    END IF
  END DO
  KK=K-1
  K=1
10  DO J=1,NL
    DO L=IK-KK,IK
      IF (UN(J)==A(L,I).AND.COUNT(A(1:NN,I)==DN(J))==0) THEN
        A(IK+1,I)=DN(J)
        K=K+1
        IK=IK+1
      END IF
    END DO
  END DO
  IF (K/=1) THEN
    KK=K-1
    K=1
    GOTO 10
  END IF
END DO
PRINT*, 'NODES REACHABLE TO EACH NODE ARE:'
DO I=1,NN
```

```
   K=1
   DO J=2,NN
      IF (A(J,I)==0) EXIT
      K=K+1
   END DO
   IF (K==1) THEN
      PRINT*, 'TO NODE(',I,'): NO NODES'
   ELSE
      PRINT*, 'TO NODE(',I,'):',(A(J,I),J=2,K)
   END IF
END DO
! FIND OUT THE NODES IMMEDIATELY UPSTREAM TO EACH NODE:
DO I=1,NN
   B(1,I)=I
   K=1
   DO L=1,NL
      IF (DN(L)==I) THEN
         B(K+1,I)=UN(L)
         K=K+1
      END IF
   END DO
END DO
PRINT*, 'NODES IMMEDIATELY UPSTREAM TO EACH NODE ARE:'
DO I=1,NN
   K=1
   DO J=2,NN
      IF (B(J,I)==0) EXIT
      K=K+1
   END DO
   IF (K==1) THEN
      PRINT*, 'TO NODE(',I,'): NO NODES'
   ELSE
      PRINT*, 'TO NODE(',I,'):',(B(J,I),J=2,K)
   END IF
END DO
! CALCULATE THE NUMBER OF PATHS FROM EACH NODE TO EACH NODE:
NP=-1
DO I=1,NN
   NP(I,0)=0
END DO
DO I=1,NN
   NP(I,I)=1
   DO J=1,NN
      IF (COUNT(A(1:NN,I)==J)==0) THEN
         NP(I,J)=0
      END IF
   END DO
END DO
100 DO I=1,NN
      DO J=1,NN
         IF (NP(I,J)/=-1) CYCLE
         IF (COUNT(NP(I,B(2:NN,J))==-1)==0) THEN
            NP(I,J)=SUM(NP(I,B(2:NN,J)))
         END IF
      END DO
   END DO
```

```
IF (COUNT(NP(1:NN,1:NN)==-1)/=0) GOTO 100
PRINT*, 'NUMBER OF PATHS FROM EACH NODE TO EACH NODE ARE:'
DO I=1,NN
   PRINT*, 'NP FROM NODE(',I,')TO NODES(',1,'-',NN, &
   ') RESPECTIVELY:',(NP(I,J),J=1,NN)
END DO
! STARTING VALUES OF PROBABILITIES:
DO I=1,NS
   DO J=0,NN
      X(I,J)=0.5_2
   END DO
END DO
TOL=SQRT(X02AJF())
! THE ACCURACY IN X TO WHICH THE SOLUTION IS REQUIRED.
IFAIL=1
! SOLVING  NON_LINEAR  EQUATIONS TO CALCULATE  THE
! PROBABILITIES  OF PATH FLOWS FROM EACH SOURCE TO
! EACH DEMAND NODE, BY CALLING NAG LIBRARY C05NBF:
CALL C05NBF(FCN,N,X,FVEC,TOL,WA,LWA,IFAIL)
DO I=1,NS
   DO J=0,NS
      IF (I/=J)THEN
         X(I,J)=0.0_2
      END IF
   END DO
END DO
DO I=1,NS
   DO J=NS+1,NN
      IF (NP(I,J)==0) THEN
         X(I,J)=0.0_2
      END IF
   END DO
END DO
DO I=NS+1,NN
   DO J=1,NS
      IF (D(I)==0.0_2) THEN
         X(J,I)=0.0_2
      END IF
   END DO
END DO
IF (IFAIL==0)THEN
   FNORM=F06EJF(N,FVEC,1)
   PRINT*, 'FINAL 2-NORM OF THE RESIDUALS=', FNORM
   DO I=2,NS
      PRINT*, 'ALFA(',I,')=',X(I,I)
   END DO
   PRINT*, 'PROBABILITIES OF PATH FLOWS FROM EACH', &
   ' SOURCE TO EACH DEMAND NODE ARE:'
   DO I=1,NS
      DO J=NS+1,NN
         IF (X(I,J)==0.0_2) CYCLE
         PRINT*, 'P(',I,'-',J,')=',X(I,J)
      END DO
   END DO
ELSE
   PRINT*, 'IFAIL=', IFAIL
```

```
    IF (IFAIL>1)THEN
      DO I=2,NS
        PRINT*, 'ALFA(',I,')=',X(I,I)
      END DO
      PRINT*, 'PROBABILITIES OF PATH FLOWS FROM EACH', &
      ' SOURCE TO EACH DEMAND NODE ARE:'
      DO I=1,NS
        DO J=NS+1,NN
          IF (X(I,J)==0.0_2) CYCLE
          PRINT*, 'P(',I,'-',J,')=',X(I,J)
        END DO
      END DO
    END IF
END IF
! CHECK PROBABILITIES:
DO I=1,NS
  SP(I)=DOT_PRODUCT(NP(I,NS+1:NN),X(I,NS+1:NN))
END DO
PRINT*, 'PROBABILITIES CHECKING:'
DO I=1,NS
  PRINT*, 'NORMALITY CONDITION AT SOURCE(',I,')=',SP(I)
END DO
! CALCULATE THE PATH FLOWS FROM EACH SOURCE TO EACH DEMAND NODE:
 DO I=1,NS
  PF(I,0:NS)=0.0_2
  PF(I,NS+1:NN)=X(I,NS+1:NN)*(-D(I))
END DO
PRINT*, 'PATH FLOWS FROM EACH SOURCE TO EACH DEMAND NODE ARE:'
DO I=1,NS
  DO J=NS+1,NN
    IF (PF(I,J)==0.0_2) CYCLE
    PRINT*, 'PF(',I,'-',J,')=',PF(I,J)
  END DO
END DO
! CALCULATE THE FINAL LINK FLOWS:
DO I=1,NL
  DO J=1,NS
    TQ(I,J)=NP(J,UN(I))*DOT_PRODUCT(NP(DN(I),1:NN),PF(J,1:NN))
  END DO
END DO
Q=SUM(TQ,DIM=2)
PRINT*, 'FINAL LINK FLOWS ARE:'
DO I=1,NL
  PRINT*, 'Q(',UN(I),'-',DN(I),')=',Q(I)
END DO
! CALCULATE THE ENTROPY VALUE OF THE NETWORK:
DO I=1,NS
  IF (D(I)==0.0_2) CYCLE
  DO J=NS+1,NN
    IF (X(I,J)==0.0_2) CYCLE
    TP(I,J)=X(I,J)*LOG(X(I,J))
  END DO
  TP(I,1)=(D(I)/SUM(D(NS+1:NN)))* &
        DOT_PRODUCT(TP(I,NS+1:NN),NP(I,NS+1:NN))
  TP(I,0)=(D(I)/SUM(D(1:NS)))*LOG(D(I)/SUM(D(1:NS)))
END DO
```

```
 S=SUM(TP(1:NS,1))-SUM(TP(1:NS,0))
 PRINT*, 'ENTROPY VALUE OF THE NETWORK IS:'
 PRINT*, 'S/K=',S
 PRINT*, 'END OF FILE'
END PROGRAM ALFA_METHOD
```

APPENDIX C

SOME OF THE ALFA METHOD COMPUTER PROGRAMME APPLICATIONS OF CHAPTER 5

C.1 EXAMPLE 1

The input file:

```
9
16
2
1 3
1 4
3 2
3 4
3 5
2 5
2 7
4 5
4 6
5 6
5 7
5 8
6 8
7 8
7 9
8 9
-60
-40
10
10
15
15
15
15
20
```

The output file:

```
NN?
# NODES = 9
NL?
# LINKS = 16
NS?
# SOURCES = 2
FOR EACH LINK INPUT UN, DN
FOR EACH NODE INPUT D, (SOURCE -VE)
NODES REACHABLE TO EACH NODE ARE:
TO NODE( 1 ): 3 4 2 5 7 6 8 9
TO NODE( 2 ): 5 7 6 8 9
TO NODE( 3 ): 2 4 5 7 6 8 9
TO NODE( 4 ): 5 6 7 8 9
TO NODE( 5 ): 6 7 8 9
TO NODE( 6 ): 8 9
TO NODE( 7 ): 8 9
TO NODE( 8 ): 9
TO NODE( 9 ): NO NODES
NODES IMMEDIATELY UPSTREAM TO EACH NODE ARE:
TO NODE( 1 ): NO NODES
TO NODE( 2 ): 3
TO NODE( 3 ): 1
TO NODE( 4 ): 1 3
TO NODE( 5 ): 3 2 4
TO NODE( 6 ): 4 5
TO NODE( 7 ): 2 5
TO NODE( 8 ): 5 6 7
TO NODE( 9 ): 7 8
NUMBER OF PATHS FROM EACH NODE TO EACH NODE ARE:
NP FROM NODE( 1 )TO NODES( 1 - 9 ) RESPECTIVELY: 1 1 1 2 4 6 5 15 20
NP FROM NODE( 2 )TO NODES( 1 - 9 ) RESPECTIVELY: 0 1 0 0 1 1 2 4 6
NP FROM NODE( 3 )TO NODES( 1 - 9 ) RESPECTIVELY: 0 1 1 1 3 4 4 11 15
NP FROM NODE( 4 )TO NODES( 1 - 9 ) RESPECTIVELY: 0 0 0 1 1 2 1 4 5
NP FROM NODE( 5 )TO NODES( 1 - 9 ) RESPECTIVELY: 0 0 0 0 1 1 1 3 4
NP FROM NODE( 6 )TO NODES( 1 - 9 ) RESPECTIVELY: 0 0 0 0 0 1 0 1 1
NP FROM NODE( 7 )TO NODES( 1 - 9 ) RESPECTIVELY: 0 0 0 0 0 0 1 1 2
NP FROM NODE( 8 )TO NODES( 1 - 9 ) RESPECTIVELY: 0 0 0 0 0 0 0 1 1
NP FROM NODE( 9 )TO NODES( 1 - 9 ) RESPECTIVELY: 0 0 0 0 0 0 0 0 1
FINAL 2-NORM OF THE RESIDUALS=  6.443927707994817E-10
ALFA( 2 )=  5.5919905516210164
PROBABILITIES OF PATH FLOWS FROM EACH SOURCE TO EACH DEMAND NODE ARE:
P( 1 - 3 )=  0.16666666666666667
P( 1 - 4 )=  8.3333333333333329E-02
P( 1 - 5 )=  3.2349922862496695E-02
P( 1 - 6 )=  2.5699029795101105E-02
P( 1 - 7 )=  2.0070668976745656E-02
P( 1 - 8 )=  8.3578566873076538E-03
P( 1 - 9 )=  7.867580062636513OE-03
P( 2 - 5 )=  0.1809004628250198
P( 2 - 6 )=  0.1437087318440901
P( 2 - 7 )=  0.1122349913372038
P( 2 - 8 )=  4.6737056133894450E-02
P( 2 - 9 )=  4.3995433020150770E-02
PROBABILITIES CHECKING:
```

NORMALITY CONDITION AT SOURCE(1)= 1.0000000000000000
NORMALITY CONDITION AT SOURCE(2)= 0.9999999999999998
PATH FLOWS FROM EACH SOURCE TO EACH DEMAND NODE ARE:
PF(1 - 3)= 10.000000000000000
PF(1 - 4)= 5.000000000000000
PF(1 - 5)= 1.9409953717498016
PF(1 - 6)= 1.5419417877060664
PF(1 - 7)= 1.20424013860473 94
PF(1 - 8)= 0.501471401238 4592
PF(1 - 9)= 0.4720548037581908
PF(2 - 5)= 7.23601851300079 17
PF(2 - 6)= 5.7483492737636031
PF(2 - 7)= 4.4893996534881513
PF(2 - 8)= 1.8694822453557780
PF(2 - 9)= 1.7598173208060308
FINAL LINK FLOWS ARE:
Q(1 - 3)= 44.404721290488 5384
Q(1 - 4)= 15.595278709511 4633
Q(3 - 2)= 10.729631864168 3293
Q(3 - 4)= 15.595278709511 4633
Q(3 - 5)= 8.07981071680874 76
Q(2 - 5)= 38.201294176352 7465
Q(2 - 7)= 12.528337687815 5703
Q(4 - 5)= 16.159621433617 4953
Q(4 - 6)= 5.0309359854054323
Q(5 - 6)= 19.439520810736 2762
Q(5 - 7)= 20.477801129894 3099
Q(5 - 8)= 7.5234043861484086
Q(6 - 8)= 9.4704567961417077
Q(7 - 8)= 12.126230157306 8676
Q(7 - 9)= 5.8799086604030153
Q(8 - 9)= 14.120091339596 9856
ENTROPY VALUE OF THE NETWORK IS:
S/K= 3.7489693125575236
END OF FILE

C.2 EXAMPLE 2

The input file:

```
9
13
3
1 4
1 5
5 4
4 6
5 8
8 6
2 7
7 5
7 9
2 9
3 8
3 9
9 8
-20
-35
-15
10
10
15
10
15
10
```

The output file:

```
NN?
# NODES = 9
NL?
# LINKS = 13
NS?
# SOURCES = 3
FOR EACH LINK INPUT UN, DN
FOR EACH NODE INPUT D, (SOURCE -VE)
NODES REACHABLE TO EACH NODE ARE:
TO NODE( 1 ): 4 5 6 8
TO NODE( 2 ): 7 9 5 8 4 6
TO NODE( 3 ): 8 9 6
TO NODE( 4 ): 6
TO NODE( 5 ): 4 8 6
TO NODE( 6 ): NO NODES
TO NODE( 7 ): 5 9 4 6 8
TO NODE( 8 ): 6
TO NODE( 9 ): 8 6
NODES IMMEDIATELY UPSTREAM TO EACH NODE ARE:
TO NODE( 1 ): NO NODES
TO NODE( 2 ): NO NODES
TO NODE( 3 ): NO NODES
TO NODE( 4 ): 1 5
TO NODE( 5 ): 1 7
TO NODE( 6 ): 4 8
TO NODE( 7 ): 2
TO NODE( 8 ): 5 3 9
TO NODE( 9 ): 7 2 3
NUMBER OF PATHS FROM EACH NODE TO EACH NODE ARE:
 NP FROM NODE( 1 )TO NODES( 1 - 9 ) RESPECTIVELY: 1 0 0 2 1 3 0 1 0
 NP FROM NODE( 2 )TO NODES( 1 - 9 ) RESPECTIVELY: 0 1 0 1 1 4 1 3 2
 NP FROM NODE( 3 )TO NODES( 1 - 9 ) RESPECTIVELY: 0 0 1 0 0 2 0 2 1
 NP FROM NODE( 4 )TO NODES( 1 - 9 ) RESPECTIVELY: 0 0 0 1 0 1 0 0 0
 NP FROM NODE( 5 )TO NODES( 1 - 9 ) RESPECTIVELY: 0 0 0 1 1 2 0 1 0
 NP FROM NODE( 6 )TO NODES( 1 - 9 ) RESPECTIVELY: 0 0 0 0 0 1 0 0 0
 NP FROM NODE( 7 )TO NODES( 1 - 9 ) RESPECTIVELY: 0 0 0 1 1 3 1 2 1
 NP FROM NODE( 8 )TO NODES( 1 - 9 ) RESPECTIVELY: 0 0 0 0 0 1 0 1 0
 NP FROM NODE( 9 )TO NODES( 1 - 9 ) RESPECTIVELY: 0 0 0 0 0 1 0 1 1
 FINAL 2-NORM OF THE RESIDUALS=   3.014200189635123 6E-10
 ALFA( 2 )=   0.4786637180902165
 ALFA( 3 )=   1.7134212843979728
 PROBABILITIES OF PATH FLOWS FROM EACH SOURCE TO EACH DEMAND NODE
ARE:
 P( 1 - 4 )=   0.1762014246845641
 P( 1 - 5 )=   0.2720849287023921
 P( 1 - 6 )=   8.407338499660395 3E-02
 P( 1 - 8 )=   0.1232920669386678
 P( 2 - 4 )=   8.434122893192670 7E-02
 P( 2 - 5 )=   0.1302371835986331
 P( 2 - 6 )=   4.024287910923451 9E-02
 P( 2 - 7 )=   0.2857142857142857
 P( 2 - 8 )=   5.901543919045865 9E-02
 P( 2 - 9 )=   8.084473387342026 9E-02
 P( 3 - 6 )=   0.1440531274970310
```

P(3 - 8)= 0.211251251540949 5
P(3 - 9)= 0.289391241924038 8
PROBABILITIES CHECKING:
NORMALITY CONDITION AT SOURCE(1)= 1.000000000000000
NORMALITY CONDITION AT SOURCE(2)= 1.000000000000000
NORMALITY CONDITION AT SOURCE(3)= 0.999999999999999
PATH FLOWS FROM EACH SOURCE TO EACH DEMAND NODE ARE:
PF(1 - 4)= 3.524028493691282 5
PF(1 - 5)= 5.441698574047841 9
PF(1 - 6)= 1.681467699932079 0
PF(1 - 8)= 2.465841338773356 7
PF(2 - 4)= 2.951943012617434 6
PF(2 - 5)= 4.558301425952157 3
PF(2 - 6)= 1.408500768823208 3
PF(2 - 7)= 10.000000000000000
PF(2 - 8)= 2.065540371666053 0
PF(2 - 9)= 2.829565685569709 6
PF(3 - 6)= 2.160796912455465 3
PF(3 - 8)= 3.168768773114242 9
PF(3 - 9)= 4.340868628860581 8
FINAL LINK FLOWS ARE:
Q(1 - 4)= 5.205496193623361 0
Q(1 - 5)= 14.79450380637663 90
Q(5 - 4)= 9.565939975064004 8
Q(4 - 6)= 4.771436168687365 9
Q(5 - 8)= 7.621350179194696 0
Q(8 - 6)= 10.22856383131263 41
Q(2 - 7)= 28.69639317394102 92
Q(7 - 5)= 12.39278634788206 19
Q(7 - 9)= 6.303606826058970 8
Q(2 - 9)= 6.303606826058970 8
Q(3 - 8)= 5.329565685569708 2
Q(3 - 9)= 9.670434314430290 0
Q(9 - 8)= 12.27764796654822 99
ENTROPY VALUE OF THE NETWORK IS:
S/K= 3.028465553638588 0
END OF FILE

C.3 EXAMPLE 3

The input file:

```
9
13
3
1 4
1 5
5 4
5 8
8 6
4 6
2 7
7 8
2 9
7 9
9 8
3 9
3 8
-30
-35
-15
10
10
20
10
20
10
```

The output file:

```
NN?
# NODES = 9
NL?
# LINKS = 13
NS?
# SOURCES = 3
FOR EACH LINK INPUT UN, DN
FOR EACH NODE INPUT D, (SOURCE -VE)
NODES REACHABLE TO EACH NODE ARE:
TO NODE( 1 ): 4 5 8 6
TO NODE( 2 ): 7 9 8 6
TO NODE( 3 ): 9 8 6
TO NODE( 4 ): 6
TO NODE( 5 ): 4 8 6
TO NODE( 6 ): NO NODES
TO NODE( 7 ): 8 9 6
TO NODE( 8 ): 6
TO NODE( 9 ): 8 6
NODES IMMEDIATELY UPSTREAM TO EACH NODE ARE:
TO NODE( 1 ): NO NODES
TO NODE( 2 ): NO NODES
TO NODE( 3 ): NO NODES
TO NODE( 4 ): 1 5
TO NODE( 5 ): 1
TO NODE( 6 ): 8 4
TO NODE( 7 ): 2
TO NODE( 8 ): 5 7 9 3
TO NODE( 9 ): 2 7 3
NUMBER OF PATHS FROM EACH NODE TO EACH NODE ARE:
NP FROM NODE( 1 )TO NODES( 1 - 9 ) RESPECTIVELY: 1 0 0 2 1 3 0 1 0
NP FROM NODE( 2 )TO NODES( 1 - 9 ) RESPECTIVELY: 0 1 0 0 0 3 1 3 2
NP FROM NODE( 3 )TO NODES( 1 - 9 ) RESPECTIVELY: 0 0 1 0 0 2 0 2 1
NP FROM NODE( 4 )TO NODES( 1 - 9 ) RESPECTIVELY: 0 0 0 1 0 1 0 0 0
NP FROM NODE( 5 )TO NODES( 1 - 9 ) RESPECTIVELY: 0 0 0 1 1 2 0 1 0
NP FROM NODE( 6 )TO NODES( 1 - 9 ) RESPECTIVELY: 0 0 0 0 0 1 0 0 0
NP FROM NODE( 7 )TO NODES( 1 - 9 ) RESPECTIVELY: 0 0 0 0 0 2 1 2 1
NP FROM NODE( 8 )TO NODES( 1 - 9 ) RESPECTIVELY: 0 0 0 0 0 1 0 1 0
NP FROM NODE( 9 )TO NODES( 1 - 9 ) RESPECTIVELY: 0 0 0 0 0 1 0 1 1
FINAL 2-NORM OF THE RESIDUALS=   4.081871956209322 9E-13
ALFA( 2 )=   0.974557574232459 3
ALFA( 3 )=   2.194599765650623 1
PROBABILITIES OF PATH FLOWS FROM EACH SOURCE TO EACH DEMAND NODE
ARE:
P( 1 - 4 )=   0.166666666666667
P( 1 - 5 )=   0.333333333333333
P( 1 - 6 )=   7.746937358532057 8E-02
P( 1 - 8 )=   0.100925212577371 6
P( 2 - 6 )=   7.549836479864351 1E-02
P( 2 - 7 )=   0.285714285714285 7
P( 2 - 8 )=   9.835743034822247 4E-02
P( 2 - 9 )=   9.635916442255813 8E-02
P( 3 - 6 )=   0.170014269115452 6
P( 3 - 8 )=   0.221490447870516 5
P( 3 - 9 )=   0.216990566028062 0
```

PROBABILITIES CHECKING:
NORMALITY CONDITION AT SOURCE(1)= 0.9999999999999999
NORMALITY CONDITION AT SOURCE(2)= 0.9999999999999999
NORMALITY CONDITION AT SOURCE(3)= 1.0000000000000002
PATH FLOWS FROM EACH SOURCE TO EACH DEMAND NODE ARE:
PF(1 - 4)= 5.0000000000000000
PF(1 - 5)= 10.0000000000000000
PF(1 - 6)= 2.3240812075596171
PF(1 - 8)= 3.0277563773211464
PF(2 - 6)= 2.6424427679525229
PF(2 - 7)= 10.0000000000000000
PF(2 - 8)= 3.4425100621877864
PF(2 - 9)= 3.3725707547895349
PF(3 - 6)= 2.5502140367317891
PF(3 - 8)= 3.3223567180577471
PF(3 - 9)= 3.2548584904209301
FINAL LINK FLOWS ARE:
Q(1 - 4)= 7.3240812075596171
Q(1 - 5)= 22.6759187924403811
Q(5 - 4)= 7.3240812075596171
Q(5 - 8)= 5.3518375848807640
Q(8 - 6)= 15.3518375848807658
Q(4 - 6)= 4.6481624151192342
Q(2 - 7)= 25.5424764150701549
Q(7 - 8)= 6.0849528301403097
Q(2 - 9)= 9.4575235849298451
Q(7 - 9)= 9.4575235849298451
Q(9 - 8)= 18.0424764150701549
Q(3 - 9)= 9.1274292452104664
Q(3 - 8)= 5.8725707547895363
ENTROPY VALUE OF THE NETWORK IS:
S/K= 2.9239736390456761
END OF FILE

C.4 THE REVERSED EXAMPLE OF EXAMPLE 1

The input file:

```
9
16
7
1 2
1 4
2 3
2 4
2 5
3 5
3 6
4 5
4 8
5 6
5 7
5 8
6 7
6 9
8 7
7 9
-20
-15
-15
-15
-15
-10
-10
40
60
```

The output file:

```
NN?
# NODES = 9
NL?
# LINKS = 16
NS?
# SOURCES = 7
FOR EACH LINK INPUT UN, DN
FOR EACH NODE INPUT D, (SOURCE -VE)
NODES REACHABLE TO EACH NODE ARE:
TO NODE( 1 ): 2 4 3 5 6 7 8 9
TO NODE( 2 ): 3 4 5 6 8 7 9
TO NODE( 3 ): 5 6 7 8 9
TO NODE( 4 ): 5 8 6 7 9
TO NODE( 5 ): 6 7 8 9
TO NODE( 6 ): 7 9
TO NODE( 7 ): 9
TO NODE( 8 ): 7 9
TO NODE( 9 ): NO NODES
NODES IMMEDIATELY UPSTREAM TO EACH NODE ARE:
TO NODE( 1 ): NO NODES
TO NODE( 2 ): 1
TO NODE( 3 ): 2
TO NODE( 4 ): 1 2
TO NODE( 5 ): 2 3 4
TO NODE( 6 ): 3 5
TO NODE( 7 ): 5 6 8
TO NODE( 8 ): 4 5
TO NODE( 9 ): 6 7
NUMBER OF PATHS FROM EACH NODE TO EACH NODE ARE:
NP FROM NODE( 1 )TO NODES( 1 - 9 ) RESPECTIVELY: 1 1 1 2 4 5 15 6 20
NP FROM NODE( 2 )TO NODES( 1 - 9 ) RESPECTIVELY: 0 1 1 1 3 4 11 4 15
NP FROM NODE( 3 )TO NODES( 1 - 9 ) RESPECTIVELY: 0 0 1 0 1 2 4 1 6
NP FROM NODE( 4 )TO NODES( 1 - 9 ) RESPECTIVELY: 0 0 0 1 1 1 4 2 5
NP FROM NODE( 5 )TO NODES( 1 - 9 ) RESPECTIVELY: 0 0 0 0 1 1 3 1 4
NP FROM NODE( 6 )TO NODES( 1 - 9 ) RESPECTIVELY: 0 0 0 0 0 1 1 0 2
NP FROM NODE( 7 )TO NODES( 1 - 9 ) RESPECTIVELY: 0 0 0 0 0 0 1 0 1
NP FROM NODE( 8 )TO NODES( 1 - 9 ) RESPECTIVELY: 0 0 0 0 0 0 1 1 1
NP FROM NODE( 9 )TO NODES( 1 - 9 ) RESPECTIVELY: 0 0 0 0 0 0 0 0 1
FINAL 2-NORM OF THE RESIDUALS=  5.644121205656478 7E-10
ALFA( 2 )=  1.4164214326698088
ALFA( 3 )=  4.355262093239017 1
ALFA( 4 )=  3.4014133797101418
ALFA( 5 )=  5.4824012344012560
ALFA( 6 )=  21.183981113138617 8
ALFA( 7 )=  42.367962227262772 5
PROBABILITIES OF PATH FLOWS FROM EACH SOURCE TO EACH DEMAND NODE
ARE:
P( 1 - 8 )=  8.799086637398186 0E-02
P( 1 - 9 )=  2.360274008780544 7E-02
P( 2 - 8 )=  0.1246321490046590
P( 2 - 9 )=  3.343142693209092 5E-02
P( 3 - 8 )=  0.3832232849652948
P( 3 - 9 )=  0.1027961191724509
P( 4 - 8 )=  0.2992933101449221
```

P(4 - 9)= 8.0282675942031173E-02
P(5 - 8)= 0.4824012344010357
P(5 - 9)= 0.1293996913997411
P(6 - 9)= 0.5000000000000000
P(7 - 9)= 0.9999999999999979
PROBABILITIES CHECKING:
NORMALITY CONDITION AT SOURCE(1)= 1.0000000000000000
NORMALITY CONDITION AT SOURCE(2)= 1.0000000000000000
NORMALITY CONDITION AT SOURCE(3)= 1.0000000000000000
NORMALITY CONDITION AT SOURCE(4)= 1.0000000000000000
NORMALITY CONDITION AT SOURCE(5)= 1.0000000000000000
NORMALITY CONDITION AT SOURCE(6)= 1.0000000000000000
NORMALITY CONDITION AT SOURCE(7)= 0.9999999999999979
PATH FLOWS FROM EACH SOURCE TO EACH DEMAND NODE ARE:
PF(1 - 8)= 1.7598173274796372
PF(1 - 9)= 0.4720548017561089
PF(2 - 8)= 1.8694822350698854
PF(2 - 9)= 0.5014714039813639
PF(3 - 8)= 5.7483492744794216
PF(3 - 9)= 1.5419417875867629
PF(4 - 8)= 4.4893996521738311
PF(4 - 9)= 1.2042401391304676
PF(5 - 8)= 7.2360185160155357
PF(5 - 9)= 1.9409953709961163
PF(6 - 9)= 5.0000000000000000
PF(7 - 9)= 9.9999999999999787
FINAL LINK FLOWS ARE:
Q(1 - 2)= 14.1200913362601828
Q(1 - 4)= 5.8799086637398190
Q(2 - 3)= 9.4704567969743607
Q(2 - 4)= 12.1262301537864090
Q(2 - 5)= 7.5234043854994139
Q(3 - 5)= 19.4395208103258881
Q(3 - 6)= 5.0309359866484717
Q(4 - 5)= 20.4778011286991877
Q(4 - 8)= 12.5283376888270404
Q(5 - 6)= 16.1596214333637498
Q(5 - 7)= 8.0798107166818749
Q(5 - 8)= 38.2012941744788677
Q(6 - 7)= 15.5952787100061094
Q(6 - 9)= 15.5952787100061094
Q(8 - 7)= 10.7296318633059240
Q(7 - 9)= 44.4047212899938870
ENTROPY VALUE OF THE NETWORK IS:
S/K= 3.7489693125575236
END OF FILE

APPENDIX D

THE CAMONET COMPUTER PROGRAMME

```
      IMPLICIT DOUBLE PRECISION (A-H,O-Z)
      PARAMETER(MXNN=20,MXNL=40,MXNLC=10,MXCN=5)
      PARAMETER(MXNLP=MXNL-MXNN+1)
      PARAMETER(N=MXNLP*MXNLC+MXNL)
      INTEGER UN(MXNLC,MXNL),DN(MXNLC,MXNL),NQL(MXNLC,MXNN),
     & ISTATE(N+MXNLC*(MXNLP+1)),IUSER(1),IWORK(3*N+2*MXNLC*(MXNLP+1)),
     & FLDIR(MXNLP*MXNLC,MXNL),HLP(MXNLC,MXNL),LCEXCN(MXNLC)
      DOUBLE PRECISION D(MXNLC,MXNN),QN(MXNLC,0:MXNN),QL(MXNLC,MXNL),
     & PQL(MXNLC,MXNN,MXCN),PQD(MXNLC,MXNN),PN(MXNN),
     & A(MXNLC,MXNN-1,MXNL),PQ(MXNL),X(N),AA(MXNN-1,MXNL+1),L(MXNL),
     & DI(MXNL),BL(N+MXNLC*(MXNLP+1)),BU(N+MXNLC*(MXNLP+1)),
     & C(MXNLC*(MXNLP+1)),CJAC(MXNLC*(MXNLP+1),N),OBJGRD(N),USER(1),
     & CLAMDA(N+MXNLC*(MXNLP+1)),R(N,N),ALFA(MXNL),PALFA(MXNL),
     & WORK(2*N*N+2*N*MXNLC*(MXNLP+1)+20*N+21*MXNLC*(MXNLP+1)),
     & PHL(MXNLC),A1(MXNN-1,MXNL),D1(MXNN),QL1(MXNL),HL(MXNLC,MXNL)
      LOGICAL OPTIMZ
      CHARACTER ANSWER*1
      COMMON/IVAR/NN,NL,NS,NLC,NEXC
      COMMON/IARRAY/UN,DN,NQL,FLDIR,HLP,LCEXCN
      COMMON/RARRAY/D,QN,PN,PQD,PQL,A,AA,PQ,QL,L,DI,ALFA
      EXTERNAL E04UCF,E04UEF,OBJFUN,CONFUN
C DATA INPUT
      OPEN(5,FILE='camonet.dat',FORM='FORMATTED')
      OPEN(6,FILE='camonet.res',FORM='FORMATTED')
      PRINT*,' OPTIMIZE ENTROPY? (Y/N) '
      READ 99999,ANSWER
      OPTIMZ=ANSWER.EQ.'Y' .OR. ANSWER.EQ.'y'
      PRINT*,' OPTIMZ =',OPTIMZ
      PRINT*,' NN ?'
      READ*,NN
      PRINT*,' # NODES =',NN
      PRINT*,' NL ?'
      READ*,NL
      PRINT*,' # LINKS =',NL
      PRINT*,' NS ?'
      READ*,NS
      PRINT*,' # SOURCES =',NS
      NLP=NL-NN+1
      PRINT*,' # LOOPS =',NLP
      PRINT*,' NLC ?'
      READ*,NLC
      PRINT*,' # LOAD CASES =',NLC
```

```
      PRINT*,' NEXC ?'
      READ*,NEXC
      PRINT*,' # EXTRA CONSTRAINTS =',NEXC
      IF(NLC.GT.MXNLC)THEN
        PRINT*,' ARRAYS TOO SMALL, NLC .GT. MXNLC. PROG STOPPED'
      ELSE IF(NEXC.GT.MXNLC)THEN
        PRINT*,' ARRAYS TOO SMALL, NEXC .GT. MXNLC. PROG STOPPED'
      ELSE IF(NLP.GT.MXNLP)THEN
        PRINT*,' ARRAYS TOO SMALL, NLP .GT. MXNLP. PROG STOPPED'
      ELSE IF(NN.GT.MXNN)THEN
        PRINT*,' ARRAYS TOO SMALL, NN .GT. MXNN. PROG STOPPED'
      ELSE IF(NL.GT.MXNL)THEN
        PRINT*,' ARRAYS TOO SMALL, NL .GT. MXNL. PROGRAM TERMINATED'
        STOP
      END IF
      DO 550 I=1,NLC
      PRINT*,' FOR LOAD CASE',I,' INPUT THE FOLLOWING:'
      PRINT*,' ------------------------------------'
      PRINT*,' FOR EACH LINK INPUT UN, DN'
      DO 100 J=1,NL
      READ*,UN(I,J),DN(I,J)
  100  CONTINUE
      PRINT*,' FOR EACH NODE INPUT D, (SOURCE -VE)'
      DO 150 J=1,NN
      READ*,D(I,J)
  150  CONTINUE
C SET UP CONTINUITY MATRIX
      DO 250 J=1,NN-1
      DO 200 K=1,NL
      IF(UN(I,K).EQ.J)A(I,J,K)=-1.0D0
      IF(DN(I,K).EQ.J)A(I,J,K)=1.0D0
  200  CONTINUE
  250  CONTINUE
      PRINT*,' INPUT (STARTING) FLOWS FOR THE LAST',NLP,' LINK(S)'
      K=I-1
      READ*,(X(NLP*K+J),J=1,NLP)
      PRINT*,' THE INPUT FLOWS ARE'
      DO 300 J=1,NLP
      K=I-1
      PRINT*,' QL(',I,',',NL-NLP+J,' ) =',X(NLP*K+J)
  300  CONTINUE
      DO 350 J=1,NLP
      K=I-1
      QL(I,NL-NLP+J)=X(NLP*K+J)
  350  CONTINUE
C COMPUTE DEPENDENT FLOWS
      DO 360 J=1,NN-1
      DO 355 K=1,NL
      A1(J,K)=A(I,J,K)
      QL1(K)=QL(I,K)
  355  CONTINUE
  360  CONTINUE
      DO 365 J=1,NN
      D1(J)=D(I,J)
  365  CONTINUE
      CALL GAUSS(MXNN-1,MXNL,NN-1,NL,NLP,A1,AA,D1,QL1)
```

```
      DO 375 J=1,NN-1
      DO 370 K=1,NL
      A(I,J,K)=A1(J,K)
      QL(I,K)=QL1(K)
  370  CONTINUE
  375  CONTINUE
      DO 380 J=1,NN
      D(I,J)=D1(J)
  380  CONTINUE
      ERR=1.0D-6
      DO 450 J=1,NN
      QIN=0.0D0
      QOUT=0.0D0
      DO 400 K=1,NL
      IF(QL(I,K).LT.0.0D0)THEN
      PRINT*,'  *** WARNING ***  QL(',I,',',UN(I,K),DN(I,K),' )'
      PRINT*,'                   IS -VE FOR LOAD CASE',I
      PRINT*,'QL(',I,',',UN(I,K),DN(I,K),' ) =',QL(I,K)
      IF(ABS(QL(I,K)).GT.ERR)PRINT*,' EXECUTION ABORTED'
      STOP
      END IF
      IF(DN(I,K).EQ.J)QIN=QIN+QL(I,K)
      IF(UN(I,K).EQ.J)QOUT=QOUT+QL(I,K)
  400  CONTINUE
      IF(ABS(QIN-QOUT-D(I,J)) .GT. ERR)THEN
      PRINT*,' FLOWS DO NOT BALANCE AT NODE',J,' FOR LOAD CASE',I
      PRINT*,' NET INTERN. FLO = ',QIN-QOUT
      PRINT*,' D(',I,',',J,')=',D(I,J)
      PRINT*,' PROGRAM STOPPED'
      STOP
      END IF
  450  CONTINUE
      PRINT*,' THE COMPLETE INPUT FLOWS ARE'
      DO 500 J=1,NL
      PRINT*,' QL(',I,',',UN(I,J),DN(I,J),' ) =',QL(I,J)
  500  CONTINUE
  550  CONTINUE
      PRINT*,' ---------------------------------------'
      PRINT*,' FOR EACH LINK INPUT (STARTING) PIPE CHARACTERISTIC ALFA'
      READ*,(X(I),I=NLP*NLC+1,NLP*NLC+NL)
      PRINT*,' THE INPUT PIPE CHARACTERISTICS ARE'
      DO 600 I=1,NL
      J=NLP*NLC+I
      PRINT*,' ALFA(',UN(1,I),DN(1,I),' ) =',X(J)
  600  CONTINUE
      NV=NLP*NLC+NL
      CALL OBJFUN(MODE,NV,X,F,OBJGRD,NSTATE,IUSER,USER)
      PRINT*,' FUNCTION VALUE FOR INPUT DATA IS'
      PRINT*,' F =',F
      IF(OPTIMZ)THEN
      PRINT*,' FOR EACH LINK INPUT LENGTH L'
      READ*,(L(I),I=1,NL)
      PRINT*,' FOR EACH LINK INPUT DIAMETER DI'
      READ*,(DI(I),I=1,NL)
      PRINT*,' FOR EACH LOOP  IN EACH  LOAD CASE  INPUT  UNIT VALUE'
      PRINT*,'     FOR  EACH LINK  EXISTED IN  THE LOOP , CLOCKWISE'
```

```
      PRINT*,'     (+VE), WITH ZERO VALUE FOR EACH LINK NOT EXISTED'
      PRINT*,'     IN THAT LOOP'
      DO 650 I=1,NLP*NLC
      READ*,(FLDIR(I,J),J=1,NL)
650   CONTINUE
      IF(NEXC.NE.0)THEN
      PRINT*,' INPUT THE PATH HEAD LOSS FOR EACH EXTRA CONSTRAINT'
      READ*, (PHL(I),I=1,NEXC)
      PRINT*,' FOR EACH  PATH  OF  HEAD  LOSS  CONSTRAINT  INPUT THE'
      PRINT*,'     CORRESPONDING  LOAD CASE NUMBER , AND  INPUT UNIT'
      PRINT*,'     VALUE  FOR EACH  LINK EXISTED IN  THE PATH , WITH'
      PRINT*,'     ZERO VALUE FOR EACH LINK NOT EXISTED IN THAT PATH'
      DO 700 I=1,NEXC
      READ*, LCEXCN(I), (HLP(I,J),J=1,NL)
700   CONTINUE
      END IF
      PRINT*,' FOR EACH LOAD CASE INPUT THE',NLP,' FLOW LOWER BOUNDS'
      READ*, (BL(I),I=1,NLP*NLC)
      PRINT*,' FOR EACH LOAD CASE INPUT THE',NLP,' FLOW UPPER BOUNDS'
      READ*, (BU(I),I=1,NLP*NLC)
      PRINT*,' INPUT PIPE CHARACTERISTIC LOWER BOUND'
      READ*, PCLB
      PRINT*,' INPUT PIPE CHARACTERISTIC UPPER BOUND'
      READ*, PCUB
      DO 800 I=NLP*NLC+1,NLP*NLC+NL
      BL(I)=PCLB
      BU(I)=PCUB
800   CONTINUE
      DO 900 I=NLP*NLC+NL+1,2*NLP*NLC+NL
      BL(I)=0.0D0
      BU(I)=0.0D0
900   CONTINUE
      IF(NEXC.NE.0)THEN
      DO 950 I=1,NEXC
      BL(2*NLP*NLC+NL+I)=PHL(I)
      BU(2*NLP*NLC+NL+I)=PHL(I)
950   CONTINUE
      END IF
      NCNLN=NLP*NLC+NEXC
      LDA=1
      LDCJ=NCNLN
      LDR=NV
      LIWORK=3*NV+2*NCNLN
      LWORK=2*NV**2+2*NV*NCNLN+20*NV+21*NCNLN
C     CALL X04AAF(1,6)
C     CALL X04ABF(1,6)
      CALL E04UEF(' DERIVATIVE LEVEL 0')
      CALL E04UEF(' MAJOR ITERATION LIMIT 1000')
      CALL E04UEF(' MINOR ITERATION LIMIT 2000')
C     CALL E04UEF(' LINESEARCH TOLERANCE 9.00D-03')
C     CALL E04UEF(' HESSIAN YES')
C     CALL E04UEF(' STEP LIMIT 1')
C     CALL E04UEF(' MAJOR PRINT LEVEL 30')
C     CALL E04UEF(' MINOR PRINT LEVEL 30')
C     CALL E04UEF(' OPTIMALITY TOLERANCE 1.0D-3')
C     CALL E04UEF(' FUNCTION PRECISION 1.0D-8')
```

```
      IFAIL=-1
      CALL E04UCF(NV,NCLIN,NCNLN,LDA,LDCJ,LDR,
     & AB,BL,BU,CONFUN,OBJFUN,ITER,ISTATE,C,CJAC,
     & CLAMDA,F,OBJGRD,R,X,IWORK,LIWORK,WORK,LWORK,
     & IUSER,USER,IFAIL)
      DO 1150 I=1,NLC
      DO 1000 J=1,NLP
      K=I-1
      QL(I,NL-NLP+J)=X(NLP*K+J)
1000  CONTINUE
      DO 1010 J=1,NN-1
      DO 1005 K=1,NL
      A1(J,K)=A(I,J,K)
      QL1(K)=QL(I,K)
1005  CONTINUE
1010  CONTINUE
      DO 1015 J=1,NN
      D1(J)=D(I,J)
1015  CONTINUE
      CALL GAUSS(MXNN-1,MXNL,NN-1,NL,NLP,A1,AA,D1,QL1)
      DO 1025 J=1,NN-1
      DO 1020 K=1,NL
      A(I,J,K)=A1(J,K)
      QL(I,K)=QL1(K)
1020  CONTINUE
1025  CONTINUE
      DO 1030 J=1,NN
      D(I,J)=D1(J)
1030  CONTINUE
      DO 1100 J=1,NN
      QIN=0.0D0
      QOUT=0.0D0
      DO 1050 K=1,NL
      IF(QL(I,K).LT.0.0D0)THEN
      PRINT*,'  *** WARNING ***  QL(',I,',',UN(I,K),DN(I,K),')'
      PRINT*,'                   IS -VE FOR LOAD CASE',I
      PRINT*,'QL(',I,',',UN(I,K),DN(I,K),')=',QL(I,K)
      END IF
      IF(DN(I,K).EQ.J)QIN=QIN+QL(I,K)
      IF(UN(I,K).EQ.J)QOUT=QOUT+QL(I,K)
1050  CONTINUE
      IF(ABS(QIN-QOUT-D(I,J)) .GT. ERR)THEN
      PRINT*,' FLOWS DO NOT BALANCE AT NODE',J,'FOR LOAD CASE',I
      END IF
1100  CONTINUE
1150  CONTINUE
      CALL OBJFUN(MODE,NV,X,F,OBJGRD,NSTATE,IUSER,USER)
      PRINT*,' IFAIL =',IFAIL
      IF (IFAIL .EQ. 0)THEN
      PRINT*,' FUNCTION VALUE ON SUCCESSFUL EXIT IS'
      PRINT*,' F=',F
      DO 1250 I=1,NLC
      PRINT*,' ALL THE OPTIMAL LINK FLOWS FOR LOAD CASE',I,' ARE'
      DO 1200 J=1,NL
      PRINT*,' QL(',I,',',UN(I,J),DN(I,J),' ) =',QL(I,J)
1200  CONTINUE
```

```
1250  CONTINUE
      PRINT*,' ALL THE OPTIMAL PIPE CHARACTERISTICS ARE'
      DO 1300 I=1,NL
      J=NLP*NLC+I
      PRINT*,' ALFA(',UN(1,I),DN(1,I),' ) =',X(J)
1300  CONTINUE
      END IF
      IF(IFAIL .NE. 0)THEN
      PRINT*,' *** IFAIL =',IFAIL,'!!!'
      PRINT*,' *** UNSUCCESSFUL EXIT !!!'
      PRINT*,' FUNCTION VALUE ON UNSUCCESSFUL EXIT IS'
      PRINT*,' F=',F
      DO 1400 I=1,NLC
      PRINT*,' ALL LINK FLOWS ON EXIT FOR LOAD CASE',I,' ARE'
      DO 1350 J=1,NL
      PRINT*,' QL(',I,',',UN(I,J),DN(I,J),' ) =',QL(I,J)
 1350  CONTINUE
 1400  CONTINUE
      PRINT*,' ALL PIPE CHARACTERISTICS ON EXIT ARE'
      DO 1450 I=1,NL
      J=NLP*NLC+I
      PRINT*,' ALFA(',UN(1,I),DN(1,I),' ) =',X(J)
 1450  CONTINUE
      END IF
      SUM=0.0D0
      DO 1500 I=NLP*NLC+1,NLP*NLC+NL
      SUM=SUM+X(I)
 1500  CONTINUE
      DO 1550 I=1,NL
      J=NLP*NLC+I
      PALFA(I)=X(J)/SUM
 1550  CONTINUE
      PRINT*,' ALL PIPE CHARACTERISTIC PROBABILITIES ARE'
      DO 1600 I=1,NL
      PRINT*,' PALFA(',UN(1,I),DN(1,I),' ) =',PALFA(I)
 1600  CONTINUE
      DO 1700 I=1,NLC
      PRINT*,' THE HEAD LOSSES IN THE LINKS FOR LOAD CASE',I,' ARE'
      DO 1650 J=1,NL
      K=NLP*NLC+J
      HL(I,J)=X(K)*L(J)*QL(I,J)**(1.852)*DI(J)**(-4.87)
      PRINT*,' HL(',I,',',UN(I,J),DN(I,J),' ) =',HL(I,J)
 1650  CONTINUE
 1700  CONTINUE
      END IF
      STOP
99999 FORMAT(A1)
      END
C
C SUBROUTINE OBJFUN COMPUTES ENTROPY VALUE FOR ANY GIVEN DATA
C
      SUBROUTINE OBJFUN (MODE,NV,X,F,OBJGRD,
     & NSTATE,IUSER,USER)
      IMPLICIT DOUBLE PRECISION (A-H,O-Z)
      PARAMETER(MXNN=20,MXNL=40,MXNLP=21,MXNLC=10,MXCN=5)
      INTEGER UN(MXNLC,MXNL),DN(MXNLC,MXNL),NQL(MXNLC,MXNN),
```

```
& IUSER(*),FLDIR(MXNLP*MXNLC,MXNL),HLP(MXNLC,MXNL),
& LCEXCN(MXNLC)
 DOUBLE PRECISION D(MXNLC,MXNN),QN(MXNLC,0:MXNN),
& QL(MXNLC,MXNL),PQL(MXNLC,MXNN,MXCN),PQD(MXNLC,MXNN),
& PN(MXNN),A(MXNLC,MXNN-1,MXNL),PQ(MXNL),X(NV),
& AA(MXNN-1,MXNL+1),OBJGRD(NV),USER(*),L(MXNL),
& DI(MXNL),ALFA(MXNL),A1(MXNN-1,MXNL),D1(MXNN),QL1(MXNL)
 COMMON/IVAR/NN,NL,NS,NLC,NEXC
 COMMON/IARRAY/UN,DN,NQL,FLDIR,HLP,LCEXCN
 COMMON/RARRAY/D,QN,PN,PQD,PQL,A,AA,PQ,QL,L,DI,ALFA
 V(P)=-P*DLOG(P)
 NLP=(NV-NL)/NLC
 ENT=0.0D0
 DO 900 I=1,NLC
 DO 100 J=1,NLP
 K=I-1
      QL(I,NL-NLP+J)=X(NLP*K+J)
100   CONTINUE
      DO 120 J=1,NN-1
      DO 110 K=1,NL
      A1(J,K)=A(I,J,K)
      QL1(K)=QL(I,K)
110   CONTINUE
120   CONTINUE
      DO 130 J=1,NN
      D1(J)=D(I,J)
130   CONTINUE
      CALL GAUSS(MXNN-1,MXNL,NN-1,NL,NLP,A1,AA,D1,QL1)
      DO 150 J=1,NN-1
      DO 140 K=1,NL
      A(I,J,K)=A1(J,K)
      QL(I,K)=QL1(K)
140   CONTINUE
150   CONTINUE
      DO 160 J=1,NN
      D(I,J)=D1(J)
160   CONTINUE
C SUM SOURCE SUPPLIES
      QN(I,0)=0.0D0
      DO 200 J=1,NS
      QN(I,0)=QN(I,0)-D(I,J)
200   CONTINUE
      DO 400 J=1,NN
      NQL(I,J)=0
      QN(I,J)=0.0D0
      IF(J.GT.NS)QN(I,J)=QN(I,J)+D(I,J)
      DO 300 K=1,NL
      IF(UN(I,K).EQ.J)THEN
      NQL(I,J)=NQL(I,J)+1
      QN(I,J)=QN(I,J)+QL(I,K)
      END IF
300   CONTINUE
400   CONTINUE
      DO 600 J=1,NN
      IF(J.GT.NS)PQD(I,J)=D(I,J)/QN(I,J)
      K=0
```

```
      DO 500 M=1,NL
      IF(UN(I,M).EQ.J)THEN
      K=K+1
      PQL(I,J,K)=QL(I,M)/QN(I,J)
      END IF
500   CONTINUE
600   CONTINUE
      S=0.0D0
      DO 800 J=1,NN
      S1=0.0D0
      DO 700 K=1,NQL(I,J)
      IF(PQL(I,J,K).NE.0.0D0)S1=S1+V(PQL(I,J,K))
700   CONTINUE
      IF(J.GT.NS)S1=S1+V(PQD(I,J))
      S=S+S1*QN(I,J)/QN(I,0)
800   CONTINUE
C ADD ENTROPY DUE TO DISTRIBUTION OF SOURCE FLOWS
      DO J=1,NS
        S=S+V(-D(I,J)/QN(I,0))
      END DO
      ENT=ENT+S
900   CONTINUE
      DPNLC=NLC
      ENT=ENT*DPNLC**(-1)
C ADD ENTROPY DUE TO PIPE CHARACTERISTICS
      SUMALFA=0.0D0
      DO I=NLP*NLC+1,NLP*NLC+NL
        SUMALFA=SUMALFA+X(I)
      END DO
      DO I=NLP*NLC+1,NLP*NLC+NL
        ENT=ENT+V(X(I)/SUMALFA)
      END DO
      F=-ENT
      RETURN
      END
C
C SUBROUTINE CONFUN COMPUTES THE VALUES OF THE NONLINEAR CONSTRAINTS
C
      SUBROUTINE CONFUN(MODE,NCNLN,NV,LDCJ,NEEDC,X,
     & C,CJAC,NSTATE,IUSER,USER)
      IMPLICIT DOUBLE PRECISION (A-H,O-Z)
      PARAMETER(MXNN=20,MXNL=40,MXNLP=21,MXNLC=10,MXCN=5)
      INTEGER UN(MXNLC,MXNL),DN(MXNLC,MXNL),NQL(MXNLC,MXNN),
     & IUSER(*),NEEDC(*),FLDIR(MXNLP*MXNLC,MXNL),HLP(MXNLC,MXNL),
     & LCEXCN(MXNLC)
      DOUBLE PRECISION D(MXNLC,MXNN),QN(MXNLC,0:MXNN),
     & QL(MXNLC,MXNL),PQL(MXNLC,MXNN,MXCN),PQD(MXNLC,MXNN),
     & PN(MXNN),A(MXNLC,MXNN-1,MXNL),PQ(MXNL),X(NV),DI(MXNL),
     & AA(MXNN-1,MXNL+1),L(MXNL),C(MXNLC*(MXNLP+1)),CJAC(LDCJ,*),
     & USER(*),ALFA(MXNL),A1(MXNN-1,MXNL),D1(MXNN),QL1(MXNL)
      COMMON/IVAR/NN,NL,NS,NLC,NEXC
      COMMON/IARRAY/UN,DN,NQL,FLDIR,HLP,LCEXCN
      COMMON/RARRAY/D,QN,PN,PQD,PQL,A,AA,PQ,QL,L,DI,ALFA
      NLP=(NV-NL)/NLC
      DO 100 I=1,NL
      J=NLP*NLC+I
```

```
      ALFA(I)=X(J)
100   CONTINUE
      DO 500 I=1,NLC
      DO 200 J=1,NLP
      K=I-1
      QL(I,NL-NLP+J)=X(NLP*K+J)
200   CONTINUE
      DO 220 J=1,NN-1
      DO 210 K=1,NL
      A1(J,K)=A(I,J,K)
      QL1(K)=QL(I,K)
210   CONTINUE
220   CONTINUE
      DO 230 J=1,NN
      D1(J)=D(I,J)
230   CONTINUE
      CALL GAUSS(MXNN-1,MXNL,NN-1,NL,NLP,A1,AA,D1,QL1)
      DO 250 J=1,NN-1
      DO 240 K=1,NL
      A(I,J,K)=A1(J,K)
      QL(I,K)=QL1(K)
240   CONTINUE
250   CONTINUE
      DO 260 J=1,NN
      D(I,J)=D1(J)
260   CONTINUE
      DO 400 J=1,NLP
      K=I-1
      C(NLP*K+J)=0.0D0
      DO 300 M=1,NL
      IF(FLDIR(NLP*K+J,M).NE.0) THEN
      C(NLP*K+J)=C(NLP*K+J)+FLDIR(NLP*K+J,M)*ALFA(M)*
     & QL(I,M)**(1.852)*L(M)*DI(M)**(-4.87)
      END IF
300   CONTINUE
400   CONTINUE
500   CONTINUE
      IF(NEXC.NE.0)THEN
      DO 700 I=1,NEXC
      C(NLP*NLC+I)=0.0D0
      DO 600 J=1,NL
      IF(HLP(I,J).NE.0) THEN
      C(NLP*NLC+I)=C(NLP*NLC+I)+HLP(I,J)*ALFA(J)*
     & QL(LCEXCN(I),J)**(1.852)*L(J)*DI(J)**(-4.87)
      END IF
600   CONTINUE
700   CONTINUE
      END IF
      RETURN
      END
C
C SUBROUTINE NAME: GAUSS
C
C PURPOSE: SOLUTION OF (NR)X(NC) (NR<NC) SIMULTANEOUS EQUATIONS BY
GAUSS
C ELIMINATION. THE LAST (NC)-(NR) VARIABLES MUST BE KNOWN AND SUPPLIED
```

```
C AS DATA. E.G IF FOR 7 (NC) VARIABLES & 5 (NR) EQUATIONS, THE VALUE
C OF THE LAST 2 VARIABLES MUST BE SUPPLIED AS DATA.
C ARGUMENTS:
C NR=NO. OF ROWS=NO. OF EQNS.
C NC=NO. COLUMNS=NO. OF VARIABLES.
C A=(NR)X(NC) MATRIX OF COEFFIEIDNTS OF THE VARIABLES X. UNCHANGED ON
C EXIT.
C AA=AUGMENTED MATRIX. CONTAINS UPPER 'TRAPEZOIDAL' MATRIX ON EXIT.
C X=VECTOR OF THE NC VARIABLES
C B=VECTOR OF THE RHS'S OF THE NR EQUATIONS. UNCHANGED ON EXIT
      SUBROUTINE GAUSS(IR,IC,NR,NC,NLPS,A,AA,B,X)
      IMPLICIT DOUBLE PRECISION (A-H,O-Z)
      DOUBLE PRECISION A(IR,IC),AA(IR,IC+1),B(IR),X(IC)
C AUGMENT MATRIX A BY MATRIX B
      DO 200 I=1,NR
      DO 100 J=1,NC
      AA(I,J)= A(I,J)
100   CONTINUE
200   CONTINUE
      DO 300 I=1,NR
      AA(I,NC+1)=B(I)
300   CONTINUE
C REDUCE AUGMENTED MATRIX TO UPPER TRAPEZOIDAL MATRIX
      DO 800 I=1,NR-1
C FIND LARGEST ELEMENT IN PIVOT COLUMN
      IPIVOT=I
      AMAX=ABS(AA(I,I))
      DO 400 J=I+1,NC
      IF(ABS(AA(J,I)).GT.AMAX)THEN
      AMAX=ABS(AA(J,I))
      IPIVOT=J
      END IF
400   CONTINUE
C PERFORM ROW EXCHANGE IF NECESSARY TO AVOID LARGE PIVOT RATIOS,
HENCE
C ROUDING OFF ERRORS
      IF(IPIVOT.NE.I)THEN
      DO 500 K=I,NC+1
      TEMP=AA(I,K)
      AA(I,K)=AA(IPIVOT,K)
      AA(IPIVOT,K)=TEMP
500   CONTINUE
      END IF
C PIVOT
      DO 700 J=I+1,NR
      PRATIO=AA(J,I)/AA(I,I)
      DO 600 K=I+1,NC+1
      AA(J,K)=AA(J,K)-AA(I,K)*PRATIO
600   CONTINUE
700   CONTINUE
800   CONTINUE
C BACKSUBSTITUTE
      DO 1000 I=NC-NLPS,1,-1
      SUM=0.0
      DO 900 K=I+1,NC
      SUM=SUM+AA(I,K)*X(K)
```

```
      X(I)=(AA(I,NC+1)-SUM)/AA(I,I)
900   CONTINUE
1000  CONTINUE
      RETURN
      END
```

APPENDIX E

SOME OF THE CAMONET COMPUTER PROGRAMME APPLICATIONS OF CHAPTER 7

E.1 EXAMPLE 1

E.1.1 RUN 1

The input file:

```
y
6
7
1
1
0
1 2
2 4
3 4
4 6
5 6
1 3
3 5
-.284
.028
.033
.075
.092
.056
.2 .1
1 1 1 1 1 1 1
1 1 1 1 1 1 1
1 1 1 1 1 1 1
1 1 -1 0 0 -1 0
0 0 1 1 -1 0 -1
.126 .093
.255 .147
1.0d-3
1.0d+3
```

The output file:

```
 OPTIMIZE ENTROPY? (Y/N)
 OPTIMZ =  T
 NN ?
 # NODES =  6
 NL ?
 # LINKS =  7
 NS ?
 # SOURCES =  1
 # LOOPS =  2
 NLC ?
 # LOAD CASES =  1
 NEXC ?
 # EXTRA CONSTRAINTS =  0
 FOR LOAD CASE  1 INPUT THE FOLLOWING:
 ------------------------------
 FOR EACH LINK INPUT UN, DN
 FOR EACH NODE INPUT D, (SOURCE -VE)
 INPUT (STARTING) FLOWS FOR THE LAST  2 LINK(S)
 THE INPUT FLOWS ARE
 QL(  1,  6 ) =   0.20000000000000
 QL(  1,  7 ) =    1.0000000000000D-01
 THE COMPLETE INPUT FLOWS ARE
 QL(  1,  1  2 ) =    8.4000000000000D-02
 QL(  1,  2  4 ) =    5.6000000000000D-02
 QL(  1,  3  4 ) =    6.7000000000000D-02
 QL(  1,  4  6 ) =    4.8000000000000D-02
 QL(  1,  5  6 ) =    8.0000000000000D-03
 QL(  1,  1  3 ) =   0.20000000000000
 QL(  1,  3  5 ) =    1.0000000000000D-01
 ------------------------------
 FOR EACH LINK INPUT (STARTING) PIPE CHARACTERISTIC ALFA
 THE INPUT PIPE CHARACTERISTICS ARE
 ALFA(  1  2 ) =    1.0000000000000
 ALFA(  2  4 ) =    1.0000000000000
 ALFA(  3  4 ) =    1.0000000000000
 ALFA(  4  6 ) =    1.0000000000000
 ALFA(  5  6 ) =    1.0000000000000
 ALFA(  1  3 ) =    1.0000000000000
 ALFA(  3  5 ) =    1.0000000000000
 FUNCTION VALUE FOR INPUT DATA IS
 F =   -3.8406898845982
 FOR EACH LINK INPUT LENGTH L
 FOR EACH LINK INPUT DIAMETER DI
 FOR EACH LOOP  IN EACH  LOAD CASE  INPUT  UNIT VALUE
    FOR  EACH LINK  EXISTED IN  THE LOOP , CLOCKWISE
    (+VE), WITH ZERO VALUE FOR EACH LINK NOT EXISTED
    IN THAT LOOP
 FOR EACH LOAD CASE INPUT THE  2 FLOW LOWER BOUNDS
 FOR EACH LOAD CASE INPUT THE  2 FLOW UPPER BOUNDS
 INPUT PIPE CHARACTERISTIC LOWER BOUND
 INPUT PIPE CHARACTERISTIC UPPER BOUND
```

Calls to E04UEF

DERIVATIVE LEVEL 0
MAJOR ITERATION LIMIT 1000
MINOR ITERATION LIMIT 2000

*** E04UCF
*** Start of NAG Library implementation details ***

Implementation title: Sun Solaris
Precision: Fortran Double Precision
Product Code: FLSOL16D
Mark: 16A

*** End of NAG Library implementation details ***

Parameters

Linear constraints.....	0	Linear feasibility.....	1.05D-08
Variables.....	9	Crash tolerance.....	1.00D-02
Infinite bound size....	1.00D+20	COLD start.....	
Infinite step size.....	1.00D+20	EPS (machine precision)	1.11D-16
Step limit.....	2.00D+00	Hessian.....	NO
Nonlinear constraints..	2	Nonlinear feasibility..	5.43D-06
Nonlinear objectiv vars	9	Optimality tolerance...	3.26D-12
Nonlinear Jacobian vars	9	Linesearch tolerance...	9.00D-01
Derivative level.....	0	Function precision.....	4.37D-15
Verify level.....	0	Monitoring file.....	-1
Major iterations limit.	1000	Major print level.....	10
Minor iterations limit.	2000	Minor print level.....	0

Difference intervals to be computed.

Workspace provided is IWORK(31), WORK(420).
To solve problem we need IWORK(31), WORK(420).

The user sets 0 out of 18 Jacobian elements.
Each iteration, 18 Jacobian elements will be estimated numerically.

The user sets 0 out of 9 objective gradient elements.
Each iteration, 9 gradient elements will be estimated numerically.

Computation of the finite-difference intervals

J	X(J)	Forward DX(J)	Central DX(J)	Error est.
1	2.00D-01	3.251179D-08	1.587252D-06	3.678735D-06

2	9.30D-02	5.760113D-09	1.445722D-06	2.076387D-05
3	1.00D+00	9.897526D-07	9.897526D-06	1.208406D-07
4	1.00D+00	9.897526D-07	9.897526D-06	1.208406D-07
5	1.00D+00	9.897526D-07	9.897526D-06	1.208406D-07
6	1.00D+00	9.897526D-07	9.897526D-06	1.208406D-07
7	1.00D+00	9.897526D-07	9.897526D-06	1.208406D-07
8	1.00D+00	9.897526D-07	9.897526D-06	1.208406D-07
9	1.00D+00	9.897526D-07	9.897526D-06	1.208406D-07

6 constant constraint gradient elements assigned.

Maj	Mnr	Step	Merit function	Violtn	Norm Gz	Cond Hz
0	1	0.0D+00	-3.669625D+00	4.4D-02	4.2D-02	1.0D+00
1	3	1.0D+00	-3.752099D+00	6.7D-01	2.3D-01	1.8D+00
2	2	4.1D-01	-3.780615D+00	7.9D-04	1.4D-01	1.5D+00
3	1	1.0D+00	-3.788903D+00	1.7D-04	4.5D-02	1.5D+00
4	1	1.0D+00	-3.791099D+00	2.1D-05	2.5D-02	1.7D+00
5	1	1.0D+00	-3.791757D+00	3.0D-06	2.2D-02	2.9D+00
6	1	1.0D+00	-3.792764D+00	1.5D-05	1.4D-02	2.4D+00
7	1	1.0D+00	-3.793033D+00	3.8D-06	5.8D-03	2.8D+00
8	1	1.0D+00	-3.793071D+00	1.4D-06	1.2D-03	2.5D+00
9	1	1.0D+00	-3.793073D+00	4.7D-09	7.6D-04	3.8D+00
10	1	1.0D+00	-3.793074D+00	3.4D-09	6.3D-04	3.2D+00
11	1	1.0D+00	-3.793075D+00	3.2D-09	4.4D-04	4.9D+00
12	1	1.0D+00	-3.793075D+00	1.5D-09	2.0D-04	4.3D+00
13	1	1.0D+00	-3.793075D+00	6.7D-10	4.6D-05	3.8D+00
14	1	1.0D+00	-3.793075D+00	2.5D-11	2.0D-05	4.5D+00
15	1	1.0D+00	-3.793075D+00	1.4D-12	1.7D-05	3.5D+00
16	1	1.0D+00	-3.793075D+00	3.6D-12	1.0D-05	2.7D+00
17	1	1.0D+00	-3.793075D+00	2.4D-12	4.4D-06	2.5D+00
18	1	1.0D+00	-3.793075D+00	1.1D-12	9.9D-07	3.4D+00
19	1	1.0D+00	-3.793075D+00	1.3D-14	3.9D-07	3.5D+00

Exit from NP problem after 19 major iterations,
23 minor iterations.

Varbl	State	Value	Lower Bound	Upper Bound	Lagr Mult	Residual
V 1	FR	0.184348	0.126000	0.255000	0.	5.8348E-02
V 2	FR	0.101208	9.300000E-02	0.147000	0.	8.2077E-03
V 3	FR	1.30355	1.000000E-03	1000.00	0.	1.303
V 4	FR	1.17704	1.000000E-03	1000.00	0.	1.176
V 5	FR	1.14555	1.000000E-03	1000.00	0.	1.145
V 6	FR	1.19679	1.000000E-03	1000.00	0.	1.196
V 7	FR	1.03561	1.000000E-03	1000.00	0.	1.035
V 8	FR	0.518965	1.000000E-03	1000.00	0.	0.5180
V 9	FR	0.586509	1.000000E-03	1000.00	0.	0.5855

N Con	State	Value	Lower Bound	Upper Bound	Lagr Mult	Residual
N 1	EQ	-1.065120E-14	0.	0.	2.295	-1.0651E-14
N 2	EQ	6.642256E-15	0.	0.	5.747	6.6423E-15

Exit E04UCF - Optimal solution found.

Final objective value = -3.793075
IFAIL = 0
FUNCTION VALUE ON SUCCESSFUL EXIT IS
F= -3.7930752928082
ALL THE OPTIMAL LINK FLOWS FOR LOAD CASE 1 ARE
QL(1, 1 2) = 9.9651705627388D-02
QL(1, 2 4) = 7.1651705627388D-02
QL(1, 3 4) = 5.0140551311425D-02
QL(1, 4 6) = 4.6792256938814D-02
QL(1, 5 6) = 9.2077430611863D-03
QL(1, 1 3) = 0.18434829437261
QL(1, 3 5) = 1.0120774306119D-01
ALL THE OPTIMAL PIPE CHARACTERISTICS ARE
ALFA(1 2) = 1.3035489749548
ALFA(2 4) = 1.1770424525642
ALFA(3 4) = 1.1455511193369
ALFA(4 6) = 1.1967903585545
ALFA(5 6) = 1.0356136950591
ALFA(1 3) = 0.51896498652445
ALFA(3 5) = 0.58650871327005
ALL PIPE CHARACTERISTIC PROBABILITIES ARE
PALFA(1 2) = 0.18718339676657
PALFA(2 4) = 0.16901766534477
PALFA(3 4) = 0.16449566054445
PALFA(4 6) = 0.17185337017314
PALFA(5 6) = 0.14870917234688
PALFA(1 3) = 7.4520889392692D-02
PALFA(3 5) = 8.4219845431497D-02
THE HEAD LOSSES IN THE LINKS FOR LOAD CASE 1 ARE
HL(1, 1 2) = 1.8210467046009D-02
HL(1, 2 4) = 8.9263038480448D-03
HL(1, 3 4) = 4.4850232239074D-03
HL(1, 4 6) = 4.1226865558273D-03
HL(1, 5 6) = 1.7571526687855D-04
HL(1, 1 3) = 2.2651747670157D-02
HL(1, 3 5) = 8.4319945128495D-03

E.1.2 RUN 2

The input file:

```
y
6
7
1
1
1
1 2
2 4
3 4
4 6
5 6
1 3
3 5
-.284
.028
.033
.075
.092
.056
.2 .1
1 1 1 1 1 1 1
1 1 1 1 1 1 1
1 1 1 1 1 1 1
1 1 -1 0 0 -1 0
0 0 1 1 -1 0 -1
20
1 0 0 1 1 0 1 0
.126 .093
.284 .284
1.0d-3
1.0d+3
```

The output file:

```
 OPTIMIZE ENTROPY? (Y/N)
 OPTIMZ =  T
 NN ?
 # NODES =  6
 NL ?
 # LINKS =  7
 NS ?
 # SOURCES =  1
 # LOOPS =  2
 NLC ?
 # LOAD CASES =  1
 NEXC ?
 # EXTRA CONSTRAINTS =  1
 FOR LOAD CASE  1 INPUT THE FOLLOWING:
 ------------------------------
 FOR EACH LINK INPUT UN, DN
 FOR EACH NODE INPUT D, (SOURCE -VE)
 INPUT (STARTING) FLOWS FOR THE LAST  2 LINK(S)
 THE INPUT FLOWS ARE
 QL(  1,  6 ) =   0.20000000000000
 QL(  1,  7 ) =    1.0000000000000D-01
 THE COMPLETE INPUT FLOWS ARE
 QL(  1,  1  2 ) =    8.4000000000000D-02
 QL(  1,  2  4 ) =    5.6000000000000D-02
 QL(  1,  3  4 ) =    6.7000000000000D-02
 QL(  1,  4  6 ) =    4.8000000000000D-02
 QL(  1,  5  6 ) =    8.0000000000000D-03
 QL(  1,  1  3 ) =   0.20000000000000
 QL(  1,  3  5 ) =    1.0000000000000D-01
 ------------------------------
 FOR EACH LINK INPUT (STARTING) PIPE CHARACTERISTIC ALFA
 THE INPUT PIPE CHARACTERISTICS ARE
 ALFA(  1  2 ) =    1.0000000000000
 ALFA(  2  4 ) =    1.0000000000000
 ALFA(  3  4 ) =    1.0000000000000
 ALFA(  4  6 ) =    1.0000000000000
 ALFA(  5  6 ) =    1.0000000000000
 ALFA(  1  3 ) =    1.0000000000000
 ALFA(  3  5 ) =    1.0000000000000
 FUNCTION VALUE FOR INPUT DATA IS
 F =   -3.8406898845982
 FOR EACH LINK INPUT LENGTH L
 FOR EACH LINK INPUT DIAMETER DI
 FOR EACH LOOP  IN EACH  LOAD CASE  INPUT  UNIT VALUE
    FOR  EACH LINK  EXISTED IN  THE LOOP , CLOCKWISE
    (+VE), WITH ZERO VALUE FOR EACH LINK NOT EXISTED
    IN THAT LOOP
 INPUT THE PATH HEAD LOSS FOR EACH EXTRA CONSTRAINT
 FOR EACH  PATH  OF  HEAD  LOSS  CONSTRAINT  INPUT THE
    CORRESPONDING  LOAD CASE NUMBER , AND  INPUT UNIT
    VALUE  FOR EACH  LINK EXISTED IN  THE PATH , WITH
    ZERO VALUE FOR EACH LINK NOT EXISTED IN THAT PATH
 FOR EACH LOAD CASE INPUT THE  2 FLOW LOWER BOUNDS
 FOR EACH LOAD CASE INPUT THE  2 FLOW UPPER BOUNDS
```

INPUT PIPE CHARACTERISTIC LOWER BOUND
INPUT PIPE CHARACTERISTIC UPPER BOUND

Calls to E04UEF

DERIVATIVE LEVEL 0
MAJOR ITERATION LIMIT 1000
MINOR ITERATION LIMIT 2000

*** E04UCF
*** Start of NAG Library implementation details ***

Implementation title: Sun Solaris
Precision: Fortran Double Precision
Product Code: FLSOL16D
Mark: 16A

*** End of NAG Library implementation details ***

Parameters

Linear constraints.....	0	Linear feasibility.....	1.05D-08
Variables.....	9	Crash tolerance.....	1.00D-02
Infinite bound size....	1.00D+20	COLD start.....	
Infinite step size.....	1.00D+20	EPS (machine precision)	1.11D-16
Step limit.....	2.00D+00	Hessian.....	NO
Nonlinear constraints..	3	Nonlinear feasibility..	5.43D-06
Nonlinear objectiv vars	9	Optimality tolerance...	3.26D-12
Nonlinear Jacobian vars	9	Linesearch tolerance...	9.00D-01
Derivative level.....	0	Function precision.....	4.37D-15
Verify level.....	0	Monitoring file.....	-1
Major iterations limit.	1000	Major print level.....	10
Minor iterations limit.	2000	Minor print level.....	0

Difference intervals to be computed.

Workspace provided is IWORK(33), WORK(459).
To solve problem we need IWORK(33), WORK(459).

The user sets 0 out of 27 Jacobian elements.
Each iteration, 27 Jacobian elements will be estimated numerically.

The user sets 0 out of 9 objective gradient elements.
Each iteration, 9 gradient elements will be estimated numerically.

Computation of the finite-difference intervals

J	X(J)	Forward DX(J)	Central DX(J)	Error est.
1	2.00D-01	3.430007D-08	1.587252D-06	4.029381D-06
2	9.30D-02	6.187888D-09	1.445722D-06	2.233526D-05
3	1.00D+00	1.063956D-06	1.063956D-05	1.299002D-07
4	1.00D+00	1.063956D-06	1.063956D-05	1.299002D-07
5	1.00D+00	1.063956D-06	1.063956D-05	1.299002D-07
6	1.00D+00	1.063956D-06	1.063956D-05	1.299002D-07
7	1.00D+00	1.063956D-06	1.063956D-05	1.299002D-07
8	1.00D+00	1.063956D-06	1.063956D-05	1.299002D-07
9	1.00D+00	1.063956D-06	1.063956D-05	1.299002D-07

10 constant constraint gradient elements assigned.

Maj	Mnr	Step	Merit function	Violtn	Norm Gz	Cond Hz	
0	6	0.0D+00	1.790036D+18	1.7D+03	0.0D+00	1.0D+00	I
1	8	5.0D-01	9.633685D+04	1.6D+01	5.2D-03	1.0D+00	LR
2	1	1.0D+00	-2.944674D+00	1.8D-01	3.2D-03	1.1D+01	R
3	2	1.0D+00	-3.405383D+00	1.8D-04	3.3D-03	1.0D+01	R
4	1	1.0D+00	-3.406177D+00	2.4D-07	3.1D-03	9.0D+00	R
5	1	1.0D+00	-3.440285D+00	6.1D-04	2.1D-03	1.1D+01	
6	1	1.0D+00	-3.489034D+00	2.5D-03	1.5D-03	3.5D+01	
7	1	1.0D+00	-3.575972D+00	1.8D-02	9.3D-04	7.0D+01	
8	1	1.0D+00	-3.640179D+00	2.7D-02	6.4D-04	1.2D+02	
9	1	1.0D+00	-3.676048D+00	2.7D-02	6.2D-04	1.7D+02	
10	1	1.0D+00	-3.689175D+00	1.3D-02	6.9D-04	2.1D+02	
11	1	1.0D+00	-3.692071D+00	3.2D-03	7.3D-04	2.1D+02	
12	1	1.0D+00	-3.693090D+00	7.1D-04	7.5D-04	9.4D+02	
13	1	1.0D+00	-3.695068D+00	1.2D-03	7.6D-04	2.2D+02	
14	1	1.0D+00	-3.699469D+00	1.1D-03	7.5D-04	3.5D+01	R
15	1	1.0D+00	-3.708202D+00	7.1D-03	6.8D-04	1.3D+02	
16	1	1.0D+00	-3.718169D+00	3.5D-02	5.5D-04	6.5D+02	
17	1	1.0D+00	-3.725819D+00	5.7D-02	4.0D-04	5.0D+02	
18	1	1.0D+00	-3.738484D+00	3.9D-02	3.1D-04	1.2D+03	R
19	1	1.0D+00	-3.746136D+00	5.2D-03	2.9D-04	8.9D+02	R
20	1	1.0D+00	-3.747099D+00	4.4D-03	2.9D-04	5.0D+02	R
21	1	1.0D+00	-3.747298D+00	5.3D-04	2.8D-04	2.1D+03	
22	1	1.0D+00	-3.747340D+00	3.8D-04	2.8D-04	9.5D+02	R
23	1	1.0D+00	-3.747355D+00	4.7D-06	2.8D-04	2.4D+02	R
24	1	1.0D+00	-3.749591D+00	7.5D-04	2.6D-04	7.4D+01	R
25	2	3.0D-01	-3.753846D+00	5.7D+02	2.6D-04	3.0D+01	R
26	2	7.4D-02	-3.758184D+00	7.4D-03	2.3D-04	1.9D+02	
27	1	3.5D-01	-3.763526D+00	1.1D-02	2.1D-04	3.1D+01	R
28	1	3.2D-01	-3.766551D+00	1.4D-02	2.0D-04	4.3D+01	R
29	1	3.6D-01	-3.768688D+00	1.6D-02	1.8D-04	5.1D+01	R
30	1	4.7D-01	-3.770258D+00	1.6D-02	1.8D-04	5.9D+01	R
31	1	1.0D+00	-3.771225D+00	1.8D-02	1.7D-04	7.2D+01	R
32	1	1.0D+00	-3.772212D+00	1.1D-03	1.7D-04	6.2D+01	R
33	1	1.0D+00	-3.772363D+00	1.5D-03	1.6D-04	8.7D+01	R
34	1	1.0D+00	-3.772650D+00	2.5D-03	1.6D-04	1.0D+02	R
35	1	1.0D+00	-3.773279D+00	6.2D-03	1.6D-04	1.1D+02	R
36	1	1.0D+00	-3.774542D+00	1.2D-02	1.5D-04	1.3D+02	R
37	1	1.0D+00	-3.776835D+00	1.9D-02	1.5D-04	1.6D+02	R
38	1	1.0D+00	-3.780207D+00	2.6D-02	1.3D-04	1.5D+02	R

```
 39    1 1.0D+00  -3.784167D+00 3.2D-02 1.0D-04 1.5D+02      R
 40    1 1.0D+00  -3.790097D+00 1.7D-02 6.8D-05 2.7D+02      R
 41    1 1.0D+00  -3.791893D+00 1.8D-02 2.6D-05 1.4D+02      R
 42    1 1.0D+00  -3.792970D+00 2.1D-03 7.6D-06 1.5D+02      R
 43    1 1.0D+00  -3.793003D+00 1.7D-04 6.4D-06 2.4D+02      R
 44    1 1.0D+00  -3.793006D+00 1.5D-05 6.2D-06 1.3D+02
 45    1 1.0D+00  -3.793007D+00 1.2D-06 6.2D-06 1.4D+02      R
 46    1 1.0D+00  -3.793008D+00 4.2D-06 6.1D-06 1.2D+02      R
 47    1 1.0D+00  -3.793009D+00 7.1D-06 6.0D-06 1.8D+02      R
 48    1 1.0D+00  -3.793014D+00 2.9D-05 5.8D-06 1.6D+02      R
 49    1 1.0D+00  -3.793023D+00 6.3D-05 5.5D-06 1.7D+02      R
 50    1 1.0D+00  -3.793040D+00 8.5D-05 4.8D-06 1.1D+02      R
 51    1 1.0D+00  -3.793060D+00 2.3D-05 3.4D-06 2.1D+01
 52    1 1.0D+00  -3.793072D+00 7.1D-05 1.6D-06 3.4D+01      R
 53    1 1.0D+00  -3.793075D+00 8.5D-05 4.8D-07 2.3D+01      R
 54    1 1.0D+00  -3.793075D+00 1.2D-05 2.0D-07 1.2D+02      R
 55    1 1.0D+00  -3.793075D+00 3.9D-07 1.1D-07 1.5D+02      R
 56    1 1.0D+00  -3.793075D+00 5.8D-08 8.6D-08 1.2D+02      R
 57    1 1.0D+00  -3.793075D+00 3.8D-09 8.4D-08 1.3D+02      R
 58    1 1.0D+00  -3.793075D+00 1.1D-10 8.3D-08 3.8D+01      R
 59    1 1.0D+00  -3.793075D+00 4.5D-10 8.2D-08 2.9D+01      R
 60    1 1.0D+00  -3.793075D+00 1.0D-09 8.0D-08 9.9D+00      R
 61    1 1.0D+00  -3.793075D+00 2.4D-09 7.4D-08 5.3D+00      R
 62    1 1.0D+00  -3.793075D+00 2.6D-09 6.2D-08 5.2D+00      R
 63    1 1.0D+00  -3.793075D+00 2.4D-09 4.1D-08 5.2D+00      R
 64    1 1.0D+00  -3.793075D+00 2.2D-09 1.9D-08 2.2D+00      R
 65    1 1.0D+00  -3.793075D+00 1.5D-09 4.8D-09 4.5D+00      R
 66    1 1.0D+00  -3.793075D+00 1.8D-10 6.6D-10 5.4D+00      R
 67    1 1.0D+00  -3.793075D+00 4.7D-13 9.9D-11 5.3D+00      C R

Exit from NP problem after    67 major iterations,
                              83 minor iterations.

Varbl State     Value        Lower Bound    Upper Bound    Lagr Mult    Residual

V  1    FR    0.184348       0.126000       0.284000        0.          5.8348E-02
V  2    FR    0.101208       9.300000E-02   0.284000        0.          8.2077E-03
V  3    FR     834.018       1.000000E-03   1000.00         0.           166.0
V  4    FR     753.081       1.000000E-03   1000.00         0.           246.9
V  5    FR     732.931       1.000000E-03   1000.00         0.           267.1
V  6    FR     765.715       1.000000E-03   1000.00         0.           234.3
V  7    FR     662.592       1.000000E-03   1000.00         0.           337.4
V  8    FR     332.037       1.000000E-03   1000.00         0.           332.0
V  9    FR     375.252       1.000000E-03   1000.00         0.           375.3

N Con State     Value        Lower Bound    Upper Bound    Lagr Mult    Residual

N  1    EQ -1.509903E-13         0.             0.       3.5875E-03 -1.5099E-13
N  2    EQ  3.339551E-13         0.             0.       8.9819E-03  3.3396E-13
N  3    EQ   20.0000           20.0000        20.0000     -3.0189E-09  2.9132E-13

Exit E04UCF - Optimal solution found.

Final objective value =   -3.793075
```

IFAIL = 0
FUNCTION VALUE ON SUCCESSFUL EXIT IS
F= -3.7930752928087
ALL THE OPTIMAL LINK FLOWS FOR LOAD CASE 1 ARE
QL(1, 1 2) = 9.9651700985929D-02
QL(1, 2 4) = 7.1651700985929D-02
QL(1, 3 4) = 5.0140553867158D-02
QL(1, 4 6) = 4.6792254853087D-02
QL(1, 5 6) = 9.2077451469129D-03
QL(1, 1 3) = 0.18434829901407
QL(1, 3 5) = 1.0120774514691D-01
ALL THE OPTIMAL PIPE CHARACTERISTICS ARE
ALFA(1 2) = 834.01797711355
ALFA(2 4) = 753.08099057484
ALFA(3 4) = 732.93088694326
ALFA(4 6) = 765.71473269237
ALFA(5 6) = 662.59190282158
ALFA(1 3) = 332.03703864103
ALFA(3 5) = 375.25214922156
ALL PIPE CHARACTERISTIC PROBABILITIES ARE
PALFA(1 2) = 0.18718313372464
PALFA(2 4) = 0.16901801116100
PALFA(3 4) = 0.16449561518617
PALFA(4 6) = 0.17185346975437
PALFA(5 6) = 0.14870905922191
PALFA(1 3) = 7.4520855798071D-02
PALFA(3 5) = 8.4219855153835D-02
THE HEAD LOSSES IN THE LINKS FOR LOAD CASE 1 ARE
HL(1, 1 2) = 11.651158391209
HL(1, 2 4) = 5.7111185097479
HL(1, 3 4) = 2.8695466350482
HL(1, 4 6) = 2.6377230990431
HL(1, 5 6) = 0.11242373718517
HL(1, 1 3) = 14.492730265909
HL(1, 3 5) = 5.3948459969058

E.1.3 RUN 3

The input file:

```
y
6
7
1
1
1
1 2
2 4
3 4
4 6
5 6
1 3
3 5
-.284
.028
.033
.075
.092
.056
.2 .1
1 1 1 1 1 1 1
1000 1000 1000 1000 1000 1000 1000
1 1 1 1 1 1 1
1 1 -1 0 0 -1 0
0 0 1 1 -1 0 -1
20
1 0 0 1 1 0 1 0
.126 .093
.284 .284
1.0d-3
1.0d+3
```

The output file:

```
 OPTIMIZE ENTROPY? (Y/N)
 OPTIMZ =  T
 NN ?
 # NODES =  6
 NL ?
 # LINKS =  7
 NS ?
 # SOURCES =  1
 # LOOPS =  2
 NLC ?
 # LOAD CASES =  1
 NEXC ?
 # EXTRA CONSTRAINTS =  1
 FOR LOAD CASE  1 INPUT THE FOLLOWING:
 ------------------------------
 FOR EACH LINK INPUT UN, DN
 FOR EACH NODE INPUT D, (SOURCE -VE)
 INPUT (STARTING) FLOWS FOR THE LAST  2 LINK(S)
 THE INPUT FLOWS ARE
 QL(  1,  6 ) =   0.20000000000000
 QL(  1,  7 ) =    1.0000000000000D-01
 THE COMPLETE INPUT FLOWS ARE
 QL(  1,  1  2 ) =    8.4000000000000D-02
 QL(  1,  2  4 ) =    5.6000000000000D-02
 QL(  1,  3  4 ) =    6.7000000000000D-02
 QL(  1,  4  6 ) =    4.8000000000000D-02
 QL(  1,  5  6 ) =    8.0000000000000D-03
 QL(  1,  1  3 ) =   0.20000000000000
 QL(  1,  3  5 ) =    1.0000000000000D-01
 ------------------------------------
 FOR EACH LINK INPUT (STARTING) PIPE CHARACTERISTIC ALFA
 THE INPUT PIPE CHARACTERISTICS ARE
 ALFA(  1  2 ) =    1.0000000000000
 ALFA(  2  4 ) =    1.0000000000000
 ALFA(  3  4 ) =    1.0000000000000
 ALFA(  4  6 ) =    1.0000000000000
 ALFA(  5  6 ) =    1.0000000000000
 ALFA(  1  3 ) =    1.0000000000000
 ALFA(  3  5 ) =    1.0000000000000
 FUNCTION VALUE FOR INPUT DATA IS
 F =   -3.8406898845982
 FOR EACH LINK INPUT LENGTH L
 FOR EACH LINK INPUT DIAMETER DI
 FOR EACH LOOP  IN EACH  LOAD CASE  INPUT  UNIT VALUE
    FOR  EACH LINK  EXISTED IN  THE LOOP , CLOCKWISE
    (+VE), WITH ZERO VALUE FOR EACH LINK NOT EXISTED
    IN THAT LOOP
 INPUT THE PATH HEAD LOSS FOR EACH EXTRA CONSTRAINT
 FOR EACH  PATH  OF  HEAD  LOSS  CONSTRAINT  INPUT THE
    CORRESPONDING  LOAD CASE NUMBER , AND  INPUT UNIT
    VALUE  FOR EACH  LINK EXISTED IN  THE PATH , WITH
    ZERO VALUE FOR EACH LINK NOT EXISTED IN THAT PATH
 FOR EACH LOAD CASE INPUT THE  2 FLOW LOWER BOUNDS
 FOR EACH LOAD CASE INPUT THE  2 FLOW UPPER BOUNDS
```

INPUT PIPE CHARACTERISTIC LOWER BOUND
INPUT PIPE CHARACTERISTIC UPPER BOUND

Calls to E04UEF

DERIVATIVE LEVEL 0
MAJOR ITERATION LIMIT 1000
MINOR ITERATION LIMIT 2000

*** E04UCF
*** Start of NAG Library implementation details ***

Implementation title: Sun Solaris
Precision: Fortran Double Precision
Product Code: FLSOL16D
Mark: 16A

*** End of NAG Library implementation details ***

Parameters

Linear constraints.....	0	Linear feasibility.....	1.05D-08
Variables.....	9	Crash tolerance.....	1.00D-02
Infinite bound size....	1.00D+20	COLD start.....	
Infinite step size.....	1.00D+20	EPS (machine precision)	1.11D-16
Step limit.....	2.00D+00	Hessian.....	NO
Nonlinear constraints..	3	Nonlinear feasibility..	5.43D-06
Nonlinear objectiv vars	9	Optimality tolerance...	3.26D-12
Nonlinear Jacobian vars	9	Linesearch tolerance...	9.00D-01
Derivative level.....	0	Function precision.....	4.37D-15
Verify level.....	0	Monitoring file.....	-1
Major iterations limit.	1000	Major print level.....	10
Minor iterations limit.	2000	Minor print level.....	0

Difference intervals to be computed.

Workspace provided is IWORK(33), WORK(459).
To solve problem we need IWORK(33), WORK(459).

The user sets 0 out of 27 Jacobian elements.
Each iteration, 27 Jacobian elements will be estimated numerically.

The user sets 0 out of 9 objective gradient elements.
Each iteration, 9 gradient elements will be estimated numerically.

Computation of the finite-difference intervals

J	X(J)	Forward DX(J)	Central DX(J)	Error est.
1	2.00D-01	1.683985D-08	1.587252D-06	1.199702D-04
2	9.30D-02	1.268873D-08	1.445722D-06	1.592184D-04
3	1.00D+00	2.645420D-06	2.645420D-05	1.482225D-07
4	1.00D+00	2.645420D-06	2.645420D-05	1.482225D-07
5	1.00D+00	2.645420D-06	2.645420D-05	1.482225D-07
6	1.00D+00	2.645420D-06	2.645420D-05	4.636651D-09
7	1.00D+00	2.645420D-06	2.645420D-05	4.636651D-09
8	1.00D+00	2.645420D-06	2.645420D-05	1.482225D-07
9	1.00D+00	2.645420D-06	2.645420D-05	4.636651D-09

10 constant constraint gradient elements assigned.

Maj	Mnr	Step	Merit function	Violtn	Norm Gz	Cond Hz
0	2	0.0D+00	-3.365138D+00	6.2D+01	3.0D-01	1.0D+00
1	1	1.0D+00	-3.775143D+00	3.7D+00	6.6D-02	1.1D+00
2	1	1.0D+00	-3.777739D+00	7.6D-02	4.4D-02	1.4D+00
3	1	1.0D+00	-3.780798D+00	4.8D-02	4.1D-02	2.1D+00
4	1	1.0D+00	-3.784204D+00	5.6D-02	5.8D-02	1.9D+00
5	1	1.0D+00	-3.787843D+00	8.2D-03	6.4D-02	8.8D+00
6	1	1.0D+00	-3.791148D+00	6.6D-02	4.1D-02	3.2D+00
7	1	1.0D+00	-3.792445D+00	1.9D-02	2.7D-02	2.9D+00
8	1	1.0D+00	-3.792956D+00	9.3D-03	1.5D-02	4.2D+00
9	1	1.0D+00	-3.793070D+00	2.4D-03	2.5D-03	4.7D+00
10	1	1.0D+00	-3.793074D+00	6.2D-05	8.7D-04	3.5D+00
11	1	1.0D+00	-3.793075D+00	2.2D-06	5.0D-04	3.3D+00
12	1	1.0D+00	-3.793075D+00	1.4D-06	1.9D-04	5.2D+00
13	1	1.0D+00	-3.793075D+00	4.4D-07	3.6D-05	2.3D+00
14	1	1.0D+00	-3.793075D+00	1.3D-08	7.3D-06	2.9D+00
15	1	1.0D+00	-3.793075D+00	6.5D-11	4.8D-06	3.4D+00
16	1	1.0D+00	-3.793075D+00	6.1D-11	1.9D-06	3.3D+00
17	1	1.0D+00	-3.793075D+00	2.8D-11	4.7D-07	4.2D+00

Exit from NP problem after 17 major iterations,
19 minor iterations.

Varbl	State	Value	Lower Bound	Upper Bound	Lagr Mult	Residual
V 1	FR	0.184348	0.126000	0.284000	0.	5.8348E-02
V 2	FR	0.101208	9.300000E-02	0.284000	0.	8.2077E-03
V 3	FR	0.834017	1.000000E-03	1000.00	0.	0.8330
V 4	FR	0.753078	1.000000E-03	1000.00	0.	0.7521
V 5	FR	0.732928	1.000000E-03	1000.00	0.	0.7319
V 6	FR	0.765712	1.000000E-03	1000.00	0.	0.7647
V 7	FR	0.662590	1.000000E-03	1000.00	0.	0.6616
V 8	FR	0.332038	1.000000E-03	1000.00	0.	0.3310
V 9	FR	0.375251	1.000000E-03	1000.00	0.	0.3743

N Con	State	Value	Lower Bound	Upper Bound	Lagr Mult	Residual
N 1	EQ	-1.103828E-11	0.	0.	3.5876E-03	-1.1038E-11

```
N  2    EQ   2.177636E-11        0.          0.      8.9819E-03  2.1776E-11
N  3    EQ    20.0000          20.0000     20.0000      7.1348E-08  1.3141E-11

Exit E04UCF - Optimal solution found.

Final objective value =   -3.793075
 IFAIL =  0
 FUNCTION VALUE ON SUCCESSFUL EXIT IS
 F=   -3.7930752928069
 ALL THE OPTIMAL LINK FLOWS FOR LOAD CASE  1 ARE
 QL(  1,  1  2 ) =    9.965182075719 5D-02
 QL(  1,  2  4 ) =    7.165182075719 5D-02
 QL(  1,  3  4 ) =    5.014047460717 4D-02
 QL(  1,  4  6 ) =    4.679229536436 9D-02
 QL(  1,  5  6 ) =    9.207704635630 7D-03
 QL(  1,  1  3 ) =   0.18434817924281
 QL(  1,  3  5 ) =    1.012077046356 3D-01
 ALL THE OPTIMAL PIPE CHARACTERISTICS ARE
 ALFA(  1  2 ) =   0.83401651024787
 ALFA(  2  4 ) =   0.75307846169771
 ALFA(  3  4 ) =   0.73292788162852
 ALFA(  4  6 ) =   0.76571235987741
 ALFA(  5  6 ) =   0.66258960959859
 ALFA(  1  3 ) =   0.33203799057462
 ALFA(  3  5 ) =   0.37525084104221
 ALL PIPE CHARACTERISTIC PROBABILITIES ARE
 PALFA(  1  2 ) =   0.18718330961534
 PALFA(  2  4 ) =   0.16901789968009
 PALFA(  3  4 ) =   0.16449538457196
 PALFA(  4  6 ) =   0.17185340095082
 PALFA(  5  6 ) =   0.14870894582715
 PALFA(  1  3 ) =    7.452127053853 4D-02
 PALFA(  3  5 ) =    8.421978881610 7D-02
 THE HEAD LOSSES IN THE LINKS FOR LOAD CASE  1 ARE
 HL(  1,  1  2 ) =    11.651163833699
 HL(  1,  2  4 ) =    5.7111170117742
 HL(  1,  3  4 ) =    2.8695264680095
 HL(  1,  4  6 ) =    2.6377191545288
 HL(  1,  5  6 ) =   0.11242243203747
 HL(  1,  1  3 ) =    14.492754377475
 HL(  1,  3  5 ) =    5.3948231904791
```

E.1.4 RUN 4

The input file:

```
y
6
7
1
1
1
1 2
2 4
3 4
4 6
5 6
1 3
3 5
-.284
.028
.033
.075
.092
.056
.2 .1
10 10 10 10 10 10 10
1000 1000 1000 1000 1000 1000 1000
.261 .235 .234 .234 .185 .367 .294
1 1 -1 0 0 -1 0
0 0 1 1 -1 0 -1
20
1 0 0 1 1 0 1 0
.126 .093
.284 .284
1.0d-3
1.0d+3
```

The output file:

```
 OPTIMIZE ENTROPY? (Y/N)
 OPTIMZ =  T
 NN ?
 # NODES =  6
 NL ?
 # LINKS =  7
 NS ?
 # SOURCES =  1
 # LOOPS =  2
 NLC ?
 # LOAD CASES =  1
 NEXC ?
 # EXTRA CONSTRAINTS =  1
 FOR LOAD CASE  1 INPUT THE FOLLOWING:
 ------------------------------
 FOR EACH LINK INPUT UN, DN
 FOR EACH NODE INPUT D, (SOURCE -VE)
 INPUT (STARTING) FLOWS FOR THE LAST  2 LINK(S)
 THE INPUT FLOWS ARE
 QL(  1,  6 ) =   0.20000000000000
 QL(  1,  7 ) =    1.0000000000000D-01
 THE COMPLETE INPUT FLOWS ARE
 QL(  1,  1  2 ) =    8.4000000000000D-02
 QL(  1,  2  4 ) =    5.6000000000000D-02
 QL(  1,  3  4 ) =    6.7000000000000D-02
 QL(  1,  4  6 ) =    4.8000000000000D-02
 QL(  1,  5  6 ) =    8.0000000000000D-03
 QL(  1,  1  3 ) =   0.20000000000000
 QL(  1,  3  5 ) =    1.0000000000000D-01
 ------------------------------------
 FOR EACH LINK INPUT (STARTING) PIPE CHARACTERISTIC ALFA
 THE INPUT PIPE CHARACTERISTICS ARE
 ALFA(  1  2 ) =   10.000000000000
 ALFA(  2  4 ) =   10.000000000000
 ALFA(  3  4 ) =   10.000000000000
 ALFA(  4  6 ) =   10.000000000000
 ALFA(  5  6 ) =   10.000000000000
 ALFA(  1  3 ) =   10.000000000000
 ALFA(  3  5 ) =   10.000000000000
 FUNCTION VALUE FOR INPUT DATA IS
 F =   -3.8406898845982
 FOR EACH LINK INPUT LENGTH L
 FOR EACH LINK INPUT DIAMETER DI
 FOR EACH LOOP  IN EACH  LOAD CASE  INPUT  UNIT VALUE
    FOR  EACH LINK  EXISTED IN  THE LOOP , CLOCKWISE
    (+VE), WITH ZERO VALUE FOR EACH LINK NOT EXISTED
    IN THAT LOOP
 INPUT THE PATH HEAD LOSS FOR EACH EXTRA CONSTRAINT
 FOR EACH  PATH  OF  HEAD  LOSS  CONSTRAINT  INPUT THE
    CORRESPONDING  LOAD CASE NUMBER , AND  INPUT UNIT
    VALUE  FOR EACH  LINK EXISTED IN  THE PATH , WITH
    ZERO VALUE FOR EACH LINK NOT EXISTED IN THAT PATH
 FOR EACH LOAD CASE INPUT THE  2 FLOW LOWER BOUNDS
 FOR EACH LOAD CASE INPUT THE  2 FLOW UPPER BOUNDS
```

INPUT PIPE CHARACTERISTIC LOWER BOUND
INPUT PIPE CHARACTERISTIC UPPER BOUND

Calls to E04UEF

DERIVATIVE LEVEL 0
MAJOR ITERATION LIMIT 1000
MINOR ITERATION LIMIT 2000

*** E04UCF
*** Start of NAG Library implementation details ***
Implementation title: Sun Solaris
Precision: Fortran Double Precision
Product Code: FLSOL16D
Mark: 16A

*** End of NAG Library implementation details ***

Parameters

Linear constraints..... 0 Linear feasibility..... 1.05D-08
Variables..... 9 Crash tolerance..... 1.00D-02

Infinite bound size.... 1.00D+20 COLD start.....
Infinite step size..... 1.00D+20 EPS (machine precision) 1.11D-16
Step limit..... 2.00D+00 Hessian..... NO

Nonlinear constraints.. 3 Nonlinear feasibility.. 5.43D-06
Nonlinear objectiv vars 9 Optimality tolerance... 3.26D-12
Nonlinear Jacobian vars 9 Linesearch tolerance... 9.00D-01

Derivative level..... 0 Function precision..... 4.37D-15
Verify level..... 0 Monitoring file..... -1

Major iterations limit. 1000 Major print level..... 10
Minor iterations limit. 2000 Minor print level..... 0

Difference intervals to be computed.

Workspace provided is IWORK(33), WORK(459).
To solve problem we need IWORK(33), WORK(459).

The user sets 0 out of 27 Jacobian elements.
Each iteration, 27 Jacobian elements will be estimated numerically.

The user sets 0 out of 9 objective gradient elements.
Each iteration, 9 gradient elements will be estimated numerically.

Computation of the finite-difference intervals

J	X(J)	Forward DX(J)	Central DX(J)	Error est.
1	2.00D-01	9.340841D-09	1.587252D-06	6.641494D-01
2	9.30D-02	5.589181D-09	1.445722D-06	1.109950D+00
3	1.00D+01	1.454981D-05	1.454981D-04	2.152935D-05
4	1.00D+01	1.454981D-05	1.454981D-04	2.152935D-05
5	1.00D+01	1.454981D-05	1.454981D-04	2.152935D-05
6	1.00D+01	1.454981D-05	1.454981D-04	6.133084D-05
7	1.00D+01	1.454981D-05	1.454981D-04	6.133084D-05
8	1.00D+01	1.454981D-05	1.454981D-04	2.152935D-05
9	1.00D+01	1.454981D-05	1.454981D-04	6.133084D-05

10 constant constraint gradient elements assigned.

Maj	Mnr	Step	Merit function	Violtn	Norm Gz	Cond Hz	
0	7	0.0D+00	6.591381D+04	2.4D+05	0.0D+00	1.0D+00	
1	3	1.0D+00	-1.906366D+00	4.2D+00	7.0D-02	1.0D+00	R
2	5	1.0D+00	-1.908304D+00	7.9D-01	0.0D+00	1.0D+00	
3	2	1.0D+00	-3.782932D+00	2.6D+00	0.0D+00	1.0D+00	R
4	4	1.2D-01	-3.822042D+00	1.8D+00	2.7D+00	1.0D+00	
5	5	2.2D-01	-3.837025D+00	1.4D+00	1.8D+00	1.0D+00	
6	2	1.3D-02	-3.838643D+00	1.4D+00	0.0D+00	1.0D+00	
7	4	1.9D-01	-3.863552D+00	1.1D+00	4.8D-01	1.0D+00	
8	4	9.5D-02	-3.870020D+00	9.8D-01	0.0D+00	1.0D+00	
9	4	6.8D-02	-3.871170D+00	8.8D-01	6.8D-01	1.0D+00	
10	5	2.6D-02	-3.872175D+00	8.5D-01	3.0D-01	1.0D+00	
11	6	1.7D-02	-3.871205D+00	8.4D-01	3.2D+00	2.8D+01	
12	3	5.2D-03	-3.863632D+00	8.3D-01	2.7D+00	3.7D+00	
13	6	4.7D-02	-3.863853D+00	8.0D-01	7.8D+00	1.5D+00	
14	5	1.7D-01	-3.861392D+00	6.3D-01	3.0D+00	1.5D+01	
15	4	1.3D-01	-3.860515D+00	5.4D-01	1.4D+01	1.5D+02	
16	3	1.6D-01	-3.860924D+00	4.5D-01	1.1D+00	3.5D+01	
17	2	1.9D-01	-3.860496D+00	3.7D-01	4.6D+00	7.4D+01	
18	1	1.0D+00	-3.860952D+00	5.4D-03	3.3D-01	6.5D+01	
19	1	1.8D-01	-3.860959D+00	4.5D-03	1.6D-01	1.7D+01	
20	1	1.0D+00	-3.860961D+00	5.5D-06	1.1D-02	1.1D+01	
21	1	1.0D+00	-3.860961D+00	3.8D-08	6.1D-04	5.0D+00	
Mnr itn		1 -- Re-solve QP subproblem.					
22	1	0.0D+00	-3.860961D+00	3.8D-08	4.5D-02	2.1D+02	C
23	1	1.0D+00	-3.860961D+00	2.6D-07	2.4D-03	1.2D+01	C
24	1	1.0D+00	-3.860961D+00	1.5D-10	2.1D-04	2.5D+01	C
25	1	1.0D+00	-3.860961D+00	4.1D-12	2.3D-06	1.5D+01	C

Exit from NP problem after 25 major iterations,
82 minor iterations.

Varbl	State	Value	Lower Bound	Upper Bound	Lagr Mult	Residual
V 1	FR	0.200028	0.126000	0.284000	0.	7.4028E-02
V 2	FR	0.110157	9.300000E-02	0.284000	0.	1.7157E-02
V 3	FR	1.301917E-03	1.000000E-03	1000.00	0.	3.0192E-04
V 4	FR	1.302051E-03	1.000000E-03	1000.00	0.	3.0205E-04
V 5	FR	1.317019E-03	1.000000E-03	1000.00	0.	3.1702E-04

V 6	FR	1.309086E-03	1.000000E-03	1000.00	0.	3.0909E-04
V 7	FR	1.297352E-03	1.000000E-03	1000.00	0.	2.9735E-04
V 8	FR	1.303317E-03	1.000000E-03	1000.00	0.	3.0332E-04
V 9	FR	1.287272E-03	1.000000E-03	1000.00	0.	2.8727E-04

N Con	State	Value	Lower Bound	Upper Bound	Lagr Mult	Residual
N 1	EQ	-3.634426E-12	0.	0.	-7.4599E-06	-3.6344E-12
N 2	EQ	1.531220E-12	0.	0.	1.9802E-04	1.5312E-12
N 3	EQ	20.0000	20.0000	20.0000	2.2851E-06	1.1902E-12

Exit E04UCF - Optimal solution found.

Final objective value = -3.860961
IFAIL = 0
FUNCTION VALUE ON SUCCESSFUL EXIT IS
F= -3.8609611360736
ALL THE OPTIMAL LINK FLOWS FOR LOAD CASE 1 ARE
QL(1, 1 2) = 8.3972275602671D-02
QL(1, 2 4) = 5.5972275602671D-02
QL(1, 3 4) = 5.6870651432302D-02
QL(1, 4 6) = 3.7842927034974D-02
QL(1, 5 6) = 1.8157072965026D-02
QL(1, 1 3) = 0.20002772439733
QL(1, 3 5) = 0.11015707296503
ALL THE OPTIMAL PIPE CHARACTERISTICS ARE
ALFA(1 2) = 1.3019171805675D-03
ALFA(2 4) = 1.3020506131335D-03
ALFA(3 4) = 1.3170187284510D-03
ALFA(4 6) = 1.3090861608795D-03
ALFA(5 6) = 1.2973518403219D-03
ALFA(1 3) = 1.3033171382885D-03
ALFA(3 5) = 1.2872724979006D-03
ALL PIPE CHARACTERISTIC PROBABILITIES ARE
PALFA(1 2) = 0.14278516766778
PALFA(2 4) = 0.14279980161808
PALFA(3 4) = 0.14444139978360
PALFA(4 6) = 0.14357141127155
PALFA(5 6) = 0.14228447309047
PALFA(1 3) = 0.14293870523600
PALFA(3 5) = 0.14117904133252
THE HEAD LOSSES IN THE LINKS FOR LOAD CASE 1 ARE
HL(1, 1 2) = 9.1842525148791
HL(1, 2 4) = 7.2239262950028
HL(1, 3 4) = 7.6835810561453
HL(1, 4 6) = 3.5918211901157
HL(1, 5 6) = 2.8686948144992
HL(1, 1 3) = 8.7245977537401
HL(1, 3 5) = 8.4067074317603

APPENDIX F

SOME OF THE EZLP COMPUTER PROGRAMME APPLICATIONS OF CHAPTER 8

F.1 THE MAXIMUM ENTROPY TRUSS DESIGN

The input file:

```
51 10
-1 2
6.195E-5 4.564E-5 3.614E-5 2.710E-5 2.478E-5
4.756E-5 3.737E-5 2.754E-5 2.180E-5 1.635E-5 1.495E-5
8.121E-5 7.425E-5
6.533E-5 4.899E-5 4.480E-5
23.795E-5 10.816E-5 8.498E-5 6.262E-5 4.957E-5 3.718E-5 3.399E-5
23.795E-5 10.816E-5 8.498E-5 6.262E-5 4.957E-5 3.718E-5 3.399E-5
1.841E-15 0.837E-15 0.658E-15 0.485E-15 0.384E-15 0.288E-15 0.263E-15
41.784E-5 18.993E-5 14.923E-5 10.996E-5 8.705E-5 6.529E-5 5.969E-5
41.784E-5 18.993E-5 14.923E-5 10.996E-5 8.705E-5 6.529E-5 5.969E-5
0 2000
1 1 1 1 1 0 0 0 0 0 0 0 0 0 0 0 0 0 0 0 0 0 0 0 0
0 0 0 0 0 0 0 0 0 0 0 0 0 0 0 0 0 0 0 0 0 0 0 0 0
0 2000
0 0 0 0 0 1 1 1 1 1 1 0 0 0 0 0 0 0 0 0 0 0 0 0 0
0 0 0 0 0 0 0 0 0 0 0 0 0 0 0 0 0 0 0 0 0 0 0 0 0
0 3464
0 0 0 0 0 0 0 0 0 0 1 1 0 0 0 0 0 0 0 0 0 0 0 0 0
0 0 0 0 0 0 0 0 0 0 0 0 0 0 0 0 0 0 0 0 0 0 0 0 0
0 3464
0 0 0 0 0 0 0 0 0 0 0 1 1 1 0 0 0 0 0 0 0 0 0 0 0
0 0 0 0 0 0 0 0 0 0 0 0 0 0 0 0 0 0 0 0 0 0 0 0 0
0 2000
0 0 0 0 0 0 0 0 0 0 0 0 0 1 1 1 1 1 1 1 0 0 0 0 0
0 0 0 0 0 0 0 0 0 0 0 0 0 0 0 0 0 0 0 0 0 0 0 0 0
0 2000
0 0 0 0 0 0 0 0 0 0 0 0 0 0 0 0 0 0 0 0 0 0 0 1 1 1
1 1 1 1 0 0 0 0 0 0 0 0 0 0 0 0 0 0 0 0 0 0 0 0 0
0 2000
0 0 0 0 0 0 0 0 0 0 0 0 0 0 0 0 0 0 0 0 0 0 0 0 0
0 0 0 0 1 1 1 1 1 1 1 0 0 0 0 0 0 0 0 0 0 0 0 0 0
0 2000
0 0 0 0 0 0 0 0 0 0 0 0 0 0 0 0 0 0 0 0 0 0 0 0 0
0 0 0 0 0 0 0 0 0 1 1 1 1 1 1 1 0 0 0 0 0 0 0 0 0
0 2000
0 0 0 0 0 0 0 0 0 0 0 0 0 0 0 0 0 0 0 0 0 0 0 0 0
0 0 0 0 0 0 0 0 0 0 0 0 0 0 0 0 0 0 0 0 1 1 1 1 1 1 1
1 0
```

10.990E-3 14.915E-3 18.840E-3 25.120E-3 27.475E-3
8.635E-3 10.990E-3 14.915E-3 18.840E-3 25.120E-3 27.475E-3
25.120E-3 27.475E-3
18.840E-3 25.120E-3 27.475E-3
3.925E-3 8.635E-3 10.990E-3 14.915E-3 18.840E-3 25.120E-3 27.475E-3
3.925E-3 8.635E-3 10.990E-3 14.915E-3 18.840E-3 25.120E-3 27.475E-3
3.925E-3 8.635E-3 10.990E-3 14.915E-3 18.840E-3 25.120E-3 27.475E-3
3.925E-3 8.635E-3 10.990E-3 14.915E-3 18.840E-3 25.120E-3 27.475E-3
3.925E-3 8.635E-3 10.990E-3 14.915E-3 18.840E-3 25.120E-3 27.475E-3

The output file:

**** PROGRAM EZLP ****

SOLUTION OF LINEAR PROGRAMMING PROBLEMS

A.B.TEMPLEMAN JULY,1985
(MODIFIED : NOV89)

THE NUMBER OF VARIABLES IS 51

THE NUMBER OF CONSTRAINTS (EXCLUDING NON-NEGATIVITY REQUIREMENTS) IS 10

THE INPUT CONSTRAINT INFORMATION IS:-

CONSTRAINT NO. 1 IS LESS THAN OR EQUAL TO A RIGHT-HAND SIDE OF 0.200000E+01

THE COEFFICIENTS OF THE LEFT-HAND SIDE FUNCTION ARE, IN THE INPUT ORDER:-

0.619500E-04	0.456400E-04	0.361400E-04	0.271000E-04	0.247800E-04
0.475600E-04	0.373700E-04	0.275400E-04	0.218000E-04	0.163500E-04
0.149500E-04	0.812100E-04	0.742500E-04	0.653300E-04	0.489900E-04
0.448000E-04	0.237950E-03	0.108160E-03	0.849800E-04	0.626200E-04
0.495700E-04	0.371800E-04	0.339900E-04	0.237950E-03	0.108160E-03
0.849800E-04	0.626200E-04	0.495700E-04	0.371800E-04	0.339900E-04
0.184100E-14	0.837000E-15	0.658000E-15	0.485000E-15	0.384000E-15
0.288000E-15	0.263000E-15	0.417840E-03	0.189930E-03	0.149230E-03
0.109960E-03	0.870500E-04	0.652900E-04	0.596900E-04	0.417840E-03
0.189930E-03	0.149230E-03	0.109960E-03	0.870500E-04	0.652900E-04
0.596900E-04				

CONSTRAINT NO. 2 IS STRICTLY EQUAL TO A RIGHT-HAND SIDE OF 0.200000E+04

THE COEFFICIENTS OF THE LEFT-HAND SIDE FUNCTION ARE, IN THE INPUT ORDER:-

0.100000E+01	0.100000E+01	0.100000E+01	0.100000E+01	0.100000E+01
0.000000E+00	0.000000E+00	0.000000E+00	0.000000E+00	0.000000E+00
0.000000E+00	0.000000E+00	0.000000E+00	0.000000E+00	0.000000E+00
0.000000E+00	0.000000E+00	0.000000E+00	0.000000E+00	0.000000E+00
0.000000E+00	0.000000E+00	0.000000E+00	0.000000E+00	0.000000E+00
0.000000E+00	0.000000E+00	0.000000E+00	0.000000E+00	0.000000E+00
0.000000E+00	0.000000E+00	0.000000E+00	0.000000E+00	0.000000E+00
0.000000E+00	0.000000E+00	0.000000E+00	0.000000E+00	0.000000E+00
0.000000E+00	0.000000E+00	0.000000E+00	0.000000E+00	0.000000E+00
0.000000E+00	0.000000E+00	0.000000E+00	0.000000E+00	0.000000E+00
0.000000E+00				

CONSTRAINT NO. 3 IS STRICTLY EQUAL TO A RIGHT-HAND SIDE OF 0.200000E+04

THE COEFFICIENTS OF THE LEFT-HAND SIDE FUNCTION ARE, IN THE INPUT ORDER:-

0.000000E+00	0.000000E+00	0.000000E+00	0.000000E+00	0.000000E+00
0.100000E+01	0.100000E+01	0.100000E+01	0.100000E+01	0.100000E+01
0.100000E+01	0.000000E+00	0.000000E+00	0.000000E+00	0.000000E+00
0.000000E+00	0.000000E+00	0.000000E+00	0.000000E+00	0.000000E+00
0.000000E+00	0.000000E+00	0.000000E+00	0.000000E+00	0.000000E+00
0.000000E+00	0.000000E+00	0.000000E+00	0.000000E+00	0.000000E+00
0.000000E+00	0.000000E+00	0.000000E+00	0.000000E+00	0.000000E+00
0.000000E+00	0.000000E+00	0.000000E+00	0.000000E+00	0.000000E+00
0.000000E+00	0.000000E+00	0.000000E+00	0.000000E+00	0.000000E+00
0.000000E+00				

CONSTRAINT NO. 4 IS STRICTLY EQUAL TO A RIGHT-HAND SIDE OF 0.346400E+04

THE COEFFICIENTS OF THE LEFT-HAND SIDE FUNCTION ARE, IN THE INPUT ORDER:-

0.000000E+00	0.000000E+00	0.000000E+00	0.000000E+00	0.000000E+00
0.000000E+00	0.000000E+00	0.000000E+00	0.000000E+00	0.000000E+00
0.000000E+00	0.100000E+01	0.100000E+01	0.000000E+00	0.000000E+00
0.000000E+00	0.000000E+00	0.000000E+00	0.000000E+00	0.000000E+00
0.000000E+00	0.000000E+00	0.000000E+00	0.000000E+00	0.000000E+00
0.000000E+00	0.000000E+00	0.000000E+00	0.000000E+00	0.000000E+00
0.000000E+00	0.000000E+00	0.000000E+00	0.000000E+00	0.000000E+00
0.000000E+00	0.000000E+00	0.000000E+00	0.000000E+00	0.000000E+00
0.000000E+00	0.000000E+00	0.000000E+00	0.000000E+00	0.000000E+00
0.000000E+00				

CONSTRAINT NO. 5 IS STRICTLY EQUAL TO A RIGHT-HAND SIDE OF 0.346400E+04

THE COEFFICIENTS OF THE LEFT-HAND SIDE FUNCTION ARE, IN THE INPUT ORDER:-

0.000000E+00 0.000000E+00 0.000000E+00 0.000000E+00 0.000000E+00
0.000000E+00 0.000000E+00 0.000000E+00 0.000000E+00 0.000000E+00
0.000000E+00 0.000000E+00 0.000000E+00 0.100000E+01 0.100000E+01
0.100000E+01 0.000000E+00 0.000000E+00 0.000000E+00 0.000000E+00
0.000000E+00 0.000000E+00 0.000000E+00 0.000000E+00 0.000000E+00
0.000000E+00 0.000000E+00 0.000000E+00 0.000000E+00 0.000000E+00
0.000000E+00 0.000000E+00 0.000000E+00 0.000000E+00 0.000000E+00
0.000000E+00 0.000000E+00 0.000000E+00 0.000000E+00 0.000000E+00
0.000000E+00 0.000000E+00 0.000000E+00 0.000000E+00 0.000000E+00
0.000000E+00

CONSTRAINT NO. 6 IS STRICTLY EQUAL TO A RIGHT-HAND SIDE OF 0.200000E+04

THE COEFFICIENTS OF THE LEFT-HAND SIDE FUNCTION ARE, IN THE INPUT ORDER:-

0.000000E+00 0.000000E+00 0.000000E+00 0.000000E+00 0.000000E+00
0.000000E+00 0.000000E+00 0.000000E+00 0.000000E+00 0.000000E+00
0.000000E+00 0.000000E+00 0.000000E+00 0.000000E+00 0.000000E+00
0.000000E+00 0.100000E+01 0.100000E+01 0.100000E+01 0.100000E+01
0.100000E+01 0.100000E+01 0.100000E+01 0.000000E+00 0.000000E+00
0.000000E+00 0.000000E+00 0.000000E+00 0.000000E+00 0.000000E+00
0.000000E+00 0.000000E+00 0.000000E+00 0.000000E+00 0.000000E+00
0.000000E+00 0.000000E+00 0.000000E+00 0.000000E+00 0.000000E+00
0.000000E+00 0.000000E+00 0.000000E+00 0.000000E+00 0.000000E+00
0.000000E+00

CONSTRAINT NO. 7 IS STRICTLY EQUAL TO A RIGHT-HAND SIDE OF 0.200000E+04

THE COEFFICIENTS OF THE LEFT-HAND SIDE FUNCTION ARE, IN THE INPUT ORDER:-

0.000000E+00 0.000000E+00 0.000000E+00 0.000000E+00 0.000000E+00
0.000000E+00 0.000000E+00 0.000000E+00 0.000000E+00 0.000000E+00
0.000000E+00 0.000000E+00 0.000000E+00 0.000000E+00 0.000000E+00
0.000000E+00 0.000000E+00 0.000000E+00 0.100000E+01 0.100000E+01
0.100000E+01 0.100000E+01 0.100000E+01 0.100000E+01 0.100000E+01
0.000000E+00 0.000000E+00 0.000000E+00 0.000000E+00 0.000000E+00
0.000000E+00 0.000000E+00 0.000000E+00 0.000000E+00 0.000000E+00
0.000000E+00 0.000000E+00 0.000000E+00 0.000000E+00 0.000000E+00
0.000000E+00

CONSTRAINT NO. 8 IS STRICTLY EQUAL TO A RIGHT-HAND SIDE OF 0.200000E+04

THE COEFFICIENTS OF THE LEFT-HAND SIDE FUNCTION ARE, IN THE INPUT ORDER:-

0.000000E+00 0.000000E+00 0.000000E+00 0.000000E+00 0.000000E+00
0.000000E+00 0.000000E+00 0.000000E+00 0.000000E+00 0.000000E+00
0.000000E+00 0.000000E+00 0.000000E+00 0.000000E+00 0.000000E+00
0.000000E+00 0.000000E+00 0.000000E+00 0.000000E+00 0.000000E+00
0.000000E+00 0.000000E+00 0.000000E+00 0.000000E+00 0.000000E+00
0.000000E+00 0.000000E+00 0.000000E+00 0.000000E+00 0.000000E+00
0.100000E+01 0.100000E+01 0.100000E+01 0.100000E+01 0.100000E+01
0.100000E+01 0.100000E+01 0.000000E+00 0.000000E+00 0.000000E+00
0.000000E+00 0.000000E+00 0.000000E+00 0.000000E+00 0.000000E+00
0.000000E+00 0.000000E+00 0.000000E+00 0.000000E+00 0.000000E+00
0.000000E+00

CONSTRAINT NO. 9 IS STRICTLY EQUAL TO A RIGHT-HAND SIDE OF 0.200000E+04

THE COEFFICIENTS OF THE LEFT-HAND SIDE FUNCTION ARE, IN THE INPUT ORDER:-

0.000000E+00 0.000000E+00 0.000000E+00 0.000000E+00 0.000000E+00
0.000000E+00 0.000000E+00 0.000000E+00 0.000000E+00 0.000000E+00
0.000000E+00 0.000000E+00 0.000000E+00 0.000000E+00 0.000000E+00
0.000000E+00 0.000000E+00 0.000000E+00 0.000000E+00 0.000000E+00
0.000000E+00 0.000000E+00 0.000000E+00 0.000000E+00 0.000000E+00
0.000000E+00 0.000000E+00 0.000000E+00 0.000000E+00 0.000000E+00
0.000000E+00 0.000000E+00 0.000000E+00 0.000000E+00 0.000000E+00
0.000000E+00 0.000000E+00 0.100000E+01 0.100000E+01 0.100000E+01
0.100000E+01 0.100000E+01 0.100000E+01 0.100000E+01 0.000000E+00
0.000000E+00 0.000000E+00 0.000000E+00 0.000000E+00 0.000000E+00
0.000000E+00

CONSTRAINT NO. 10 IS STRICTLY EQUAL TO A RIGHT-HAND SIDE OF 0.200000E+04

THE COEFFICIENTS OF THE LEFT-HAND SIDE FUNCTION ARE, IN THE INPUT ORDER:-

0.000000E+00 0.000000E+00 0.000000E+00 0.000000E+00 0.000000E+00
0.000000E+00 0.000000E+00 0.000000E+00 0.000000E+00 0.000000E+00
0.000000E+00 0.000000E+00 0.000000E+00 0.000000E+00 0.000000E+00
0.000000E+00 0.000000E+00 0.000000E+00 0.000000E+00 0.000000E+00
0.000000E+00 0.000000E+00 0.000000E+00 0.000000E+00 0.000000E+00
0.000000E+00 0.000000E+00 0.000000E+00 0.000000E+00 0.000000E+00
0.000000E+00 0.000000E+00 0.000000E+00 0.000000E+00 0.000000E+00
0.000000E+00 0.000000E+00 0.000000E+00 0.000000E+00 0.000000E+00
0.000000E+00 0.000000E+00 0.000000E+00 0.000000E+00 0.100000E+01
0.100000E+01 0.100000E+01 0.100000E+01 0.100000E+01 0.100000E+01
0.100000E+01

THE OBJECTIVE FUNCTION IS TO BE MINIMIZED AND ITS COEFFICIENTS OF VARIABLES ARE, IN THE INPUT ORDER:-

0.109900E-01	0.149150E-01	0.188400E-01	0.251200E-01	0.274750E-01
0.863500E-02	0.109900E-01	0.149150E-01	0.188400E-01	0.251200E-01
0.274750E-01	0.251200E-01	0.274750E-01	0.188400E-01	0.251200E-01
0.274750E-01	0.392500E-02	0.863500E-02	0.109900E-01	0.149150E-01
0.188400E-01	0.251200E-01	0.274750E-01	0.392500E-02	0.863500E-02
0.109900E-01	0.149150E-01	0.188400E-01	0.251200E-01	0.274750E-01
0.392500E-02	0.863500E-02	0.109900E-01	0.149150E-01	0.188400E-01
0.251200E-01	0.274750E-01	0.392500E-02	0.863500E-02	0.109900E-01
0.149150E-01	0.188400E-01	0.251200E-01	0.274750E-01	0.392500E-02
0.863500E-02	0.109900E-01	0.149150E-01	0.188400E-01	0.251200E-01
0.274750E-01				

PHASE ONE COMPLETED

SOLUTION POINT REACHED

OPTIMUM VALUES OF THE 51 INPUT VARIABLES ARE:-

X(1) = 0.200000E+04	X(2) = 0.000000E+00	X(3) = 0.000000E+00
X(4) = 0.000000E+00	X(5) = 0.000000E+00	X(6) = 0.200000E+04
X(7) = 0.000000E+00	X(8) = 0.000000E+00	X(9) = 0.000000E+00
X(10) = 0.000000E+00	X(11) = 0.000000E+00	X(12) = 0.346400E+04
X(13) = 0.000000E+00	X(14) = 0.346400E+04	X(15) = 0.000000E+00
X(16) = 0.000000E+00	X(17) = 0.000000E+00	X(18) = 0.200000E+04
X(19) = 0.000000E+00	X(20) = 0.000000E+00	X(21) = 0.000000E+00
X(22) = 0.000000E+00	X(23) = 0.000000E+00	X(24) = 0.624127E+03
X(25) = 0.137587E+04	X(26) = 0.000000E+00	X(27) = 0.000000E+00

X(28) = 0.000000E+00 X(29) = 0.000000E+00 X(30) = 0.000000E+00

X(31) = 0.200000E+04 X(32) = 0.000000E+00 X(33) = 0.000000E+00

X(34) = 0.000000E+00 X(35) = 0.000000E+00 X(36) = 0.000000E+00

X(37) = 0.000000E+00 X(38) = 0.000000E+00 X(39) = 0.200000E+04

X(40) = 0.000000E+00 X(41) = 0.000000E+00 X(42) = 0.000000E+00

X(43) = 0.000000E+00 X(44) = 0.000000E+00 X(45) = 0.000000E+00

X(46) = 0.200000E+04 X(47) = 0.000000E+00 X(48) = 0.000000E+00

X(49) = 0.000000E+00 X(50) = 0.000000E+00 X(51) = 0.000000E+00

THE OPTIMUM VALUE OF THE OBJECTIVE FUNCTION IS 0.265518E+03

THE ROW NUMBERS OF THE ACTIVE CONSTRAINTS ARE:-

1 2 3 4 5 6 7 8 9 10

**** END OF SOLUTION ****

APPENDIX G

THE TRUSS2D COMPUTER PROGRAMME

```
C     PROGRAM TRUSS2D(INPUT,OUTPUT)
C PROGRAM FOR 2-D TRUSSES USING CODE NUMBERS.
C INPUT IS IN FREE FORM.
C ********
      DIMENSION BGK(100,30),XL(60),SINW(60),COSW(60),SK(4,4),AR(60),
     1NC(60,4),QL(100),P(60)
      PRINT 4
    4 FORMAT(///' *** TRUSS ANALYSIS USING CODE NUMBERS ***'/,
     1/'INPUT IS IN FREE FORM.'/)
      PRINT 8
    8 FORMAT(' TYPE THE NO. OF MEMBERS, THE NO. OF EXTERNAL ',
     1'DISPLACEMENTS,'/' AND THE VALUE OF E.')
      READ*,NM,ND,E
      PRINT 12
   12 FORMAT(' TYPE THE MEMBER END COORDINATES, MEMBER 1, 2, ETC.,'/
     1' IN THE ORDER:'/'  XI  YI  XJ  YJ')
      DO 16 I=1,NM
      READ*,XI,YI,XJ,YJ
      XL(I)=SQRT((YJ-YI)**2+(XJ-XI)**2)
      SINW(I)=(YJ-YI)/XL(I)
   16 COSW(I)=(XJ-XI)/XL(I)
      PRINT 20
   20 FORMAT(' TYPE THE MEMBER AREAS - A(1), A(2), ETC.')
      READ*,(AR(I),I=1,NM)
      PRINT 24
   24 FORMAT(' TYPE THE CODE NUMBERS; MEMBER 1, 2, ETC.')
      DO 28 I=1,NM
   28 READ*,(NC(I,J),J=1,4)
      PRINT 32
   32 FORMAT(' TYPE THE ELEMENTS OF Q.')
      READ*,(QL(I),I=1,ND)
      PRINT 36
   36 FORMAT(//' INPUT VALUES:'//' MEMBER',30X,'CODE'/,
     1' NUMBER    LENGTH        AREA        NUMBERS'/)
      DO 40 I=1,NM
   40 PRINT 44,I,XL(I),AR(I),(NC(I,J),J=1,4)
   44 FORMAT(2X,I4,2E13.5,1X,4I3)
      PRINT 48,E
   48 FORMAT(/' THE VALUE OF E IS ',E11.5)
      PRINT 52
   52 FORMAT(1X/' ID NO.    LOADS APPLIED '/)
      DO 56 I=1,ND
```

```
56 PRINT 60,I,QL(I)
60 FORMAT(2X,I3,4X,E13.5)
   IBND=0
   DO 64 I=1,NM
   DO 64 J=1,3
   JJ=J+1
   DO 64 K=JJ,4
   IF(NC(I,J).EQ.0.OR.NC(I,K).EQ.0)GO TO 64
   M=IABS(NC(I,J)-NC(I,K))
   IF(M.GT.IBND)IBND=M
64 CONTINUE
   IBND=IBND+1
   PRINT 68,IBND
68 FORMAT(/' THE BANDWIDTH IS ',I2)
   IF(IBND.LE.30)GO TO 72
   PRINT 70
70 FORMAT(/' BANDWIDTH EXCEEDS DIMENSION.'/)
   STOP
72 DO 76 I=1,ND
   DO 76 J=1,IBND
76 BGK(I,J)=0.
   DO 84 N=1,NM
   SK(1,1)=COSW(N)**2
   SK(3,3)=SK(1,1)
   SK(1,2)=SINW(N)*COSW(N)
   SK(3,4)=SK(1,2)
   SK(1,4)=-SK(1,2)
   SK(2,3)=SK(1,4)
   SK(1,3)=-SK(1,1)
   SK(2,2)=SINW(N)**2
   SK(4,4)=SK(2,2)
   SK(2,4)=-SK(2,2)
   DO 80 I=1,4
   DO 80 J=I,4
80 SK(I,J)=(E*AR(N)/XL(N))*SK(I,J)
   DO 84 I=1,4
   DO 84 J=I,4
   K=NC(N,I)
   L=NC(N,J)
   IF(K.EQ.0.OR.L.EQ.0)GO TO 84
   IF(K.LE.L)GO TO 82
   IT=K
   K=L
   L=IT
82 IPOS=L-K+1
   BGK(K,IPOS)=BGK(K,IPOS)+SK(I,J)
84 CONTINUE
   CALL BNDSOL(BGK,QL,ND,IBND)
   DO 88 N=1,NM
   C=E*AR(N)/XL(N)
   SK(1,3)=COSW(N)
   SK(1,1)=-SK(1,3)
   SK(1,4)=SINW(N)
   SK(1,2)=-SK(1,4)
   P(N)=0.
   DO 88 J=1,4
```

```
   K=NC(N,J)
   IF(K.EQ.0)GO TO 88
   P(N)=P(N)+C*SK(1,J)*QL(K)
88 CONTINUE
   PRINT 92
92 FORMAT(//' OUTPUT VALUES '//'  ID NO.  DEFLECTIONS',3X,
  1'AXIAL FORCE'/)
   IF(NM-ND)96,106,106
96 DO 98 I=1,NM
98 PRINT 100,I,QL(I),P(I)
100 FORMAT(3X,I3,2X,2E14.5)
   J=NM+1
   DO 102 I=J,ND
102 PRINT 104,I,QL(I)
104 FORMAT(3X,I3,2X,E14.5)
   GO TO 120
106 DO 108 I=1,ND
108 PRINT 100,I,QL(I),P(I)
   IF(NM.EQ.ND)GO TO 120
   J=ND+1
   DO 110 I=J,NM
110 PRINT 112,I,P(I)
112 FORMAT(3X,I3,16X,E14.5)
120 PRINT 124
124 FORMAT(/' ANALYSIS COMPLETE.'///)
   STOP
   END
   SUBROUTINE BNDSOL(BGK,Q,NDIS,MB)
   DIMENSION BGK(100,30),Q(100),F(30)
   N=0
500 N=N+1
   Q(N)=Q(N)/BGK(N,1)
   IF(N-NDIS)550,700,550
550 DO 600 K=2,MB
   F(K)=BGK(N,K)
600 BGK(N,K)=BGK(N,K)/BGK(N,1)
   DO 660 L=2,MB
   I=N+L-1
   IF(NDIS-I)660,640,640
640 J=0
   DO 650 K=L,MB
   J=J+1
650 BGK(I,J)=BGK(I,J)-F(L)*BGK(N,K)
   Q(I)=Q(I)-F(L)*Q(N)
660 CONTINUE
   GO TO 500
700 N=N-1
   IF(N)750,900,750
750 DO 800 K=2,MB
   L=N+K-1
   IF(NDIS-L)800,770,770
770 Q(N)=Q(N)-BGK(N,K)*Q(L)
800 CONTINUE
   GO TO 700
900 RETURN
   END
```